Effects of sevoflurane in the treatment of Acute Respiratory Distress Syndrome : a translational approach

Ruoyang Zhai

UNIVERSITÉ CLERMONT AUVERGNE ANNÉE 2023

ECOLE DOCTORALE
DES SCIENCES DE LA VIE, SANTE, AGRONOMIE, ENVIRONNEMENT

Thèse

Présentée à l'Université Clermont Auvergne

pour l'obtention du grade de DOCTEUR D'UNIVERSITE
(Décret du 5 juillet 1984)

Spécialité : **Biologie Santé**

soutenue le 24 mars 2023 par

ZHAI Ruoyang

Effects of sevoflurane in the treatment of Acute Respiratory Distress Syndrome: a translational approach

---

Professeur Matthieu JABAUDON Directeur	Université Clermont Auvergne, Clermont-Fd
Professeure Beatrice BECK SCHIMMER Rapporteur	University of Zurich, Zurich, Switzerland
Professeure Anne-claire LUKASZEWICZ Rapporteur	Université de Lyon, Lyon
Professeur Vincent SAPIN Membre	Université Clermont Auvergne, Clermont-Fd

Equipe 10 « Approches translationnelles des lésions épithéliales et de leur réparation »
iGReD, INSERM, CNRS
Faculté de Médecine, Université Clermont Auvergne
28 place Henri Dunant - BP 38
63001 Clermont-Ferrand Cedex, France

Acknowledgements

First of all, I would like to express my sincere gratitude to the eminent members of the jury, thank you for accepting to be my jury members to examine my thesis work and to give me expert advises on my thesis subject. I will always be grateful and remember having such a jury composed of scientific leaders in our domain:

I would like to thank my thesis supervisor, professor Matthieu JABAUDON. This thesis would not be here without your supervision, your suggestions, your encouragement and your leadership. I have learned a lot from you, and I will not forget those priceless lessons in my future career. Your optimism, your work attitude, and your humor sense will always be an example to me. Thank you for all these times. I will never forget that sentence " **If you're going through hell, keep going.**" Still, I sincerely wish your next Ph.D. student will be someone who kills fewer cells and mouses...

I would like to show how i'm grateful to Professor Anne-claire LUKASZEWICZ and Professor Beatrice BECK SCHIMMER, it is such an honor to have two outstanding woman scientific leaders in the field of intensive care and anesthesiology at the same time in my jury. Thank you for your time and your expertise in my thesis work and its optimization.

I would like to thank Professor Vincent SAPIN, the captain of our research fleet, thank you for all those supportive moments and wise suggestions. Your powerful theory about "a successful research work is always a good story" will always be helpful for my future works. Those oolong times with sportive/political/cultural discussion will not be forgotten and remain good memories of these four years.

I would like also thank Pr. Martin SCHLAPFER and Pr. Julie BASTARACHE, for all your suggestions and expertise during these three years as jury members of my thesis committee.

Secondly, I would like to show my sincere gratitude to members of the laboratory and research partners:

Loic and Corinne, the “seniors” of our team, thank you for your advice of seniors, for your all-time care, for all those scientific discussions, also for the teaching advises for my teaching missions, thank you for all time being supportive even the heaviest moment.

Karen, Damien, Geoffroy, and Regine, Thank you for your encouragement and your help during my thesis work!

Fanny, Audrey, Coline, Julia, Ines, “girls in next office”, Thank you for your all-time encouragement, your help, your advice, your jokes, and your cakes! Fanny, my battle bud in another trench, I won’t forget those moments we doubt all on HMGB1, RAP, and the RAGE, but also those weird clips of Theo Lavabo. Audrey, I won’t forget those warm and funny little geek moments. Coline, the promise of the creation of our journal “negative results” still hold! Julia and Ines, our Indiana jones of the team, and our co-owner of A549 cells, I wish I could join you for the next adventure. Those moments won’t be forgotten, they just live forever.

Charlotte, Cécile, Camille, and Woodys, “ the bureau of legends”, as a task force team, this thesis work won’t be here without your contributions. Charlotte, AKA Lab manager and UCA employee wellness finder, and the pro of ELISA, thank you for all those times, it will be hard to forget that time we fish those lost tubes in azote! Maybe we’ll meet at the parents' meeting of our daughters! Cécile, AKA the sainte gate keeper of anima facility and the secret guardian of relic, thank you to lead us holding such a big animal experimental project, I won’t forget the mission code: Phenotype and all those lunch discussions! Camille, AKA the sport coach and the firewoman of the project deadline, thanks for holding those hard mission which seems impossible, thank you for laughing at all my jokes which were not funny at all, don’t forget your lifelong membership of my boardgame clud! Woodys, AKA the emperor of

Western Blot, thank you for all those experiences and suggestions, all those brainstorming moments, I do wish you find an attractive CDI like all those times we hope!

What a team! Those memories are unskippable chapters of this thesis.

Raiko, Randy, Jules, " those REA cool guys", I remember the beginning of all this story, and it seems is still yesterday, thank you for all your support and your help! A good pinte of beer is when you want!

I would like also to thank Julie for all those ELLA moments! Thank you Christelle for all those microscopy formations and help!

A big thank you to all our laboratory members in iGReD, this outstanding laboratory, and its great people, thank you all for filling my four years of wonderful memories!

Life is composed of work and life, a thesis work won't be here without my family and friends.

I would like to first thank all my friends for your support to my thesis, my designated lawyer and my best bro Boyu, Weizhe, Shenggen, Zonghuan, Yanru, Héléna and Tim, Clarisse and Samuel, Benoit and Gustave, Aline, Marie, Bertille and Marie, other "famillia" members, Mélissa, J-B, Hugo, Aymeric, and Lorine… Thank you!

And last, a special part to my formidable family, words are limited, but emotions are in my heart.

To my parents, my parents-in-law, and my family: I'm so proud to have you on my back and I'm so grateful for all those years of support. I'm the last person who has self-confidence and you always encourages me, today, I finally make it. We made it!

I won't thank COVID-19 for separating my family in China, and I'm so glad that we could finally meet, not through the cold internet!

And there we are, the part reserved for my wife and children, my beloved guardian unicorn, and my little elf of happiness, Tifany and Alice. I have written many versions to express my most complicated emotions for my beloved wife and daughter, but I think there will never be a better version than a warmful hug, as you always do when I cry with stress or my sad moments when experiments failed. Or a big smile you did to me when every time I'm in the downside.

Life is too short but too many blanks remain to be filled, and all I want to do is to keep any precious moments special for you, thank you, and I love you.

*"**Soyons reconnaissants aux personnes qui nous donnent du bonheur ; elles sont les charmants jardiniers par qui nos âmes sont fleuries**"*

— Marcel Proust

List of Tables and Figures

Abbreviations

AGEs: advanced glycation end-products

ALI: acute lung injury

AQP: aquaporin

ARDS: acute respiratory distress syndrome

BALF: bronchoalveolar lavage fluid

BCL: B-cell lymphoma

CCL: Chemokine ligand

COPD: Chronic Obstructive Pulmonary Disease

ENaC: The epithelial sodium channel

FiO_2: The fraction of inspired oxygen (FiO_2)

HMGB1: High mobility group box 1 protein

ICUs: Intensive care units

IL: Interleukins

LPS: Lipopolysaccharide

MAPK: Mitogen-activated protein kinase

MMPs: Matrix metalloproteinase

Na K ATPase: Sodium–potassium pump

NFKB: Nuclear factor-kappa B

NIV: Non-invasive ventilation

PaO_2: The partial pressure of oxygen

PI3K: Phosphoinositide 3-kinase

pMLC: Phosphorylated Myosin Light Chain

PRRs: Pattern recognition receptors

RAGE: Receptor for advanced glycation end-products

Rho: Ras homologous proteins

ROCK: Rho Kinase

SP: Surfactant protein

sRAGE: soluble Receptor for advanced glycation end-products

TNF: Tumor necrosis factor

TLR: Toll-like receptor

TJ: Tight junctions

VILI: Ventilator-induced lung injury

ZO: Zonula occludens

Table of contents

1. Abstract

Acute respiratory distress syndrome (ARDS) is a major cause of respiratory failure with a high mortality rate.It is characterized by diffuse alveolar damage, alveolar edema, and hypoxemic respiratory loss which cause heavy healthcare costs. Currently available treatments for ARDS remain primarily supportive, and no pharmacological approach is successfully translated into clinical application. There are two major processes during the physiopathological development of ARDS which lead to the formation of lung edema: alveolar barrier dysfunction and the impairment of alveolar fluid clearance following alveolar epithelial injury and inflammation. The receptor for advanced glycation end products (RAGE) was indicated to be involved during those processes, with the high potential of its soluble as a biomarker for ARDS diagnostic and prognostic. Volatile halogenated agents, such as sevoflurane or isoflurane, are increasingly used in intensive care units as sedative agents with their ideal intrinsic characteristics as a sedative. Furthermore, numerous pre-clinical and clinical studies indicate its lung protective effects for ARDS patients. However, its mechanisms of such beneficial effects remain to be clarified.

The main objectives of this thesis work are multiple, through experimental and translational *in vivo* and *in vitro* models of ARDS, to **1**) Asses the beneficial lung protective effects of sevoflurane in ARDS, including its effects on ARDS physiological features, lung fluid clearance, and alveolar permeability. **2**) Investigate the precise mechanism of observed effects of sevoflurane, including mechanistic studies and involved proteins' function and expression. **3**) Explore the role of RAGE in lung epithelial injury and repair and its eventual mediation role of the beneficial effects of sevoflurane.

During this thesis work, we advanced from many angles: First, our work found in our A549 cells wound healing model, the important role of RAGE in the lung injury repair

process, as its ligand, HMGB1, and AGEs promoted RAGE-dependent wound healing of lung alveolar epithelial cells, which is possible through enhanced cell migration and proliferation. Secondly, our work in murine *in vitro* and *in vivo* ARDS models, an improvement of experimental features, with decreased indices of permeability and preserved epithelial structures in cells and mice, by at least in a part, increasing expression of ZO-1 and the inhibition of RhoA activity and pMLC as well as actin cytoskeleton rearrangement following lung epithelial injury. Additionally, RAGE may play a mediating role in the effects of sevoflurane on acute lung injury. Furthermore, our work in porcine *in vivo* ARDS models confirmed the lung protective effects of sevoflurane on ARDS features, with improved oxygenation, restored alveolar permeability, and improved AFC. Our study suggests the protective effect of sevoflurane on AFC may be explained by the restoration of impaired lung expression of epithelial channels AQP-5, Na, K, ATPase, and ENaC during ARDS.

Taken together, this thesis work explained more precisely the protective effects of halogenated agents and the new revelation of its potential mechanism, and hence supports the high interest in the use of inhaled sedation in intensive care for ARDS patients. This work may give some new insights for research on the effects of sevoflurane on ARDS and its resolution.

Keywords: Acute respiratory distress syndrome; Sevoflurane; Lung epithelial barrier function; Lung wound repair; Alveolar fluid clearance; Epithelial channels: Junction proteins; Intracellular pathways; Receptor for advanced glycation end-products.

2. Introduction

2.1 Acute Respiratory Distress Syndrome

2.1.1 Definition and epidemiology

The specific diagnostic criteria for Acute Respiratory Distress Syndrome (ARDS) have evolved since its discovery. In 1967, the first case report on ARDS described an acute onset of tachypnœa, hypoxæmia, loss of compliance, and diffuse alveolar infiltration seen on chest radiographs[1]. And in 1988, Murray and al. established the first ARDS 4-point scoring system with a quantitative assessment based on the degree of hypoxemia, the level of Positive end-expiratory pressure (PEEP), static respiratory compliance, and the extent of radiographic infiltrations[2]. Those first diagnostic criteria were then updated in 1994 by the American-European Consensus Conference (AECC Definition): arterial hypoxemia with Partial Pressure of Oxygen (PaO_2)/The fraction of inspired oxygen (FiO_2)ratio <300 mmHg and PaO_2/FiO_2 ratio < 200 mmHg to define Acute Lung Injury (ALI) and ARDS, with bilateral radiographic opacities without evidence of left atrial hypertension. These criteria were once more updated in 2012 by The Berlin Definition with better feasibility, reliability, and validity. This new definition is composed of 4 principal elements (Table 1): timing frame, chest imaging, the origin of edema, and oxygenation evaluation.

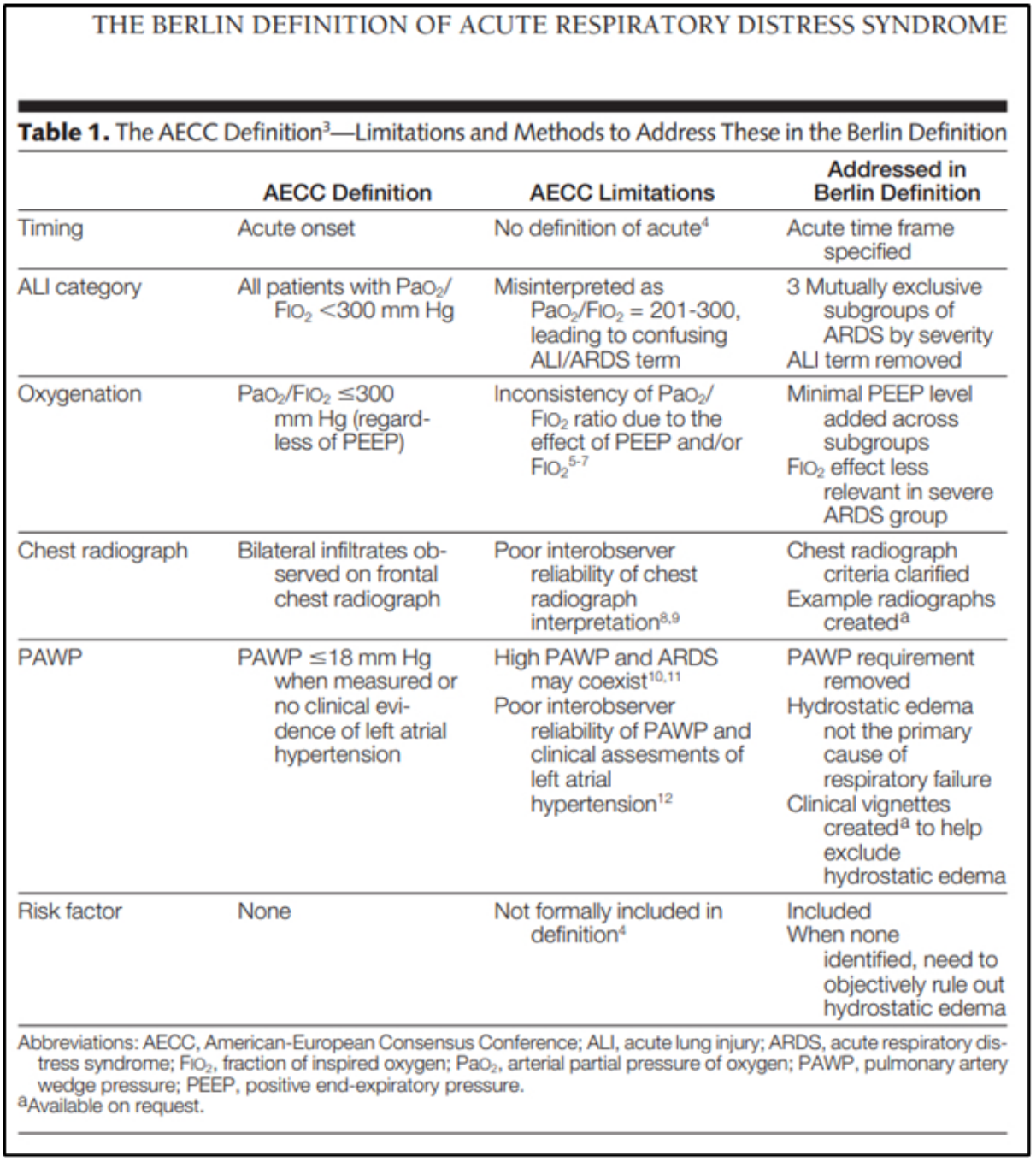

THE BERLIN DEFINITION OF ACUTE RESPIRATORY DISTRESS SYNDROME

Table 1. The AECC Definition[3]—Limitations and Methods to Address These in the Berlin Definition

	AECC Definition	AECC Limitations	Addressed in Berlin Definition
Timing	Acute onset	No definition of acute[4]	Acute time frame specified
ALI category	All patients with PaO_2/FIO_2 <300 mm Hg	Misinterpreted as PaO_2/FIO_2 = 201-300, leading to confusing ALI/ARDS term	3 Mutually exclusive subgroups of ARDS by severity ALI term removed
Oxygenation	PaO_2/FIO_2 ≤300 mm Hg (regardless of PEEP)	Inconsistency of PaO_2/FIO_2 ratio due to the effect of PEEP and/or FIO_2[5-7]	Minimal PEEP level added across subgroups FIO_2 effect less relevant in severe ARDS group
Chest radiograph	Bilateral infiltrates observed on frontal chest radiograph	Poor interobserver reliability of chest radiograph interpretation[8,9]	Chest radiograph criteria clarified Example radiographs created[a]
PAWP	PAWP ≤18 mm Hg when measured or no clinical evidence of left atrial hypertension	High PAWP and ARDS may coexist[10,11] Poor interobserver reliability of PAWP and clinical assesments of left atrial hypertension[12]	PAWP requirement removed Hydrostatic edema not the primary cause of respiratory failure Clinical vignettes created[a] to help exclude hydrostatic edema
Risk factor	None	Not formally included in definition[4]	Included When none identified, need to objectively rule out hydrostatic edema

Abbreviations: AECC, American-European Consensus Conference; ALI, acute lung injury; ARDS, acute respiratory distress syndrome; FIO_2, fraction of inspired oxygen; PaO_2, arterial partial pressure of oxygen; PAWP, pulmonary artery wedge pressure; PEEP, positive end-expiratory pressure.

[a]Available on request.

Table 1. **The limitations of AECC definition and the Berlin Definition**

Resource: ARDS Definition Task Force, Ranieri, V. M., Rubenfeld, G. D., Thompson, B. T., Ferguson, N. D., Caldwell, E., Fan, E., Camporota, L., & Slutsky, A. S. (2012). Acute respiratory distress syndrome: the Berlin Definition. *JAMA: The Journal of the American Medical Association*, *307*(23), 2526–2533.

For advancing under the background where limited information exists about the epidemiology, recognition, management, and outcomes of patients with acute respiratory distress syndrome (ARDS), an international, multicenter, prospective cohort study called LUNG SAFE was established in 50 countries in 2014. In this very large observational study, researchers have concluded a 10.4% prevalence among all 29144 intensive care units (ICUs) admissions with precisely 30.0% for mild ARDS (95% Confidence interval (CI), 28.2%-31.9%); 46.6% for moderate ARDS, 46.6% (95% CI, 44.5%-48.6%); and 23.4% for severe ARDS (95% CI, 21.7%-25.2%). This high prevalence was associated with a high hospital mortality rate, 34.9% (95% CI, 31.4%-38.5%) for those with mild, 40.3% (95% CI, 37.4%-43.3%) for those with moderate, and 46.1% (95% CI, 41.9%-50.4%) for those with severe ARDS. Nonetheless, in this study, ARDS was underdiagnosed and undertreated. Only 60.2% of all patients with ARDS were clinician-recognized and 34.0% of patients got the recognition of ARDS at the time of fulfilling ARDS criteria (95% CI, 32.0-36.0). Only fewer than two-thirds of patients with ARDS were treated with an optimal tidal volume[3].

ARDS could be triggered in different clinical situations, including pneumonia by bacterial, and viral causes which are the most common cause of ARDS, extrapulmonary sepsis, gastric fluid aspiration, transfusions, severe trauma, injurious mechanical ventilation, and/or reperfusion of ischemic tissues, among other causes[4] (Figure 1). Additionally, several risk factors have been associated with ARDS, including alcohol abuse, tobacco, air pollution, and hypoalbuminemia, studies have proved chronic alcohol abuse increases the risk of ARDS and multiple organ failure in septic shock, and cigarette smoke exposure has been proven associated independently with the risk of ARDS.

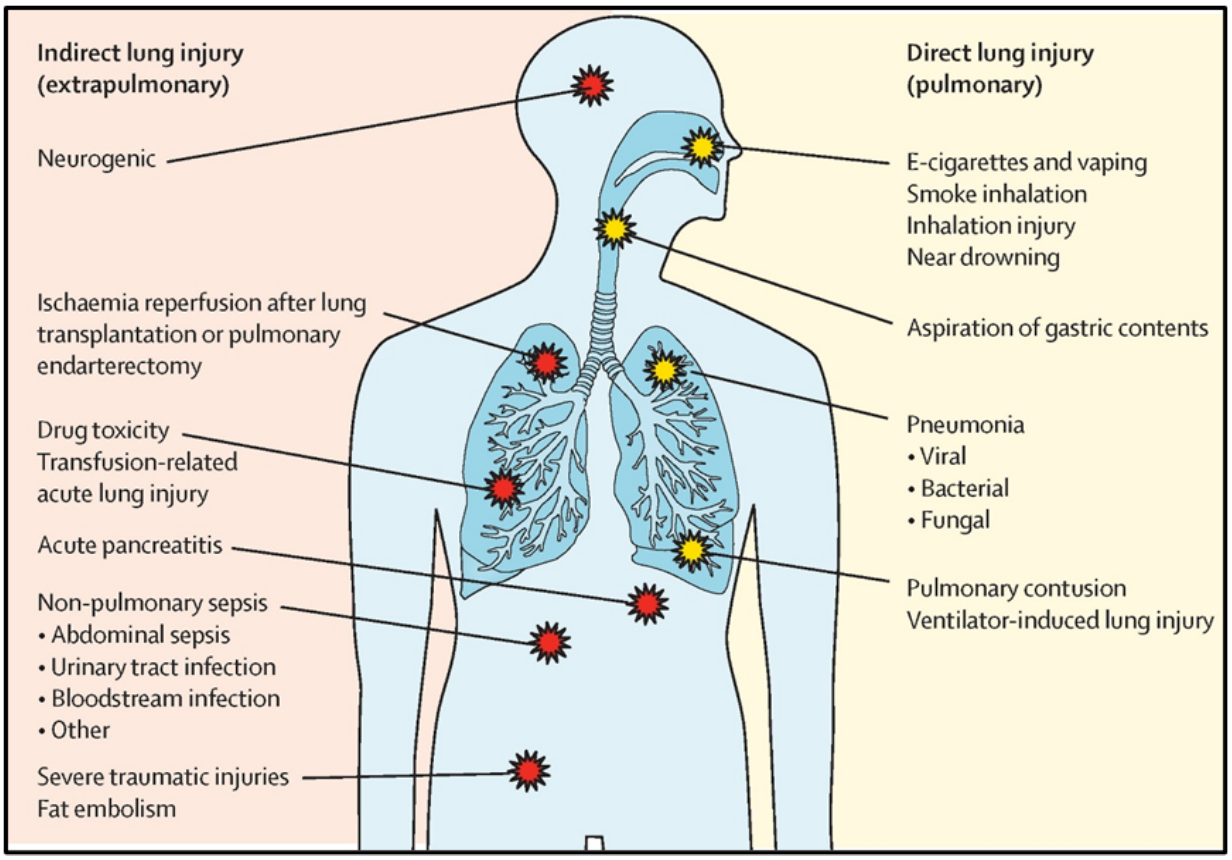

Figure 1. **Causes of acute respiratory distress syndrome**

A schematic summary of indirect and direct causes of ARDS

Resource: Bos, L. D. J., & Ware, L. B. (2022). Acute respiratory distress syndrome: causes, pathophysiology, and phenotypes. *The Lancet*, *400*(10358), 1145–1156.

In blunt and penetrating injury cases, the severity and duration of trauma, chest injury, the number of blood transfusions, the presence of traumatic brain injury, and the quantity of crystalloid fluids can each be a risk factor for developing ARDS[5].

2.1.2 Physiopathology of ARDS

In ARDS, an injury response is referred to as the exudative phase of ARDS within 24 hours of the inciting direct or indirect insult of the patient. This exudative phase is characterized by innate immune cell-mediated damage of the alveolar endothelial and epithelial barriers and the accumulation of protein-rich edema fluid within the interstitium and alveoli[4]: The presence of Damage-associated molecular pattern, e.g., High mobility group box 1 protein (HMGB1), or Pathogen Associated Molecular Pattern, e.g., lipopolysaccharide (LPS) in alveolus activates resident macrophages into highly inflammatory M1 macrophages, via the pattern recognition receptors, e.g., the receptor for advanced glycation end products (RAGE) or toll-like receptors (TLR). This activation leads to the release of potent proinflammatory mediators (e.g., interleukin (IL) -6, IL-17, Tumor necrosis factor (TNF)) and chemokines (e.g., IL-8, chemokine ligand (CCL)-2) which amplifies the inflammatory responses with neutrophil accumulation. This neutrophilic inflammation contributes then to acute lung injury in ARDS, leading to **1**) impaired barrier function notably the tight junction and adherens junctions injury with increased epithelial permeability[6] and **2**) Alveolar type II and type I pneumocyte aggressions with impaired surfactant secretion and also impaired alveolar clearance[7,8]. And at final a formation of protein-rich edema hence respiratory failure (Figure 2).

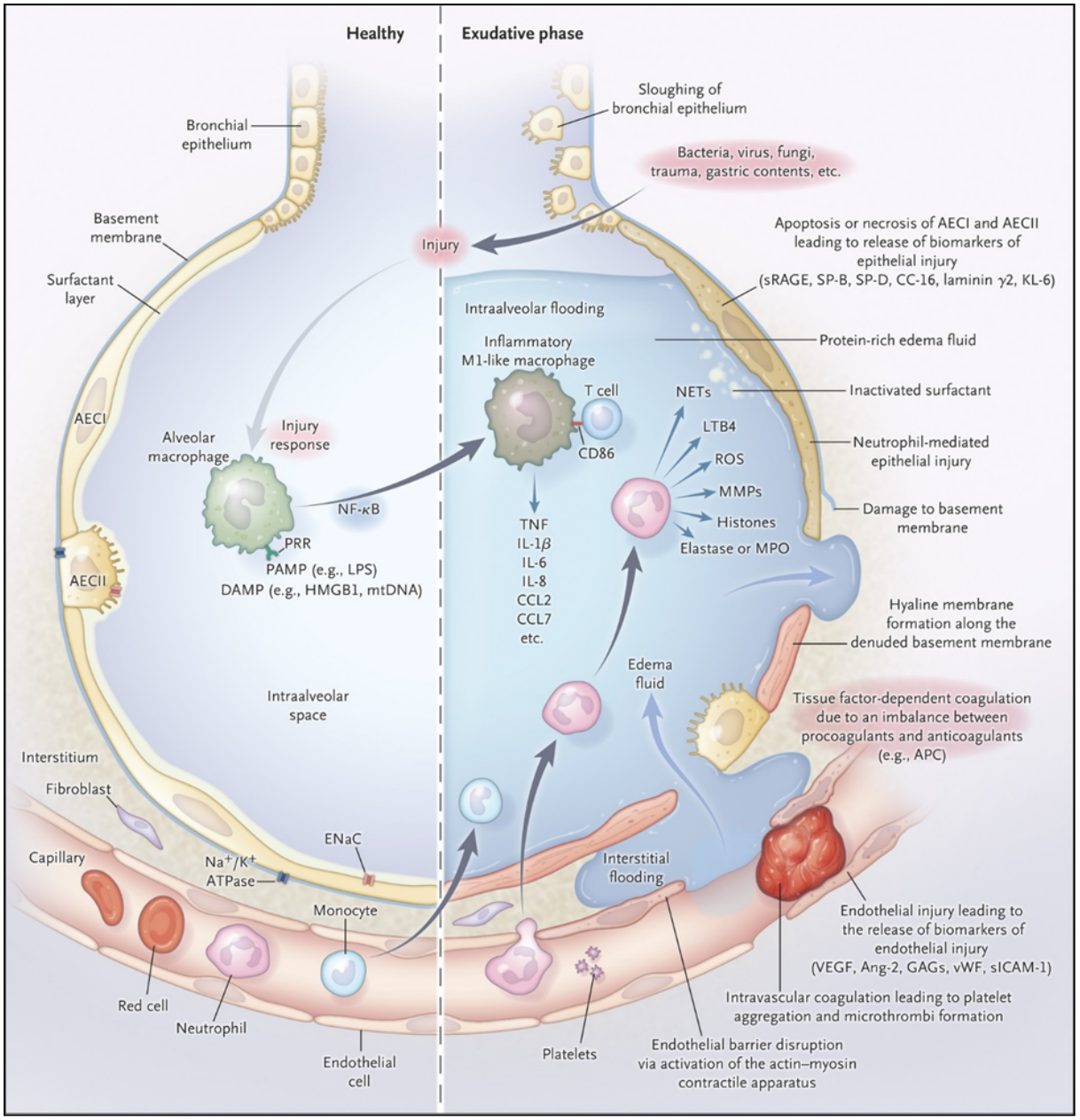

Figure 2. **The Healthy Lung and the Exudative Phase of ARDS.**

Left: the healthy alveolus. Right: the alveolus in the exudative phase during ARDS.

Following the aggression, macrophages are activated by secreting pro-inflammatory cytokines, causing epithelial damage. These lesions lead to the loss of the barrier function of the alveolar epithelium, to the formation of alveolar edema, to the alteration of alveolar fluid clearance, and therefore to impaired gas exchange.

Resource: Thompson, B. T., Chambers, R. C., & Liu, K. D. (2017). Acute Respiratory Distress Syndrome. *The New England Journal of Medicine*, *377*(19), 1904–1905.

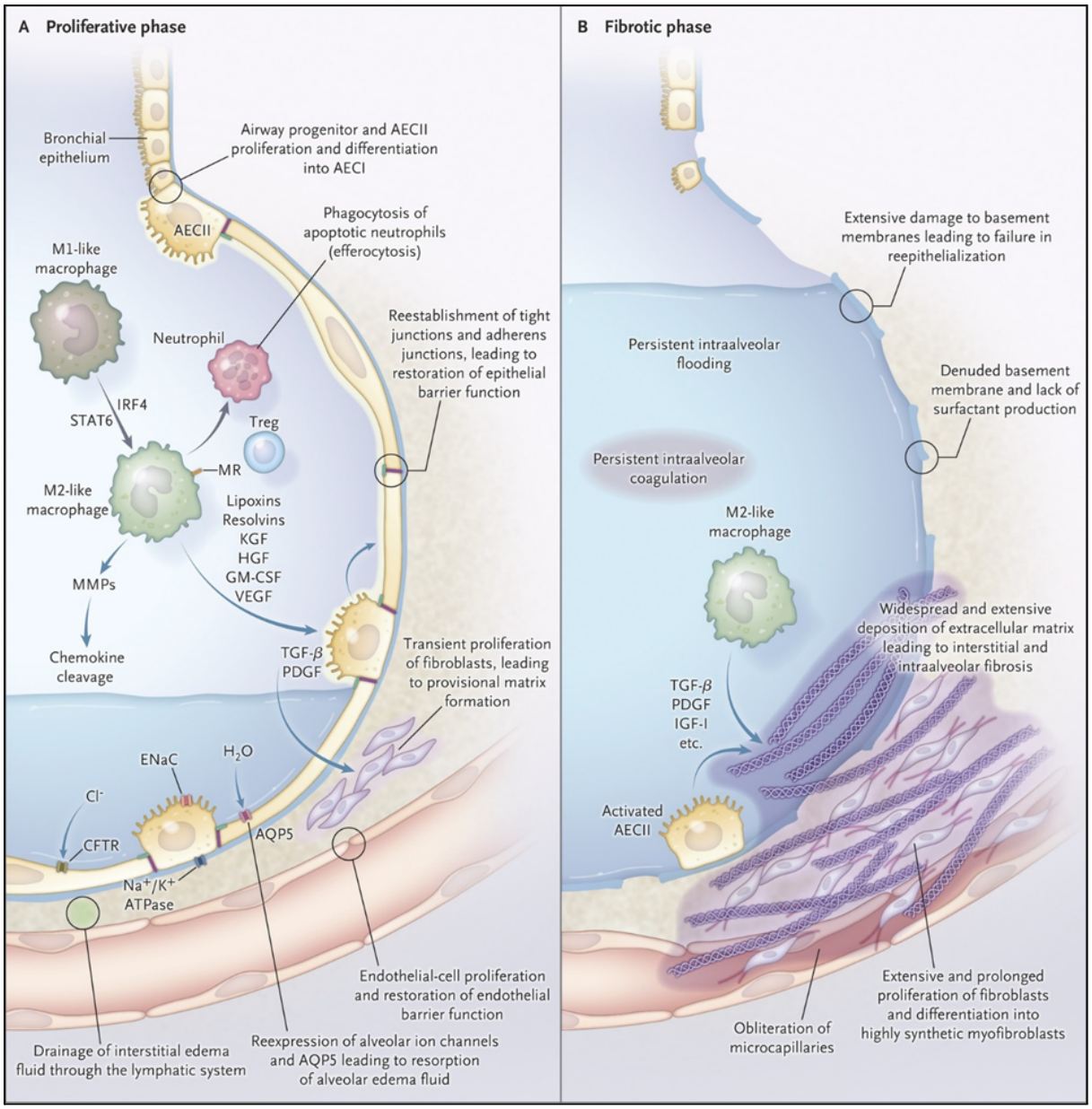

Figure 3. **The Proliferative and Fibrotic Phases of ARDS.**

Left: the alveolus in the proliferative phase during ARDS. Right: the alveolus in the fibrotic phase during ARDS.

Resource: Thompson, B. T., Chambers, R. C., & Liu, K. D. (2017). Acute Respiratory Distress Syndrome. *The New England Journal of Medicine*, *377*(19), 1904–1905.

This early phase of inflammation is followed by the proliferative phase (Figure 3), which is principally characterized by the proliferation of type 2 pneumocytes and its transdifferentiation to type 1 pneumocytes[9,10], re-establishment of tight junctions and adherens junctions in both epithelial and endothelial cells leading to restoration of epithelial and endothelial integrity, re-expression of epithelial ion channels and Aquaporin(AQP)-5 leading to the reabsorption of alveolar edema. This phase of restoration of alveolar structure and function could be followed by, in some instances, a fibrotic phase with persistent interalveolar coagulation, unsolved edema, and interstitial and interalveolar fibrosis, which is associated with increased mortality and prolonged mechanical ventilation days[4].

2.1.3 Current therapeutic strategy of ARDS

Before the beginning of this section, it is essential to point out that, to date, there are still no specific drugs or therapies which are capable of treating or directly preventing ARDS/ALI[11]. However, numerous supportive strategies allow for maintaining optimal management for patients including such as lower tidal volume ventilation, positive end-expiratory pressure (PEEP), and fluid management for ARDS[12,13], along with current discoveries on neuromuscular blockade [14] and prone positioning[15].

Most clinicians use invasive mechanical ventilation for patients with ARDS, particularly those with moderate or severe ARDS. Noninvasive ventilation (NIV) may reduce the work of breathing and increase the pulmonary shunt, thereby improving gas exchange while avoiding the need for deep sedation and reducing the risk of nosocomial pneumonia. Recently, a meta-analysis of 13 studies, including 540 patients with ARDS treated with NIV, showed an intubation rate varying between 30% and 86% and a mortality rate ranging from 15% to 71%[16]. However, its use remains controversial due to the high risk of failure and the possible risk of delaying tracheal intubation and invasive ventilation. The use of high PEEP

allows the reopening of non-ventilated alveoli and decreases the intrapulmonary shunt, which could make it possible to reduce the repetitive opening and closing of the alveoli with each respiratory cycle, the use of adjustment of optimal PEEP is also one important strategy to improve oxygenation[12,17]. The optimization of driving pressure is proven to be strongly associated with increased survival which may be involved in most cases of the mentioned respiratory intervention strategy[18]. However, the possible alveolar derecruitment, cyclic opening and closing of atelectatic alveoli, and distal small airways leading to ventilator-induced lung injury (VILI) if inadequate low positive end-expiratory pressure (PEEP) is applied. On the other hand, high PEEP levels may be associated with excessive lung parenchyma stress and strain and negative hemodynamic effects, resulting in systemic organ injury.

The purpose of mechanical ventilation is to guarantee sufficient gas exchange, allowing both an increase in arterial oxygenation (PaO_2) and the elimination of CO2, while reducing the activity of the respiratory muscles[19]. The effect of mechanical ventilation on oxygenation is bidirectional: it titrates the inspired fraction of oxygen (FiO_2); then, it makes it possible to provide, during the inspiratory phase, a positive pressure sufficient to ensure the opening of non- or poorly ventilated pulmonary units. However, these same lung units can collapse again without the application of a sufficient level of PEEP during the expiratory phase[20]. And unfortunately, a ventilatory strategy completely devoid of adverse effects does not exist, this strategy must be adapted to each patient based on hemodynamic status, gas exchange, alveolar recruit ability, and respiratory mechanics. The last years of literature have made it possible to better understand how the use of high tidal volumes and high levels of pressure can damage the lung[21,22]: ventilatory strategies based on the use of a high tidal volume can cause both developments of pulmonary edema in people without ARDS[23,24] and worsening of existing disease[25,26]. These effects are mainly attributable to alveolar

overdistension, which causes endothelial and epithelial damage, and then the activation of a pro-inflammatory cascade. This same pro-inflammatory cascade can also be promoted by lesions linked to the cyclic opening and reopening of the alveoli, called atelectotrauma[27,28]. The application of high levels of PEEP, allowing the reopening of unventilated alveoli and decreasing the intrapulmonary shunt, could decrease the repetitive opening and closing of the alveoli with each respiratory cycle[17]. Two large randomized controlled studies compared high levels of PEEP with lower levels[29,30], no advantage of one strategy over the other was found. could be highlighted in terms of becoming patients. This seemingly contradictory finding can be interpreted by considering the concept of lung recruitment, defined as the extent of collapsed lung regions to which aeration can be restored with increasing air pressure.

ARDS is a frequently involved syndrome in critical care, its management is also suitable for The **ABCDEF** bundle which includes: **A** as Assess, Prevent, and Manage Pain, **B** as Both Spontaneous Awakening Trials (SAT) and Spontaneous Breathing Trials (SBT), **C** as the Choice of analgesia and sedation, **D** as Delirium: Assess, Prevent, and Manage, **E** as Early mobility and Exercise, and **F** as Family engagement and empowerment[31]. Moreover, a current review indicates, the adaptation of this bundle in patients with ARDS should be adapted with an additional option "R" (R = Respiratory-drive-control). This additional option is suggested to be considered to take priority in the management of mechanical-ventilator and respiratory-drive related parameters, with the caution of avoiding the unnecessary use of medications (particularly opioids, sedatives, and neuromuscular blocking agents) which can delay ventilator liberation and worsen other patient's outcomes[32]. This evidence-based strategy bundle should also be helpful for optimizing ARDS patients' recovery and outcomes.

2.1.4 Phenotypes of ARDS: opportunity and challenges

The heterogeneity of ARDS is associated with distinct clinical, and biological differences, distinct outcomes which may explain the difficulty of recognition[33], and distinct responses of patients to therapy[34,35]. Additionally, in the current definition of ARDS, there is until today no specific etiological, physio-pathological, or biological criteria resulting in a clear understanding of the heterogeneity of patients. This heterogeneity also leads to inappropriate subsets identification of patients, which may at least partially explain a considerable number of negative trials on pharmacological agents, including β-agonists, corticosteroids, anticoagulants, statins, and surfactant treatment. Additionally, numeral benefit effects proven in preclinical studies were poorly translated from to clinical trials due to the limitations of those models associated with the heterogeneity of ARDS. Increasing literature indicates the identification of subphenotypes of ARDS, with prognostic and predictive enrichment, and is one approach to resolve the clinical and biological complexity that may be a key for further treatment studies.

Although the "subtypes" of ARDS have long been recognized by practitioners, the concept of phenotype or endotype has emerged much more recently[36]. The largest challenge in phenotyping ARDS is the lack of a simple diagnostic test, resulting in the reliance on a consensus definition developed by experts. The discovery, or rather the recognition of these ARDS subtypes makes it possible to consider the evaluation of targeted therapies according to the pathophysiological mechanisms involved in a given patient, which would represent a major advance for the application of future personalized medicine[37].

Recent reviews suggested that the heterogeneity of ARDS may be based on 3 main categories of information: the etiology of ARDS, the physio-pathological mechanistic, and the biology (Figure 4) which will make it possible to propose different phenotypes of ARDS.

An example of an ARDS phenotype is the hypo- or hyper-inflammatory profile of patients with the syndrome[34]. These profile differences could be retrospectively highlighted for the first time in a series of studies by applying the principle of latent class analysis which consists of combining different biological and clinical parameters to identify subgroups (or phenotypes) of patients[38–40]. Analyzing about forty parameters, it was possible to highlight a hyper-inflammatory profile characterized by exaggerated inflammation with high plasma concentrations of sTFNR, Il-6 or 8, RAGE, protein C, and bicarbonate. The hyper-inflammatory profile was associated with increased mortality compared to the hypo-inflammatory profile[38,39]. It is interesting to note that these profiles seem stable over time and are also suitably generalizable to observational studies[41–43]. And when these profiles are retrospectively applied to large cohorts of randomized controlled trials, different effects of the treatment studied appear between the hyper- and hypo-inflammatory profiles while the result was considered negative[38,39,44–46].

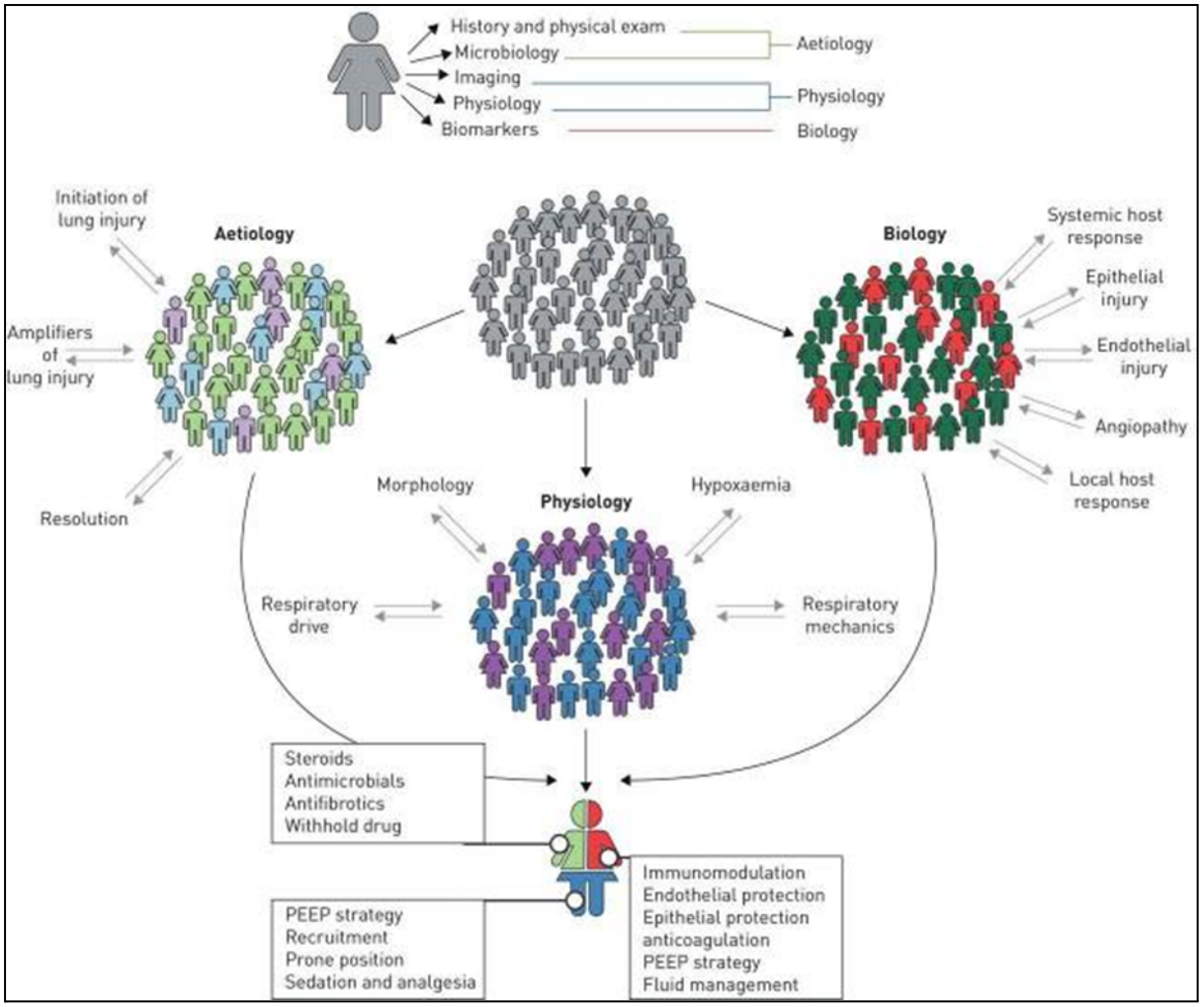

Figure 4. **Principal domains of information for ARDS phenotypes**

ARDS patients profile can be phenotyped in three domains: Etiology profile, Physiology profile and Biology profile.

Resource: Thompson, B. T., Chambers, R. C., & Liu, K. D. (2017). Acute Respiratory Distress Syndrome. *The New England Journal of Medicine*, *377*(19), 1904–1905.

Faced with the challenging situation under numerous negative results of the latest clinical trials and thanks to this notion of ARDS phenotype, it seems the personalized medicine strategy, with the adapted therapeutic approach based on the data of a given group of patients having the same phenotype, has been more than more considered. The application of this principle in recent years in the field of hematology or in respiratory pathologies other than ARDS such as asthma or Chronic Obstructive Pulmonary Disease (COPD) has made it possible to improve the understanding of the physio-pathological mechanisms involved and to improve and offer patients specific therapeutic care[47]. These promising data can be applied to ARDS in order to offer personalized medicine. Nevertheless, certain specificities must be taken into account due to the complexity of the mechanisms involved during ARDS due to the rapid evolution of ARDS which requires practitioners to adapt their treatment, sometimes very early. It is therefore essential to define, among patients with ARDS, clinical and biological criteria (with the help of biomarkers) to distinguish between the existing different ARDS phenotypes[47].

The identification of phenotypes or endotypes of patients necessitates the use of specific biomarkers. Determining how biomarker-derived approaches should be integrated to guide future ARDS research remains a major challenge, and it is suggested that [48] :

- Biological tests could be useful to identify patients with any of the following predominant biological patterns of lung injury and repair in ARDS: epithelial injury, endothelial dysfunction, and systemic inflammatory response.
- Inclusive and collaborative biobanks of samples typically require hundreds of samples to allow the identification of phenotypes and should reflect the diversity within patients with ARDS.

- Longitudinal sampling could provide additional insights into biological dynamics and treatment responses over time.

Future clinical trials should be taking into consideration all those phenotypes and heterogeneities, in the hope to find an effective therapeutic strategy and to offer patients individualized medicine[49–51].

2.2 Halogenated agents in ARDS

2.2.1 Sedative agents in intensive care

Sedation is used in intensive care to improve comfort and tolerance, such as during mechanical ventilation, invasive interventions, and/or nursing care[52]. Current sedation practices in intensive care still make strong use of benzodiazepines as well as propofol and/or ketamine, these molecules being most often associated with opioids to have a synergistic action.

Benzodiazepines are a class of drugs well-known for intensive care. However, in recent years, numerous data underline the harmful consequences of prolonged and high-dose use of benzodiazepines[53], which would be linked to delayed awakening related to the long hepatic metabolism cycle. These excesses of sedation are associated in the short term with an increase in tolerance to hypnotics, the incidence of withdrawal syndromes, and also delirium. And by long term with the appearance of cognitive disorders such as depression, anxiety, or even post-traumatic stress. Propofol, another widely used anesthetic agent, also induces certain adverse effects impacting the outcome of patients. In addition to a higher cost compared to benzodiazepines, propofol induces significant hemodynamic variations, an increase in plasma triglyceride concentrations, or even the appearance of a propofol infusion syndrome[54].

With the widespread use of benzodiazepines and propofol, their respective effects are now better described and better known than before, prompting practitioners to develop alternative sedation strategies. In addition, the recent pandemic linked to the SARS-COV-2 virus has highlighted the possibility of a shortage in the supply of drugs conventionally used to sedate patients in intensive care, leading to a new complexity in the management of intravenous sedation[55]. Apart from certain specific situations, it is now accepted that patients

should no longer have so-called “deep” sedation in favor of so-called “light” sedation, leaving the patient the possibility of interacting with the environment and with caregivers. Besides the choice of the applied molecule, the prognosis of patients is impacted by a global sedation strategy, starting with the systematic questioning of its indication by clinicians.

2.2.2 Halogenated agents and inhaled sedation in intensive care

Halogenated agents are molecules with a carbon skeleton and several halogen atoms (chlorine, fluorine, or bromine), the most used halogenated agents clinically in France are sevoflurane, isoflurane and desflurane (Figure 5). The physical characteristics of halogenated agents have major implications for their use in clinical practice and the solubility of gases in plasma is inversely correlated to their rapid onset and offset of action. Thus, an anesthetic gas with low solubility in plasma will allow rapid induction of narcosis and be rapidly eliminated after interruption of its administration, leading to rapid awakening. The gas/blood partition coefficient is, therefore, the most decisive criterion for the rapidity of the action of the gas and patient awakening. These characteristics, which are suitable for the use of halogenated agents in the operating room, remain suitable as well in the ICU setting. Halogenated agents are liquid at room pressure and temperature (except desflurane), and must, therefore, be transformed into breathable vapor by vaporizers dedicated to each gas, depending on their boiling temperatures.

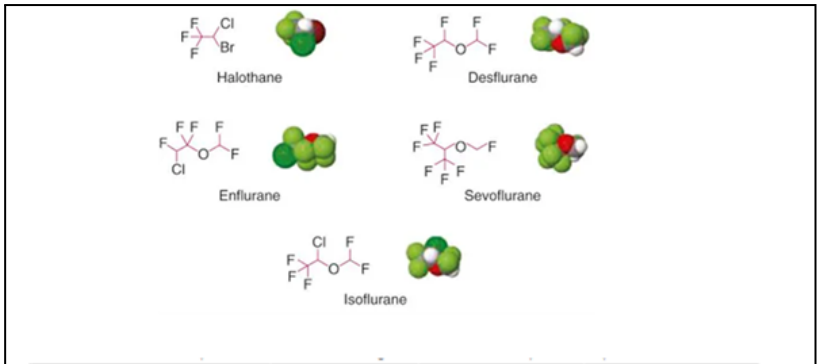

Parameters	Iso vs Des	Iso vs Sevo	Sevo vs Des
Time to opening eyes		2,4 (1,8 ; 2,9)* S	1,4 (-0,1 ; 2,9)
Time to obey commands	4,6 (1,1 ; 8,2)* D	2,4 (1,8 ; 2,9)* S	2,7 (1,2 ; 4,1)* D
Time to home ready	6,4 (-8,7 ; 21,5)	5,1 (2,8 ; 7,4)* S	2,0 (-16 ; 12)
Time to home discharge		25 (0,4 ; 50)* S	2,1 (-18 ; 13)

Figure 5. **Principal halogenated agents and an anesthetic parameter comparison between Isoflurane/Sevoflurane/Desflurane**

Resource: Gupta, A., Stierer, T., Zuckerman, R., Sakima, N., Parker, S. D., & Fleisher, L. A. (2004). Comparison of recovery profile after ambulatory anesthesia with propofol, isoflurane, sevoflurane and desflurane: a systematic review. *Anesthesia and Analgesia*, *98*(3), 632–641, table of contents.

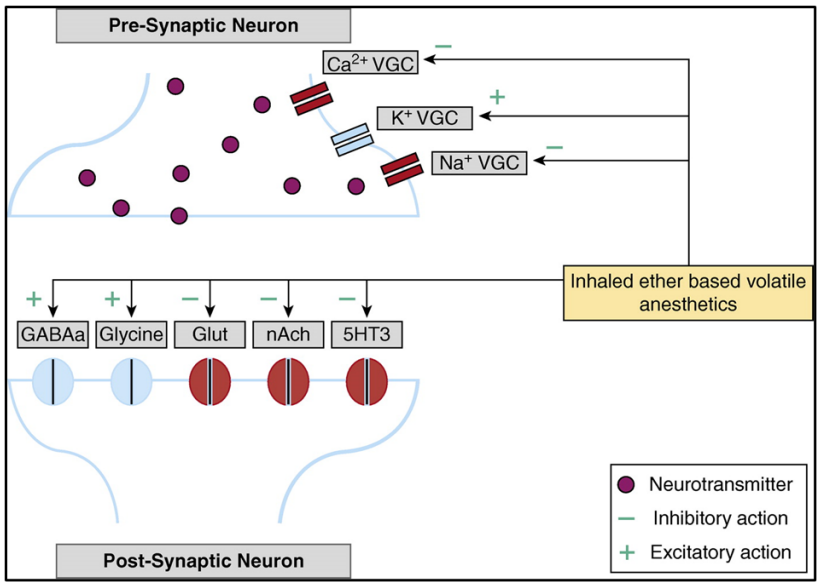

Figure 6. **The modern theory of volatile anesthetic activity involves complex interaction with multiple proteins on the pre- and postsynaptic nerve membrane as well as nonneural tissue.**

Resource: Jerath, A., Parotto, M., Wasowicz, M., & Ferguson, N. D. (2016). Volatile Anesthetics. Is a New Player Emerging in Critical Care Sedation? *American Journal of Respiratory and Critical Care Medicine*, *193*(11), 1202–1212

In general, the action of halogenated agents involves complex mechanisms via interactions with membrane proteins at the pre-and post-synaptic levels, both in nervous tissues and other types of tissue. Overall, volatile halogenated agents reduce presynaptic excitation and neurotransmitter release through the inhibition of sodium and calcium voltage-gated channels (VGCs) and induce depolarization through the activation of potassium channels. Volatile anesthetics reduce neurotransmitter activity in the postsynaptic membrane by enhancing inhibitory ion channel activity mediated by γ-aminobutyric acid (GABAa) and glycine receptors as well as inhibiting excitatory ion channels mediated by nicotinic acetylcholine (nAch), serotonin type 3 (5HT3), glutamate (glut), N-methyl-d-aspartate, and α-amino-3-hydroxy-5-methyl-4-isoxazole propionic acid receptors. Volatile anesthetics are also likely to possess widespread effects on G-protein–coupled receptors and intracellular signaling pathways on the nerve and other cell types[56,57] (Figure 6). Of note, halogenated agents have a bronchodilator effect through direct action on the bronchial smooth muscle and inhibition of the transmission of the vagal impulse at the level of the postganglionic fiber. They also inhibit the hypoxic pulmonary vasoconstriction response in a dose-related manner.

One of the typical characteristics of halogenated agents is their rapid reaction on patients: fast-onset (1–2 min) and fast-offset (4–7 min) drugs with moderate analgesic effects that induce a dose-dependent reduction in respiratory drive and allow light-to-deep sedation targets. Thus, their use for inhaled sedation can fit into an analgesia-first strategy for minimizing sedation within the "ABCDEF" bundle in ARDS management. End-tidal gas fractions are good surrogates of cerebral concentrations of the drugs and, although sedation should first be adapted using validated clinical scores[58], monitoring such end-tidal gas fractions could represent an efficient way of titrating sedation to a patient's needs (usual range of 0.2–1.4%)[59,60]. Importantly, halogenated agents undergo pulmonary elimination and

have a low level of hepatic metabolism (metabolism rate of 2–5% for sevoflurane, 0.2% for isoflurane, and 0.02% for desflurane), without the production of active metabolites (fluorine ions) or alteration in hepatic/renal lab tests in patients[57].

Thanks to the improvement of devices for delivering halogenated agents in intensive care, inhaled sedation has been more widely used, in particular by overcoming several technical constraints; more than 230 million patients undergoing major surgery each year require general anesthesia and mechanical ventilation[61]. The miniaturization of halogen administration devices such as the Sedaconda-ACD (Sedana Medical, Uppsala, Sweden), or the MIRUS system (Carelide, Mouvaux, France) have notably become compatible with resuscitation ventilators[57]. Nevertheless, the use of inhaled sedation remains dependent on the availability of these materials within the units.

2.2.3. Halogenated agents: benefits and limitations in intensive care

Specific prospective data regarding the use of inhaled sedation in the intensive care unit (ICU) to prevent or treat lung injury is lacking[57,62]. However, a retrospective analysis of patients receiving inhaled sedation suggests an association between its use and reductions in 1-year and in-hospital mortality, perhaps related to a significant increase in ventilator-free days compared to intravenous sedation[63]. Numerous trials now support the efficacy and safety of inhaled sevoflurane for the sedation of ICU patients[64–66], and sevoflurane is associated with shorter wake-up and extubation times[67]. As the use of volatile agents gains popularity in the ICU setting, evidence suggesting that sevoflurane may also protect against inflammatory lung injury may provide insight into the potential additional benefit these agents can offer for the lung-injured patient. Preclinical studies have shown that inhaled sevoflurane improves gas exchange[68–70], reduces alveolar edema[70], and attenuates pulmonary and systemic

inflammation[71–73] in experimental models of ARDS. Isoflurane also showed lung protective effects after injury by maintaining the integrity of the alveolar–capillary barrier, possibly by modulating the expression of a key tight junction protein[74–76]. However, further studies are needed to verify to what extent the experimental evidence of organ protection from inhaled sevoflurane could be translated to humans. Of note, a pilot single-center randomized controlled trial (RCT) from our group found that early use of inhaled sevoflurane in patients with ARDS was associated with improved oxygenation, reduced levels of some pro-inflammatory markers and reduced lung epithelial injury, as assessed by plasma and alveolar sRAGE, the soluble receptor for advanced glycation end-products[77].

2.3 Receptor for advanced glycation end products (RAGE)

2.3.1 RAGE and RAGE ligands

The receptor for advanced glycation end-products (RAGE) is a transmembrane receptor belonging to the immunoglobulin superfamily. It has been described as a receptor recognizing pro-inflammatory molecular patterns and thus belongs to the group of pattern-recognition receptors (PRRs). This protein, of approximately 46 kDa, comprises 3 major domains: an extracellular domain (itself subdivided into domains V, C1, C2) allowing the attachment of various ligands, a transmembrane domain and a cytoplasmic part essential for signal transduction. The N-terminal domain has a signal peptide at its end and is morphologically comparable to the variable domains of the Ig. The V-C1 duo forms an interdependent functional unit characterized by the presence of many positive electrical charges, while the C2 domain, autonomous and attached to V-C1 via a flexible 5 aa link, is electrically negatively charged[78](Figure 7). Associated with the transmembrane part, the intracellular domain is an essential part of the signaling pathways involving the RAGE pathway[79]. In addition to the full-length, transmembrane form of RAGE, there are also truncated variants of the membrane receptor and several soluble isoforms, generally grouped together in the literature as soluble RAGE (sRAGE) and which can be produced by proteolytic cleavage of the part extra-cellular form by proteases from the matrix metalloproteinases (MMPs) family[80,81] or by alternative splicing (esRAGE, for endogenous secretory RAGE)[82].

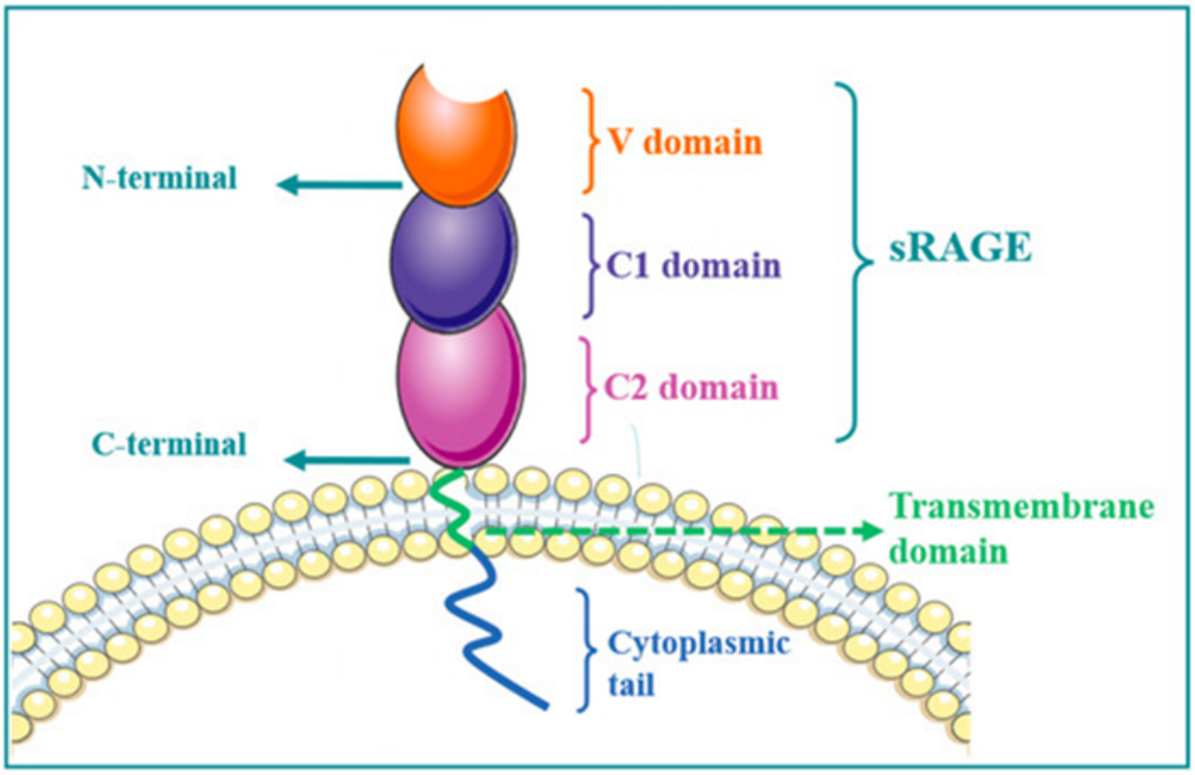

Figure 7. **Structral organization of RAGE**

Resource: Yue, Q.; Song, Y.; Liu, Z.; Zhang, L.; Yang, L.; Li, J. Receptor for Advanced Glycation End Products (RAGE): A Pivotal Hub in Immune Diseases. Molecules 2022, 27, 4922. https://doi.org/10.3390/molecules27154922

In parallel with the complete form of RAGE, the RAGE protein is subject to alternative splicing phenomena resulting in the production of numerous transcript variants with distinct functionalities such as antagonistic soluble forms or variants with altered extracellular domains. In descending order the main isoforms of RAGE are: the complete form of RAGE (mRAGE), a secreted form of RAGE v1 (esRAGE) and an N-terminal truncated form (Nt-RAGE). However, other isoforms of RAGE exist and come from mechanisms other than alternative splicings, such as mechanisms involving metalloprotease 10 (ADAM-10) or extracellular matrix metalloprotease type 9 (MMP-9)[83–85]. The soluble form of RAGE can act as a decoy, diverting RAGE ligands thus preventing them from binding to a functional form of RAGE. The precise role of the soluble form of RAGE has yet

to be clearly elucidated to date. Concentrations of the soluble form of RAGE are inversely correlated with RAGE activity, but the precise mechanisms of regulation remain unknown. Some hypotheses tend to believe that the production of soluble forms of RAGE could be regulated by a negative feedback loop triggered by the activation of RAGE itself to avoid self-activation during pathological situations producing ligands of rage. These soluble forms of RAGE are also found both in plasma and in other fluids such as the alveolar fluid of patients with lung damage. However, the mechanisms allowing the passage of soluble forms of RAGE from the lungs into the bloodstream remains to this day completely unknown.

As described in its name, RAGE was first identified as an advanced glycation end-products (AGEs) receptor. AGEs are compounds resulting from the Maillard reaction, a non-enzymatic glyco-oxidative reaction[86]. However, several other molecules belonging to the category of DAMPs (also called alarmins or endogenous danger signals) can bind to RAGE, such as amphoteric (HMGB1, for high–mobility group box 1 protein), S100 proteins, β-amyloid fibrils[87–89]). In addition to advanced glycation end-products (AGEs), many additional ligands have been described[90–103]. Among many other ligands, RAGE interacts with *β*-amyloid proteins[92,93] and amyloid protein A[94]. RAGE can also bind proteins of the S100/calgranulin family, a family of proteins that accumulate extracellularly during chronic inflammation phenomena[95,96]. Another pro-inflammatory RAGE ligand described is the HMGB1 protein (amphoterin) which is released by necrotizing cells[97–100]. In parallel with these ligands involved in the phenomena of chronic inflammation, degenerative pathologies and immune response[100], RAGE can also interact directly with the surface proteins of bacteria[101], prions[102] or leukocytes[103]. RAGE can be defined as a pattern-recognition receptor (PRR)[91,103–105] and shares similarities with toll-like receptors (TLR)[106]. It has to be mentioned that there are receptors other than RAGE capable of binding AGEs, such as macrophage scavenger receptor (SR), oligosaccharyltransferase-48（OST-48）, 80 K-H phosphoprotein

(80 K-H), galectin-3, lectine-like oxidized low density lipoprotein, fasciclin EGF-like receptors, laminin-type EGF-like receptors, or domain -containing scavenger 1/2[107] and CD36[108]. Faced with these diversities of receptors and ligands, the mechanisms that can explain why and how a ligand will bind to a specific type of receptor and/or in a specific tissue of the body remain little studied til today. However, it is recognized that the association between AGEs and its receptors is involved in the mechanisms of endocytosis and degradation of AGEs in parallel with the signal transduction activity of the RAGE receptor itself.

2.3.2 RAGE principal signaling pathway

The great diversity of the repertoire of potential ligands explains, at least in part, the ability of RAGE to activate numerous signaling pathways that regulate a number of physiological and pathological processes such as proliferation, apoptosis, autophagy and cell inflammation[109] (Figure 8). Indeed, and schematically, the activation of RAGE by its ligands induces the pro-inflammatory signaling pathways NF-κB, MAP kinase and PI3 Kinase, resulting in the secretion of pro-inflammatory cytokines. Moreover, the activation of NF-κB by the RAGE pathway results in positive feedback that increases the expression of RAGE itself, and results in an intense and sustained inflammatory signal, bring into play an intracellular signaling cascade which is a first line of cellular defense of organism[89,110]. Secondary to the activation of RAGE, IκBα is rapidly degraded after having been phosphorylated, and this removal of inhibition allows the translocation of NF-κB into the nucleus. NF-κB then binds to specific DNA sequences activating the transcription of many NF-κB-dependent genes such as genes coding for cytokines, adhesion molecules, prothrombotic and vasoconstrictive proteins, but also RAGE itself. same. A large number of genes coding for anti-apoptotic factors such as B-cell lymphoma (Bcl)-XL, Bcl-2, and the

Bcl-2 homolog A1 are dependent on NF-κB[111–113]. NF-κB is also involved in cell survival maintenance mechanisms. The long-term maintenance of the long-lasting endogenous negative feedback loop appears to be specific to the activation of the RAGE-NF-κB axis. RAGE activates NF-κB by degrading IκBα to IκBβ, which will allow the synthesis of NF-κBp65 with IκBβ[110]. *De novo* transcription of p65 mRNAs leads to excess production of the NF-κBp65 complex, greater than the formation of IκBβ necessary to maintain the NF-κBp65 complex in the cytoplasm. In addition, a mechanism of hyperphosphorylation of IκBβ has been shown in parallel, sequestering at the nuclear level the NF-κB which has just been synthesized[114,115]. The synthesis itself of IκBβ has a role in promoting the activation of NF-κB via the RAGE-NF-κB axis[110]. The expression of RAGE is induced by NF-κB[112], and therefore the prolonged activation of NF-κB induces the production of the RAGE receptor, a cycle that allowing the maintenance and amplification of the RAGE-NF-κB axis signal.

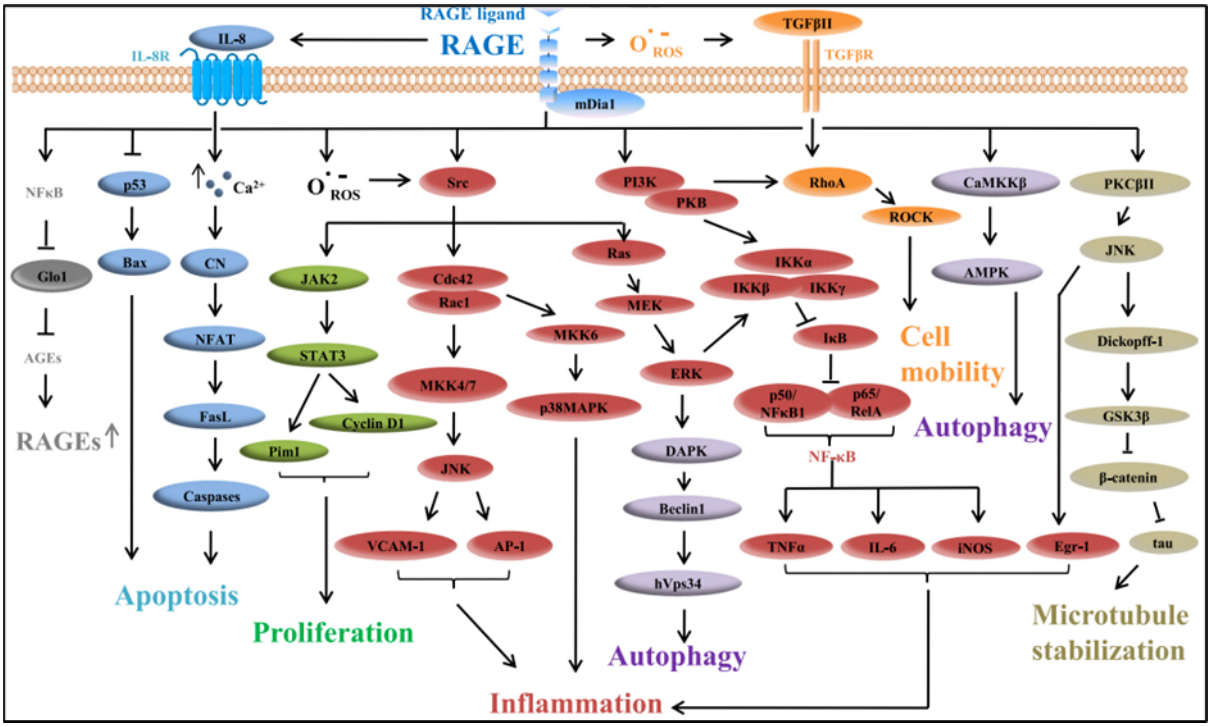

Figure 8. **Visual summary of RAGE-Dependent signaling pathways**

Resource: Xie, J., Méndez, J. D., Méndez-Valenzuela, V., & Aguilar-Hernández, M. M. (2013). Cellular signaling of the receptor for advanced glycation end products (RAGE). Cellular Signaling, 25(11), 2185–2197.

The role of RAGE in cell migration has been described in various cell types (immune cells, astrocytes, vascular smooth muscle cells, endothelial cells, chondrocytes, mesangial cells, microglia), for example, Manfredi et al. demonstrated that the expression of RAGE was essential for the migration of dendritic cells to the lymph nodes[116]. Some experimental data have shown, for example, that the interaction of RAGE with HMGB1 leads to the activation of Rac1/Cdc42, MAPK, PI3K/Akt pathways, leading to migratory processes and even tumor growth and metastasis under pathological conditions[117–120]. The binding of AGEs at RAGE stimulates, among other things, migration phenomena involved in carcinogenesis through the ERK1/2 pathway, or in the healing process of keratocytes through the NFκB pathway, as does the S100A4/RAGE/ERK axis, which is involved in colorectal cancer. described[121–123]). However, the reverse effect of RAGE has been also observed in myoblasts, where inactivation of RAGE increases proliferation and promotes tumor formation in vivo, while expression of RAGE reduces migration during rhabdomyosarcoma, a malignant muscle tumor[124,125].

On cell survival, interestingly, RAGE exhibits dichotomous effects between apoptosis and survival depending on various parameters. It has been shown that doses of the order of nM of S100β stimulate the expression of the anti-apoptotic protein Bcl-2 and therefore the cell survival of neuroblastomas and gliomas but conversely, higher doses of S100β (μM) induce apoptosis[126,127]. Furthermore, totally reduced form of HMGB1 induces the survival and proliferation of cancer cells by inducing the Beclin-1 protein, while the oxidized form is responsible for apoptosis (via the activation of caspases 3 and 9) and necrosis.[128,129]. As for AGEs, studies have demonstrated their proapoptotic effect through the stimulation of TGFβ within osteocytes[130].

The activation of RAGE can induce the generation of reactive oxygen species (ROS) via in particular the enzymatic complex NADPH[131,132].

As we can conclude in what we have discussed just in the above paragraphs, most RAGE ligands are involved in inflammation and cell migration, and proliferation mechanisms. In fact, the basal expression of RAGE, which is low under physiological conditions, will be strongly increased in response to an inflammatory process[133]. Most RAGE ligands are secreted by immune cells such as monocytes, macrophages, neutrophils or leukocytes[133]. Surprisingly, while many receptors self-regulate negatively with increasing concentration of their respective ligands, activating RAGE by its ligands increases the expression of the receptor itself[112,134]. Upon activation of the RAGE receptor, the transcription factor NF-κB is translocated at the nuclear level and binds at the level to the promoter of the RAGE gene which induces the transcription of the messenger RNA of RAGE[112]. In parallel, NF-κB also binds to the glyoxalase I(Glo1) promoter region, which will inhibit its transcription. The Glo1 protein is involved in the inactivation of AGE precursors by catalyzing the transformation of lactate and therefore decreasing the production of AGEs. Thus, the activation of RAGE itself increases the formation of AGEs by suppressing Glo1 expression[134]. An abnormally high expression and activation of RAGE, and therefore an exaggerated immune and inflammatory response, are implicated in the development of numerous human pathologies such as diabetes, cardiovascular pathologies, tumor pathologies, or Alzheimer's disease[134].

2.3.3 RAGE and ARDS

In a pathological situation, the lung is directly exposed to many external pathogens, external antigens, and danger signals or also called alarmins. The mechanisms of innate immunity involve a large number of PRRs such as RAGE or TLR receptors in order to recognize danger signals such as molecular patterns associated with pathogens or damage-associated molecular patterns[135]. It is also important to point out, at the beginning of this section, that both transmembrane full-length and soluble form of RAGE is abundantly expressed in the lung tissue[81,136–140]. In the early 2000s, Schmidt et al. built the first theory about a "two-hit" mechanism in the inflammatory cascade and RAGE may be importantly involved in this process[91,141]. In this theory, the first hit would be the activation of RAGE by its ligands and the second hit of this cellular disruption would reflect the excess accumulation of pathogenic bacteria, pro-inflammatory stimuli, modified molecules, ischemic damage, and other factors as well. During infection, innate immunity is activated by PAMPs expressed within the infecting microorganisms. This results in the expression of pro-inflammatory cytokines and chemokines ultimately leading to inflammatory processes and tissue damage. These mechanisms are generally encountered during pathologies such as diabetes, neurodegenerative diseases, arteriosclerosis, or even autoimmune diseases[91,142,143]. During ARDS, the immune system will be activated by PAMPs from external pathogens and by DAMPs linked to cell death or from the activation of immune cells and the degradation of the cell matrix[144,145].

It should also be noted that soluble forms of RAGE can act as a "decoy" by binding to ligands and preventing the interaction of these ligands with the transmembrane form of RAGE. In this context, the RAGE pathway seems to be under the control of complex

regulatory pathways, and these effects are most likely dependent on a balance, or an imbalance, between the accumulation of RAGE ligands, the expression of its form complete membrane and its soluble forms[146,147]. This soluble form of RAGE was first proven as a marker of epithelial damage specific to type 1 pneumocyte and also a mediator of inflammation in 2004 by Shirasawa et al.[148]. Later in the decade, the first studies to determine the role of RAGE in lung injury were conducted in 2006 by Uchida et al.[149] in which a rapid rise in serum and bronchoalveolar lavage fluid(BALF) concentrations was found after pulmonary insult by hydrochloric acid in a mouse model. Intratracheal administration of lipopolysaccharide(LPS) in mice is also associated with an elevation of sRAGE in BALF[150]. Su et al. proved in different factor-triggered ARDS experimental models the role of RAGE as a direct indicator of lung injury the elevation of excess lung water and pulmonary vascular permeability index were shown to be associated with the elevation of sRAGE concentrations in BALF[151]. Recently, two studies of our research team proved, in a mouse model of direct epithelial injury by lung instillation of hydrochloric acid, RAGE inhibition was associated with improved alveolar fluid clearance function and restoration of expression of the epithelial channel Aquaporin-5[152], and in a piglet model where comparable data in terms of improvement in pulmonary function were found as the administration of a RAGE inhibitor was associated with an improvement in oxygenation and a reduction in the level of pulmonary lesions[153]. These experimental data highlighted the prominent role of sRAGE as a marker of type 1 pneumocyte injury and that sRAGE is correlated with the severity of ARDS.

In a clinical vision, the biggest value digging recently on sRAGE must be the application of sRAGE as a biomarker in order to help in diagnostic approaches, risk stratification and identification of potential therapeutic targets, in particular by providing valuable assistance for the characterization of the physio-pathological mechanisms involved in ARDS, due to its special characteristic in the term of lack of recognition and heterogeneity.

The recent use of biomarkers has made it possible to identify different ARDS phenotypes with distinct characteristics with their own prognosis and responses to therapies [154]. In a first clinical study, Jabaudon et al. found sRAGE concentrations are higher in ARDS patients during sepsis[155]. Later, in the same clinical team, more proofs of sRAGE is revealed, as serum and lung concentrations are correlated and an increase in sRAGE and a decrease in esRAGE and AGEs have been observed in ARDS[156]. In this study, RAGE isoforms exhibited high alveolar-plasma concentration ratios, strongly suggesting an alveolar origin. sRAGE is also associated with the morphology of lung involvement in ARDS. sRAGE is also associated with the non-focal morphology of lung involvement in ARDS[156,157]. The RAGE receptor may also have prognostic value in patients with ARDS variations as sRAGE concentration is associated with patient mortality[158]. In ARDS patients, the application of an alveolar recruitment maneuver is associated with a transient decrease in sRAGE, itself associated with an increase in oxygenation[159]. During the operative period, variations in sRAGE concentration are associated with the occurrence of postoperative ARDS in patients at risk of operative complications operated for major abdominal surgery[160]. Later, first randomized trial in our team proved, the use of inhaled sedation with sevoflurane is associated with improved oxygenation and a probable decrease in epithelial lesions as evidenced by a plasmatic and alveolar decrease in sRAGE[77].

However, the modulation of RAGE and the RAGE role in the pathogenesis ARDS need still to be clarified. Until today, no study exists in humans showing a potential interest in the modulation of RAGE during ARDS. In other pathologies such as Alzheimer's disease, the use of a protein inhibitor of RAGE(azeliragon (TTP448), vTv Terapeutics, High Point, NC, USA) was tested in 399 patients but did not show a real benefit on the pathology. Nevertheless, the use of this low-dose RAGE inhibitor appeared to have a safe use profile in the study patients. On the other hand, there are preclinical data suggesting a potential interest

in modulating the RAGE pathway during lung injury. The use of a protein inhibitor of RAGE, RAGE Antagonist Peptide(RAP) in *in vitro* and *in vivo* models of lung injury was associated with a decrease in pro-inflammatory cytokines such as Il-6 and the transcription factor NF -KB[161].

2.4. Alveolar epithelial barrier function in ARDS: Important factors and signaling pathway

2.4.1 Alveolar epithelium

A human lung, in good terms of health, plays the most crucial role in every term of a life: respiration. And more precisely, with thousands of human alveolar structures facilitate the carbon dioxide and oxygen exchange across the distal alveolar-capillary unit. The alveolar epithelium was composed only of two types of cells: Type I and Type II pneumocytes. Pneumocytes type I(ATI) covered more than 90% of the surface of epithelium with a thick and flat morphology, connected tightly with endothelial cells of alveolar capillaries, and pneumocyte type II(ATII) have a distinct morphology with characteristic lamellar bodies and distinct apical microvilli[162]. The major role of ATI cells, as they occur almost the total epithelial surface, is to compose a thin barrier that allows the efficient gas exchange. The role of ATII cells was for long time considered as a secretory cell of surfactant, since the blood–air interface on the epithelium side produces a collapsing tension, which is lowered by the pulmonary surfactant lining the alveolar surface, assuring alveolar stability during breathing[163] (Figure 9). The surfactant, also called surfactant-associated protein(SP), is a family of phospholipid-protein complexes with 90% of lipid and 10% of protein. There are five of them, from SP-A to SP-D[164], and one recently discovered surfactant called SP-G also called SFTA2[165].

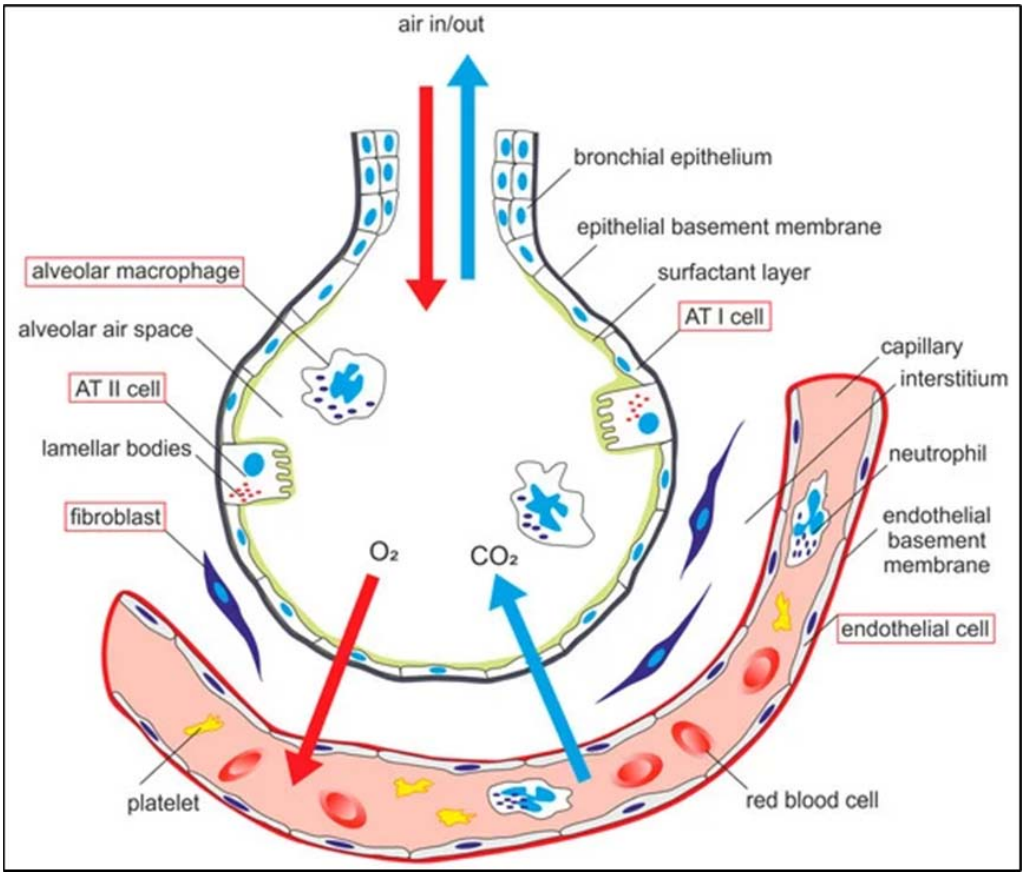

Figure 9. **Alveolar-capillary structure with ATI and ATII cells**

Resource: Nova Z, Skovierova H, Calkovska A. Alveolar-Capillary Membrane-Related Pulmonary Cells as a Target in Endotoxin-Induced Acute Lung Injury. *International Journal of Molecular Sciences*. 2019; 20(4):831. https://doi.org/10.3390/ijms20040831

In cases of lung insults, ATI cells showed high mortality[166]. The process of repair of the disrupted surface and the renewal of ATI cells is called re-epithelization and has been clarified in experimental models of lung insults in recent years, ATII cells were proven to be able to enter a self-renewal cycle and act as progenitors of new ATI through a transdifferentiation process, controlled by TGF-β and BMP signaling[10,167–170]. After the ATI cell loss, the survived ATII cells orchestrate the re-epithelization, with proliferation and then

transdifferentiation from ATII with massive covers over the alveolar surface area, and a morphological change from cuboidal form to thin squamous form[10], this process is characterized by a change of ATII biomarkers to ATI biomarkers expression in ATII cells.

2.4.2 Alveolar barrier function: the role of junction proteins and epithelial permeability

As mentioned above, one of the major roles of the lung epithelium is the physical barrier between the lumen and the underlying submucosa, which limits the pathogen entry and ensures a balanced fluid transport. One of the critical components of this epithelial barrier is the junction proteins: Tight junction proteins (TJs), represented by claudins, zona occludins (ZO), and junctional adhesion molecules (JAM). The lateral structure of adjacent alveolar epithelial cells is sealed by TJ complexes, in ATI-ATI cases, the sealed band is narrow, and in ATII-ATII cases, the sealed band is much broader[166]. (Figure 10) Among different TJ families, the claudin family is a family of transmembrane proteins, claudins expressed abundantly at alveolar epithelium levels were claudin-3, 4, and 18[171]. Jin et al. found that claudin-3 is predominantly expressed in ATII cells and is involved more in ATI-ATII junctions level than in ATI-ATI levels[172], and claudin-3 alterations were found associated with increased permeability and decreased alveolar barrier function in 2011 which is opposing to the previous conclusion found in 2003[173,174]. Opposite to claudin-3, claudin-4 was proven in numerous studies to have a sealing role that decreases paracellular permeability[175–177]. Another indispensable tight junction protein family is the zona occludens family(ZO-1, ZO-2, and ZO-3), this family of cytoplasmic, scaffolding protein is localized at the alveolar epithelial junctional sites, ZO1 proteins play a critical role in assuring the connection with other TJs because it contains all domains necessary to assure protein binding to all other major transmembrane barrier proteins: notably ZO-1/Claudins complexe[178,179],

adherens junction proteins E-cadherin[178] and with cytoskeletal proteins f-actins[178,180–182]. As mentioned above, Adherens junction protein, particularly E–cadherin in alveoli, is mainly responsible for maintaining cell-cell adhesion[6,183]. Those actors in lung homeostasis maintain the normal epithelial function barrier and regulated permeability.

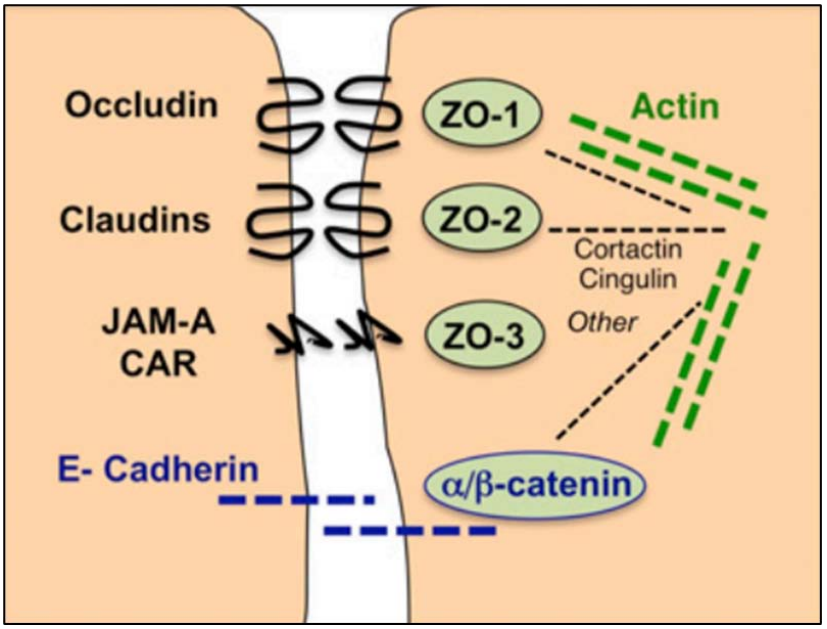

Figure 10. **Alveolar epithelial junctions**

Resource: Rezaee, F., & Georas, S. N. (2014). Breaking Barriers. New Insights into Airway Epithelial Barrier Function in Health and Disease. American Journal of Respiratory Cell and Molecular Biology, 50(5), 857–869.

A significant body of evidence indicates that the development of acute lung injury leads to the dysfunction of alveolar epithelial junctions and the disassembly of the epithelial barrier[175,178,184–188]. There are also a number of cell signaling pathways that are involved in the disassembly of lung epithelial junctions during acute lung injury, including the PI3K/Akt pathway[189,190] and the Rho/ROCK pathway[191–193]. Dysregulation of these pathways has been shown to disrupt epithelial junctions and to contribute to the development and progression of acute lung injury[194–196].

2.4.3. Alveolar Fluid Clearance

Besides the lung barrier function, another physiological key process in alveolar homeostasis is the lung fluid balance, this process is essential for the maintenance of a physiological alveolar fluid volume and electrolyte composition is regulated by active ion transport mechanisms. In ATI and ATII cells, ion transport proteins play the principal regulatory role of this alveolar fluid clearance balance, allowing transepithelial sodium (Na+), chloride (Cl−), and potassium (K+) transports. Three prominent proteins in this category are sodium channels (ENaC), Na/K-ATPase, and aquaporin (AQP)-5. The epithelial sodium channel ENaC, composed of 3 subunits (α, β, γ), is located at the level of the apical membrane of type I and II pneumocytes and participates in the absorption of sodium ions. The latter, after a passive migration towards the basolateral pole of the pneumocytes, are expelled thanks to the Na/K-ATPase pump. This transmembrane protein is made up of a catalytic α subunit (due to ATPase activity) and a regulatory β subunit, which plays a role in addressing molecules on the surface of the catalytic subunit. By consuming the energy provided by the degradation of ATP, it exchanges three sodium ions for two potassium ions, a process which will lead to a change in osmolarity and the expulsion of liquid into the pulmonary capillary circulation. Sodium channels located at the apical surface (amiloride sensitive ENaCs and amiloride insensitive channels). The aquaporin family, which are small transmembrane proteins of about 28 kDa, has 10 members in mammals. Three aquaporins are expressed at the pulmonary level: AQP-1 (at the level of the microvascular endothelium), AQP-4 (on the basolateral membrane of pneumocytes), and AQP-5 (on the apical membrane of type I pneumocytes). These proteins, which form pores in the cell membrane, provide significant and specific permeability of water molecules, and play an important role in alveolar fluid clearance (Figure 11).

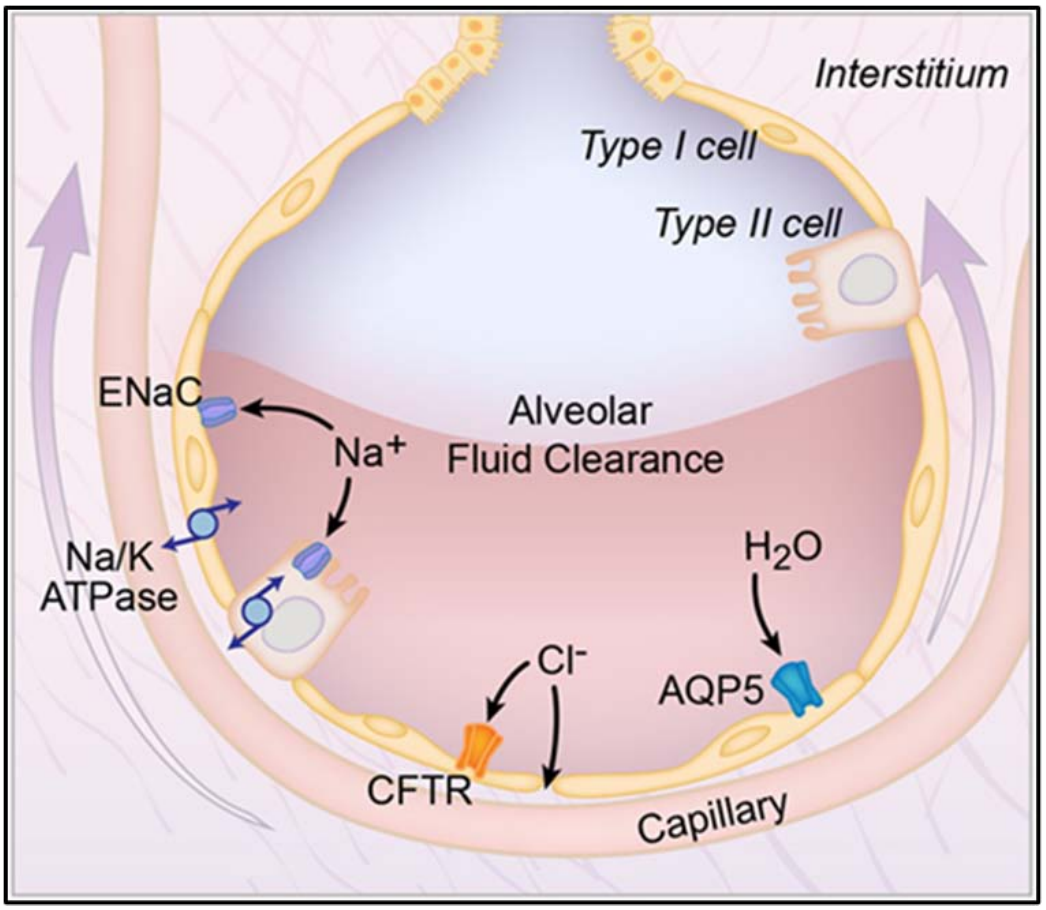

Figure 11. **Alveolar fluid Clearance Pathways**

Resource: Huppert, L. A., & Matthay, M. A. (2017). Alveolar Fluid Clearance in Pathologically Relevant Conditions: In Vitro and In Vivo Models of Acute Respiratory Distress Syndrome. Frontiers in Immunology, 8, 371.

During acute lung injury, alveolar fluid clearance can be impaired, leading to the accumulation of excess fluid in the alveoli and the development of alveolar edema and directly associated with increased mortality[197,198].

2.4.4 RAGE/Rho/Rock/MLC/F-actin pathway and alveolar homeostasis

One of the important downstream signaling pathways following the activation of RAGE is the Rho/ROCK pathway[199]. (Figure 12) The small GTPase, RhoA, which belongs to the Rho subfamily, controls cell adhesion and its motility via actin-cytoskeleton reorganization and actin-myosin filament bundles regulation. ROCK (Rho-associated coiled-coil-forming protein kinase) is a downstream target protein of Rho. ROCK is divided into two isoforms, ROCKI and ROCKII. Functional differences between ROCK-I and ROCKII remain unknown, there are multiple downstream signals that ROCK activation participate, notably in cell-cell adhesion regulation including cytoskeleton rearrangement, cell contraction, and stress fiber assembly, but also involved in apoptosis, cell proliferation, and migration[200–205].Particularly, main involved processes of Rho/ROCK pathway are on cytoskeleton rearrangement, cell contraction, and stress fiber assembly was after the active form of RhoA binds to ROCK, ROCK phosphorylates myosin phosphatase, resulting in an increase in myosin light chain (MLC) phosphorylation, which triggered the polymerization of G-actin to F-actin and induces cytoskeletal changes.

Numerous studies revealed the strong association and pivotal role of Rho/ROCK pathway in the disruption of epithelial barrier junctions and increased permeability[206], which in ARDS context, favorise the formation of edema and impaired alveolar fluid clearance[195,207]. There have been several studies that have investigated the relationship between F-actin and alveolar injury, and have shown that F-actin may play a role in the development and progression of alveolar injury. The increased formation of F-actin may contribute to the increased permeability of the alveoli and the accumulation of fluid in the alveoli in patients with ARDS. The study found that the increased formation of F-actin was associated with an

increase in the permeability of the alveoli and the accumulation of fluid in the alveoli in the mice with lung injury[208,209].

Figure 12. **RAGE/RHO/ROCK pathway**

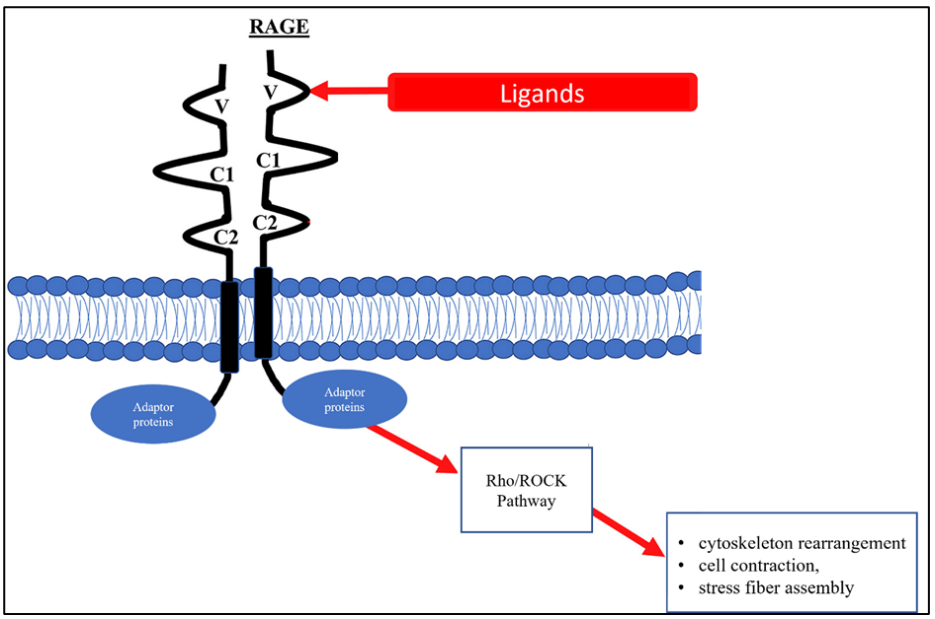

Resource: Personal artwork following literature

3. Research objectives

Our research objectives were multiple with different hypothesizes to test surrounding sevoflurane's high potential protective effects in the ARDS context and its precise mechanism, in both *in vivo* and *in vitro* models of ARDS:

First of all, we hypothesized that in sterile inflammation-induced acute lung injury, the exposure to sevoflurane may have beneficial effects on

- **Lung alveolar epithelial injury and ARDS physiological features (PaO_2/FiO_2)**
- **Lung epithelial barrier function protection and repair**
- **Alveolar Fluid Clearance improvement**

The mechanistic regulation of those eventual protective effects should also be discussed, following encouraging existed evidence:

- **Sevoflurane could decrease lung alveolar epithelial permeability through the Rho/pMLC/F-actin regulation**
- **Sevoflurane protective effects on alveolar fluid clearance is, at least partly, through the protection of epithelial of ion and water transport**

And finally, with all the high potential that RAGE showed in other studies, it is indispensable to discuss the possible role of RAGE in lung epithelial repair in our research :

- **RAGE has an important role in the process of alveolar re-epithelization, the test of this hypothesis will establish a solid ground to discuss for the next hypothesis.**
- **Effects of sevoflurane on lung epithelial permeability could be, at least partially, mediated by RAGE.**

4. Results

4.1 Inhaled anesthesics for sedation of intensive care patients

4.1.1 Review of the literature on inhaled ICU sedation

Inhaled sedation in the intensive care unit. Anaesth Crit Care Pain Med. 2022 Jul 27;41(5):101133. **(Study N°1)**

Matthieu Jabaudon, **Ruoyang Zhai**, Raiko Blondonnet, Woodys Lenga Ma Bonda

4.2 Use of preclinical models of ARDS for mechanistic investigations of lung alveolar injury and repair

4.2.1 Review of the literature on preclinical and clinical models of ARDS

From preclinical to clinical models of acute respiratory distress syndrome. Signa Vitae 2022. Vol.18, Issue 1, January 2022 pp.3-14. doi: 10.22514/sv.2021.228 **(Study N°2)**

Ruoyang Zhai, Woodys Lenga Ma Bonda, Gustavo Matute-Bello, Matthieu Jabaudon

4.2.2 Explore roles of the RAGE pathway in alveolar epithelial wound healing

The receptor for advanced glycation end-products enhances lung epithelial wound repair: An in vitro study. *Exp. Cell Res.* **391**, 112030 (2020)**(Study N°3)**

Ruoyang Zhai, Raiko Blondonnet, Ebrahim Ebrahimi, Corinne Belville, Jules Audard, Christelle Gross, Helena Choltus, Fanny Henrioux, Jean-Michel Constantin, Bruno Pereira, Loic Blanchon, Vincent Sapin, Matthieu Jabaudon

4.3 Mechanistic approaches to the effects of sevoflurane on lung epithelial injury and function

4.3.1 Effects of sevoflurane on RAGE mediated-lung epithelial barrier function

Effects of sevoflurane on lung epithelial permeability in experimental models of acute respiratory distress syndrome **(Study N°4)**

Ruoyang Zhai, Woodys Lenga Ma Bonda, Charlotte Leclaire, Cécile Saint-Béat, Camille Theilliere, Corinne Belville, Randy Coupet, Raiko Blondonnet, Damien Bouvier, Loic Blanchon, Vincent Sapin, Matthieu Jabaudon (*Submitted for Publication*)

4.3.2 Effects of volatile anesthetics sevoflurane and isoflurane on lung alveolar epithelial injury and function: a randomized laboratory trial in piglets

Effects of volatile anesthetics sevoflurane and isoflurane on lung alveolar epithelial injury and function: a randomized laboratory trial in piglets **(Study N°5)**

Ruoyang Zhai, Raiko Blondonnet, Bertille Paquette, Corinne Belville, Bruno Pereira, Woodys Lenga Ma Bonda, Damon-Soubeyran Christelle, Loic Blanchon, Vincent Sapin, Matthieu Jabaudon (*In Preparation*)

STUDY N°1

Inhaled sedation in the intensive care unit

Jabaudon M, **Zhai R**, Blondonnet R, Bonda WLM. **Anaesth Crit Care Pain Med. 2022 Jul 27;41(5):101133.**

ELSEVIER

Anaesthesia Critical Care & Pain Medicine

Volume 41, Issue 5, October 2022, 101133

Review article

Inhaled sedation in the intensive care unit

Matthieu Jabaudon [a, b], Ruoyang Zhai [b], Raiko Blondonnet [a, b], Woodys Lenga Ma Bonda [b]

[a] Department of Perioperative Medicine, CHU Clermont-Ferrand, Clermont-Ferrand, France

[b] GReD, Université Clermont Auvergne, CNRS, INSERM, Clermont-Ferrand, France

Available online 27 July 2022, Version of Record 1 August 2022.

Scientific Knowledge of the Subject

Sedation is used to improve comfort and tolerance in the Intensive Care Unit (ICU), such as during mechanical ventilation, invasive interventions, and/or nursing care[52]. However, sedation should not be considered as a goal and should always be integrated in an "ABCDEF" bundle for ICU liberation[210,211]. Such a bundle should always give priority to the adaptation of ventilator settings for patient-ventilator asynchrony prevention or treatment over the unnecessary administration of medications, such as sedatives, opioids, and neuromuscular blocking agents, which can delay liberation from mechanical ventilation and the ICU, thus worsening patient outcomes[32,212].

Current sedation practice largely relies on intravenous agents, such as propofol and dexmedetomidine, or midazolam, however, both of them has its limites[32,210,212–214]. During past years, the use of halogenated agents, such as sevoflurane and isoflurane, in the sedation of patients in the Intensive Care Unit (ICU), is now feasible through dedicated vaporizers and scavenging systems[57,215–217]. In addition to their function as sedative agents, these molecules have many intrinsic characteristics with potential therapeutic benefits that could be especially relevant to ICU patients for example in COVID-19 cases[55,218].

Contributions of this study to the field

In this review, we summarized the pharmacological basis and practical aspects of the use of volatile anesthetics for ICU sedation, and reviewed and discussed available evidence supporting inhaled sedation as a viable alternative to intravenous sedation.

We also pointed out the availability of halogenated agents and devices allowing their use in intensive care depends on countries, which should be taken into consideration.

However, encouragingly, inhaled sedation is being increasingly accepted as an alternative to intravenous sedation, particularly for desired short-term sedation in intensive care.

Anaesth Crit Care Pain Med 41 (2022) 101133

Contents lists available at ScienceDirect

Anaesthesia Critical Care & Pain Medicine

journal homepage: www.elsevier.com

Review article

Inhaled sedation in the intensive care unit

Matthieu Jabaudon [a,b,*], Ruoyang Zhai [b], Raiko Blondonnet [a,b], Woodys Lenga Ma Bonda [b]

[a] Department of Perioperative Medicine, CHU Clermont-Ferrand, Clermont-Ferrand, France
[b] GReD, Université Clermont Auvergne, CNRS, INSERM, Clermont-Ferrand, France

ARTICLE INFO

Article history:
Available online 27 July 2022

Keywords:
inhaled sedation
isoflurane
sevoflurane
intensive care unit
acute respiratory distress syndrome

ABSTRACT

Inhaled sedation with halogenated agents, such as isoflurane or sevoflurane, is now feasible in intensive care unit (ICU) patients through dedicated vaporisers and scavenging systems. Such a sedation strategy requires specific equipment and adequate training of ICU teams. Isoflurane and sevoflurane have ideal pharmacological properties that allow efficient, well-tolerated, and titratable light-to-deep sedation. In addition to their function as sedative agents, these molecules may have clinical benefits that could be especially relevant to ICU patients. Our goal was to summarise the pharmacological basis and practical aspects of inhaled ICU sedation, review the available evidence supporting inhaled sedation as a viable alternative to intravenous sedation, and discuss the remaining areas of uncertainty and future perspectives of development.

Contents

Introduction

In the intensive care unit (ICU), sedation is used to improve comfort and tolerance, such as during mechanical ventilation, invasive interventions, and/or nursing care [1]. However, sedation itself should not be considered as a goal and priority should always be given to analgesia and the adaptation of ventilator settings for patient-ventilator asynchrony prevention or treatment over the unnecessary administration of medications, such as sedatives, opioids, and neuromuscular blocking agents, which can delay liberation from mechanical ventilation and the ICU, thus worsening patient outcomes [2–4]. Current sedation practise largely relies on intravenous agents, such as propofol and dexmedetomidine. Recent surveys of sedation practices have also found that midazolam and propofol continue to be widely used for ICU sedation [5]. However, non-benzodiazepine strategies should be preferred for ICU sedation, as the use of benzodiazepines is associated with decreased ventilator-free days, increased risk of delirium, and worse long-term outcomes overall [3,4]. Propofol use is not directly associated with prolonged sedation and/or delirium,

* Corresponding author.
E-mail address: mjabaudon@chu-clermontferrand.fr (M. Jabaudon).

https://doi.org/10.1016/j.accpm.2022.101133

and propofol is more titratable than midazolam; however, it may cause hypertriglyceridaemia and propofol-related infusion syndrome, typically at higher doses. Dexmedetomidine is an alpha-2 agonist that does not reduce respiratory drive, has co-analgesic properties, and may have cardiac toxicity in some patients at higher doses. A deep level of sedation is not possible with dexmedetomidine alone, and using multiple agents may be considered in some situations [3,4,6].

Although volatile anaesthetics such as isoflurane or sevoflurane have long been used to provide general anaesthesia in the operating theatre, inhaled ICU sedation is now an available option to provide ICU sedation, at least in those countries where specific devices have been developed and approved for use with modern halogenated agents such as isoflurane, sevoflurane or desflurane [7–10]. In addition to their function as sedative agents, these molecules have many intrinsic characteristics with potential therapeutic benefits that could be especially relevant to ICU patients. The use of volatile anaesthetics for ICU sedation has increased in some regions during the recent coronavirus disease 2019 (COVID-19) pandemic, given intravenous drug shortages and the need to expand ICU bed capacity [11,12]. In this article, our goal was to summarise the pharmacological basis and practical aspects of the use of volatile anaesthetics for ICU sedation, to review the available evidence supporting inhaled sedation as a viable alternative to intravenous sedation, and to discuss areas of uncertainty and future perspectives of the field.

History and Pharmacological Basis

In the early nineteenth century, nitrous oxide (N_2O) and ether were the first volatile anaesthetics to be used for medical purposes. Halogenated agents have been used in humans for almost 150 years to induce general anaesthesia; halothane was the first fluorocarbon molecule synthesised in 1951, but it was soon abandoned due to concerns about liver toxicity. More modern molecules such as isoflurane, sevoflurane, and desflurane emerged in 1972, 1990, and 1992, respectively [13]. Halogenated agents take their name from the presence of atoms from the halogen group in their molecular structure. Note that methoxyflurane, which is also a halogenated agent, was initially abandoned in the 1970s because of renal toxicity, but is currently being used again through self-administered inhalation for rapid pain relief in the prehospital setting.

Halogenated agents are molecules with a carbon skeleton and several halogen atoms (chlorine, fluorine or bromine). The chemical structures of the main halogenated agents in use today are presented in Fig. 1. The physical characteristics of halogenated agents—those related to solubility in the blood or organs in particular—have major implications for their use in clinical practice; indeed, the solubility of gases in plasma is inversely correlated to their rapid onset and offset of action. Thus, an anaesthetic gas that is not very soluble in plasma will allow rapid induction of narcosis and be rapidly eliminated after interruption of its administration, leading to rapid awakening. The gas/blood partition coefficient is, therefore, the most decisive parameter for the rapidity of action of the gas and patient awakening. These characteristics, which are true for the use of halogenated agents in the operating theatre, remain true in the ICU setting. Halogenated agents are liquid at room pressure and temperature (except desflurane), and must, therefore, be transformed into breathable vapour by vaporisers dedicated to each gas, depending on their boiling temperatures.

The action of halogenated agents involves complex mechanisms via interactions with membrane proteins at the pre- and post-synaptic levels, both in nervous tissues and other types of tissue. Overall, they reduce presynaptic excitation and neurotransmitter release, reduce neurotransmitter activity in the postsynaptic membrane, exert anti-N-methyl-D-aspartate effects [9], have anticonvulsant effects, and can cause isoelectric electroencephalogram with burst suppression at high doses. Of note, halogenated agents have a bronchodilator effect through direct action on the bronchial smooth muscle and inhibition of the transmission of the vagal impulse at the level of the postganglionic fibre. They also inhibit the hypoxic pulmonary vasoconstriction response in a dose-related manner.

Halogenated agents are fast-onset (1–2 min) and fast-offset (4–7 min) drugs that induce a dose-dependent reduction in respiratory drive and allow light-to-deep sedation targets. Although isoflurane or sevoflurane use has been associated with a decrease

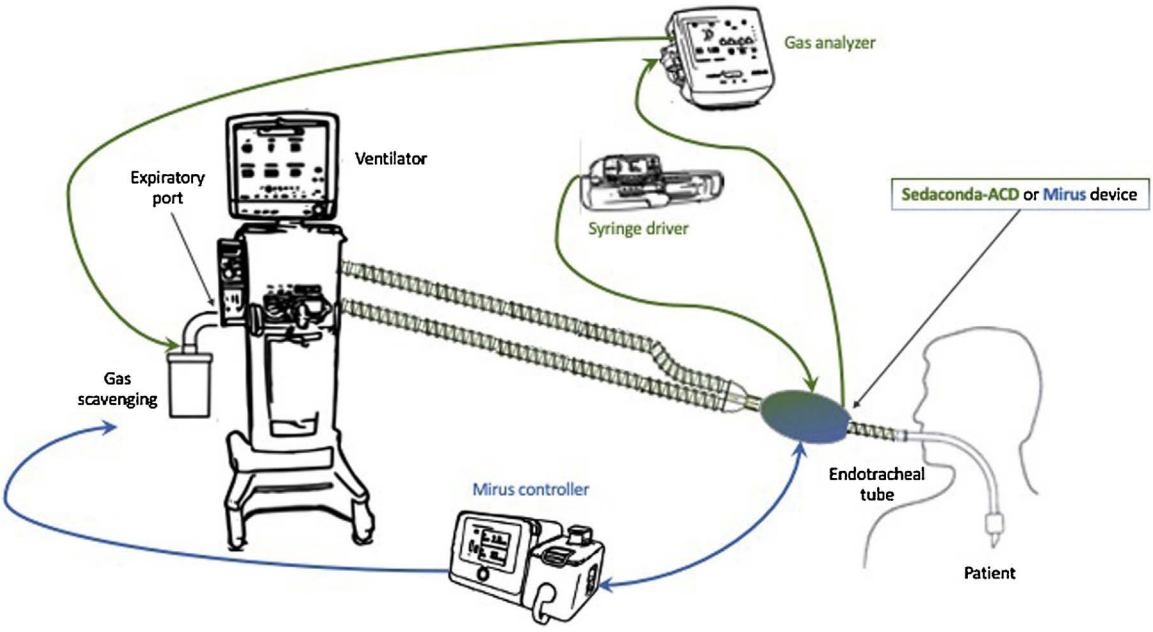

Fig. 1. Schematic view of the bedside equipment setup for delivering inhaled sedation in the intensive care unit. A Sedaconda-ACD (equipment setup in green) or Mirus (equipment setup in blue) device is placed between the Y-piece of the ventilator breathing circuit and the endotracheal tube. Use of these devices does not require additional antimicrobial filtration or humidification. Expired volatile anaesthetic agent is scavenged at the ventilator expiratory port.

in opioid requirements in some studies [14,15], whether these agents have specific analgesic effects and which mechanisms may explain such effects remains unknown. End-tidal gas fractions are good surrogates of cerebral concentrations of the drugs and, although sedation should first be adapted using validated clinical scores [16], monitoring such end-tidal gas fractions could represent an efficient way of titrating sedation to a patient's needs (usual range of 0.2–1.4%) [17,18]. Importantly, halogenated agents undergo pulmonary elimination and have a low level of hepatic metabolism (metabolism rate of 2–5% for sevoflurane, 0.2% for isoflurane, and 0.02% for desflurane), without the production of active metabolites (fluorine ions) or alteration in hepatic/renal lab tests in patients [9].

Practical Aspects

Devices and general set-up

Volatiles were first vaporised to ICU patients through anaesthesia machines to manage severe medical conditions, such as refractory asthma, bronchospasm and status epilepticus, or to achieve sedation in patients with high requirements, such as those with a history of drug abuse [7,19–23].

Nowadays, the anaesthetics machine has been repurposed to meet ICU demand in the current pandemic [24,25]. Anaesthetic machine reflectors have been specifically developed to ventilate critically ill patients. Two major systems have been used: the Anaesthetic Conserving Device (Sedaconda-ACD, Sedana Medical, Danderyd, Sweden) and the Mirus system (Mirus, TIM GmbH, Koblenz, Germany). These devices are inline miniature vaporisers with humidification and antiviral filter properties. It connects between the endotracheal tube and Y-piece of the respiratory circuit attached to a gas monitoring module (allowing continuous surveillance of end-tidal gas concentrations and carbon dioxide) and a gas-scavenging device (either active or passive). They are compatible with most modern ventilators, but heated humidifiers should not be used with them as these devices already have good heat and moisture exchanger properties.

The Sedaconda-ACD device contains no electrical components and is compatible with magnetic resonance imaging and computed tomography scanners; the latest Sedaconda-ACD-S version has a smaller dead space of 50 mL and can, therefore, allow tidal volumes as low as 200 mL. The Sedaconda-ACD allows for the passive vaporisation of sevoflurane and isoflurane, delivered continuously to the device in a liquid form via an electric syringe pump. After priming the agent line with 1.5 mL of the agent, indicative pump rates for isoflurane and sevoflurane are 2–7 mL/h and 4–10 mL/h, respectively, to obtain end-tidal fractions of 0.2–0.7% and 0.5–1.4%, respectively [18]. The Sedaconda-ACD also contains a layer of activated charcoal that captures $>$ 80% of the exhaled agent, which can be redelivered during the next inspiration. The Mirus system can be used to deliver isoflurane, sevoflurane or desflurane while adjusting infusion rates through the automatic control of anaesthetic concentration targets [26]. In patients with high volume secretions, both devices may need more frequent replacement ($<$ 24 h for the Sedaconda-ACD; $<$ 7 days for the Mirus system), and mini vaporisers should be removed from the circuit when inhaled sedation is stopped, in order to minimise the work of breathing [27].

Both medical and paramedical teams should be familiar with these technical concerns before using inhaled sedation in practice [9,11], and adequate training on technology and drug features should be considered before using these systems. This may be simpler in European ICUs, where anaesthesiology-trained intensivists are predominant, compared to some other regions; implementation of inhaled ICU sedation should always involve cross-disciplinary collaboration between anaesthesiologists, intensivists, nurses, and respiratory therapists.

Potential adverse events and current limitations

The prolonged use of inhaled sedation (*e.g.,* for $>$ 48 h) has shown good safety with equivalent effects on haemodynamic stability, no hepatorenal toxicity, and possibly less agitation compared to intravenous agents [28–31].

The risk of malignant hyperthermia triggered by halogenated agents is very rare but should be rapidly identified, as it requires urgent treatment. Malignant hyperthermia occurs within genetically susceptible patients and combines hyperthermia, hypercarbia and haemodynamic instability. The triggering drug (and device in the case of halogenated agents) should be immediately removed and specific treatment relies on intravenous dantrolene sodium. Such symptoms should ideally be separated from more common ICU events such as new sepsis and deteriorating lung function.

Among others, non-specific adverse events include decreased cardiac output and arterial pressure (dose-dependent), as well as respiratory depression (dose-dependent). Halogenated agents have equivocal effects on cerebral blood flow, with increased intracranial pressure and cerebral vasodilation, but decreased cerebral oxygen consumption and improved regional blood flow. However, they should be avoided when there is a risk of increased intracranial pressure. During pregnancy or in patients and healthcare professionals at risk of pregnancy, the use of sevoflurane seems safe, but the "precautionary principle" should be applied to limit exposure as much as possible, although exposure levels of healthcare workers seem very low [32]. There is little evidence to suggest that low dose isoflurane exposure has any clinically significant teratogenic effects, though isoflurane in combination with N_2O can be teratogenic in rats [33,34]. The exposure of pregnant mice to isoflurane for 4 h caused reduced foetal weight and congenital malformations at doses above 6000 ppm. If a patient or a healthcare worker is pregnant or probably pregnant, a precautionary use should be applied to limit exposure as much as possible. However, inhaled anaesthetics deemed to be safe and the level of exposure to healthcare workers seem very low [33,35]. Unfortunately, there are no clinical data available during pregnancy. More recently, a few cases of diabetes insipidus have been reported after the prolonged use of high-dose sevoflurane, but the causality remains under debate [36–38].

Available Evidence

Published clinical trials of adult patients who underwent sedation with volatile anaesthetics in the intensive care unit are listed in Table 1.

Potential Benefits of inhaled ICU sedation

Halogenated agents are short-acting drugs, which are easy to titrate to the targeted level from light-to-deep sedation. In a small randomised controlled trial, assigning ICU patients expected to require sedation for more than 24 h to sevoflurane (n = 19), propofol (n = 14) or midazolam (n = 14), sevoflurane was associated with significantly shorter wake-up and extubation times, decreased use of opioids, and less vasopressor requirement compared to both midazolam and propofol [14]. A first systematic review and meta-analysis of eight trials (523 patients) published before 2015 confirmed a reduction in extubation times (defined as the time between discontinuing sedation and tracheal extubation)

Table 1
Published randomised controlled trials and quasi-randomised controlled trials of adult patients who underwent sedation with volatile anaesthetics (sevoflurane, isoflurane, or desflurane) in the intensive care unit.

Study	Subjects	Inhaled sedation group (drug, n)	Intravenous sedation group (drug, n)	Mean sedation duration	Target sedation level	Included outcomes
Sackey et al. [39]	Medical patients expected to need > 12 h sedation	Isoflurane (n = 20)	Midazolam (n = 20)	Maximum: 96 h Inhaled: 52 h IV: 32 h	BBSS -1 to +1	Awakening time, extubation time
Sackey et al. [40]	Medical patients expected to need > 12 h sedation	Isoflurane (n = 10)	Midazolam (n = 7)	Maximum: 96 h Inhaled: 44.2 h IV: 61.3 h	BBSS -1 to +1	ICU LOS, delirium
Mesnil et al. [14]	Medical patients expected to need ≥ 24 h sedation	Sevoflurane (n = 19)	Propofol (n = 14) Midazolam (n = 14)	Inhaled: 50 h Propofol: 57 h Midazolam: 50 h	RSS 3-4	Awakening time, extubation time, ICU LOS, delirium, serum creatinine
Georgevici et al. [16]	Surgical patients requiring postoperative invasive MV after major abdominal, vascular, or orthopaedic interventions	Isoflurane (n = 10) Sevoflurane (n = 10) Desflurane (n = 10)	None	Isoflurane: 18 h Sevoflurane: 17 h Desflurane: 18 h	Age-adjusted MAC 0.55	RASS, BPS, EEG monitoring (Narcotrend index)
Jerath et al. [47]	Patients with normal or mildly reduced left ventricular systolic function and receiving postoperative sedation after coronary artery bypass graft surgery	Isoflurane or Sevoflurane (n = 67)	Propofol (n = 74)	Not reported	RASS -1 to +1	Serum troponin, extubation times, sedation and pain scores, analgesia requirement, shivering, postoperative nausea and vomiting, and ICU and hospital LOS
Jabaudon et al. [28]	Patients within 24 h of moderate or severe ARDS (Berlin criteria)	Sevoflurane (n = 25)	Midazolam (n = 25)	Sevoflurane: 48 h IV: 48 h	BIS 40–50	Arterial oxygenation, alveolar and plasma levels of cytokines and soluble form of the receptor for advanced glycation end-products, physiologic variables, compliance of the respiratory system, airway resistance, vasopressor requirement, duration of mechanical ventilation, ICU LOS, 30-day mortality
Hellström et al. [48]	Surgical patients after coronary artery bypass surgery with cardiopulmonary bypass	Sevoflurane (n = 49)	Propofol (n = 50)	Sevoflurane: 2.8 h IV: 3.1 h	MAAS 2-3 for a minimum of 2 h	Duration of sedation, wake-up times, minor adverse events, ICU/hospital LOS and ICU memory tool
Hellström et al. [49]	Surgical patients after coronary artery bypass grafting with cardiopulmonary bypass	Sevoflurane (n = 50)	Propofol (n = 50)	Sevoflurane: 2.9 h IV: 3.7 h	MAAS 2-3 for a minimum of 2 h	Serum troponin, adverse cardiac events, need for haemodynamic support
Meiser et al. [41]	Surgical patients after major surgery	Desflurane (n = 28)	Propofol (n = 28)	Desflurane: 11.5 h IV: 9.7 h	BIS 60	Emergence time, time to first response, time to eyes open, time to squeeze hand, time to extubation, time to saying birth date and to recall words memorised preoperatively
Meiser et al. [15]	Patients under MV	Isoflurane (n = 150)	Propofol (n = 151)	Isoflurane: 11.5 h IV: 9.7 h	RASS -4 to -1	Percentage of time in sedation range, opioid requirements, spontaneous breathing, time to wake-up and extubation, and adverse events

MV: mechanical ventilation; IV: intravenous; BBSS: Bloomsbury sedation scale; LOS: length of stay; RASS: Richmond agitation sedation scale; RSS: Ramsay sedation scale; MAC: end-expiratory minimal alveolar concentration; BPS: behavioural pain scale; EEG: electroencephalography; BIS: bispectral index; ARDS: acute respiratory distress syndrome; MAAS: motor activity assessment scale.

when using inhaled sedation with desflurane, sevoflurane or isoflurane, compared to intravenous midazolam or propofol (difference in means, −53 minutes; 95% confidence interval [CI], −75 to −30; $P < 10^{-5}$). Differences were greater when comparing inhaled sedation with midazolam (−292 minutes; 95% CI, −384 to −200; $P < 10^{-5}$) than with propofol (−29 minutes; 95% CI, −47 to −11; $P = 10^{-3}$), and there was no significant difference in the incidence of adverse events (such as nausea and vomiting or changes in serum creatinine) related to the proportion of time spent in target sedation, length of stay, or death between inhaled and intravenous sedation strategies [29,39–41]. In another meta-analysis of 13 randomised and quasi-randomised controlled trials (1,027 patients) published before 2017, awakening and extubation times were shorter with inhaled sedation than with intravenous sedation (midazolam or propofol), although there were no differences in the lengths of ICU and hospital stays [30]. These findings contrast with those from a retrospective study in surgical ICU ventilated patients receiving prolonged sedation (> 96 h), in which patients receiving inhaled isoflurane (n = 72) had more ventilator-free days at day 60, more hospital-free days at 6 months, and decreased mortality, compared to patients receiving midazolam or propofol (n = 128) [42]. However, in-hospital and one-year

mortality rates were high in patients from the control group (63% and 70%, respectively) in this study, which had inherent limitations due to a small sample size and a retrospective, single-centre design.

There is now important literature to support the overall safety of administering inhaled sedation to ICU patients through specific devices, without the risk of tolerance or withdrawal and with no major adverse effects, such as effects on respiratory mechanics or renal or liver function [14,27,29–31,43–45]. In addition, inhaled sedation consistently decreased the need for opioid analgesics and other sedatives across multiple studies, including in patients with COVID-19 [12,31,46]. In the meta-analysis by Kim et al., inhaled sedation was also associated with lower serum troponin levels 6 h after ICU admission, compared to intravenous sedation [30,47–49]. This potential benefit of myocardial protection converges with previous results from another meta-analysis of 68 studies in patients undergoing cardiac surgery, in which the use of halogenated agents (sevoflurane, isoflurane or desflurane), compared to total intravenous anaesthesia, was associated with fewer postoperative pulmonary complications and decreased mortality (odds ratio for overall mortality, 95% CI, 0.35 to 0.85) [50]. The Mortality in Cardiac Surgery Randomized Controlled Trial of Volatile Anesthetics (MYRIAD trial) was a pragmatic, multicentre, single blind trial of halogenated agents *vs.* total intravenous anaesthesia in patients undergoing elective coronary artery bypass grafting. More than 5,000 patients were enrolled in this large trial that did not find any benefit of volatile anaesthetics in decreasing the primary outcome of mortality at one year, which was low in this trial (2.8% in the volatile anaesthetics group *vs.* 3.0% in the total intravenous anaesthesia group).

Recent research also suggests that inhaled sedation could be associated with some kidney-protective effects through attenuated renal tubular necrosis and decreased effects of pro-inflammatory cytokines [51–53]. Because animal and human studies support the protective effects of pre-treatment with halogenated agents before prolonged liver [54], brain [55] or heart [56] ischaemia, the hypothesis of end-organ protective properties of inhaled sedation has gained growing interest [9]. In the following section, we will focus on the effects of inhaled sedation on the lungs of patients with, or at risk of ARDS.

End-organ Protection? The case of the lungs

Multiple preclinical investigations suggest that isoflurane and sevoflurane may possess important lung-protective effects mediated via mechanisms that could be very relevant to the pathogenesis and resolution of ARDS [57].

In vitro, sevoflurane reduced the secretion of inflammatory mediators and the chemotactic activity and adherence of neutrophils in cultured alveolar epithelial cells after lipopolysaccharide (LPS) challenge [58,59], and alveolar macrophages treated with sevoflurane after LPS had increased phosphorylation of the extracellular-regulated kinase, an anti-inflammatory and anti-apoptotic kinase [60,61]. *In vivo*, studies in various mouse, rat and pig models of ARDS found that isoflurane and sevoflurane reduced alveolar and systemic levels of pro-inflammatory cytokines [62–66]. Inhaled sedation was also associated with improved arterial oxygenation and decreased lung alveolar oedema in experimental ARDS [66,67]. In particular, isoflurane was able to restore epithelial tight junction integrity in a double-hit mouse model of nebulised LPS plus ventilator-induced lung injury [68], and sevoflurane may have protective effects on some mechanisms of transepithelial fluid transport in vitro and in vivo [63,69].

A single-centre, randomised, controlled clinical pilot trial of inhaled sevoflurane *vs.* intravenous midazolam enrolled 50 patients within 24 h of moderate-severe ARDS onset, as defined by the Berlin criteria, across three French ICUs [28]. In this trial, the duration of the intervention was 48 h under neuromuscular blockade with cisatracurium and conditions of deep sedation (as assessed by a bispectral index value of 40-50) and lung-protective ventilation (tidal volume of 6 – 8 mL/kg predicted body weight, positive end-expiratory pressure of $\geq$ 5 cmH_2O, inspiratory plateau pressure of $<$ 30 cmH_2O). The use of the larger Sedaconda-ACD device (instrumental dead space volume of 100 mL) was not associated with increased airway resistance or arterial carbon dioxide. The primary endpoint of arterial oxygenation was better over time (5 days) in patients receiving sevoflurane, an effect most pronounced on day 2 and day 3 after randomisation. The levels of pro-inflammatory cytokines and of soluble receptor for advanced glycation end products, a marker of lung epithelial injury, were decreased in both the plasma and the bronchoalveolar lavage fluid with sevoflurane, compared to intravenous midazolam. Although this pilot trial was not adequately powered to assess major clinical outcomes (30-day mortality of 36% with sevoflurane *versus* 40% with midazolam, $P = 0.9$), there was a non-significant increase in the number of ventilator-free days at day 30 in patients treated with sevoflurane, compared to those treated with midazolam (median, interquartile, 13.0 [1.0 – 20.0] *versus* 5.5 [0.0 – 28.0], respectively, $P = 0.4$).

In patients with COVID-19-related ARDS, inhaled isoflurane was associated with improved arterial oxygenation and lung function, as well as decreased opioid and sedative consumptions [12,46,70]. The feasibility of inhaled sedation with isoflurane under extracorporeal membrane oxygenation [71], of co-administration of sevoflurane and inhaled nitric oxide [72], and of a strategy of light sedation with sevoflurane and spontaneous breathing during prone positioning [73], has also been reported in patients with ARDS.

Currently, at least two large trials are enrolling patients with ARDS to assess the effects of inhaled sedation on major clinical outcomes. The Canadian Sedating with Volatile Anesthetics Critically Ill COVID-19 Patients in ICU: Effects On Ventilatory Parameters And Survival (SAVE-ICU) trial is a multicentre, open-label, pragmatic, randomised controlled trial that aims at randomising 752 mechanically ventilated patients with hypoxaemic acute respiratory failure and proven or suspected COVID-19 to either intravenous sedation (with any sedation supplied by the participating hospital) or inhaled sedation with isoflurane or sevoflurane, depending on the availability of both drugs (ClinicalTrials.gov: NCT04415060). Primary outcome measures will be hospital mortality, ventilator-free and ICU-free days at day 30, and quality of life at 3 and 12 months after discharge. In parallel, the French Sevoflurane for Sedation in ARDS (SESAR) trial aims at recruiting a total of 700 patients within 24 h of moderate-severe ARDS onset (PaO_2/FiO_2 $<$ 150 mmHg under a positive end-expiratory pressure of at least 8 cmH_2O) to evaluate whether sedation with inhaled sevoflurane (administered through the Sedaconda-ACD-S) will increase the number of ventilator-free days through day 28, as defined as the number of days alive and off the ventilator at 28 days (thereby considering death as a competing event) (primary outcome) and decrease all-cause 90-day mortality (key secondary outcome), compared to a sedation strategy of intravenous propofol (ClinicalTrials.gov: NCT04235608). Findings from the SAVE-ICU and SESAR trials will also be invaluable to inform the impact of inhaled sedation on neurocognitive function and long-term outcomes, in addition to contributing to better understanding of the potential clinical benefits of halogenated agents for ICU sedation. Meanwhile, although this sedation strategy is already being applied routinely in some centres, a recent panel of experts suggested that inhaled sedation with isoflurane or sevoflurane could be considered as a second or third-line strategy (propofol being the first line) within an "ABCDEF-R" bundle (R for Respiratory-drive-control) for patients with ARDS [4].

Table 2
Current ongoing prospective clinical studies of inhaled isoflurane, sevoflurane or desflurane in adult ICU patients, as registered on ClinicalTrials.gov.

Study	ClinicalTrials.gov Identifier	Study population	Number to recruit	Intervention: volatile anaesthetics (with device when available)	Comparator	Primary outcome(s)	Secondary outcomes
Comparison of an Inhaled Sedation Strategy to an Intravenous Sedation Strategy in Intensive Care Unit Patients Treated With Invasive Mechanical Ventilation (INASED)	NCT04341350	Adult patients requiring mechanical ventilation for at least 24 and sedation	250 (multicentre)	Isoflurane (Sedaconda ACD-S, Sedana Medical)	Propofol	Occurrence of a delirium in intensive care [Time Frame: 28 days]	Mortality in intensive care [Time Frame: Through exit from the intensive care unit] Mortality at day 28 [Time Frame: 28 days] Hospital cost per patient [Time Frame: Through study completion, an average of 1 year] Number of days with vasopressors or inotropic agents [Time Frame: Through exit from the intensive care unit] Number of days with sedation [Time Frame: Through exit from the intensive care unit] Cumulative dose anaesthetics drugs [Time Frame: Through exit from the intensive care unit] Duration of anaesthetics drugs [Time Frame: Through exit from the intensive care unit] Maximum dose of vasopressors or inotropic agents [Time Frame: Through exit from the intensive care unit] Ventilation free days at 28 days following randomisation [Time Frame: 28 days] Incidence and duration of delirium [Time Frame: 28 days] Length of ICU stay [Time Frame: Through exit from the intensive care unit, an average of 28 days] Requirement of patients physical restraints [Time Frame: Through exit from the intensive care unit] Self-aggressive act [Time Frame: Through exit from the intensive care unit] Hetero-aggressive act [Time Frame: Through exit from the intensive care unit] Evaluation of cognitive functions [Time Frame: at ICU discharge and 3 and 12 months after ICU discharge]
Comparison of Extubation Delay After Prolonged Sedation (ISOREA)	NCT04710914	Adult patients admitted to the intensive care unit for septic shock and requiring sedation for more than 3 days	59 (single-center)	Isoflurane (Mirus, TIM GmbH)	Midazolam	The delay between the first sedation stop and extubation [Time Frame: 10 days]	Wake-up time [Time Frame: 10 days] Total duration of sedation and mechanical ventilation [Time Frame: 90 days] Total duration of intensive care and hospital stay [Time Frame: 90 days] A measure of overall survival at 90 days defined by the duration between the inclusion date and the date of death [Time Frame: 90 days] Measurement of wake-up time defined by the duration between the day of the first sedation stop and a RASS score of 0 [Time Frame: 10 days] Incidence of intercurrent events [Time Frame: 90 days] Doses of vasopressor, hypnotic and opioid drugs administered [Time Frame: 3 days] Number of days without mechanical ventilation [Time Frame: 90 days] Measurement of midazolam and two active metabolites, 1-OHM and 1-OHMG [Time Frame: 24, 48 and 96 hours] Costs of sedative treatments (midazolam and isoflurane) and the devices needed to administer them (syringes and tubing for midazolam, reflector and filter exchanger for isoflurane) [Time Frame: 90 days]

Table 2 (*Continued*)

Study	ClinicalTrials.gov Identifier	Study population	Number to recruit	Intervention: volatile anaesthetics (with device when available)	Comparator	Primary outcome(s)	Secondary outcomes
Sedating With Volatile Anaesthetics Critically Ill COVID-19 Patients in ICU: Effects On Ventilatory Parameters And Survival (SAVE-ICU)	NCT04415060	Adult patients under mechanical ventilation and expected to remain mechanically ventilated at the end of the next day; Receiving IV sedation by infusion or bolus for $\leq$ 72 hours to facilitate mechanical ventilation; Proven or suspected COVID-19, or COVID-19 negative patients with PaO_2/FiO_2 $\leq$ 300 mmHg during the 12 h prior to enrolment	752 (Multicentre)	Isoflurane or Sevoflurane	IV sedation (any drugs)	Hospital Mortality [Time Frame: 2 years] Ventilator-Free Days [Time Frame: 30 days] ICU-Free Days [Time Frame: 30 days] Participant Quality of Life at 3 and 12 months after discharge [Time Frame: 365 days]	Median Daily Oxygenation [Time Frame: 3 days] Delirium and Coma Free Days [Time Frame: 14 days] Adjunctive ARDS therapies [Time Frame: 30 days] Hospital-Free Days [Time Frame: 60 days] Disability [Time Frame: 365 days] Cost Utility Analysis [Time Frame: 365 days]
SEvoflurane for Sedation in ARds (SESAR)	NCT04235608	Adult patients within 24 h of ARDS (Berlin criteria) with PaO_2/FiO_2 $<$ 150 mmHg under positive end-expiratory pressure $\geq$8 cmH_2O	700 (Multicentre)	Sevoflurane (Sedaconda ACD-S, Sedana Medical)	Propofol	Number of days alive and off the ventilator [Time Frame: 28 days]	Key secondary endpoint: survival [Time Frame: 90 days] Secondary endpoints: mortality [Time Frames: 7, 14, and 28 days] Exploratory outcomes: Ventilator-free days through day 7 and day 14 Organ failure-free days through day 7 ICU-free and hospital-free days through day 28 Measures of respiratory function through day 7 Use of rescue procedures for refractory hypoxaemia through day 28 ICU-acquired delirium through day 28 Long-term outcome assessments at 3 and 12 months Healthcare-related costs during ICU and hospital stay Exploratory biologic outcomes (mechanistic studies) Safety outcomes: changes in haemodynamic measures and in KDIGO criteria for acute kidney injury; supraventricular tachycardia or new onset atrial fibrillation; severe hypercapnic acidosis with pH $<$ 7.15; development of malignant hyperthermia, of propofol-related infusion syndrome, and of pneumothorax or bronchopleural fistula persistent despite drainage

ICU: intensive care unit; COVID-19: Coronavirus disease 2019; PaO2: partial pressure of oxygen in arterial blood; FiO2: fraction of inspired oxygen; ARDS: acute respiratory distress syndrome; KDIGO: kidney disease improving global outcomes.

Challenges and Perspectives

Large-scale studies are urgently awaited to further confirm the efficacy and safety of inhaled ICU sedation. The main current ongoing prospective clinical studies of inhaled isoflurane, sevoflurane or desflurane in adult ICU patients are summarised in Table 2. The phase III multicentre randomised controlled SEDACONDA trial found that isoflurane is efficacious as a sole sedative and non-inferior to propofol in maintaining targeted sedation levels [15]. This trial is the largest trial of inhaled sedation that has been completed to date, with 301 adult patients under mechanical ventilation enrolled across 21 centres in Germany and three centres in Slovenia. It will also allow pre-planned analyses in patients with acute respiratory failure/ARDS and evaluation of long-term neuropsychological effects (up to one year after randomisation).

Indeed, multiple areas of uncertainty persist. For example, whether inhaled sedation with halogenated agents could decrease the risk of delirium and/or post-intensive care syndrome, compared to the current practice of intravenous sedation, deserves further investigation. Unfortunately, available meta-analyses were unable to address the impact of inhaled sedation on ICU-related delirium. Data from a pilot follow-up study on short-term recovery from and longer-term evaluations of memory, quality of life, and symptoms of anxiety or post-traumatic stress suggest that inhaled sedation might be associated with less cognitive consequences, compared to midazolam [40]. The Inhaled Sedation in ICU (INASED) investigators are currently enrolling patients (a total expected sample size of 250 patients) in a French multicentre, randomised, controlled, open-label trial of isoflurane *vs.* propofol that was designed to assess the effect of the two sedation strategies on the occurrence of delirium (primary outcome, as assessed twice a day by the confusion assessment method for the ICU) as well as cognitive and functional outcomes at 3 and 12 months (secondary outcomes) [74].

Healthcare-related cost analyses of inhaled *vs.* intravenous sedation should also be the focus of future research. As a matter of fact, there is no available cost-effectiveness study that considers direct and indirect costs in relation to any beneficial clinical outcomes of inhaled sedation, such as faster awakening and extubation times, and decreased lengths of ICU and hospital stay. In European centres, the Sedaconda-ACD is commonly used and costs approximately 70 – 80€. In a series of 15 patients under sedation with isoflurane for an average of 4 days, the cost of midazolam/sufentanil sedation was similar to that of isoflurane/sufentanil sedation, even when including the drug, device, and scavenging costs [75]. A short-term postoperative sedation randomised controlled trial comparing desflurane to propofol sedation showed the overall drug costs for volatiles were lower (95€ desflurane *vs.* 171€ propofol) and cost neutral with the addition of the Sedaconda-ACD device [41], while another study of sevoflurane for short-term sedation found that inhaled sedation is more expensive than intravenous propofol sedation [76]. The cost-effectiveness of isoflurane *vs.* sevoflurane for inhaled sedation also warrants further investigation, as sevoflurane is usually more expensive than isoflurane in most countries.

The risk of room and environmental pollution is also a major question when performing inhaled sedation in the ICU. Based on currently available data, there is no significant pollution when the anaesthetic reflectors are correctly set up and used in accordance with recommendations from their manufacturers. Clinical teams should monitor and prevent potential leaks to the respiratory circuit and replace vaporisers (every 24 h for the Sedaconda-ACD and Sedaconda-ACD-S, and every seven days for the Mirus) and gas scavenging filters regularly. Using a closed suction system can be helpful for patients with important secretions requiring frequent tracheal suctioning. Devices and empty syringes should be disposed according to local protocols, and it is recommended that syringes with larger amounts of residual halogenated agents (> 20 mL) should be disposed of with the special hospital waste. The use of air conditioning and gas scavenging systems is recommended. Because desflurane's carbon dioxide equivalent is 50 times higher than that of sevoflurane and 23 times higher than that of isoflurane, inhaled desflurane may not represent a viable option for ICU sedation. Peak concentrations of waste halogenated agents have been shown during the handling of the system, especially during the preparation of syringes and device replacement. However, multiple studies reported room pollution below 1.5 ppm for the Sedaconda-ACD with scavenging, which is far below the recommended exposure limits, with scavenging, even in countries with lowest recommendations (ranging from 2 to 50 ppm) [32,35,77]. To minimise room pollution, the Swedish and American authorities recommend that ICU rooms are equipped with air conditioning that has at least 6 air changes per hour; however, although one study found that effective air conditioning was one of the main reasons for low values of waste halogenated agent [32], low values of waste gas could be maintained with air conditioning below the recommendations (4 air changes per hour) in another study [77].

Using halogenated agents for ICU sedation is gaining popularity, and a 2019 survey of French ICUs highlighted that 80% of respondents were "satisfied or very satisfied" with the technique [10]. In this declarative survey, the main indications of inhaled sedation were severe asthma or bronchospasm, ARDS, and failure of intravenous sedation. However, most of them had only used inhaled sedation for < 5 years and in < 20 patients per year, and the main reasons for not using inhaled sedation included the unavailability of the device (40% of responses) and lack of familiarity with the technique (35% of responses). Overall, almost 75% of respondents answered that inhaled sedation was probably a seducing and viable alternative to intravenous sedation, thus prompting further diffusion and evaluation of this strategy, the pursuit of continuous efforts to specifically train ICU staff in charge of sedation, and efforts to further simplify the set-up and use of systems dedicated to inhaled sedation, such as the Sedaconda-ACD and the Mirus.

Conclusion

Taken together, the evidence available to date supports the potential clinical benefits of using halogenated agents for ICU sedation, although further research is needed to confirm its efficacy and safety in large populations of critically ill patients, and its specific effects on important outcomes, such as lung and neurocognitive functions, among others. The availability and practices of inhaled ICU sedation largely vary across countries, and both the drugs (isoflurane, sevoflurane) and the devices (Sedaconda-ACD, Mirus) are not yet labelled worldwide for ICU sedation. However, the use of inhaled sedation may represent more than an alternative to intravenous sedation, and some national guidelines, such as in Germany, already suggest that inhaled sedation should be considered as a first-line strategy for mechanically ventilated patients for whom short wake-up times are targeted [8].

Funding

This work was supported by grants from the the French Agence Nationale de la Recherche and the Direction Générale de l'Offre de Soins ("Programme de Recherche Translationnelle en Santé" 2020; ANR-20-CE17-

0015) and the "Fonds Européen de Développement Régional" (European Union, FEDER Auvergne 2020) (Matthieu Jabaudon).

The funders had no influence in the preparation of this article.

Conflicts of Interest

Matthieu Jabaudon is a principal investigator of the SEvoflurane for Sedation in ARds (SESAR) (ClinicalTrials.gov Identifier: NCT04235608) and the ISCA study (ClinicalTrials.gov Identifier: NCT04383730), which are co-funded and funded, respectively, by grants from Sedana Medical. Matthieu Jabaudon received fees from Sedana Medical for participation in a scientific advisory panel in 2019; Matthieu Jabaudon received consulting fees from Abbvie in 2020 and 2021. Neither Sedana Medical nor Abbvie has had any influence in preparing this manuscript. The other authors do not have any interests to disclose.

Ethical Statement

Not applicable to this review article.

References

[1] Weinert CR, Calvin AD. Epidemiology of sedation and sedation adequacy for mechanically ventilated patients in a medical and surgical intensive care unit. Crit Care Med 2007;35:393–401.
[2] Ely EW. The ABCDEF Bundle: Science and Philosophy of How ICU Liberation Serves Patients and Families. Crit Care Med 2017;45:321–30.
[3] Devlin JW, Skrobik Y, Gélinas C, Needham DM, Slooter AJC, Pandharipande PP, et al. Clinical Practice Guidelines for the Prevention and Management of Pain, Agitation/Sedation, Delirium, Immobility, and Sleep Disruption in Adult Patients in the ICU. Crit Care Med 2018;46:e825–73.
[4] Chanques G, Constantin J-M, Devlin JW, Ely EW, Fraser GL, Gélinas C, et al. Analgesia and sedation in patients with ARDS. Intensive Care Med 2020;46:2342–56.
[5] Payen J-F, Chanques G, Mantz J, Hercule C, Auriant I, Leguillou J-L, et al. Current Practices in Sedation and Analgesia for Mechanically Ventilated Critically Ill PatientsA Prospective Multicenter Patient-based Study. Anesthesiology 2007;106:687–95.
[6] Shehabi Y, Howe BD, Bellomo R, Arabi YM, Bailey M, Bass FE, et al. Early Sedation with Dexmedetomidine in Critically Ill Patients. N Engl J Med 2019;380:2506–17.
[7] Soukup J, Schärff K, Kubosch K, Pohl C, Bomplitz M, Kompardt J. State of the art: sedation concepts with volatile anesthetics in critically Ill patients. J Crit Care 2009;24:535–44.
[8] DAS-Taskforce 2015, Baron R, Binder A, Biniek R, Braune S, Buerkle H, et al. Evidence and consensus based guideline for the management of delirium, analgesia, and sedation in intensive care medicine. Revision 2015 (DAS-Guideline 2015) - short version. Ger Med Sci 2015;13. Doc19.
[9] Jerath A, Parotto M, Wasowicz M, Ferguson ND. Volatile Anesthetics. Is a New Player Emerging in Critical Care Sedation? Am J Respir Crit Care Med 2016;193:1202–12.
[10] Blondonnet R, Quinson A, Lambert C, Audard J, Godet T, Zhai R, et al. Use of volatile agents for sedation in the intensive care unit: A national survey in France. PLoS One 2021;16e0249889.
[11] Jerath A, Ferguson ND, Cuthbertson B. Inhalational volatile-based sedation for COVID-19 pneumonia and ARDS. Intensive Care Med 2020;46:1563–6.
[12] Ferrière N, Bodenes L, Bailly P, L'Her E. Shortage of anesthetics: Think of inhaled sedation! J Crit Care 2021;63:104–5.
[13] Meiser A. Inhaled sedation in the intensive care unit: A new option and its technical prerequisites. Springer Fachmedien Wiesbaden; 2019.
[14] Mesnil M, Capdevila X, Bringuier S, Trine P-O, Falquet Y, Charbit J, et al. Long-term sedation in intensive care unit: a randomized comparison between inhaled sevoflurane and intravenous propofol or midazolam. Intensive Care Med 2011;37:933–41.
[15] Meiser A, Volk T, Wallenborn J, Guenther U, Becher T, Bracht H, et al. Inhaled isoflurane via the anaesthetic conserving device versus propofol for sedation of invasively ventilated patients in intensive care units in Germany and Slovenia: an open-label, phase 3, randomised controlled, non-inferiority trial. Lancet Respir Med 2021;9:1231–40.
[16] Georgevici A-I, Kyprianou T, Herzog-Niescery J, Procopiuc L, Loganathan S, Weber TP, et al. Negative drift of sedation depth in critically ill patients receiving constant minimum alveolar concentration of isoflurane, sevoflurane, or desflurane: a randomized controlled trial. Crit Care 2021;25:141.
[17] Sackey PV, Radell PJ, Granath F, Martling CR. Bispectral index as a predictor of sedation depth during isoflurane or midazolam sedation in ICU patients. Anaesth Intensive Care 2007;35:348–56.
[18] Blanchard F, Perbet S, James A, Verdonk F, Godet T, Bazin J-E, et al. Minimal alveolar concentration for deep sedation (MAC-DS) in intensive care unit patients sedated with sevoflurane: A physiological study. Anaesth Crit Care Pain Med 2020;39:429–34.
[19] Breheny FX, Kendall PA. Use of isoflurane for sedation in intensive care. Crit Care Med 1992;20:1062–4.
[20] Sackey PV, Martling C-R, Radell PJ. Three cases of PICU sedation with isoflurane delivered by the "AnaConDa.". Paediatr Anaesth 2005;15:879–85.
[21] Redaelli S, Mangili P, Ormas V, Sosio S, Peluso L, Ponzoni F, et al. Prolonged sedation in ARDS patients with inhaled anesthetics: our experience. Crit Care 2013;17P386.
[22] Sethi R, Mahon SV. Tracheal extubation under deep sevoflurane anesthesia: A novel strategy for weaning difficulties in intensive care. J Anaesthesiol Clin Pharmacol 2013;29:238–40.
[23] Hamanaka N, Taniguchi A, Tanigami H, Yoshiya I. [Sevoflurane inhalation reduced bronchospasm after extubation]. Masui 1996;45:1131–4.
[24] Hanidziar D. Use of anaesthesia machines for mechanical ventilation and sedation in patients with COVID-19 ARDS. Br J Anaesth 2021;10. S0007-0912(21)00275-0.
[25] Bottiroli M, Calini A, Pinciroli R, Mueller A, Siragusa A, Anelli C, et al. The repurposed use of anesthesia machines to ventilate critically ill patients with Coronavirus Disease 2019 (COVID-19). BMC Anesthesiol 2021;21:155.
[26] Daume P, Weis J, Bomberg H, Bellgardt M, Volk T, Groesdonk HV, et al. Washout and Awakening Times after Inhaled Sedation of Critically Ill Patients: Desflurane Versus Isoflurane. J Clin Med Res 2021;10:665.
[27] Chabanne R, Perbet S, Futier E, Ben Said NA, Jaber S, Bazin J-E, et al. Impact of the anesthetic conserving device on respiratory parameters and work of breathing in critically ill patients under light sedation with sevoflurane. Anesthesiology 2014;121:808–16.
[28] Jabaudon M, Boucher P, Imhoff E, Chabanne R, Faure J-S, Roszyk L, et al. Sevoflurane for Sedation in Acute Respiratory Distress Syndrome. A Randomized Controlled Pilot Study. Am J Respir Crit Care Med 2017;195:792–800.
[29] Jerath A, Panckhurst J, Parotto M, Lightfoot N, Wasowicz M, Ferguson ND, et al. Safety and Efficacy of Volatile Anesthetic Agents Compared With Standard Intravenous Midazolam/Propofol Sedation in Ventilated Critical Care Patients: A Meta-analysis and Systematic Review of Prospective Trials. Anesth Analg 2017;124:1190–9.
[30] Kim HY, Lee JE, Kim HY, Kim J. Volatile sedation in the intensive care unit: A systematic review and meta-analysis. Medicine 2017;96:e8976.
[31] Jerath A, Wong K, Wasowicz M, Fowler T, Steel A, Grewal D, et al. Use of Inhaled Volatile Anesthetics for Longer Term Critical Care Sedation: A Pilot Randomized Controlled Trial. Critical Care Explorations 2020;2:e0281.
[32] Herzog-Niescery J, Vogelsang H, Gude P, Seipp H-M, Bartz H, Uhl W, et al. The impact of the anesthetic conserving device on occupational exposure to isoflurane among intensive care healthcare professionals. Minerva Anestesiol 2018;84:25–32.
[33] Fujinaga M, Baden JM, Yhap EO, Mazze RI. Reproductive and teratogenic effects of nitrous oxide, isoflurane, and their combination in Sprague-Dawley rats. Anesthesiology 1987;67:960–4.
[34] Mazze RI, Fujinaga M, Baden JM. Reproductive and teratogenic effects of nitrous oxide, fentanyl and their combination in Sprague-Dawley rats. Br J Anaesth 1987;59:1291–7.
[35] Mazze RI, Wilson AI, Rice SA, Baden JM. Fetal development in mice exposed to isoflurane. Teratology 1985;32:339–45.
[36] Muyldermans M, Jennes S, Morrison S, Soete O, François P-M, Keersebilck E, et al. Partial Nephrogenic Diabetes Insipidus in a Burned Patient Receiving Sevoflurane Sedation With an Anesthetic Conserving Device-A Case Report. Crit Care Med 2016;44:e1246–1250.
[37] Maussion E, Combaz S, Cuisinier A, Chapuis C, Payen J-F. Renal dysfunction during sevoflurane sedation in the ICU: A case report. Eur J Anaesthesiol 2019;36:377–9.
[38] L'Heudé M, Poignant S, Elaroussi D, Espitalier F, Ferrandière M, Laffon M. Nephrogenic diabetes insipidus associated with prolonged sedation with sevoflurane in the intensive care unit. Br J Anaesth 2019;122:e73–5.
[39] Sackey PV, Martling C-R, Granath F, Radell PJ. Prolonged isoflurane sedation of intensive care unit patients with the Anesthetic Conserving Device. Crit Care Med 2004;32:2241–6.
[40] Sackey PV, Martling C-R, Carlswärd C, Sundin O, Radell PJ. Short- and long-term follow-up of intensive care unit patients after sedation with isoflurane and midazolam–a pilot study. Crit Care Med 2008;36:801–6.
[41] Meiser A, Sirtl C, Bellgardt M, Lohmann S, Garthoff A, Kaiser J, et al. Desflurane compared with propofol for postoperative sedation in the intensive care unit. Br J Anaesth 2003;90:273–80.
[42] Bellgardt M, Bomberg H, Herzog-Niescery J, Dasch B, Vogelsang H, Weber TP, et al. Survival after long-term isoflurane sedation as opposed to intravenous sedation in critically ill surgical patients: Retrospective analysis. Eur J Anaesthesiol 2016;33:6–13.
[43] Bourdeaux D, Sautou-Miranda V, Montagner A, Perbet S, Constantin JM, Bazin J-E, et al. Simple assay of plasma sevoflurane and its metabolite hexafluoroisopropanol by headspace GC–MS. Journal of Chromatography B 2010;878:45–50.
[44] Perbet S, Bourdeaux D, Sautou V, Pereira B, Chabanne R, Constantin JM, et al. A pharmacokinetic study of 48-hour sevoflurane inhalation using a disposable delivery system (AnaConDa®) in ICU patients. Minerva Anestesiol 2014;80:655–65.
[45] Perbet S, Bourdeaux D, Lenoire A, Biboulet C, Pereira B, Sadoune M, et al. Sevoflurane for procedural sedation in critically ill patients: A pharmacokinetic comparative study between burn and non-burn patients. Anaesth Crit Care Pain Med 2018;37:551–6.
[46] Flinspach AN, Zacharowski K, Ioanna D, Adam EH. Volatile Isoflurane in Critically Ill Coronavirus Disease 2019 Patients-A Case Series and Systematic Review. Crit Care Explor 2020;2:e0256.

[47] Jerath A, Beattie SW, Chandy T, Karski J, Djaiani G, Rao V, et al. Volatile-based short-term sedation in cardiac surgical patients: a prospective randomized controlled trial. Crit Care Med 2015;43:1062–9.
[48] Hellström J, Öwall A, Bergström J, Sackey PV. Cardiac outcome after sevoflurane versus propofol sedation following coronary bypass surgery: a pilot study. Acta Anaesthesiol Scand 2011;55:460–7.
[49] Hellström J, Öwall A, Sackey PV. Wake-up times following sedation with sevoflurane versus propofol after cardiac surgery. Scand Cardiovasc J 2012;46:262–8.
[50] Uhlig C, Bluth T, Schwarz K, Deckert S, Heinrich L, De Hert S, et al. Effects of Volatile Anesthetics on Mortality and Postoperative Pulmonary and Other Complications in Patients Undergoing Surgery: A Systematic Review and Meta-analysis. Anesthesiology 2016;124:1230–45.
[51] Hashiguchi H, Morooka H, Miyoshi H, Matsumoto M, Koji T, Sumikawa K. Isoflurane Protects Renal Function Against Ischemia and Reperfusion Through Inhibition of Protein Kinases, JNK and ERK. Anesthesia & Analgesia 2005;101:1584–9.
[52] Obal D, Rascher K, Favoccia C, Dettwiler S, Schlack W. Post-conditioning by a short administration of desflurane reduced renal reperfusion injury after differing of ischaemia times in rats. Br J Anaesth 2006;97:783–91.
[53] Fukazawa K, Lee HT. Volatile anesthetics and AKI: risks, mechanisms, and a potential therapeutic window. J Am Soc Nephrol 2014;25:884–92.
[54] Lv X, Yang L, Tao K, Liu Y, Yang T, Chen G, et al. Isoflurane preconditioning at clinically relevant doses induce protective effects of heme oxygenase-1 on hepatic ischemia reperfusion in rats. BMC Gastroenterol 2011;11:31.
[55] Sakai H, Sheng H, Yates RB, Ishida K, Pearlstein RD, Warner DS. Isoflurane Provides Long-term Protection against Focal Cerebral Ischemia in the Rat. Anesthesiology 2007;106:92–9.
[56] Hert SGD, De Hert SG, Van der Linden PJ, Cromheecke S, Meeus R, ten Broecke PW, et al. Choice of Primary Anesthetic Regimen Can Influence Intensive Care Unit Length of Stay after Coronary Surgery with Cardiopulmonary Bypass. Anesthesiology 2004;101:9–20.
[57] O'Gara B, Talmor D. Lung protective properties of the volatile anesthetics. Intensive Care Med 2016;42:1487–9.
[58] Suter D, Spahn DR, Blumenthal S, Reyes L, Booy C, Z'graggen BR, et al. The immunomodulatory effect of sevoflurane in endotoxin-injured alveolar epithelial cells. Anesth Analg 2007;104:638–45.
[59] Yue T, Roth Z'graggen B, Blumenthal S, Neff SB, Reyes L, Booy C, et al. Post-conditioning with a volatile anaesthetic in alveolar epithelial cells in vitro. Eur Respir J 2008;31:118–25.
[60] Steurer M, Schläpfer M, Steurer M, Z'graggen BR, Booy C, Reyes L, et al. The volatile anaesthetic sevoflurane attenuates lipopolysaccharide-induced injury in alveolar macrophages. Clin Exp Immunol 2009;155:224–30.
[61] Kim S-H, Li M, Pyeon T-H, So K-Y, Kwak S-H. The volatile anesthetic sevoflurane attenuates ventilator-induced lung injury through inhibition of ERK1/2 and Akt signal transduction. Korean J Anesthesiol 2015;68:62–9.
[62] Du X, Jiang C, Lv Y, Dull RO, Zhao Y-Y, Schwartz DE, et al. Isoflurane promotes phagocytosis of apoptotic neutrophils through AMPK-mediated ADAM17/Mer signaling. PLoS One 2017;12e0180213.
[63] Fortis S, Spieth PM, Lu W-Y, Parotto M, Haitsma JJ, Slutsky AS, et al. Effects of anesthetic regimes on inflammatory responses in a rat model of acute lung injury. Intensive Care Med 2012;38:1548–55.
[64] Ohsumi A, Marseu K, Slinger P, McRae K, Kim H, Guan Z, et al. Sevoflurane Attenuates Ischemia-Reperfusion Injury in a Rat Lung Transplantation Model. Ann Thorac Surg 2017;103:1578–86.
[65] Voigtsberger S, Lachmann RA, Leutert AC, Schläpfer M, Booy C, Reyes L, et al. Sevoflurane ameliorates gas exchange and attenuates lung damage in experimental lipopolysaccharide-induced lung injury. Anesthesiology 2009;111:1238–48.
[66] Ferrando C, Aguilar G, Piqueras L, Soro M, Moreno J, Belda FJ. Sevoflurane, but not propofol, reduces the lung inflammatory response and improves oxygenation in an acute respiratory distress syndrome model: A randomised laboratory study. Eur J Anaesthesiol 2013;30:455–63.
[67] Kellner P, Müller M, Piegeler T, Eugster P, Booy C, Schläpfer M, et al. Sevoflurane Abolishes Oxygenation Impairment in a Long-Term Rat Model of Acute Lung Injury. Anesth Analg 2017;124:194–203.
[68] Englert JA, Macias AA, Amador-Munoz D, Pinilla Vera M, Isabelle C, Guan J, et al. Isoflurane Ameliorates Acute Lung Injury by Preserving Epithelial Tight Junction Integrity. Anesthesiology 2015;123:377–88.
[69] Schläpfer M, Leutert AC, Voigtsberger S, Lachmann RA, Booy C, Beck-Schimmer B. Sevoflurane reduces severity of acute lung injury possibly by impairing formation of alveolar oedema. Clin Exp Immunol 2012;168:125–34.
[70] Hanidziar D, Baldyga K, Ji CS, Lu J, Zheng H, Wiener-Kronish J, et al. Standard Sedation and Sedation With Isoflurane in Mechanically Ventilated Patients With Coronavirus Disease 2019. Crit Care Explor 2021;3:e0370.
[71] Meiser A, Bomberg H, Lepper PM, Trudzinski FC, Volk T, Groesdonk HV. Inhaled Sedation in Patients With Acute Respiratory Distress Syndrome Undergoing Extracorporeal Membrane Oxygenation. Anesth Analg 2017;125:1235–9.
[72] 36th International Symposium on Intensive Care and Emergency Medicine: Brussels, Belgium. 15-18 March 2016. Crit Care 2016;20:94.
[73] Heider J, Bansbach J, Kaufmann K, Heinrich S, Loop T, Kalbhenn J. Does volatile sedation with sevoflurane allow spontaneous breathing during prolonged prone positioning in intubated ARDS patients? A retrospective observational feasibility trial. Ann Intensive Care 2019;9:41.
[74] Bailly P, Egreteau P-Y, Ehrmann S, Thille AW, Guitton C, Grillet G, et al. Inased (inhaled sedation in ICU) trial protocol: a multicentre randomised open-label trial. BMJ Open 2021;11e042284.
[75] L'her E, Dy L, Pili R, Prat G, Tonnelier J-M, Lefevre M, et al. Feasibility and potential cost/benefit of routine isoflurane sedation using an anesthetic-conserving device: a prospective observational study. Respir Care 2008;53:1295–303.
[76] Röhm KD, Wolf MW, Schöllhorn T, Schellhaass A, Boldt J, Piper SN. Short-term sevoflurane sedation using the Anaesthetic Conserving Device after cardiothoracic surgery. Intensive Care Med 2008;34:1683–9.
[77] Sackey PV, Martling C-R, Nise G, Radell PJ. Ambient isoflurane pollution and isoflurane consumption during intensive care unit sedation with the Anesthetic Conserving Device. Crit Care Med 2005;33:585–90.

STUDY N°2

From preclinical to clinical models of acute respiratory distress syndrome

Ruoyang Zhai, Woodys Lenga Ma Bonda, Gustavo Matute-Bello, Matthieu Jabaudon. **Signa Vitae 2022. Vol.18, Issue 1, January 2022 pp.3-14**. doi: 10.22514/sv.2021.228

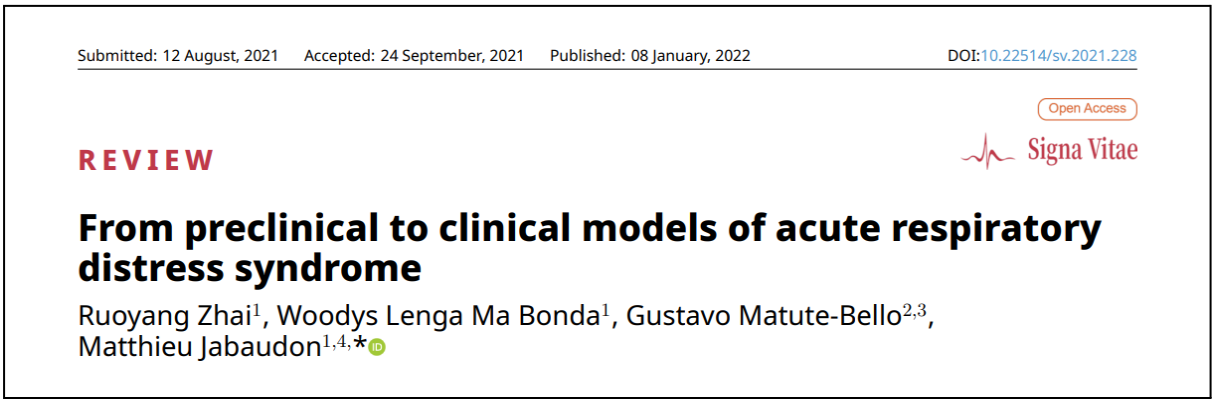

Submitted: 12 August, 2021 Accepted: 24 September, 2021 Published: 08 January, 2022 DOI:10.22514/sv.2021.228

Open Access

REVIEW

Signa Vitae

From preclinical to clinical models of acute respiratory distress syndrome

Ruoyang Zhai[1], Woodys Lenga Ma Bonda[1], Gustavo Matute-Bello[2,3], Matthieu Jabaudon[1,4,*]

Scientific Knowledge of the Subject

Specific pharmacological therapy is still lacking for acute respiratory distress syndrome (ARDS). This situation may be partly explained by the poor clinical translation of promising therapies from preclinical models, which can be attributable to the intrinsic limitations of the models[219,220].

Research efforts have been held back in part by the difficulty of modeling human ARDS in animals, mainly due its heterogeneity, with many clinical or biological/functional variations among patients, in addition to its distinct causative factors, such as pulmonary or extrapulmonary sepsis, gastric fluid aspiration, transfusions, severe trauma, injurious mechanical ventilation, and/or reperfusion of ischemic tissues, among other causes[221–225]. In this perspective, various preclinical models of "acute lung injury" that mimic the causes of clinical "ARDS" have been used to better understand the mechanisms of injury and its repair, and to develop novel therapies targeting these mechanism[226].

Although most preclinical studies on ARDS have been performed using animal models, other preclinical in vitro models are available and, more recently, the use of clinical models of ARDS has also broadened our ability to decipher injury or repair mechanisms and to identify novel targets for therapy development.

Contributions of this study to the field

In this review, we summarized multiple *in vitro*, *ex vivo*, and *in vivo* experimental models of ARDS which have been developed in recent years, and their strengths and limitations. However, no single model can truly reproduce the complexity and heterogeneity of clinical ARDS. Combining multiple preclinical approaches with *in vivo* and clinical

investigations is probably the most promising strategy for future mechanistic and therapeutic research

Despite some failed experiments, some studies succeeded in advancing our knowledge of the complex mechanisms of ARDS pathophysiology and the clinical translation of a few therapeutic interventions, such as lung-protective mechanical ventilation, neuromuscular blockade, and corticoid therapy[12,14,227]. Therefore, the judicious and imaginative use of a broad range of experimental and analytical approaches is of paramount importance in developing translational discovery research, with the goal of developing prediction medicine strategies to ultimately improve patient outcomes.

Submitted: 12 August, 2021 Accepted: 24 September, 2021 Published: 08 January, 2022 DOI:10.22514/sv.2021.228

Open Access
Signa Vitae

REVIEW

From preclinical to clinical models of acute respiratory distress syndrome

Ruoyang Zhai[1], Woodys Lenga Ma Bonda[1], Gustavo Matute-Bello[2,3], Matthieu Jabaudon[1,4,*]

[1]GReD, Université Clermont Auvergne, CNRS, INSERM, 63000 Clermont-Ferrand, France
[2]Center for Lung Biology, Division of Pulmonary, Critical Care and Sleep Medicine, Department of Medicine, University of Washington, Seattle, WA 98105, USA
[3]Medical Research Service, VA Puget Sound Healthcare System, Seattle, WA 98105, USA
[4]Department of Perioperative Medicine, CHU Clermont-Ferrand, 63000 Clermont-Ferrand, France

***Correspondence**
mjabaudon@chu-clermontferrand.fr
(Matthieu Jabaudon)

Abstract

Various preclinical models that mimic the clinical causes of acute respiratory distress syndrome (ARDS) have been used to better understand the mechanisms of acute lung injury and its repair and to investigate novel therapies targeting such mechanisms. Despite important preclinical and clinical research efforts in recent decades, few candidate therapies with promising preclinical effects have been successfully translated into the clinical scenario, which could be attributable to the intrinsic limitations of the models as well as to the incorrect identification of appropriate phenotypes of patients to target with novel therapies that have proven beneficial in select preclinical models. However, current translational research strategies based on the use of multiple complementary preclinical and clinical models hold the promise of revolutionizing intensive care by using granular knowledge that should allow for a better diagnosis, greater predictability of the disease course, and the development of targeted therapies while ensuring patient safety through reduced adverse effects. Our goal was to summarize the strengths and limitations of the available models of ARDS, including animal, *in vitro*, and clinical models, and to discuss the current challenges and perspectives for research.

Keywords

Acute respiratory distress syndrome; Acute lung injury; Preclinical models; Translational research

1. Introduction

The acute respiratory distress syndrome (ARDS) is a severe form of acute lung injury characterized by the onset of hypoxemic respiratory failure associated with noncardiogenic pulmonary edema and dysregulated inflammatory responses [1–3]. The incidence of the syndrome is high, representing approximately 10% of patients admitted to the intensive care unit (ICU) and, despite important preclinical and clinical research efforts since its first description in 1967 [4], the syndrome is still associated with high mortality rates and long-term impacts on survivors [5]. Substantial progress has been made in improving supportive intensive care, such as the application of lung-protective mechanical ventilation, but specific pharmacological therapy is still lacking. Although this may be due to the incorrect identification of appropriate subsets of patients to target with novel therapies that have proven beneficial in select preclinical models, it may also be explained by the poor clinical translation of promising therapies from preclinical models, which can be attributable to the intrinsic limitations of the models [6, 7].

Research efforts have been held back in part by the difficulty of modeling human ARDS in animals, mainly due its heterogeneity, with many clinical or biological/functional variations among patients, in addition to its distinct causative factors, such as pulmonary or extrapulmonary sepsis, gastric fluid aspiration, transfusions, severe trauma, injurious mechanical ventilation, and/or reperfusion of ischemic tissues, among other causes [3, 8–11]. In this perspective, various preclinical models of "acute lung injury" that mimic the causes of clinical "ARDS" have been used to better understand the mechanisms of injury and its repair, and to develop novel therapies targeting these mechanisms [12].

Ideally, a comprehensive model of acute lung injury should be able to reproduce all the relevant features of ARDS pathophysiology, including all the physiological, functional, biological, and pathological symptoms related to injury and their consequences. However, such an ideal model mimicking the clinical scenario does not exist, and all the preclinical models have intrinsic limitations and strengths [13, 14]. Importantly, the "ideal" model may not always be the one that best reproduces human ARDS, but the one that is best suited to answer a specific scientific question. For example, despite all their limitations, mouse models remain key for mechanistic studies because of the ease of genetic manipulations, the ability to generate a large cohort in a short time, etc. Large animal models have more translational value but are less well suited to mechanistic studies. This leads to a proposed stepwise approach for animal studies, with reductionistic, targeted ro-

dent models as an initial step to identify potential mechanisms or therapeutic targets, and increasingly translational models (e.g., large animals) as recommended pre-clinical steps as the research gets closer to the bedside (e.g., testing of novel therapeutics). Although most preclinical studies on ARDS have been performed using animal models, other preclinical *in vitro* models are available and, more recently, the use of clinical models of ARDS has also broadened our ability to decipher injury or repair mechanisms and to identify novel targets for therapy development.

In this narrative review, our goal was to summarize the strengths and limitations of the available models of acute lung injury, including animal, *in vitro*, and clinical models, and to discuss the current challenges and prospects for research.

2. *In vivo* models of ARDS

Live animal models of ARDS play an important role as a bridge between clinical and laboratory studies in research translation. The consensus criteria of an *in vivo* model include acute onset of injury, altered alveolar-capillary membrane, alveolar inflammation, and lung histopathological changes that, together, lead to physiological impairment, such as arterial hypoxemia or impaired alveolar fluid clearance (Table 1, Ref. [14]) [14, 15]. Despite the many anatomical and physiological differences between animals and humans influencing the response of the lung to an acute injurious stimulus and affecting the evaluation of lung injury, *in vivo* models are frequently used as a reliable tool to test hypotheses with variably controlled parameters [14]. The latest updates on what constitutes an animal model of ARDS have focused on the clinical presentation, highlighted the importance of some degree of pre-existing lung injury, suggested the use of mechanical ventilation (to better coincide with the most frequent clinical scenario), and recommended the assessment of physiological outcomes to test potential therapeutic candidates [13, 14, 16]. Since no single animal model can fully replicate all the pathophysiological features of ARDS, multiple animal models have been developed, with the goal of replicating, sometimes in a very caricatural way, the clinical risk factors for ARDS, such as aspiration, pulmonary/extra-pulmonary infections, and mechanical ventilation-induced lung injury, among others [2, 3]. Schematically, preclinical ARDS can be caused *in vivo* through direct lung injury (such as after pneumonia or acid installation) or indirect lung injury (such as after peritonitis). "Double-hit" models have also been developed, which are intended to mimic clinical scenarios combining a specific risk factor (such as pneumonia) and a superimposed injury (such as hyperoxia or injurious ventilation) [17].

Different animal species have been used in the models, from large animals, such as non-human primates, pigs, dogs, cattle, sheep, and rabbits, to smaller animals, such as rats and mice. Larger animals are believed to better replicate human conditions, but these models are expensive and require specialized animal facilities. Models using smaller animals, such as mice, are more widely accessible and are a very powerful research tool, as the animals can be genetically modified in multiple ways to facilitate the detailed mechanistic study of complex pathways [13, 18–20].

2.1 Lipopolysaccharide-induced sepsis models

Lipopolysaccharide (LPS), often named endotoxin, is composed of a polar lipid head group (lipid A) and a chain of repeating disaccharides. It is present on the outer membrane of Gram-negative bacteria such as *escherichia coli* and *haemophilus influenzae*. The host response to LPS plays an important role as a mediator of bacterial sepsis via its binding with toll-like receptor 4 and the subsequent secretion of inflammatory mediators [21, 22]. LPS-induced lung injury caused by pulmonary or extra-pulmonary sepsis is one of the most commonly used ARDS models [13]. LPS can be administered into the lungs by intratracheal instillation or inhalation to produce direct lung injury in which the alveolar epithelium is the primary structure that is damaged. LPS can also be administered intraperitoneally or intravenously to reproduce peritonitis or blood infection, respectively, with marked systemic inflammatory response. Interestingly, repeated or continuous LPS exposure has been shown to exacerbate lung injury in models of extrapulmonary ARDS [23]. The LPS model ideally mimics a neutrophilic inflammatory response with increases in intrapulmonary cytokines and is, therefore, typically suitable for studies of inflammatory processes [13, 18]. However, it has significant disadvantages. First, the responses to LPS are highly variable among animal species, depending on the presence or absence of specific lung intravenous macrophages; for example, rodents are more tolerant to endotoxin exposure than pigs or sheep. Rodent models have been widely used to study LPS-induced lung injury due to their availability, easy accommodation, and relatively low cost. However, rodents are small animals with limited blood volume available for serial sampling [13, 24]. The endotoxin preparations used in animal studies may also vary in serotype and purity and can be contaminated with bacterial lipoproteins and other bacterial materials [25]. The duration of LPS exposure may also introduce some variability in the published results. In addition, the LPS model is often associated with mild changes in alveolar-capillary permeability and degrees of endothelial and epithelial injury, thus limiting clinical translation.

2.2 Live bacteria-induced sepsis models

Intrapulmonary or intravenous administration of live bacteria is another option to induce sepsis in animal models. Intratracheal instillation or inhalation of live bacteria, such as *streptococcus pneumoniae* or *pseudomonas aeruginosa*, can cause ARDS and, depending on the importance of the bacterial inoculum, systemic manifestations of sepsis [26–28]. The intravenous administration of live bacteria is followed within an hour by an initial phase of hypotension and leukopenia, which can progress to septic shock, intravascular coagulation, and death [13, 14]. Typically, live bacteria-induced sepsis models induce increased permeability, interstitial edema, and neutrophilic alveolitis. They are often used for studies of bacterial sepsis-induced lung injury. The intratracheal administration of live bacteria often results in localized pneumonia (rather than ARDS) in histological studies; however, the unilateral administration of bacteria can result in lung injury in the

TABLE 1. Features of experimental acute respiratory distress syndrome in animals and their main relevant measures in animals, as proposed by the official American Thoracic Society workshop report published in 2011 [14].

Features of experimental ARDS	Very relevant measures
Histological evidence of tissue injury	• Accumulation of neutrophils in the alveolus or the interstitium
	• Presence of hyaline membranes
	• Presence of proteinaceous debris in the alveolus
	• Thickening of the alveolar wall
	• Enhanced injury as measured by a standardized histology score
Alteration of the alveolar-capillary barrier	• Increase in extravascular lung water content
	• Accumulation of an exogenous tracer in the alveolar spaces or the extravascular compartment
	• Increase in total bronchoalveolar protein concentration
	• Increase in concentration of high molecular weight proteins in bronchoalveolar fluid (such as albumin, immunoglobulin M (IgM))
	• Increase in the microvascular filtration coefficient
Inflammatory response	• Increase in the absolute number of neutrophils in bronchoalveolar fluid
	• Increase in lung myeloperoxidase activity or protein concentration
	• Increase in the concentrations of proinflammatory cytokines in lung tissue or bronchoalveolar fluid
Physiological dysfunction	• Hypoxemia
	• Increased alveolar–arterial oxygen difference

It is recommended that at least three of the four "main" features are present in animal models of acute respiratory distress syndrome, and that at least one of the "very relevant" measures is performed for each feature of interest. This list of measures is indicative and may not be exhaustive, meaning that other measures may be relevant.

contralateral lung, depending on the bacterial dose. Therefore, the main technical issue with this model resides in the potential variability in the doses of live bacteria being administered.

Although viral infections are less frequent clinical causes of ARDS than bacterial infections outside of some specific pandemics (e.g., the coronavirus disease 2019 pandemic) [3, 5], animal models of viral pneumonia-induced lung injury are also being used to study the specific responses to or test the potential therapies for pathogens, such as influenza viruses or coronaviruses [29, 30].

2.3 Acid aspiration model

Gastric aspiration is one of the common causes leading to the development of ARDS in patients [31, 32]. This neutrophil-dependent form of lung injury is characterized by damage to the alveolar epithelium, alveolar hemorrhage, and intra-alveolar and interstitial edema. One of the most important features of this toxic process is the low pH of the gastric content, and hydrochloric acid (HCl) intratracheal instillation is the most used method to mimic gastric aspiration in animals, in particular in mice or larger animals such as pigs. This model induces the pathophysiological hallmarks of ARDS, with neutrophil recruitment and moderate effects on mortality [13]. The acid aspiration model is particularly useful for studying mechanisms of disruption of the alveolar-capillary barrier and of neutrophil recruitment. In addition, this reproducible model can be used to study the resolution phase of ARDS over multiple days after injury [33–35]. However, the narrow margin between injurious and noninjurious acid concentrations remains a limitation.

2.4 Abdominal sepsis models

Multiple models of peritonitis-induced lung injury have been described. In the cecal ligation and puncture (CLP) model, the cecum is ligated and punctured with a needle. The severity of the injury depends on the number of holes in the cecum and the size of the needle. In contrast to models using LPS and live bacteria, in which the effects are almost immediate, the effects of CLP develop over days, and the onset is less abrupt and consistent [13]. The main features of CLP-induced lung injury are mild hypoxemia, neutrophilic inflammation, and interstitial and alveolar edema, thus providing a complex representation of clinical extra-pulmonary sepsis [13]. Abdominal sepsis models can, therefore, be useful to study mechanisms of indirect lung injury due to sepsis. However, mortality is high, ranging from 25% at 18 h to 70–90% at 30 h, and it requires invasive surgery, although alternative surgical methods have been reported, such as colon ascendens stent peritonitis and laparoscopic cecal ligation [36, 37]. Other investigators have used intraperitoneal inoculation of fibrin clots containing controlled inoculum of bacteria, such as *escherichia coli*, to reproduce peritonitis-induced lung injury in mice and rabbits; in this model, lung injury more likely occurred at high doses, with overwhelmed host response, while lower doses only caused mild lung injury, such as in CLP model [38]. A more reliable and titratable model of peritonitis by the intraperitoneal injection of cecal slurry has been recently used to induce indirect ARDS [39, 40]. This model was first adapted from a neonatal necrotizing enterocolitis model [41]. Briefly, cecal contents are collected from euthanized donor mice, resuspended, and filtered before intraperitoneal injection.

2.5 Ventilator-induced lung injury

The use of ventilator-induced lung injury models has largely contributed to our understanding of the clinical benefits of lung-protective strategies of mechanical ventilation [42, 43]. Ventilation with high tidal volumes, especially without positive end-expiratory pressure, is associated with alveolar recruitment of inflammatory cells, changes in water and protein permeability, and histological injury, and, in general, severe hypoxemia develops within several hours [13, 14]. Although increased alveolar cytokine release has been reported in isolated lung preparations from mice and rats, it may not be present in all species. In addition, these models generally use very high tidal volumes (20–30 mL/kg body weight), which are not necessarily very relevant for clinical translation. However, they are very useful to study mechanical stretch and the activation of specific intracellular pathways involved in mechanotransduction. The effects of moderate increases in tidal volumes or of other changes in ventilator settings are best investigated in a "double-hit" model, following another primary insult.

2.6 Hyperoxia model

Prolonged exposure to hyperoxia may cause hyperoxia-induced lung injury in humans, with alveolar edema and endothelial and epithelial injury [44]. Animal models of hyperoxia have been used as direct lung injury models, sometimes as a secondary hit after peritonitis or LPS [45, 46]. The mechanism of hyperoxia-induced lung injury remains unclear and may be mediated by reactive oxygen species. The hyperoxia model provides an excellent model to study lung repair after lung injury. However, the major limitations are that this model requires specific equipment and prolonged exposure (for 72 h in many studies) [13].

2.7 Ischemia/Reperfusion model

Ischemia and reperfusion following lung transplantation or at other nonpulmonary sites can lead to a wide range of effects, including lung injury. This injury is associated with alveolar edema, epithelial and endothelial injury, inflammatory responses, massive production of free reactive oxygen species, and hypoxemia [13, 47]. Direct lung ischemia is generally induced by clamping the pulmonary artery, followed by reperfusion of the pulmonary and bronchial circulations. This model reproduces the development of acute lung injury after lung, intestinal or peripheral ischemia and reperfusion in humans and is probably more clinically relevant to transplantation studies than to ARDS. Of note, innovative approaches have been developed to allow non-invasive and repetitive in vivo microscopy of ectopic lung tissue using dorsal skinfold chambers in transplantation studies [48]. The main limitation of the ischemia/reperfusion model is that it requires specific surgical skills and equipment [13, 49, 50].

2.8 Models of viral infections

Live animal models of acute lung injury can be used to study the mechanisms of ARDS due to viruses, such as influenza viruses or, more recently, the severe acute respiratory syndrome coronavirus 2 (SARS-CoV-2) [51–54]. Results from these models have emphasized the major role of the inflammatory host immune response to infection as a major contributor to lung injury. Although most airborne viruses initially affect the respiratory epithelium, the role of endothelial dysfunction has not been well established, and pathogen-specific pathways may contribute to diffuse alveolar damage [55]. Small animal models are widely used to study viral infections; however, translation may require genetic modifications (to the animal and/or the virus) to make the model susceptible, for example to SARS-CoV-2 [54]. Animal models can be rapidly mobilized to better understand the mechanisms of emerging viruses, such as during the recent coronavirus disease 2019 (COVID-19) pandemic, and to test new diagnostic, preventive, and/or therapeutic approaches [30].

2.9 Other models

The oleic acid model was first used to mimic clinical ARDS, although it is primarily based on the induction of fat embolism [56]. The intravenous administration of oleic acid leads to direct lung endothelial injury caused by necrosis and microvascular thrombosis. This model is rather reproducible, rapidly reproduces the most basic features of experimental ARDS in large animal models (pigs/piglets, sheep, dogs) [57–59], and is particularly useful to study lung mechanics, ventilatory strategies, and ventilation/perfusion distribution during acute lung injury. However, it is now seldom performed; its main limitations include a high mortality rate, a difficult application in smaller animals, and unclear effects on alveolar inflammation [13, 60].

Alveolar surfactant proteins regulate surface tension during breathing, and surfactant deficiency and dysfunction are frequent during ARDS [3], primarily due to decreased secretion by injured alveolar type II epithelial cells [61]. Surfactant depletion can be modeled by repeated saline lavage of the lungs and this model has good value to study surfactant functions and to assess the effects of ventilation strategies in animals. It induces rapid and reproducible, yet transient, hypoxemia and alveolar recruitment but only modest lung injury per se and very little neutrophil recruitment [13, 60, 62, 63].

Whether the bleomycin model is a good acute lung injury model is still discussed by many researchers, as it is one the few that leads to an acute inflammatory phase followed by a fibrotic phase that eventually resolves [13, 14].

3. *In vitro* models of ARDS

In vitro cell culture models can provide a direct link to lung cell responses in a simplified way and represent valuable methods to investigate basic biological and functional mechanisms and roles for specific cell types, receptors or pathways. They allow the manipulation of one or multiple variables through rigorously controlled, bias-free experiments to investigate the variation in quantitative protein markers, physiological functions, and/or gene expression in response to multiple conditions, including candidate therapies targeting precise mechanisms of injury or repair.

A monoculture of either alveolar epithelial, lung endothelial, or alveolar macrophages, among other cell types, can be performed to test mechanistic hypotheses or optimize the experimental parameters in subsequent *in vivo* or clinical research. *In vitro* monocultures can also be used to study important cellular functions, such as wound healing after a scratch assay [64] or transepithelial fluid transport by alveolar epithelial cells (often called “alveolar fluid clearance” *in vivo*), using transwell experiments [65, 66]. For example, monolayer cultures of commercialized, immortalized or primary isolated alveolar epithelial type I (AT I) or type II (AT II) cells have been used to mimic the alveolar epithelium and its barrier function [67]). Non-sterile inflammation was first studied in 2D monoculture or classical culture models exposed to LPS *in vitro*, mimicking the clinical infection with Gram-negative bacteria [68–72]. In contrast, the setting of sterile inflammation can be studied *in vitro* by exposing cultured cells to a mixture of cytokines, such as interleukin-1 beta, tumor necrosis factor alpha, and interferon gamma [65, 73, 74]. In addition, some biological mechanisms of mechanical ventilation-induced lung injury have been investigated *in vitro* through exposure to cyclic mechanical stretch, hypercapnia or hyperoxia [75–79]. Interestingly, alveolar epithelial cells or alveolar progenitor cells (such as induced pluripotent stem cells-derived AT2-like cells) can be differentiated at the air-liquid interface, inducing cell polarization, epithelial barrier formation through the establishment of intercellular junctions, and surfactant production.

However, monocultures are unable to reproduce the complexity of the alveolar-capillary environment, and, for example, a traditional submersion culture model does not reproduce the air-liquid environment of human alveoli. The main advances have, therefore, come from modeling the human airway at the air-liquid interface, building co-culture models (such as of epithelial cells and endothelial cells or macrophages), and developing 3D-engineered lung cellular environments. *In vitro* co-culture or multicellular models can better reproduce the *in vivo* environment, compared to 2D monocultures [80]. Unlike 2D cultures, co-culture or multicellular systems can model complex interactions between different cell types in a more relevant environment, such as a model of alveolar-capillary barrier using epithelial and endothelial cells [81, 82]. For example, a 3D multicellular model composed of an alveolar epithelial cell layer cultured in interaction with alveolar macrophages on one side and monocyte-derived dendritic cells on the other has been recently described [67, 81, 83]. *Ex vivo* organoid cultures have also been proposed to better model the multiple features of ARDS. These are 3D models assembled from cultured human alveolar stem cells to reproduce all the characteristics of a functional human alveolus *in vitro* [84]. These cultures are long-term, feeder-free, and chemically defined systems that represent a very powerful model to investigate complex mechanisms, such as those involved in severe acute respiratory syndrome coronavirus 2 infection [85–87]. Ultimately, the combination of microfluidic bioengineering and 3D cell culture has led

to the development of "lung-on-a-chip" models comprising a full alveolar-capillary interface that can be exposed to cyclic ventilation and perfusion [88–90]. This model requires long-term cultures of human cell lines, and it is only very recently that the use of primary human alveolar epithelial cells has been reported [91].

4. Human models of ARDS

4.1 Human in vivo models of ARDS

Because a recognized shortcoming in human ARDS research is the difficulty in translating the findings from bench to bedside, novel *in vivo* models have been successfully developed to investigate the mechanisms of lung injury or therapies for ARDS. These models are major breakthroughs in translational ARDS research and have clear advantages in allowing potentially effective therapies to be readily investigated *in vivo* in humans and to inform subsequent clinical trials in patients.

Seminal studies included intravenous administrations of LPS to human volunteers [92, 93]; however, in some studies, direct lung instillations of LPS [94] or other agents, such as leukotriene B4 (produced by human alveolar macrophages, with potent chemotactic activity for neutrophils) [95], were performed using bronchoscopy. More recently, the inhalation of low-dose LPS by healthy humans was successfully used to replicate alveolar epithelial cell activation, alveolar inflammation, and systemic inflammatory response without causing significant adverse effects [96–99]. In this recently developed human *in vivo* model, lung injury is only transient, and inflammation has mainly been investigated within a few hours after LPS exposure.

4.2 Human ex vivo models of ARDS

An *ex vivo* human lung preparation has recently been proposed to better reflect the *in vivo* settings of experimental ARDS [100]. In this model, donor human lungs that have been rejected for transplantation are ventilated and perfused *ex vivo* and used to study the mechanisms of lung injury, isolate multiple primary lung cell types, and test potential therapies before clinical translation into trials. The model allows for analyses of physiological indices, such as oxygenation and alveolar fluid clearance, and the sampling of multiple tissues and fluids up to 6–10 hours in most experiments [101]. Although the *ex vivo* human lung preparation is rather convenient, inexpensive, and the model closest to clinical conditions, ethical and practical issues in obtaining human lungs for research may exist depending on the country. The main limitation of *ex vivo* models resides in the heterogeneity in human lungs due to donor-specific and pre-procurement variables that limit baseline comparisons of measures among experimental lungs. Notably, in addition to its use in ARDS research, the *ex vivo* human lung preparation is being largely used in conditioning or therapeutic studies of donor lungs before transplantation [102].

5. Perspectives and challenges

Multiple models of acute lung injury induced by the main clinical risk factors for ARDS have been developed *in vitro* (from monocultures to more complex constructions), *in vivo* in animals, *ex vivo* (using human or animal lung preparations), and *in vivo* in human volunteers (Table 2). While no single model can truly reproduce the complexity and heterogeneity of clinical ARDS, combining multiple preclinical approaches with *in vivo* and clinical investigations is probably the most promising strategy for future mechanistic and therapeutic research (Fig. 1). Each experimental model has its limitations. For example, despite the recent developments of 3D cultures and lung organoids, *in vitro* models may probably never reproduce the clinical setting, but they are still very useful to inform mechanistic and drug discovery studies [6]. Recent animal studies are able to better reflect the multiple-hit hypothesis for ARDS pathogenesis, and they can be used to investigate the different phases of ARDS, from onset (such as in the hydrochloric acid and the oleic acid models) to recovery (such as in the hyperoxia acid and the bleomycin models), thus allowing studies of preventive ARDS therapies and the combined effects of pre-existing lung injury and exposure to high lung stress through mechanical ventilation use in the intensive care unit [14, 17, 103]. Animal studies typically use young and healthy animals, and older animals should also be investigated to better reflect the clinical picture of ARDS as a disease of aging. In addition, they do not reproduce the common clinical ARDS settings of patient comorbidities and multiorgan failure, with a prolonged need for intensive care over multiple days, if not weeks, and most studies do not take into consideration the impact of ventilatory settings (e.g., the level of positive end-expiratory pressure) on oxygenation. To distinguish models of acute lung injury from conditions that reflect more subacute or chronic lung injury, maximal lung injury should be evident within 24 hours of exposure to the inciting stimulus [14]. However, although some animal models allow studies of lung injury over multiple days and can capture the different phases of ARDS over time [33], most of them are limited to the first few hours after injury, thus limiting clinical translation and the ability to explore the nonlinearity of biological processes. Another limitation that is particularly relevant in mice is the profound impact of strain variability in murine models of injury; not only a particular observation may not be translatable to humans, but it may not even be translatable to other strains of mice. This highlights the need to restrict mice to mechanistic questions and use more translational models for preclinical studies.

Human models, *in vivo* or *ex vivo*, represent major progress toward the clinical translation of basic findings. In addition to the development of novel preclinical and clinical ARDS models, such as the lung-on-a-chip *in vitro* and the *ex vivo* human lung preparation, recent evolutions in the field of translational ARDS research have been made possible by the refinement of experimental techniques. In particular, the field of genome editing now offers a broad range of opportunities to develop investigational or therapeutic strategies by downregulating or upregulating the expression of a specific gene *in vitro* and *in vivo*, such as with the gene knockout or knockdown techniques based on ribonucleic acid interference or the clustered regularly interspaced short palindromic repeats (CRISPR)/CRISPR-associated protein (Cas) system (capable of site-specific deoxyribonucleic acid

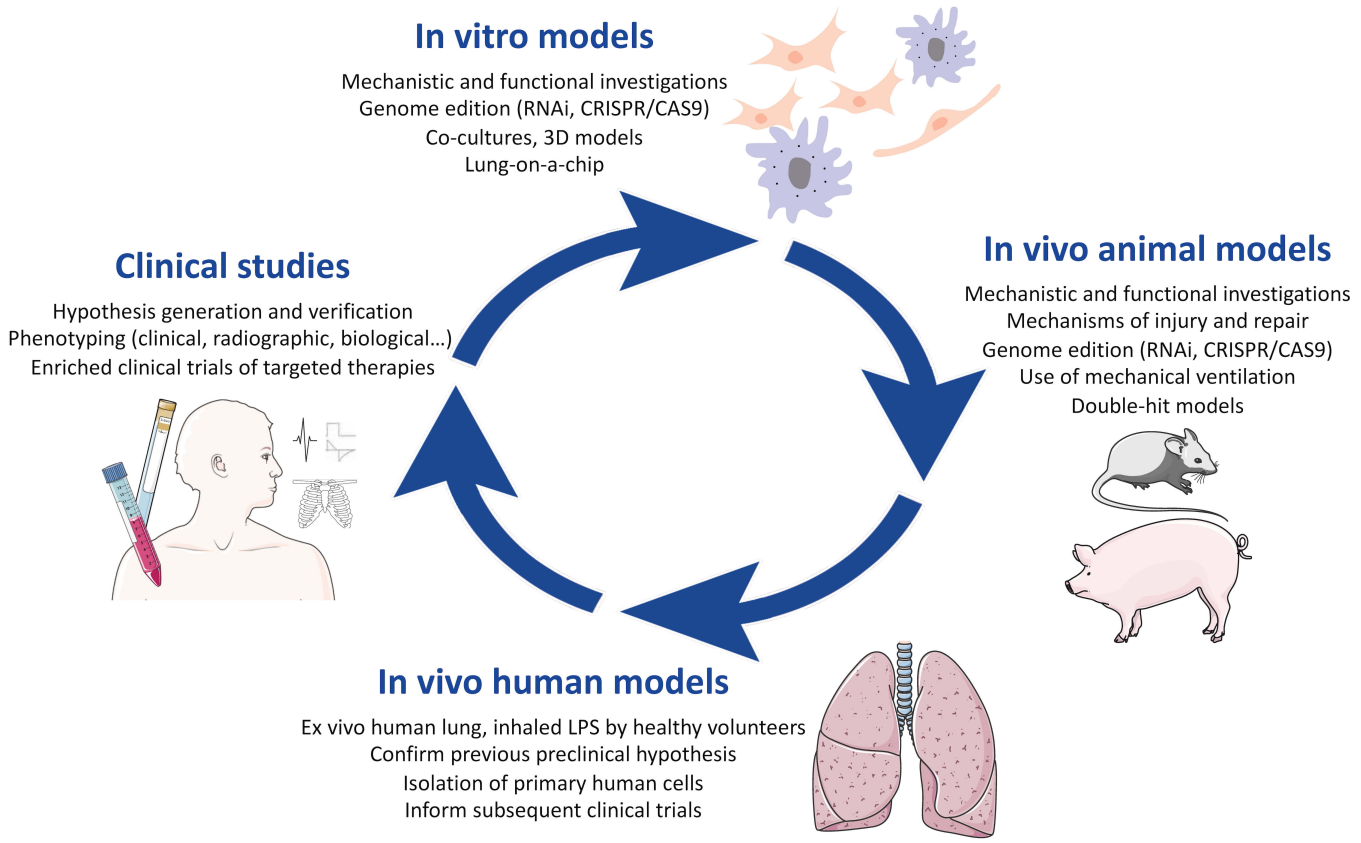

FIGURE 1. Schematic view of a translational research framework based on multiple experimental preclinical approaches and clinical studies. RNAi, interference ribonucleic acid; CRISPR, clustered regularly interspaced short palindromic repeats; CAS9, CRISPR-associated protein 9; LPS, lipopolysaccharide.

cleavage) [89, 104]. Novel methods have also improved our ability to understand the functional significance of polymorphisms or genes identified through genome-wide studies or transcriptomic screens in models and patients, to investigate the potential pathogenic causality for markers or mediators and the potential value of targeting treatment in specific genetic backgrounds. Such innovative approaches have been successfully deployed in COVID-19 research [30].

These traditional and novel experimental designs are important pieces, along with the acquisition of granular clinical, physiological, and biological data (e.g., from bronchoalveolar fluid and blood samples to study mechanisms of lung and systemic responses, respectively, to injury) within clinical studies, in identifying new drug targets, developing targeted therapies, and ultimately selecting patients most likely to benefit. Such strategies of trial enrichment, in which patients are selected who are more likely to develop an outcome, such as mortality (prognostic enrichment), and/or when they are more likely to respond to a targeted therapy (predictive enrichment), hold the promise of precision approaches for ARDS [105–107]. In such a translational framework, preclinical models may reveal that a biological/functional trait or marker has a causal role in the severity of ARDS and suggest that measuring this marker could have value for endotype identification [34, 105, 108, 109]. Ideally, such markers (e.g., biological or radiographic indices) could help in selecting patients to enroll in future precision trials and monitoring their individual responses to the intervention being tested [103, 110–112]. This would require markers that are rapidly available to inform potential trial eligibility. Of note, the first clinical study evaluating a point-of-care assay to prospectively identify hyper- and hypo-inflammatory phenotypes in patients with ARDS and hypoxemic acute respiratory failure is currently enrolling patients (ClinicalTrials.gov Identifier: NCT04009330), and the preliminary results in patients with COVID-19 have been published [113]. However, it remains uncertain to date whether available preclinical models may be representative of known clinical ARDS phenotypes/endotypes or may be helpful to identify phenotype-specific therapy responsive traits [114]. The performance of candidate markers over time during the natural course of ARDS and their kinetics under candidate therapies should also be rigorously evaluated [10]. In addition, even when a diagnostic or therapeutic precision approach is consistently supported by findings across combined preclinical and clinical ARDS models, it should not be associated with adverse effects that may preclude its application to improve patient outcomes.

In conclusion, multiple experimental models have been developed in the last few decades, with major recent developments in the fields of *in vitro*, *ex vivo*, and *in vivo* experimental ARDS. While some of these experiments failed, others succeeded in advancing our knowledge of the complex mechanisms of ARDS pathophysiology and the clinical translation of a few therapeutic interventions, such as lung-protective

TABLE 2. Non-exhaustive list of preclinical and clinical models of acute respiratory distress syndrome.

Setting	Model	Injury feature	Technical notes
Live animal models	Lipopolysaccharide-induced sepsis	Pulmonary or systemic sepsis	Variable response to injury across species
	Live bacteria-induced sepsis		Variability in the doses of live bacteria administered
	Acid aspiration	Direct lung injury	Mimics aspiration of gastric contents
			Narrow margin between injury and absence of injury
	Abdominal sepsis	Peritonitis-induced indirect lung injury	Invasive surgery required with high mortality
			Intraperitoneal injection of cecal slurry more reliable and titratable
	Ventilator-induced lung injury	Direct alveolar injury with severe hypoxemia	High tidal volumes not relevant for clinical translation
	Hyperoxia	Hyperoxia-induced injury	Requires prolonged exposure and specific equipment
	Ischemia-reperfusion	Induced by clamping the pulmonary artery lung or other nonpulmonary arteries	Requires specific surgical skills and equipment
	Viral infection	Acute lung injury of viral causes (mostly airborne viruses)	Can be rapidly mobilized to better understand the mechanisms of emerging viruses
			Translation may require genetic modifications to the animal and/or the virus
In vitro models	Submerged monoculture	Cell injury of sterile or non-sterile causes	Reproducible for testing and establishing experimental conditions
			Submerged cultures or cultures at the air-liquid interface
	Multicellular co-culture	Cell injury of sterile or non-sterile causes in a more relevant multicellular environment	Can model complex interactions between different cell types
	Organoid culture		
	Lung-on-a-chip	Cell injury of sterile or non-sterile causes in a human lung-like environment	Allows multicellular co-culture
			Reproduces all characteristics of a functional human alveolus unit
Human *in vivo* models	Lipopolysaccharide-induced sepsis in human volunteers	Intravenous administration or direct lung instillation of high-dose lipopolysaccharide	Seminal models
		Inhalation of low-dose lipopolysaccharide	Transient lung injury and rapid investigation of inflammation
Human *ex vivo* models	*Ex vivo* human lung preparation	Donor human lungs rejected for transplantation are ventilated and perfused *ex vivo* before exposure to sterile or non-sterile injuries	Most translatable model, allows for analyses of physiological indices
			Rather convenient and inexpensive but potential ethical and practical issues

mechanical ventilation, neuromuscular blockade, and corticoid therapy [115–117]. Therefore, the judicious and imaginative use of a broad range of experimental and analytical approaches is of paramount importance in developing translational discovery research, with the goal of developing prediction medicine strategies to ultimately improve patient outcomes.

AUTHOR CONTRIBUTIONS

RZ, WLMB, and GMB were involved in the conception and design of the review, in writing the paper, and in its revision prior to submission. MJ takes responsibility for the content of the paper and was involved in the conception and design of the review, in writing the paper, and in its revision prior to submission.

ETHICS APPROVAL AND CONSENT TO PARTICIPATE

Not applicable.

ACKNOWLEDGMENT

The authors wish to thank Mrs. Charlotte Leclaire and Mrs. Cécile Saint-Béat at Université Clermont Auvergne, for their opinions and suggestions to improve this review.

FUNDING

This research received no external funding.

CONFLICT OF INTEREST

The authors declare no conflict of interest.

REFERENCES

[1] ARDS Definition Task Force, Ranieri VM, Rubenfeld GD, Thompson BT, Ferguson ND, Caldwell E, *et al*. Acute respiratory distress syndrome: the Berlin Definition. Journal of the American Medical Association. 2012; 307: 2526–33.

[2] Thompson BT, Chambers RC, Liu KD. Acute Respiratory Distress Syndrome. The New England Journal of Medicine. 2017; 377: 562–572.

[3] Matthay MA, Zemans RL, Zimmerman GA, Arabi YM, Beitler JR, Mercat A, *et al*. Acute respiratory distress syndrome. Nature Reviews Disease Primers. 2019; 5: 18.

[4] Ashbaugh DG, Bigelow DB, Petty TL, Levine BE. Acute respiratory distress in adults. Lancet. 1967; 2: 319–323.

[5] Bellani G, Laffey JG, Pham T, Fan E, Brochard L, Esteban A, *et al*. Epidemiology, Patterns of Care, and Mortality for Patients with Acute Respiratory Distress Syndrome in Intensive Care Units in 50 Countries. Journal of the American Medical Association. 2016; 315: 788–800.

[6] Matthay MA, Zimmerman GA, Esmon C, Bhattacharya J, Coller B, Doerschuk CM, *et al*. Future research directions in acute lung injury: summary of a National Heart, Lung, and Blood Institute working group. American Journal of Respiratory and Critical Care Medicine. 2003; 167: 1027–1035.

[7] Matthay MA, McAuley DF, Ware LB. Clinical trials in acute respiratory distress syndrome: challenges and opportunities. The Lancet Respiratory Medicine. 2018; 5: 524–534.

[8] Calfee CS, Eisner MD, Ware LB, Thompson BT, Parsons PE, Wheeler AP, *et al*. Trauma-associated lung injury differs clinically and biologically from acute lung injury due to other clinical disorders. Critical Care Medicine. 2007; 35: 2243–2250.

[9] Tejera P, Meyer NJ, Chen F, Feng R, Zhao Y, O'Mahony DS, *et al*. Distinct and replicable genetic risk factors for acute respiratory distress syndrome of pulmonary or extrapulmonary origin. Journal of Medical Genetics. 2012; 49: 671–680.

[10] Delucchi K, Famous KR, Ware LB, Parsons PE, Thompson BT, Calfee CS. Stability of ARDS subphenotypes over time in two randomised controlled trials. Thorax. 2018; 73: 439–445.

[11] Wilson JG, Calfee CS. ARDS Subphenotypes: Understanding a Heterogeneous Syndrome. Critical Care. 2020; 24: 102.

[12] Juffermans NP, Radermacher P, Laffey JG. The importance of discovery science in the development of therapies for the critically ill. Intensive Care Medicine Experimental. 2020; 8: 17.

[13] Matute-Bello G, Frevert CW, Martin TR. Animal models of acute lung injury. American Journal of Physiology-Lung Cellular and Molecular Physiology. 2008; 295: L379–L399.

[14] Matute-Bello G, Downey G, Moore BB, Groshong SD, Matthay MA, Slutsky AS, *et al*. An official American Thoracic Society workshop report: features and measurements of experimental acute lung injury in animals. American Journal of Respiratory Cell and Molecular Biology. 2011; 44: 725–738.

[15] Matthay MA. Resolution of pulmonary edema. Thirty years of progress. American Journal of Respiratory and Critical Care Medicine. 2014; 189: 1301–1308.

[16] Oakley C, Koh M, Baldi R, Soni S, O'Dea K, Takata M, *et al*. Ventilation following established ARDS: a preclinical model framework to improve predictive power. Thorax. 2019; 74: 1120–1129.

[17] Laffey JG, Kavanagh BP. Fifty Years of Research in ARDS. Insight into Acute Respiratory Distress Syndrome. From Models to Patients. American Journal of Respiratory and Critical Care Medicine. 2017; 196: 18–28.

[18] Bastarache JA, Blackwell TS. Development of animal models for the acute respiratory distress syndrome. Disease Models & Mechanisms. 2009; 2: 218–223.

[19] Aeffner F, Bolon B, Davis IC. Mouse Models of Acute Respiratory Distress Syndrome: a Review of Analytical Approaches, Pathologic Features, and Common Measurements. Toxicologic Pathology. 2015; 43: 1074–1092.

[20] Cockrell AS, Yount BL, Scobey T, Jensen K, Douglas M, Beall A, *et al*. A mouse model for MERS coronavirus-induced acute respiratory distress syndrome. Nature Microbiology. 2016; 2: 16226.

[21] Lu Y, Yeh W, Ohashi PS. LPS/TLR4 signal transduction pathway. Cytokine. 2008; 42: 145–151.

[22] Ciesielska A, Matyjek M, Kwiatkowska K. TLR4 and CD14 trafficking and its influence on LPS-induced pro-inflammatory signaling. Cellular and Molecular Life Sciences. 2021; 78: 1233–1261.

[23] Cheng D, Han W, Chen SM, Sherrill TP, Chont M, Park G, *et al*. Airway epithelium controls lung inflammation and injury through the NF-kappa B pathway. Journal of Immunology. 2007; 178: 6504–6513.

[24] Kohman RA, Crowell B, Kusnecov AW. Differential sensitivity to endotoxin exposure in young and middle-age mice. Brain, Behavior, and Immunity. 2010; 24: 486–492.

[25] Tapping RI, Akashi S, Miyake K, Godowski PJ, Tobias PS. Toll-like receptor 4, but not toll-like receptor 2, is a signaling receptor for Escherichia and Salmonella lipopolysaccharides. Journal of Immunology. 2000; 165: 5780–5787.

[26] Su X, Looney MR, Gupta N, Matthay MA. Receptor for advanced glycation end-products (RAGE) is an indicator of direct lung injury in models of experimental lung injury. American Journal of Physiology-Lung Cellular and Molecular Physiology. 2009; 297: L1–L5.

[27] Matthay MA, Goolaerts A, Howard JP, Lee JW. Mesenchymal stem cells for acute lung injury: preclinical evidence. Critical Care Medicine. 2010; 38: S569–S573.

[28] Asmussen S, Ito H, Traber DL, Lee JW, Cox RA, Hawkins HK, *et al*. Human mesenchymal stem cells reduce the severity of acute lung injury in a sheep model of bacterial pneumonia. Thorax. 2014; 69: 819–825.

[29] Rosas LE, Doolittle LM, Joseph LM, El-Musa H, Novotny MV, Hickman-Davis JM, *et al*. Postexposure Liponucleotide Prophylaxis and Treatment Attenuates Acute Respiratory Distress Syndrome in Influenza-

infected Mice. American Journal of Respiratory Cell and Molecular Biology. 2021; 64: 677–686.

[30] Cleary SJ, Pitchford SC, Amison RT, Carrington R, Robaina Cabrera CL, Magnen M, *et al*. Animal models of mechanisms of SARS-CoV-2 infection and COVID-19 pathology. British Journal of Pharmacology. 2020; 177: 4851–65.

[31] Marik PE. Aspiration pneumonitis and aspiration pneumonia. The New England Journal of Medicine. 2001; 344: 665–671.

[32] Raghavendran K, Nemzek J, Napolitano LM, Knight PR. Aspiration-induced lung injury. Critical Care Medicine. 2011; 39: 818–826.

[33] Patel BV, Wilson MR, Takata M. Resolution of acute lung injury and inflammation: a translational mouse model. The European Respiratory Journal. 2012; 39: 1162–1170.

[34] Jabaudon M, Blondonnet R, Roszyk L, Bouvier D, Audard J, Clairefond G, *et al*. Soluble Receptor for Advanced Glycation End-Products Predicts Impaired Alveolar Fluid Clearance in Acute Respiratory Distress Syndrome. American Journal of Respiratory and Critical Care Medicine. 2015; 192: 191–199.

[35] Chimenti L, Morales-Quinteros L, Puig F, Camprubi-Rimblas M, Guillamat-Prats R, Gómez MN, *et al*. Comparison of direct and indirect models of early induced acute lung injury. Intensive Care Medicine Experimental. 2020; 8: 62.

[36] Traeger T, Koerner P, Kessler W, Cziupka K, Diedrich S, Busemann A, *et al*. Colon ascendens stent peritonitis (CASP)–a standardized model for polymicrobial abdominal sepsis. Journal of Visualized Experiments. 2010; 46: 2299.

[37] Kuhn R, Schubert D, Tautenhahn J, Nestler G, Schulz H, Bartelmann M, *et al*. Effect of intraperitoneal application of an endotoxin inhibitor on survival time in a laparoscopic model of peritonitis in rats. World Journal of Surgery. 2005; 29: 766–770.

[38] Matute-Bello G, Frevert CW, Kajikawa O, Skerrett SJ, Goodman RB, Park DR, *et al*. Septic shock and acute lung injury in rabbits with peritonitis: failure of the neutrophil response to localized infection. American Journal of Respiratory and Critical Care Medicine. 2001; 163: 234–243.

[39] Shaver CM, Paul MG, Putz ND, Landstreet SR, Kuck JL, Scarfe L, *et al*. Cell-free hemoglobin augments acute kidney injury during experimental sepsis. American Journal of Physiology-Renal Physiology. 2019; 317: F922–F929.

[40] Meegan JE, Shaver CM, Putz ND, Jesse JJ, Landstreet SR, Lee HNR, *et al*. Cell-free hemoglobin increases inflammation, lung apoptosis, and microvascular permeability in murine polymicrobial sepsis. PLoS ONE. 2020; 15: e0228727.

[41] Wynn JL, Scumpia PO, Delano MJ, O'Malley KA, Ungaro R, Abouhamze A, *et al*. Increased mortality and altered immunity in neonatal sepsis produced by generalized peritonitis. Shock. 2007; 28: 675–683.

[42] Webb HH, Tierney DF. Experimental pulmonary edema due to intermittent positive pressure ventilation with high inflation pressures. Protection by positive end-expiratory pressure. American Review of Respiratory Disease. 1974; 110: 556–565.

[43] Dreyfuss D, Saumon G. Ventilator-induced lung injury: lessons from experimental studies. American Journal of Respiratory and Critical Care Medicine. 1998; 157: 294–323.

[44] Kallet RH, Matthay MA. Hyperoxic Acute Lung Injury. Respiratory Care. 2013; 58: 123–141.

[45] Vuichard D, Ganter MT, Schimmer RC, Suter D, Booy C, Reyes L, *et al*. Hypoxia aggravates lipopolysaccharide-induced lung injury. Clinical and Experimental Immunology. 2005; 141: 248–260.

[46] Hauser B, Barth E, Bassi G, Simon F, Gröger M, Öter S, *et al*. Hemodynamic, metabolic, and organ function effects of pure oxygen ventilation during established fecal peritonitis-induced septic shock. Critical Care Medicine. 2009; 37: 2465–2469.

[47] Eltzschig HK, Eckle T. Ischemia and reperfusion–from mechanism to translation. Nature Medicine. 2011; 17: 1391–1401.

[48] Regelin N, Heyder S, Laschke MW, Hadizamani Y, Borgmann M, Moehrlen U, *et al*. A murine model to study vasoreactivity and intravascular flow in lung isograft microvessels. Scientific Reports. 2019; 9: 5170.

[49] Fard N, Saffari A, Emami G, Hofer S, Kauczor H, Mehrabi A. Acute respiratory distress syndrome induction by pulmonary ischemia–reperfusion injury in large animal models. Journal of Surgical Research. 2014; 189: 274–284.

[50] Rocco PRM, Nieman GF. ARDS: what experimental models have taught us. Intensive Care Medicine. 2016; 42: 806–810.

[51] Su HC, Nguyen KB, Salazar-Mather TP, Ruzek MC, Dalod MY, Biron CA. NK cell functions restrain T cell responses during viral infections. European Journal of Immunology. 2001; 31: 3048–3055.

[52] Lang PA, Lang KS, Xu HC, Grusdat M, Parish IA, Recher M, *et al*. Natural killer cell activation enhances immune pathology and promotes chronic infection by limiting CD8+ T-cell immunity. Proceedings of the National Academy of Sciences of the United States of America. 2012; 109: 1210–1215.

[53] Zhou G, Juang SWW, Kane KP. NK cells exacerbate the pathology of influenza virus infection in mice. European Journal of Immunology. 2013; 43: 929–938.

[54] Johansen MD, Irving A, Montagutelli X, Tate MD, Rudloff I, Nold MF, *et al*. Animal and translational models of SARS-CoV-2 infection and COVID-19. Mucosal Immunology. 2020; 13: 877–891.

[55] Hendrickson CM, Matthay MA. Viral pathogens and acute lung injury: investigations inspired by the SARS epidemic and the 2009 H1N1 influenza pandemic. Seminars in Respiratory and Critical Care Medicine. 2013; 34: 475–486.

[56] Schuster DP. ARDS: clinical lessons from the oleic acid model of acute lung injury. American Journal of Respiratory and Critical Care Medicine. 1994; 149: 245–260.

[57] Hartmann EK, Bentley A, Duenges B, Klein KU, Boehme S, Markstaller K, *et al*. TIP peptide inhalation in oleic acid-induced experimental lung injury: a post-hoc comparison. BMC Research Notes. 2013; 6: 385.

[58] Prat NJ, Meyer AD, Langer T, Montgomery RK, Parida BK, Batchinsky AI, *et al*. Low-Dose Heparin Anticoagulation during Extracorporeal Life Support for Acute Respiratory Distress Syndrome in Conscious Sheep. Shock. 2015; 44: 560–568.

[59] Du G, Wang S, Li Z, Liu J. Sevoflurane Posttreatment Attenuates Lung Injury Induced by Oleic Acid in Dogs. Anesthesia and Analgesia. 2017; 124: 1555–1563.

[60] Ballard-Croft C, Wang D, Sumpter LR, Zhou X, Zwischenberger JB. Large-Animal Models of Acute Respiratory Distress Syndrome. The Annals of Thoracic Surgery. 2012; 93: 1331–1339.

[61] Raghavendran K, Willson D, Notter RH. Surfactant therapy for acute lung injury and acute respiratory distress syndrome. Critical Care Clinics. 2011; 27: 525–559.

[62] Muellenbach RM, Kredel M, Bernd Z, Johannes A, Kuestermann J, Schuster F, *et al*. Acute respiratory distress induced by repeated saline lavage provides stable experimental conditions for 24 hours in pigs. Experimental Lung Research. 2009; 35: 222–233.

[63] Russ M, Boerger E, von Platen P, Francis RCE, Taher M, Boemke W, *et al*. Surfactant Depletion Combined with Injurious Ventilation Results in a Reproducible Model of the Acute Respiratory Distress Syndrome (ARDS). Journal of Visualized Experiments. 2021.

[64] Zhai R, Blondonnet R, Ebrahimi E, Belville C, Audard J, Gross C, *et al*. The receptor for advanced glycation end-products enhances lung epithelial wound repair: an in vitro study. Experimental Cell Research. 2020; 391: 112030.

[65] Lee JW, Fang X, Dolganov G, Fremont RD, Bastarache JA, Ware LB, *et al*. Acute lung injury edema fluid decreases net fluid transport across human alveolar epithelial type II cells. The Journal of Biological Chemistry. 2007; 282: 24109–24119.

[66] Fang X, Matthay MA. Measurement of Protein Permeability and Fluid Transport of Human Alveolar Epithelial Type II Cells under Pathological Conditions. Methods in Molecular Biology. 2018; 122: 121–128.

[67] Drasler B, Karakocak BB, Tankus EB, Barosova H, Abe J, Sousa de Almeida M, *et al*. An Inflamed Human Alveolar Model for Testing the Efficiency of Anti-inflammatory Drugs in vitro. Frontiers in Bioengineering and Biotechnology. 2020; 8: 987.

[68] King P. Haemophilus influenzae and the lung (Haemophilus and the lung). Clinical and Translational Medicine. 2012; 1: 10.

[69] Camprubí–Rimblas M, Guillamat-Prats R, Lebouvier T, Bringué J, Chimenti L, Iglesias M, *et al*. Role of heparin in pulmonary cell populations in an in-vitro model of acute lung injury. Respiratory Research. 2017; 18: 89.

[70] Tojo K, Tamada N, Nagamine Y, Yazawa T, Ota S, Goto T. Enhancement of glycolysis by inhibition of oxygen-sensing prolyl hydroxylases protects alveolar epithelial cells from acute lung injury. The FASEB Journal. 2018; 32: 2258–2268.
[71] Pooladanda V, Thatikonda S, Bale S, Pattnaik B, Sigalapalli DK, Bathini NB, *et al*. Nimbolide protects against endotoxin-induced acute respiratory distress syndrome by inhibiting TNF-α mediated NF-κB and HDAC-3 nuclear translocation. Cell Death & Disease. 2019; 10: 81.
[72] Wu D, Fu X, Zhang Y, Li Q, Ye L, Han S, *et al*. The protective effects of C16 peptide and angiopoietin-1 compound in lipopolysaccharide-induced acute respiratory distress syndrome. Experimental Biology and Medicine. 2020; 245: 1683–1696.
[73] Bastarache JA, Wang L, Geiser T, Wang Z, Albertine KH, Matthay MA, *et al*. The alveolar epithelium can initiate the extrinsic coagulation cascade through expression of tissue factor. Thorax. 2007; 62: 608–616.
[74] Metz JK, Wiegand B, Schnur S, Knoth K, Schneider-Daum N, Groß H, *et al*. Modulating the Barrier Function of Human Alveolar Epithelial (hAELVi) Cell Monolayers as a Model of Inflammation. Alternatives to Laboratory Animals. 2020; 48: 252–267.
[75] Otulakowski G, Engelberts D, Gusarova GA, Bhattacharya J, Post M, Kavanagh BP. Hypercapnia attenuates ventilator-induced lung injury via a disintegrin and metalloprotease-17. The Journal of Physiology. 2016; 592: 4507–4521.
[76] Wang T, Gross C, Desai A, Zemskov E, Wu X, Garcia AN, *et al*. Endothelial Cell Signaling and Ventilator-Induced Lung Injury (VILI): Molecular Mechanisms, Genomic Analyses & Therapeutic Targets. American Journal of Physiology-Lung Cellular and Molecular Physiology. 2017; 312: L452–L476.
[77] Joelsson JP, Myszor IT, Arason AJ, Ingthorsson S, Cherek P, Windels GS, *et al*. Innovative in vitro method to study ventilator induced lung injury. ALTEX. 2019; 36: 634–642.
[78] Monjezi M, Jamaati H, Noorbakhsh F. Attenuation of ventilator-induced lung injury through suppressing the pro-inflammatory signaling pathways: a review on preclinical studies. Molecular Immunology. 2021; 135: 127–136.
[79] Pao H-P, Liao W-I, Tang S-E, Wu S-Y, Huang K-L, Chu S-J. Suppression of Endoplasmic Reticulum Stress by 4-PBA Protects Against Hyperoxia-Induced Acute Lung Injury via Up-Regulating Claudin-4 Expression. Frontiers in Immunology. 2021; 12: 674316.
[80] Fitzgerald KA, Malhotra M, Curtin CM, O' Brien FJ, O' Driscoll CM. Life in 3D is never flat: 3D models to optimise drug delivery. Journal of Controlled Release. 2015; 215: 39–54.
[81] Rothen-Rutishauser BM, Kiama SG, Gehr P. A three-dimensional cellular model of the human respiratory tract to study the interaction with particles. American Journal of Respiratory Cell and Molecular Biology. 2005; 32: 281–289.
[82] Blank F, Rothen-Rutishauser B, Gehr P. Dendritic cells and macrophages form a transepithelial network against foreign particulate antigens. American Journal of Respiratory Cell and Molecular Biology. 2007; 36: 669–677.
[83] Viola H, Chang J, Grunwell JR, Hecker L, Tirouvanziam R, Grotberg JB, *et al*. Microphysiological systems modeling acute respiratory distress syndrome that capture mechanical force-induced injury-inflammation-repair. APL Bioengineering. 2019; 3: 041503.
[84] Nikolić MZ, Rawlins EL. Lung Organoids and their Use to Study Cell-Cell Interaction. Current Pathobiology Reports. 2017; 5: 223–231.
[85] Katsura H, Sontake V, Tata A, Kobayashi Y, Edwards CE, Heaton BE, *et al*. Human Lung Stem Cell-Based Alveolospheres Provide Insights into SARS-CoV-2-Mediated Interferon Responses and Pneumocyte Dysfunction. Cell Stem Cell. 2020; 27: 890–904.e8.
[86] Salahudeen AA, Choi SS, Rustagi A, Zhu J, van Unen V, de la O SM, *et al*. Progenitor identification and SARS-CoV-2 infection in human distal lung organoids. Nature. 2020; 588: 670–675.
[87] Youk J, Kim T, Evans KV, Jeong Y, Hur Y, Hong SP, *et al*. Three-Dimensional Human Alveolar Stem Cell Culture Models Reveal Infection Response to SARS-CoV-2. Cell Stem Cell. 2020; 27: 905–919.e10.
[88] Huh D, Leslie DC, Matthews BD, Fraser JP, Jurek S, Hamilton GA, *et al*. A human disease model of drug toxicity-induced pulmonary edema in a lung-on-a-chip microdevice. Science Translational Medicine. 2012; 4: 159ra147.
[89] Meyer NJ, Calfee CS. Novel translational approaches to the search for precision therapies for acute respiratory distress syndrome. the Lancet. Respiratory Medicine. 2017; 5: 512–523.
[90] da Silva da Costa FA, Soares MR, Malagutti-Ferreira MJ, da Silva GR, Lívero FADR, Ribeiro-Paes JT. Three-Dimensional Cell Cultures as a Research Platform in Lung Diseases and COVID-19. Tissue Engineering and Regenerative Medicine. 2021; 18: 735–745.
[91] Huang D, Liu T, Liao J, Maharjan S, Xie X, Pérez M, *et al*. Reversed-engineered human alveolar lung-on-a-chip model. Proceedings of the National Academy of Sciences. 2021; 118: e2016146118.
[92] Wyshock EG, Suffredini AF, Parrillo JE, Colman RW. Cofactors V and VIII after endotoxin administration to human volunteers. Thrombosis Research. 1995; 80: 377–389.
[93] DeLa Cadena RA, Majluf-Cruz A, Stadnicki A, Agosti JM, Colman RW, Suffredini AF. Activation of the contact and fibrinolytic systems after intravenous administration of endotoxin to normal human volunteers: correlation with the cytokine profile. Immunopharmacology. 1996; 33: 231–237.
[94] Luca R, Lijnen HR, Suffredini AF, Pepper MS, Steinberg KP, Martin TR, *et al*. Increased angiostatin levels in bronchoalveolar lavage fluids from ARDS patients and from human volunteers after lung instillation of endotoxin. Thrombosis and Haemostasis. 2002; 87: 966–971.
[95] Martin TR, Pistorese BP, Chi EY, Goodman RB, Matthay MA. Effects of leukotriene B4 in the human lung. Recruitment of neutrophils into the alveolar spaces without a change in protein permeability. The Journal of Clinical Investigation. 1989; 84: 1609–1619.
[96] Shyamsundar M, McKeown STW, O'Kane CM, Craig TR, Brown V, Thickett DR, *et al*. Simvastatin decreases lipopolysaccharide-induced pulmonary inflammation in healthy volunteers. American Journal of Respiratory and Critical Care Medicine. 2009; 179: 1107–1114.
[97] Shyamsundar M, McAuley DF, Ingram RJ, Gibson DS, O'Kane D, McKeown ST, *et al*. Keratinocyte growth factor promotes epithelial survival and resolution in a human model of lung injury. American Journal of Respiratory and Critical Care Medicine. 2014; 189: 1520–1529.
[98] Moazed F, Burnham EL, Vandivier RW, O'Kane CM, Shyamsundar M, Hamid U, *et al*. Cigarette smokers have exaggerated alveolar barrier disruption in response to lipopolysaccharide inhalation. Thorax. 2016; 71: 1130–1136.
[99] Hamid U, Krasnodembskaya A, Fitzgerald M, Shyamsundar M, Kissenpfennig A, Scott C, *et al*. Aspirin reduces lipopolysaccharide-induced pulmonary inflammation in human models of ARDS. Thorax. 2017; 72: 971–980.
[100] Lee JW, Fang X, Gupta N, Serikov V, Matthay MA. Allogeneic human mesenchymal stem cells for treatment of E. coli endotoxin-induced acute lung injury in the ex vivo perfused human lung. Proceedings of the National Academy of Sciences. 2009; 106: 16357–16362.
[101] Ross JT, Nesseler N, Lee J, Ware LB, Matthay MA. The ex vivo human lung: research value for translational science. JCI Insight. 2019; 4: e128833.
[102] Shaver CM, Ware LB. Primary graft dysfunction: pathophysiology to guide new preventive therapies. Expert Review of Respiratory Medicine. 2017; 11: 119–128.
[103] Beitler JR, Goligher EC, Schmidt M, Spieth PM, Zanella A, Martin-Loeches I, *et al*. Personalized medicine for ARDS: the 2035 research agenda. Intensive Care Medicine. 2016; 42: 756–767.
[104] Jagrosse ML, Dean DA, Rahman A, Nilsson BL. RNAi therapeutic strategies for acute respiratory distress syndrome. Translational Research. 2019; 214: 30–49.
[105] Jabaudon M, Blondonnet R, Audard J, Fournet M, Godet T, Sapin V, *et al*. Recent directions in personalised acute respiratory distress syndrome medicine. Anaesthesia Critical Care & Pain Medicine. 2018; 37: 251–258.
[106] Matthay MA, Arabi YM, Siegel ER, Ware LB, Bos LDJ, Sinha P, *et al*. Phenotypes and personalized medicine in the acute respiratory distress syndrome. Intensive Care Medicine. 2020; 46: 2136–2152.
[107] Jabaudon M, Blondonnet R, Ware LB. Biomarkers in acute respiratory distress syndrome. Current Opinion in Critical Care. 2021; 27: 46–54.
[108] Jabaudon M, Futier E, Roszyk L, Chalus E, Guerin R, Petit A, *et al*. Soluble form of the receptor for advanced glycation end products is a

marker of acute lung injury but not of severe sepsis in critically ill patients. Critical Care Medicine. 2011; 39: 480–488.

[109] Mrozek S, Jabaudon M, Jaber S, Paugam-Burtz C, Lefrant J, Rouby J, *et al*. Elevated Plasma Levels of sRAGE are Associated with Nonfocal CT-Based Lung Imaging in Patients with ARDS: a Prospective Multicenter Study. Chest. 2016; 150: 998–1007.

[110] Sinha P, Calfee CS. Phenotypes in acute respiratory distress syndrome: moving towards precision medicine. Current Opinion in Critical Care. 2019; 25: 12–20.

[111] Jabaudon M, Audard J, Pereira B, Jaber S, Lefrant J-Y, Blondonnet R, *et al*. Early Changes Over Time in the Radiographic Assessment of Lung Edema Score Are Associated With Survival in ARDS. Chest. 2020; 158: 2394–2403.

[112] Jabaudon M, Pereira B, Laroche E, Roszyk L, Blondonnet R, Audard J, *et al*. Changes in Plasma Soluble Receptor for Advanced Glycation End-Products Are Associated with Survival in Patients with Acute Respiratory Distress Syndrome. Journal of Clinical Medicine Research. 2021; 10: 2076.

[113] Sinha P, Calfee CS, Cherian S, Brealey D, Cutler S, King C, *et al*. Prevalence of phenotypes of acute respiratory distress syndrome in critically ill patients with COVID-19: a prospective observational study. The Lancet Respiratory Medicine. 2020; 8: 1209–1218.

[114] Carla A, Pereira B, Boukail H, Audard J, Pinol-Domenech N, De Carvalho M, *et al*. Acute respiratory distress syndrome subphenotypes and therapy responsive traits among preclinical models: protocol for a systematic review and meta-analysis. Respiratory Research. 2020; 21: 81.

[115] Papazian L, Forel J, Gacouin A, Penot-Ragon C, Perrin G, Loundou A, *et al*. Neuromuscular blockers in early acute respiratory distress syndrome. The New England Journal of Medicine. 2010; 363: 1107–1116.

[116] Acute Respiratory Distress Syndrome Network, Brower RG, Matthay MA, Morris A, Schoenfeld D, Thompson BT, *et al*. Ventilation with lower tidal volumes as compared with traditional tidal volumes for acute lung injury and the acute respiratory distress syndrome. The Acute Respiratory Distress Syndrome Network. The New England Journal of Medicine. 2000; 342: 1301–1308.

[117] Villar J, Ferrando C, Martínez D, Ambrós A, Muñoz T, Soler JA, *et al*. Dexamethasone treatment for the acute respiratory distress syndrome: a multicentre, randomised controlled trial. Lancet Respiratory Medicine. 2020; 8: 267–276.

How to cite this article: Ruoyang Zhai, Woodys Lenga Ma Bonda, Gustavo Matute-Bello, Matthieu Jabaudon. From pre-clinical to clinical models of acute respiratory distress syndrome. Signa Vitae. 2022;18(1):3-14. doi:10.22514/sv.2021.228.

STUDY N°3

The receptor for advanced glycation end-products enhances lung epithelial wound repair: An *in vitro* study

Zhai, R., Blondonnet, R., Ebrahimi, E., Belville, C., Audard, J., Gross, C., Cholthus, H., Henrioux, F., Constantin, J.-M., Pereira, B., Blanchon, L., Sapin, V., & Jabaudon, M. (2020). ***Experimental Cell Research*, *391*(2), 112030.**

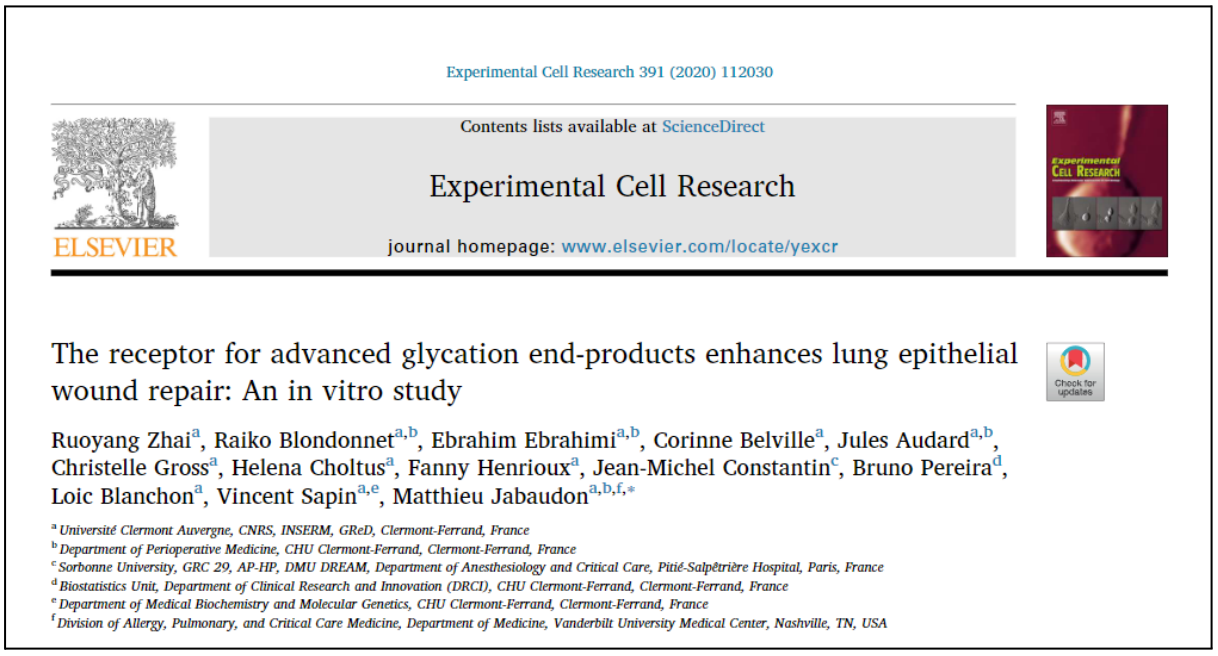

Experimental Cell Research 391 (2020) 112030

Contents lists available at ScienceDirect

Experimental Cell Research

journal homepage: www.elsevier.com/locate/yexcr

The receptor for advanced glycation end-products enhances lung epithelial wound repair: An in vitro study

Ruoyang Zhai[a], Raiko Blondonnet[a,b], Ebrahim Ebrahimi[a,b], Corinne Belville[a], Jules Audard[a,b], Christelle Gross[a], Helena Cholthus[a], Fanny Henrioux[a], Jean-Michel Constantin[c], Bruno Pereira[d], Loic Blanchon[a], Vincent Sapin[a,e], Matthieu Jabaudon[a,b,f,*]

[a] Université Clermont Auvergne, CNRS, INSERM, GReD, Clermont-Ferrand, France
[b] Department of Perioperative Medicine, CHU Clermont-Ferrand, Clermont-Ferrand, France
[c] Sorbonne University, GRC 29, AP-HP, DMU DREAM, Department of Anesthesiology and Critical Care, Pitié-Salpêtrière Hospital, Paris, France
[d] Biostatistics Unit, Department of Clinical Research and Innovation (DRCI), CHU Clermont-Ferrand, Clermont-Ferrand, France
[e] Department of Medical Biochemistry and Molecular Genetics, CHU Clermont-Ferrand, Clermont-Ferrand, France
[f] Division of Allergy, Pulmonary, and Critical Care Medicine, Department of Medicine, Vanderbilt University Medical Center, Nashville, TN, USA

Scientific Knowledge of the Subject

The alteration of alveolar epithelial barrier integrity with increased epithelial permeability is critical in the pathophysiology of acute respiratory distress syndrome (ARDS) [163,197,228,229]. Current evidence suggests re-epithelization of the alveolar surface as a key process that is required to restore the integrity and function of the lung alveolar epithelial barrier[224]**.** However, its precise mechanisms remain underinvestigated[224,230,231]. The receptor for advanced glycation end-products (RAGE) may play a key role in lung homeostasis[81,140], as prooved in existed evidence in lung repair mechanisms such as peripheral nerve regeneration through the recruitment of axonal outgrowth pathways[232,233] or extracellular matrix synthesis and wound repair in human bronchial epithelial cells through stimulation by HMGB1[234]. However, whether modulation of RAGE pathway might affect lung alveolar epithelial wound repair remains unknown.

Contributions of this study to the field

In this study, we found both HMGB1 and AGEs promoted RAGE-dependent wound healing of lung alveolar epithelial cells in our A549 cells wound healing model. In addition, both RAGE ligands increased cell proliferation in a RAGE-dependent manner. Treatment with HMGB1 increased cell migration at 12 h only, with no effect of RAP, whereas AGEs stimulated their migration in a RAGE-dependent manner 48 h after injury.

These results confirmed the important role of RAGE in alveolar epithelial repair, with its involvement in lung epithelial cell migration and proliferation.

Experimental Cell Research 391 (2020) 112030

Contents lists available at ScienceDirect

Experimental Cell Research

journal homepage: www.elsevier.com/locate/yexcr

The receptor for advanced glycation end-products enhances lung epithelial wound repair: An in vitro study

Ruoyang Zhai[a], Raiko Blondonnet[a,b], Ebrahim Ebrahimi[a,b], Corinne Belville[a], Jules Audard[a,b], Christelle Gross[a], Helena Choltus[a], Fanny Henrioux[a], Jean-Michel Constantin[c], Bruno Pereira[d], Loic Blanchon[a], Vincent Sapin[a,e], Matthieu Jabaudon[a,b,f,*]

[a] Université Clermont Auvergne, CNRS, INSERM, GReD, Clermont-Ferrand, France
[b] Department of Perioperative Medicine, CHU Clermont-Ferrand, Clermont-Ferrand, France
[c] Sorbonne University, GRC 29, AP-HP, DMU DREAM, Department of Anesthesiology and Critical Care, Pitié-Salpêtrière Hospital, Paris, France
[d] Biostatistics Unit, Department of Clinical Research and Innovation (DRCI), CHU Clermont-Ferrand, Clermont-Ferrand, France
[e] Department of Medical Biochemistry and Molecular Genetics, CHU Clermont-Ferrand, Clermont-Ferrand, France
[f] Division of Allergy, Pulmonary, and Critical Care Medicine, Department of Medicine, Vanderbilt University Medical Center, Nashville, TN, USA

ARTICLE INFO

Keywords:
Receptor for advanced glycation end-products
Lung epithelial injury
Wound healing
Cell migration
Cell proliferation

ABSTRACT

Re-epithelialization of the alveolar surface is a key process of lung alveolar epithelial barrier repair after acute lung injury. The receptor for advanced glycation end-products (RAGE) pathway plays key roles in lung homeostasis, and its involvement in wound repair has been already reported in human bronchial epithelial cells. However, its effects on lung alveolar epithelial repair after injury remain unknown. We investigated whether RAGE stimulation with its ligands high–mobility group box 1 protein (HMGB1) or advanced glycation end-products (AGEs), alone or associated with RAGE inhibition using RAGE antagonist peptide, affects in vitro wound healing in human alveolar epithelial A549 cells. We further asked whether these effects could be associated with changes in cell proliferation and migration. We found that treatment of A549 cells with HMGB1 or AGEs promotes RAGE-dependent wound healing after a scratch assay. In addition, both RAGE ligands increased cell proliferation in a RAGE-dependent manner. Treatment with HMGB1 increased migration of alveolar epithelial cells at 12 h, independently of RAGE, whereas AGEs stimulated migration as measured 48 h after injury in a RAGE-dependent manner. Taken together, these results suggest that RAGE pathway is involved in lung alveolar epithelial wound repair, possibly through enhanced cell migration and proliferation.

Credit author statement

Raiko Blondonnet, Corinne Belville, Jean-Michel Constantin, Loic Blanchon, Vincent Sapin, and Matthieu Jabaudon designed the study protocol. Ruoyang Zhai, Raiko Blondonnet, Ebrahim Ebrahimi, Corinne Belville, Jules Audard, Christelle Gross, Helena Choltus, and Fanny Henrioux performed the experiments and were responsible for the data collection strategy and preparation. Matthieu Jabaudon and Bruno Pereira were responsible for data management and statistical analysis. Ruoyang Zhai, Raiko Blondonnet, Ebrahim Ebrahimi, Corinne Belville, Loic Blanchon, Vincent Sapin, and Matthieu Jabaudon were responsible for initial drafting and manuscript revisions. All authors provided critical revisions to the manuscript and approved its submission to Experimental Cell Research.

1. Introduction

Alteration of alveolar epithelial barrier integrity with increased epithelial permeability plays a central role in the pathophysiology of the acute respiratory distress syndrome (ARDS) [1–4], a severe condition associated with significant morbidity and mortality, long-term physical or psychological consequences, and high healthcare-associated costs [5–7]. The lung alveolar epithelial barrier is composed of alveolar type (AT)-I cells, covering 95% of the alveolar epithelial surface, and of AT-II cells. Previous research suggests that re-epithelization of the alveolar surface is a key process that is required to restore the integrity and function of the lung alveolar epithelial barrier [8]. Although this repair process may involve the proliferation and migration of AT-II cells, its precise mechanisms remain underinvestigated [8–10].

* Corresponding author. Department of Perioperative Medicine, CHU Clermont-Ferrand; Université Clermont Auvergne, CNRS UMR, INSERM, GReD, 1 Place Lucie Aubrac, 63003, Clermont-Ferrand, Cedex 1, France.
E-mail address: mjabaudon@chu-clermontferrand.fr (M. Jabaudon).

https://doi.org/10.1016/j.yexcr.2020.112030
Received 30 March 2020; Received in revised form 17 April 2020; Accepted 19 April 2020
Available online 21 April 2020
0014-4827/

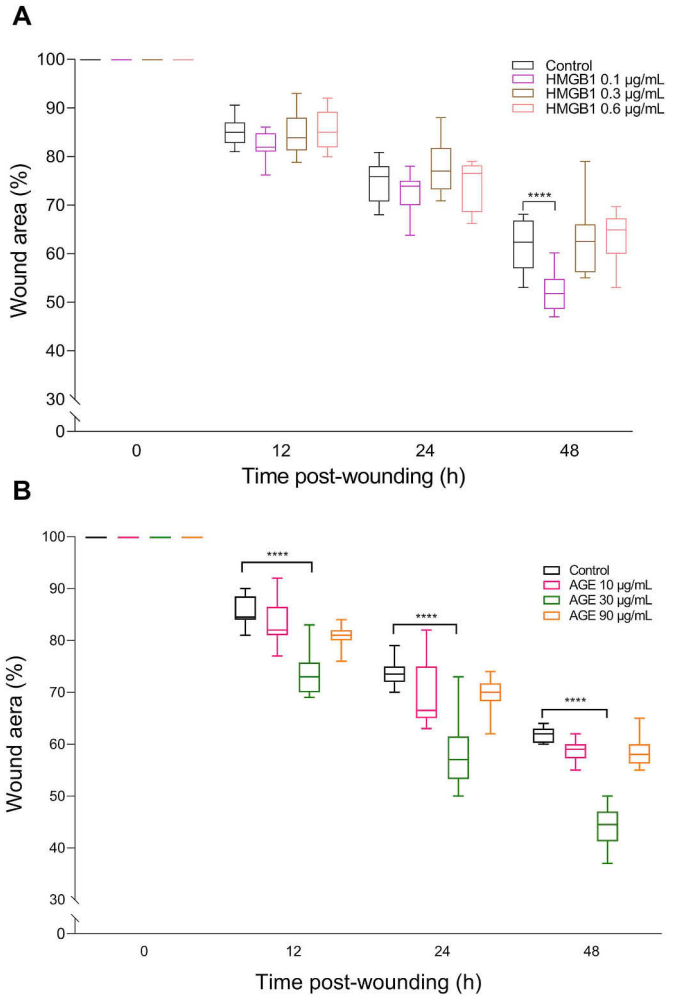

Fig. 1. Dose-response effect of HMGB1 and AGEs on the wound healing of A549 cells. A) Wound healing was assessed up to 48 h using a scratch assay of A549 cells treated with culture medium (Control) or with different concentrations of recombinant HMGB1 (0.1, 0.3, and 0.6 µg/mL). HMGB1 promotes wound healing, compared to the control condition within concentrations of 0.1–0.6 µg/mL; its effect on wound area was more pronounced with the minimum effective dose of 0.1 µg/mL, which was therefore used in subsequent experiments. Values are reported as box plots with median values and interquartile ranges, and upper/lower limits (outliers). Measurements were performed in duplicate in six independent experiments. ****$p < 10^{-4}$. **B)** Wound healing was assessed up to 48 h using a scratch assay of A549 cells treated with culture medium (Control) or with different concentrations of recombinant AGEs (10, 30 and 90 µg/mL). AGEs promote wound healing, compared to the control condition at the concentration of 30 µg/mL; this minimum effective dose was therefore used in subsequent experiments. Values are reported as box plots with median values and interquartile ranges, and upper/lower limits (outliers). Measurements were performed in duplicate in six independent experiments. ****$p < 10^{-4}$. *HMGB1: high-mobility group box 1 protein. AGEs: advanced glycation end-products.*

The receptor for advanced glycation end-products (RAGE) is a membrane signal transduction receptor that can induce various intracellular pathways by binding to multiple ligands, such as S100 proteins, high–mobility group box 1 protein (HMGB1), and advanced glycation end-products (AGEs), among others [11–16]. RAGE is abundantly expressed in the lung tissue, both as transmembrane full-length and soluble forms, and RAGE pathway may play a key role in lung homeostasis [17,18]. Recent clinical and preclinical research has suggested that soluble RAGE (sRAGE) could be a biomarker of lung epithelial injury associated with severity and outcome in ARDS [19–25]. Moreover, RAGE inhibition or *AGER* gene deficiency decreased lung injury in animal models of experimental ARDS from both septic or non-septic causes [26–29]. Although the RAGE pathway has a major role in initiating and perpetuating nuclear factor-kappa B (NF-κB)-mediated inflammation, it also contributes, among many other potential effects [11], to repair mechanisms such as peripheral nerve regeneration through the recruitment of axonal outgrowth pathways [14,30] or extracellular matrix synthesis and wound repair in human bronchial epithelial cells through stimulation by HMGB1 [31]. However, whether modulation of RAGE pathway might affect lung alveolar epithelial wound repair remains unknown.

In this study, we investigated whether treatment with RAGE agonists (HMGB1 and AGEs), alone or combined with a RAGE antagonist, would affect wound healing of lung alveolar epithelial cells in vitro. We further hypothesized that modulation of the RAGE pathway might affect some major processes of wound healing in these cells, such as proliferation or migration.

2. Materials and methods

2.1. Reagents and antibodies

Cell culture Roswell Park Memorial Institute (RPMI 1640) medium 1640, fetal bovine serum (FBS), antibiotics (streptomycin, penicillin, amphotericin B), and phosphate buffered saline (PBS) were obtained from Fisher Scientific (Illkirch, France). Human recombinant HMGB1 was obtained from Sigma-Aldrich (Saint Quentin-Fallavier, France). AGEs (ab51995) was purchased from Abcam (Paris, France). RAGE antagonist peptide (RAP) was obtained from Calbiochem® Merck Millipore (Molsheim, France).

2.2. Cell culture

Human adenocarcinoma-derived alveolar AT-II epithelial cells (A549) were obtained from the American Tissue Culture Collection (CCL-185, LGC Standard®, Molsheim, France). After thawing, cells were cultured in a 95% humidified air atmosphere at 37 °C with a CO_2 concentration of 5% in a RPMI-1640 culture medium enriched with 5% FBS and supplemented with 10 mg/mL streptomycin, 10,000 U/mL penicillin, and 25 µg/mL amphotericin B (Fisher Scientific, France).

2.3. In vitro model of alveolar epithelium wound healing (scratch assay)

Cells (2×10^5 per well) were cultured for 72 h in six 9.5 cm^2 well-plates (Corning, Samois-sur-Seine, France) until 100% confluence was

Table 1
Wound area (in %) of A549 cells treated by different concentrations of HMGB1 and AGEs at different time points after a scratch assay. The wound area is expressed as the fraction of the initial wound (100% at h0). Data are presented as medians and interquartile ranges [IQR] and were analyzed using random effects models; when time by group interaction was significant, post-hoc comparisons between groups at each timepoint were performed using the same models. *HMGB1: high-mobility group box 1 protein. AGEs: advanced glycation end-products.*

Time post-wounding (h)	Experimental conditions				p value for time by group interaction	p value for post-hoc comparisons
	Control (A)	HMGB1 0.1 μg/mL (B)	HMGB1 0.3 μg/mL (C)	HMGB1 0.6 μg/mL (D)		
12	85.8 [84.7–87.0]	81.9 [81.0–84.5]	83.8 [80.6–86.5]	84.9 [81.9–88.4]	$< 10^{-4}$	A versus B: > 0.05 A versus C: > 0.05 A versus D: > 0.05 B versus C: > 0.05 B versus D: > 0.05 C versus D: > 0.05
24	78.0 [75.7–78.0]	73.9 [70.0–75.0]	77.0 [74.8–79.5]	76.5 [72.3–78.2]	$< 10^{-4}$	A versus B: > 0.05 A versus C: > 0.05 A versus D: > 0.05 B versus C: 0.04 B versus D: > 0.05 C versus D: > 0.05
48	64.5 [62.7–67.0]	51.8 [49.2–54.4]	63.5 [56.9–66.0]	64.9 [61.2–67.3]	$< 10^{-4}$	A versus B: $< 10^{-4}$ A versus C: > 0.05 A versus D: > 0.05 B versus C: 0.003 B versus D: 0.004 C versus D: > 0.05

Time post-wounding (h)	**Control (A)**	**AGEs 10 μg/mL (B)**	**AGEs 30 μg/mL (C)**	**AGEs 90 μg/mL (D)**	**p value for time by group interaction**	**p value for post-hoc comparisons**
12	84.5 [84.0–87.5]	82.0 [81.0–85.5]	73.0 [70.0–75.2]	81.0 [80.0–82.0]	$< 10^{-4}$	A versus B: > 0.05 A versus C: $< 10^{-4}$ A versus D: 0.002 B versus C: $< 10^{-4}$ B versus D: > 0.05 C versus D: 10^{-4}
24	73.5 [72.0–75.0]	66.5 [65.0–75.0]	57.0 [53.7–60.5]	70.0 [68.8–71.3]	$< 10^{-4}$	A versus B: > 0.05 A versus C: $< 10^{-4}$ A versus D: 0.02 B versus C: 0.005 B versus D: > 0.05 C versus D: $< 10^{-4}$
48	62.0 [60.8–63.0]	59.0 [57.8–60.0]	44.5 [41.7–47.0]	58.0 [56.8–60.0]	$< 10^{-4}$	A versus B: 0.002 A versus C: $< 10^{-4}$ A versus D: 0.007 B versus C: $< 10^{-4}$ B versus D: > 0.05 C versus D: $< 10^{-4}$

obtained. The tip of a 200-μL pipette was applied perpendicular to the surface of the cell monolayer to create a thin "wound". After three washes with PBS (1X), wounded cells were either left untreated (control) or treated with RAGE agonists alone or combined with RAP (12.5 μg/mL), before being incubated at 37 °C with 95% humidified air and 5% CO_2. The dose of RAP was chosen based on the findings from previous studies [29,32–34]. The wound area was observed immediately after the scratch (h0) and 12, 24, and 48 h after treatment using a Nikon polarized optical microscope with 40x magnification and a digital camera body. Images were recorded prior to their analysis using the Fiji image processing software (Wayne Rasband, National Institute of Mental Health, Bethesda, Maryland, USA) [35]. Measurements of the wounded area were made from edge to edge by manually delimiting the lesion surface. This experiment was repeated six times (with each condition performed in duplicate). After testing three concentrations of RAGE agonists HMGB1 (0.1, 0.3, and 0.6 μg/mL) and

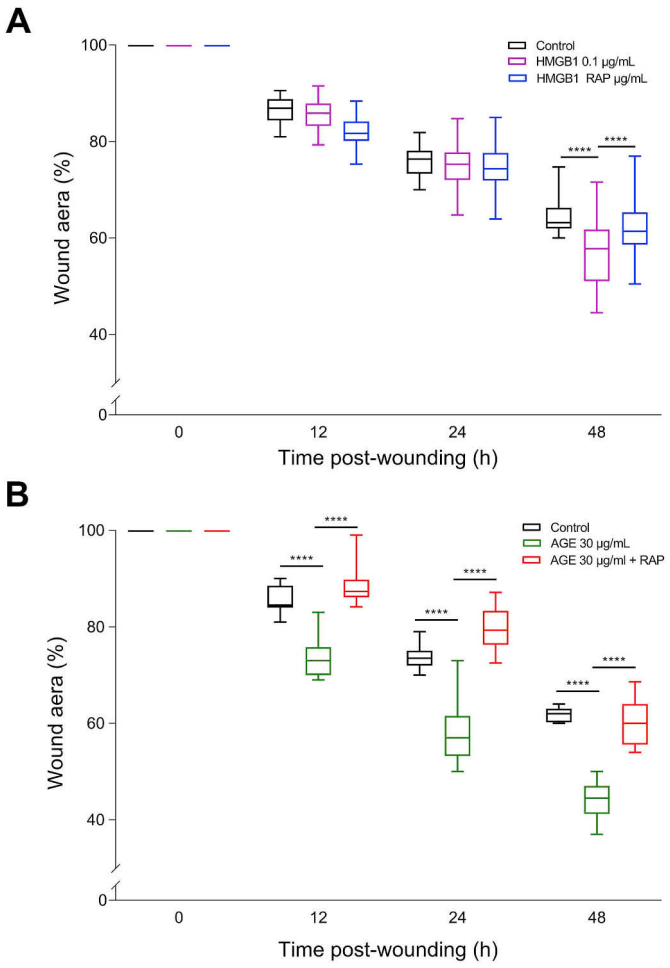

Fig. 2. The effect of RAGE modulation on lung epithelial wound healing in vitro. Wound healing was assessed in lung epithelial A549 cells treated with **A)** HMGB1 (0.1 µg/mL) or **B)** AGEs (30 µg/mL), alone or combined with RAP (12.5 µg/mL). The wound area, as measured every 12 h, is expressed as the fraction of the initial wound (100% at h0). ****$p < 10^{-4}$. *RAGE: receptor for advanced glycation end-products. HMGB1: high-mobility group box 1 protein. AGEs: advanced glycation end-products. RAP: RAGE antagonist peptide.*

AGEs (10, 30, and 90 µg/mL) for their effect on wound area, subsequent experiments were performed using the minimum effective concentration of each.

2.4. Cell migration assay

Epithelial cell migration was assessed with the CytoSelect™ 96-well cell migration assay (CBA-106; 8 µm Fluorometric format; Biolabs, London, United Kingdom). At 12 and 48 h after scratch wounding, cells were suspended in a serum-free medium and placed in the upper chamber. Three hundred microliters of chemoattractant media containing 5% FBS was then added to the lower chamber. After a 24 h incubation, migratory cells that had passed through the polycarbonate membrane (8 µm pore size) were dislodged from the underside of the membrane with a detachment solution. The dislodged cells were then stained with CyQuant® GR Dye (Fisher Scientific, Hampton, USA), diluted in a lysis buffer, and quantified by fluorescence measurement at 480 nm/520 nm (Zeiss LSM 800, Carl Zeiss SAS, Marly Le Roi, France). This experiment, performed in triplicate, was independently repeated three times.

2.5. Cell proliferation assay

At 12 and 48 h after scratch wounding, A549 cells were stained with 5-Bromo-2′-deoxy-uridine (BrdU) at 10 µM using a BrdU Labeling and Detection Kit II (11299964001; Roche Diagnostics, Meylan, France). After 45 min, they were washed three times with PBS, and fixed with an ethanol fixative solution (50 mM glycine, pH = 2, in 70% ethanol) for 20 min at −20 °C. After three washes in PBS, the cells were incubated with an anti-BrdU antibody (1/25) for 60 min at 37 °C. The cells were washed three times with PBS, followed by incubation with an anti-mouse-Ig-alkaline phosphatase (1:25 dilution) for 60 min at 37 °C. The color substrate solution was added to the cells after three washes in PBS, and the bound anti-BrdU antibody was visualized by light microscopy (Zeiss Axio Observer, Carl Zeiss SAS, Marly Le Roi, France). Proliferation was expressed as the ratio of BrdU-positive cells to the total number of cells. This experiment, performed in triplicate, was independently repeated three times.

2.6. Statistical analysis

All analyses were performed using Prism 6 (GraphPad Software, La Jolla, CA, USA) and Stata version 15 (StataCorp, College Station, TX, USA). The tests were two-sided, with a type I error set at 5%. Continuous data were expressed as mean ± standard deviation (SD) or median [interquartile range] according to statistical distribution (assumption of normality was assessed using the Shapiro-Wilk test). Continuous parameters were compared between experimental groups using analysis of variance or the Kruskal-Wallis test when *t*-test assumptions were not met (normality studied using Shapiro-Wilk and assumption of homoscedasticity verified by Fisher-Snedecor test). Random effects models were used to analyze the longitudinal evolution of variables: (i) considering between- and within-experiment variability (random subject effects: random intercept and slope) and (ii) evaluating fixed effects: group, time, and time by group interaction. The residual normality was checked for all models. Values were log-transformed for all variables to achieve normality prior to performing random effects models.

Table 2
Wound area (in %) of A549 cells treated by different HMGB1 or AGEs, alone or combined with RAP at different time points after a scratch assay. The wound area is expressed as the fraction of the initial wound (100% at h0). Data are presented as medians and interquartile ranges [IQR] and were analyzed using random effects models; when time by group interaction was significant, post-hoc comparisons between groups at each timepoint were performed using the same models. *HMGB1: high-mobility group box 1 protein. AGEs: advanced glycation end-products. RAP: RAGE antagonist peptide.*

Time post-wounding (h)	Experimental conditions			p value for time by group interaction	p value for post-hoc comparisons
	Control (A)	HMGB1 0.1 μg/mL (B)	HMGB1 0.1 μg/mL + RAP (C)		
12	86.9 [84.8–88.7]	85.8 [85.4–87.7]	81.7 [80.6–83.5]	$< 10^{-4}$	A versus B: > 0.05 A versus C: > 0.05 B versus C: > 0.05
24	76.4 [73.8–78.0]	75.3 [68.3–77.7]	72.5 [71.8–76.2]	$< 10^{-4}$	A versus B: > 0.05 A versus C: > 0.05 B versus C: > 0.05
48	63.2 [62.0–65.2]	57.7 [49.2–61.5]	59.3 [58.3–63.4]	$< 10^{-4}$	A versus B: $< 10^{-4}$ A versus C: > 0.05 B versus C: $< 10^{-4}$

Time post-wounding (h)	**Control (A)**	**AGEs 30 μg/mL (B)**	**AGEs 30 μg/mL + RAP (C)**	**p value for time by group interaction**	**p value for post-hoc comparisons**
12	83.5 [84.0–87.5]	73.0 [70.0–75.3]	87.3 [86.5–89.5]	$< 10^{-4}$	A versus B: $< 10^{-4}$ A versus C: > 0.05 B versus C: $< 10^{-4}$
24	73.5 [72.0–75.0]	57.0 [53.8–60.5]	79.3 [76.6–82.4]	$< 10^{-4}$	A versus B: $< 10^{-4}$ A versus C: > 0.05 B versus C: $< 10^{-4}$
48	62.0 [60.8–63.0]	44.5 [41.8–47.0]	60.0 [55.9–63.9]	$< 10^{-4}$	A versus B: $< 10^{-4}$ A versus C: > 0.05 B versus C: $< 10^{-4}$

3. Results

3.1. Both HMGB1 and AGEs promote dose-dependent and RAGE-dependent wound healing of lung alveolar epithelial cells

We first tested different treatment concentrations of HMGB1 and AGEs for their effect on wound area after the scratch assay (Fig. 1 and Table 1). Both RAGE ligands had dose- and time-dependent effects towards better wound healing of epithelial cells. Compared to controls, cells treated with HMGB1 (0.1 μg/mL) had better wound healing (time by group interaction, $p = 0.008$) at 24 h and 48 h after injury ($p = 0.04$ and $p < 10^{-4}$, respectively, for post-hoc comparisons). A similar effect was found after treatment with AGEs (30 μg/mL) (time by group interaction, $p < 10^{-4}$), compared to untreated cells, at 24 h and 48 h after injury ($p = 0.005$ and $p = 0.0001$, respectively, for post-hoc comparisons) ($p = 10^{-4}$). The minimum effective doses of HMGB1 (0.1 μg/mL) and AGEs (30 μg/mL) were used in subsequent experiments.

Co-treatment with RAP (12.5 μg/mL) significantly reduced the effects of both HMGB1 (time by group interaction, $p < 10^{-4}$) and AGEs (time by group interaction, $p < 10^{-4}$) on wound area, with most detrimental effects on wound healing observed at 48 h for HMGB1 and at 12 h for AGEs (Fig. 2 and Table 2).

3.2. HMGB1 and AGEs have distinct effects on the migration of lung alveolar epithelial cells during wound healing

After injury, cells treated with HMGB1 (0.1 μg/mL) showed higher migration at 12 h, but not at 48 h, compared to controls (Fig. 3A); RAP did not influence cell migration after treatment with HMGB1 at both timepoints (Fig. 3A). Cells treated with AGEs (30 μg/mL) had reduced migration at 12 h but increased migration at 48 h after injury, compared to controls. Treatment with RAP significantly counteracted these effects at both timepoints (Fig. 3B and Table 3).

3.3. Both HMGB1 and AGEs increase lung alveolar epithelial cell proliferation in a RAGE-dependent manner during wound healing

Treatment with HMGB1 (0.1 μg/mL) enhanced cell proliferation at both 12 h and 48 h after injury. These effects were significantly inhibited in presence of RAP at both timepoints (Fig. 4A). Treatment with AGEs (30 μg/mL) increased cell proliferation at both timepoints after

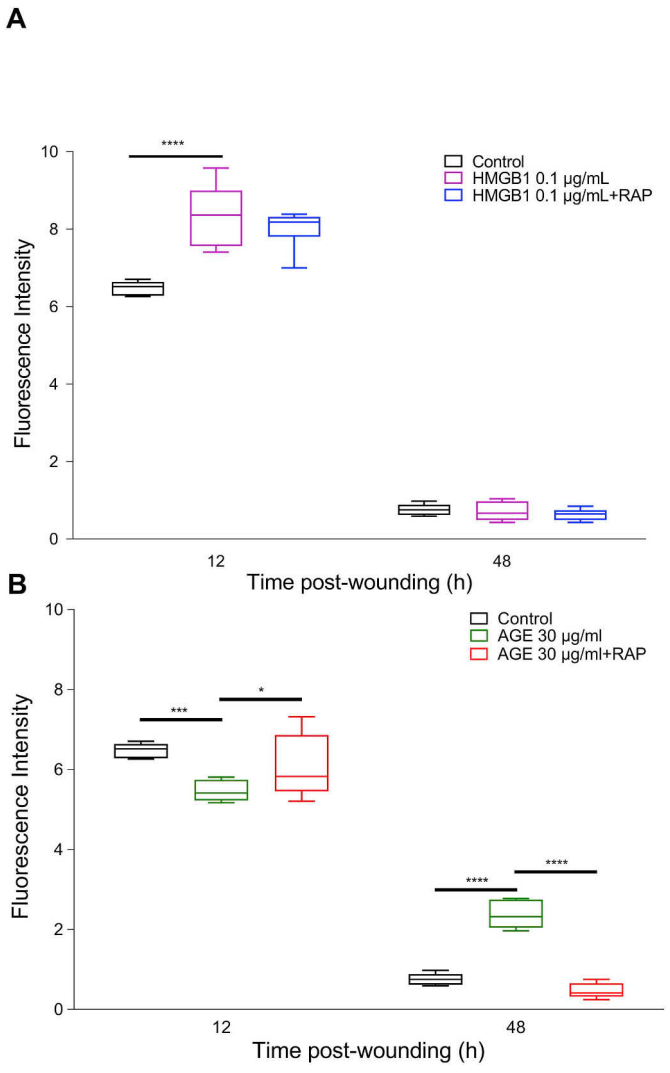

Fig. 3. Effects of treatment with HMGB1 and AGEs, and of RAGE inhibition by RAP, on the migration of A549 cells during wound healing. The migration of A549 cells, as expressed as fluorescence intensity (with higher intensity corresponding to higher migration) was assessed at 12 and 48 h after a scratch assay using the CytoSelect™ 96-well cell migration assay (CBA-106; 8 µm Fluorometric format; Biolabs, London, United Kingdom). *$p < 0.05$, ***$p < 0.001$, ****$p < 10^{-4}$. **A)** Cells treated with recombinant HMGB1 (0.1 µg/mL) had increased migration, compared to controls, at 12 h but not at 48 h. Treatment with RAP (12.5 µg/mL) did not influence this effect. **B)** Cells treated with recombinant AGEs (30 µg/mL) had decreased migration at 12 h, but increased migration at 48 h, compared to controls. Both effects of AGEs on migration were significantly counteracted after treatment with RAP (12.5 µg/mL). *RAGE: receptor for advanced glycation end-products. HMGB1: high-mobility group box 1 protein. AGEs: advanced glycation end-products. RAP: RAGE antagonist peptide.*

injury, which was abrogated by RAP treatment at both timepoints (Fig. 4B and Table 4).

4. Discussion

In this study, HMGB1 and AGEs promoted RAGE-dependent wound healing of lung alveolar epithelial cells after a scratch assay. In addition, both RAGE ligands increased cell proliferation in a RAGE-dependent manner. Treatment with HMGB1 increased cell migration at 12 h only, with no effect of RAP, whereas AGEs stimulated their migration in a RAGE-dependent manner 48 h after injury.

There is growing evidence supporting the involvement of RAGE pathway in mechanisms of cell and tissue repair after injury. Indeed, the AGE/RAGE axis promotes wound healing of human corneal epithelial cells [36] and HMGB1/RAGE axis promotes keratinocyte healing in vitro [15], with improved healing of diabetic human and mouse skin [37]. In addition, HMGB1 improves scratch wound healing of human bronchial epithelial cells via toll-like receptor (TLR)-4 and RAGE-mediated increase in extracellular matrix synthesis and modulation of cell-matrix adhesion [31]. However, in our dose-response experiments, higher doses of HMGB1 (> 0.1 µg/mL) and AGEs (> 30 µg/mL) were associated with no protective effect on wound healing, suggesting a non-linear dose-response to increasing concentrations of alarmins [38], such as RAGE ligands, and subsequent effects that can be either physiological or pathological to multiple cellular processes [11,39,40]. In our study, the activation of RAGE by both HMGB1 (0.1 µg/mL) and AGEs (30 µg/mL) promoted scratch wound healing whereas the use of a RAGE competitive antagonist abrogated these effects, thus supporting for the first time that previous findings of RAGE pathway as a promoter of wound healing may also hold true in the lung alveolar epithelium. Such findings should now be further explored in the clinical setting of ARDS to better understand the complex mechanisms involved in alveolar epithelium repair after injury, including the spreading, migration, and proliferation of alveolar epithelial cells [41].

Here we found that both HMGB1 and AGEs promote A549 cell migration during wound healing. Lung alveolar epithelial cells treated with HMGB1 acquired higher migration, compared to controls, at 12 h but not at 48 h. Although the significance of these discrepant findings remains uncertain, pro-migratory effects of HMGB1 may decrease with time, as previously reported by Huang et al. in another study on RAGE activation by HMGB1 [42]. Concurrent treatment with RAP did not decrease the pro-migratory effect of HMGB1, suggesting that the activation of RAGE by HMGB1 may not be involved in epithelial cell migration during wound healing. Indeed, multiple studies support the interaction of HMGB1 with TLR-4, rather than with RAGE, as the main mechanism responsible for smooth muscle cell migration [43] or motility of human non-small lung cancer cells [44]. In contrast, some studies suggest an important role of RAGE activation by HMGB1 in cell migration, such as in mouse endothelial progenitor cells [45], monocytes [46], neural progenitor cells [47] or glial tumor cells [48]. Consistent with this hypothesis that RAGE is implicated in the process of cell migration; Huttunen et al. could inhibit transendothelial migration

Table 3
Cell migration, as expressed as fluorescence intensity, of lung epithelial A549 cells treated with HMGB1 or AGEs, alone or combined with RAP, at different time points after a scratch assay. Higher intensity corresponds to higher migration. Data are presented as medians and interquartile ranges [IQR] and were analyzed using random effects models; when time by group interaction was significant, post-hoc comparisons between groups at each timepoint were performed using the same models. *HMGB1: high-mobility group box 1 protein. AGEs: advanced glycation end-products. RAP: RAGE antagonist peptide.*

Time post-wounding (h)	Experimental conditions			p value for time by group interaction	p value for post-hoc comparisons
	Control (A)	HMGB1 0.1 μg/mL (B)	HMGB1 0.1 μg/mL + RAP (C)		
12	6.51 [6.33–6.60]	8.40 [7.73–8.70]	8.18 [8.09–8.27]	$< 10^{-4}$	A versus B: $< 10^{-4}$ A versus C: $< 10^{-4}$ B versus C: > 0.05
48	0.75 [0.65–0.84]	0 .66 [0.52–0.91]	0.64 [0.53–0.70]	$< 10^{-4}$	A versus B: > 0.05 A versus C: > 0.05 B versus C: > 0.05
Time post-wounding (h)	**Control (A)**	**AGEs 30 μg/mL (B)**	**AGEs 30 μg/mL + RAP (C)**	**p value for time by group interaction**	**p value for post-hoc comparisons**
12	6.51 [6.33–6.60]	5.41 [5.27–5.67]	5.83 [5.60–6.50]	$< 10^{-4}$	A versus B: $< 10^{-3}$ A versus C: > 0.05 B versus C: 0.03
48	0.75 [0.65–0.84]	2.31 [2.11–2.65]	0.41 [0.35–0.58]	$< 10^{-4}$	A versus B: $< 10^{-4}$ A versus C: > 0.05 B versus C: $< 10^{-4}$

of melanoma cells in vivo and in vitro by blocking the HMGB1-binding site of RAGE [49], while Yang et al. reported that HMGB1 could induce migration of human dendritic cells via RAGE pathway [50]. In addition to the RAGE-dependent beneficial effects of HMGB1 on A549 cell wound healing, we also found that treatment by AGEs (30 μg/mL) both decreased cell migration at 12 h and increased migration at 48 h, compared to controls, and that RAGE inhibition with RAP consistently counteracted these effects at both timepoints. Although future studies are needed to understand whether early pro-inflammatory effects of AGEs might explain, at least in part, decreased migration 12 h after AGEs treatment, the pro-migratory effect of AGEs at 48 h after lung alveolar epithelial cell scratch wounding is similar to previous findings in retinal pericytes [51].

Cell proliferation is also an important contributor to wound healing, together with migration. Here, treatment with both HMGB1 and AGEs significantly increased cell proliferation at 12 and 48 h after scratch wounding, compared to controls, whereas simultaneous treatment with RAP counteracted these effects at both timepoints. Although this study is the first to report the importance of RAGE modulation in the proliferation of lung alveolar epithelial cells, these findings are consistent with previous in vitro studies in keratinocytes and fibroblasts [15]. Similarly, blocking the HMGB1/RAGE axis through treatment with recombinant sRAGE, acting as a decoy receptor that prevents interaction between RAGE and its ligands, or after transfection of a truncated RAGE, was able to suppress proliferation of glial cells in mice [48]. We also observed that the anti-proliferative effect of RAP could be less pronounced at 12 h after treatment with HMGB1 than with AGEs (Fig. 4). Indeed, a previous study found synergistic effects of RAGE and TLR activation on human bronchial epithelial wound healing, such that inhibition of both RAGE and TLR-4 was needed to abrogate the proliferative effects of HMGB1 [31]. Our study is, however, unable to support that the effects of AGEs on lung alveolar epithelial cell proliferation might be more dependent on RAGE pathway than those of HMGB1. In particular, whether our use of an S100P-derived competitive antagonist for RAGE (RAP, Calbiochem® Merck Millipore, Molsheim, France) could bring different results than the use of an HMGB1-derived recombinant RAGE antagonist peptide deserves further investigation [52].

This study has some limitations. First, we only used adenocarcinoma AT II-like alveolar epithelial cells as an in vitro cell model of the human lung alveolar epithelium. More translational studies of primary human epithelial cell cultures that include proinflammatory conditions and the integration of a more realistic environment (including, but not limited to, the presence of an extracellular matrix and of innate immunity cells) are now needed to further increase our understanding of the roles of RAGE pathway in mechanisms relevant to lung alveolar epithelial repair after injury, including studies of the potential roles of RAGE in cell transdifferentiation [53–55]. In the meanwhile, whether such RAGE-

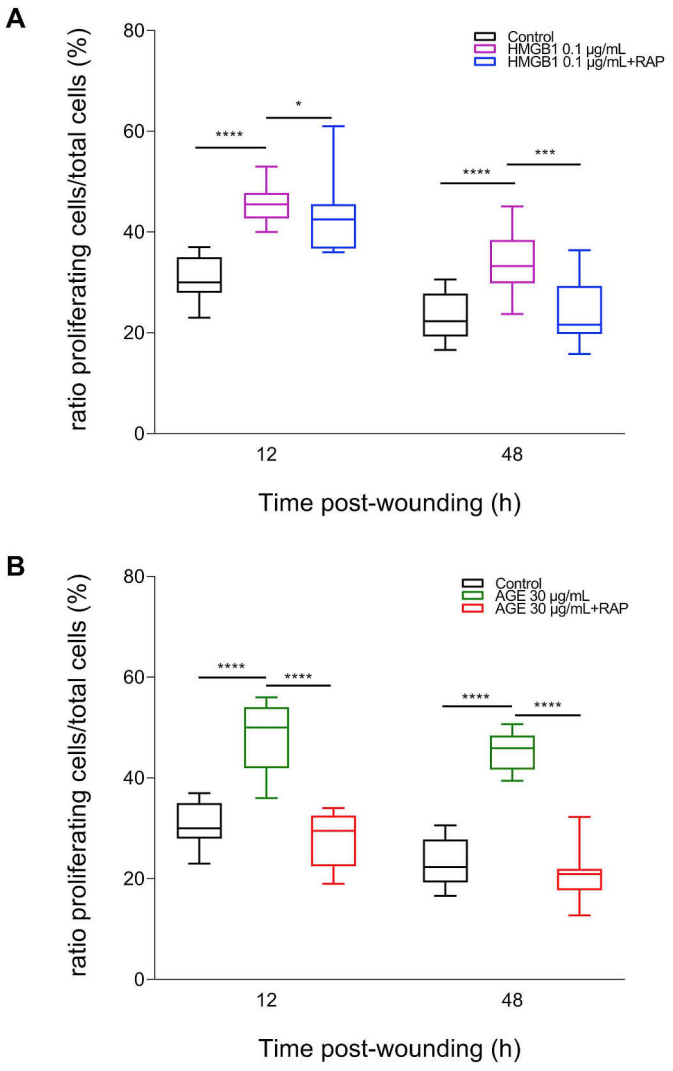

Fig. 4. Effects of treatment with HMGB1 and AGEs, and of RAGE inhibition by RAP, on the proliferation capacity of A549 cells during wound healing. Proliferation capacity of A549 cells was assessed using a BrdU Labeling and Detection Kit II *(11299964001; Roche Diagnostics, Meylan, France). Results are expressed as the ratio (in %) of proliferating cells to the total number of cells at 12 and 48 h after a scratch assay.* ***A)*** *Cells treated* with recombinant HMGB1 (0.1 µg/mL) had increased proliferation capacity, compared to controls, at 12 and 48 h. Treatment with RAP (12.5 µg/mL) significantly counteracted this effect at both timepoints. **B)** Cells treated with recombinant AGEs (30 µg/mL) had increased proliferation capacity, compared to controls, at 12 and 48 h. Treatment with RAP (12.5 µg/mL) significantly counteracted this effect at both timepoints. *p < 0.05, ***p < 0.001, ****p < 10^{-4}. *RAGE: receptor for advanced glycation end-products. HMGB1: high-mobility group box 1 protein. AGEs: advanced glycation end-products. RAP: RAGE antagonist peptide.*

dependent mechanisms favoring lung epithelial wound healing could have clinical relevance in patients with acute lung injury such as ARDS also deserves further investigation. Second, we used RAP as a competitive RAGE antagonist [32]. However, how other strategies of RAGE inhibition, such as RAGE knockout animals, treatment with recombinant sRAGE, RNA interference or CRISPR-CAS9 methods would affect lung epithelial cell wound healing remains unknown. Finally, in this study, we did not investigate intracellular pathways (such as Mitogen-activated protein kinase ERK 1/2, JAK/STAT, JNK, Rho GTPase, PI3K/Akt, and NF-κB) through which RAGE could affect lung epithelial wound repair, and the mechanisms explaining these effects deserve further investigation [11].

In conclusion, HMGB1 and AGEs promote in vitro wound healing of human alveolar epithelial cells in a RAGE-dependent manner. These effects could be explained, at least in part, by increased cell migration and proliferation. Future studies are now warranted to better understand the precise signaling pathways through which the RAGE pathway affects lung epithelial wound repair.

Funding

This work was supported by grants from the Auvergne Regional Council: "Programme Nouveau Chercheur de la Region Auvergne" 2013 and the French *Agence Nationale de la Recherche and the Direction Générale de l'Offre de Soins*: "Programme de Recherche Translationnelle en Sante ANR-13-PRTS-0010". RZ was funded by a PhD grant from the *Ecole Doctorale des Sciences de la Vie, Santé, Agronomie, Environnement* (ED SVSAE, ED 65, Université Clermont Auvergne). The funders had no influence in the study design, conduct, and analysis or in the preparation of this article.

Data availability

The datasets generated during the current study are available from the corresponding author on reasonable request.

Declaration of competing interest

This work was supported by grants from the Auvergne Regional Council and the French *Agence Nationale de la Recherche* and the *Direction Générale de l'Offre de Soins*. RZ was funded by a PhD grant from the *Ecole Doctorale des Sciences de la Vie, Santé, Agronomie, Environnement* (ED SVSAE, ED 65, Université Clermont Auvergne). The funders had no influence in the study design, conduct, and analysis or in the preparation of this article.

The authors state that they have no conflict of interest to declare in relationship with this work.

Table 4
Proliferation capacity, as expressed by the ratio (in %) of proliferating cells to the total number of cells, of lung epithelial A549 cells treated with HMGB1 or AGEs, alone or combined with RAP, at different time points after a scratch assay. Data are presented as medians and interquartile ranges [IQR] and were analyzed using random effects models; when time by group interaction was significant, post-hoc comparisons between groups at each timepoint were performed using the same models. *HMGB1: high-mobility group box 1 protein. AGEs: advanced glycation end-products. RAP: RAGE antagonist peptide.*

Time post-wounding (h)	Experimental conditions			p value for time by group interaction	p value for post-hoc comparisons
	Control (A)	HMGB1 0.1 μg/mL (B)	HMGB1 0.1 μg/mL + RAP (C)		
12	30.0 [28.0–33.0]	45.5 [44.3–47.3]	42.5 [38.3–44.5]	$< 10^{-4}$	A versus B: $< 10^{-4}$ A versus C: $< 10^{-4}$ B versus C: 0.01
48	22.3 [19.5–25.3]	33.2 [30.8–38.3]	21.6 [20.3–27.9]	$< 10^{-4}$	A versus B: $< 10^{-4}$ A versus C: > 0.05 B versus C: 10^{-4}
Time post-wounding (h)	**Control (A)**	**AGEs 30 μg/mL (B)**	**AGEs 30 μg/mL + RAP (C)**	**p value for time by group interaction**	**p value for post-hoc comparisons**
12	30.0 [28.0–33.0]	50.0 [42.0–54.0]	29.5 [23.5–31.5]	$< 10^{-4}$	A versus B: $< 10^{-3}$ A versus C: > 0.05 B versus C: 0.03
48	22.3 [19.5–25.3]	45.9 [42.3–48.3]	20.9 [18.6–21.9]	$< 10^{-4}$	A versus B: $< 10^{-4}$ A versus C: > 0.05 B versus C: $< 10^{-4}$

Acknowledgements

The authors wish to thank the staff from the Université Clermont Auvergne, CNRS, INSERM, GReD (Clermont-Ferrand, France) who helped and supported this work.

Appendix A. Supplementary data

Supplementary data to this article can be found online at https://doi.org/10.1016/j.yexcr.2020.112030.

References

[1] M.A. Matthay, J.P. Wiener-Kronish, Intact epithelial barrier function is critical for the resolution of alveolar edema in humans, Am. Rev. Respir. Dis. 142 (1990) 1250–1257.
[2] L.B. Ware, M.A. Matthay, Alveolar fluid clearance is impaired in the majority of patients with acute lung injury and the acute respiratory distress syndrome, Am. J. Respir. Crit. Care Med. 163 (2001) 1376–1383.
[3] L. Guillot, N. Nathan, O. Tabary, G. Thouvenin, P. Le Rouzic, H. Corvol, S. Amselem, A. Clement, Alveolar epithelial cells: master regulators of lung homeostasis, Int. J. Biochem. Cell Biol. 45 (2013) 2568–2573.
[4] J. Villar, H. Zhang, A.S. Slutsky, Lung repair and regeneration in ARDS: role of PECAM1 and wnt signaling, Chest 155 (2019) 587–594.
[5] M.S. Herridge, C.M. Tansey, A. Matté, G. Tomlinson, N. Diaz-Granados, A. Cooper, C.B. Guest, C.D. Mazer, S. Mehta, T.E. Stewart, P. Kudlow, D. Cook, A.S. Slutsky, A.M. Cheung, Canadian Critical Care Trials Group, Functional disability 5 years after acute respiratory distress syndrome, N. Engl. J. Med. 364 (2011) 1293–1304.
[6] G. Bellani, J.G. Laffey, T. Pham, E. Fan, L. Brochard, A. Esteban, L. Gattinoni, F. van Haren, A. Larsson, D.F. McAuley, M. Ranieri, G. Rubenfeld, B.T. Thompson, H. Wrigge, A.S. Slutsky, A. Pesenti, LUNG SAFE investigators, ESICM trials group, epidemiology, patterns of care, and mortality for patients with acute respiratory distress syndrome in intensive care units in 50 countries, J. Am. Med. Assoc. 315 (2016) 788–800.
[7] B.T. Thompson, R.C. Chambers, K.D. Liu, Acute respiratory distress syndrome, N. Engl. J. Med. 377 (2017) 562–572.
[8] M.A. Matthay, R.L. Zemans, G.A. Zimmerman, Y.M. Arabi, J.R. Beitler, A. Mercat, M. Herridge, A.G. Randolph, C.S. Calfee, Acute respiratory distress syndrome, Nat Rev Dis Primers 5 (2019) 18.
[9] I.Y. Adamson, D.H. Bowden, The type 2 cell as progenitor of alveolar epithelial regeneration. A cytodynamic study in mice after exposure to oxygen, Lab. Invest. 30 (1974) 35–42.
[10] J.L. McQualter, K. Yuen, B. Williams, I. Bertoncello, Evidence of an epithelial stem/progenitor cell hierarchy in the adult mouse lung, Proc. Natl. Acad. Sci. U. S. A. 107 (2010) 1414–1419.
[11] J. Xie, J.D. Méndez, V. Méndez-Valenzuela, M.M. Aguilar-Hernández, Cellular signalling of the receptor for advanced glycation end products (RAGE), Cell. Signal. 25 (2013) 2185–2197.
[12] H.M. Lander, J.M. Tauras, J.S. Ogiste, O. Hori, R.A. Moss, A.M. Schmidt, Activation of the receptor for advanced glycation end products triggers a p21(ras)-dependent mitogen-activated protein kinase pathway regulated by oxidant stress, J. Biol. Chem. 272 (1997) 17810–17814.
[13] M. Tafani, L. Schito, L. Pellegrini, L. Villanova, G. Marfe, T. Anwar, R. Rosa, M. Indelicato, M. Fini, B. Pucci, M.A. Russo, Hypoxia-increased RAGE and P2X7R expression regulates tumor cell invasion through phosphorylation of Erk1/2 and Akt and nuclear translocation of NF-{kappa}B, Carcinogenesis 32 (2011) 1167–1175.
[14] H.J. Huttunen, C. Fages, H. Rauvala, Receptor for advanced glycation end products (RAGE)-mediated neurite outgrowth and activation of NF-kappaB require the cytoplasmic domain of the receptor but different downstream signaling pathways, J. Biol. Chem. 274 (1999) 19919–19924.
[15] E. Ranzato, M. Patrone, M. Pedrazzi, B. Burlando, HMGb1 promotes scratch wound closure of HaCaT keratinocytes via ERK1/2 activation, Mol. Cell. Biochem. 332 (2009) 199–205.
[16] B.I. Hudson, M.E. Lippman, Targeting RAGE signaling in inflammatory disease, Annu. Rev. Med. 69 (2018) 349–364.
[17] T.K. Mukherjee, S. Mukhopadhyay, J.R. Hoidal, Implication of receptor for advanced glycation end product (RAGE) in pulmonary health and pathophysiology, Respir. Physiol. Neurobiol. 162 (2008) 210–215.
[18] M.A. Queisser, F.M. Kouri, M. Königshoff, M. Wygrecka, U. Schubert, O. Eickelberg, K.T. Preissner, Loss of RAGE in pulmonary fibrosis: molecular relations to functional changes in pulmonary cell types, Am. J. Respir. Cell Mol. Biol. 39 (2008) 337–345.
[19] M. Shirasawa, N. Fujiwara, S. Hirabayashi, H. Ohno, J. Iida, K. Makita, Y. Hata, Receptor for advanced glycation end-products is a marker of type I lung alveolar cells, Gene Cell. 9 (2004) 165–174.
[20] T. Uchida, M. Shirasawa, L.B. Ware, K. Kojima, Y. Hata, K. Makita, G. Mednick, Z.A. Matthay, M.A. Matthay, Receptor for advanced glycation end-products is a marker of type I cell injury in acute lung injury, Am. J. Respir. Crit. Care Med. 173 (2006) 1008–1015.
[21] C.S. Calfee, L.B. Ware, M.D. Eisner, P.E. Parsons, B.T. Thompson, N. Wickersham, M.A. Matthay, Nhlbi Ards Network, Plasma receptor for advanced glycation end products and clinical outcomes in acute lung injury, Thorax 63 (2008) 1083–1089.
[22] T. Mauri, S. Masson, A. Pradella, G. Bellani, A. Coppadoro, M. Bombino, S. Valentino, N. Patroniti, A. Mantovani, A. Pesenti, R. Latini, Elevated plasma and alveolar levels of soluble receptor for advanced glycation endproducts are associated with severity of lung dysfunction in ARDS patients, Tohoku J. Exp. Med. 222 (2010) 105–112.
[23] M. Jabaudon, E. Futier, L. Roszyk, E. Chalus, R. Guerin, A. Petit, S. Mrozek, S. Perbet, S. Cayot-Constantin, C. Chartier, V. Sapin, J.-E. Bazin, J.-M. Constantin, Soluble form of the receptor for advanced glycation end products is a marker of acute lung injury but not of severe sepsis in critically ill patients, Crit. Care Med. 39 (2011) 480–488.
[24] M. Jabaudon, R. Blondonnet, L. Roszyk, D. Bouvier, J. Audard, G. Clairefond, M. Fournier, G. Marceau, P. Déchelotte, B. Pereira, V. Sapin, J.-M. Constantin, Soluble receptor for advanced glycation end-products predicts impaired alveolar fluid clearance in acute respiratory distress syndrome, Am. J. Respir. Crit. Care Med. 192 (2015) 191–199.
[25] M. Jabaudon, R. Blondonnet, B. Pereira, R. Cartin-Ceba, C. Lichtenstern, T. Mauri, R.M. Determann, T. Drabek, R.D. Hubmayr, O. Gajic, F. Uhle, A. Coppadoro,

A. Pesenti, M.J. Schultz, M.V. Ranieri, H. Brodska, S. Mrozek, V. Sapin, M.A. Matthay, J.-M. Constantin, C.S. Calfee, Plasma sRAGE is independently associated with increased mortality in ARDS: a meta-analysis of individual patient data, Intensive Care Med. 44 (2018) 1388–1399.
[26] M.A.D. van Zoelen, M. Schouten, A.F. de Vos, S. Florquin, J.C.M. Meijers, P.P. Nawroth, A. Bierhaus, T. van der Poll, The receptor for advanced glycation end products impairs host defense in pneumococcal pneumonia, J. Immunol. 182 (2009) 4349–4356.
[27] L. Ramsgaard, J.M. Englert, M.L. Manni, P.S. Milutinovic, J. Gefter, J. Tobolewski, L. Crum, G.M. Coudriet, J. Piganelli, R. Zamora, Y. Vodovotz, J.J. Enghild, T.D. Oury, Lack of the receptor for advanced glycation end-products attenuates E. coli pneumonia in mice, PloS One 6 (2011) e20132.
[28] R. Blondonnet, J. Audard, C. Belville, G. Clairefond, J. Lutz, D. Bouvier, L. Roszyk, C. Gross, M. Lavergne, M. Fournet, L. Blanchon, C. Vachias, C. Damon-Soubeyrand, V. Sapin, J.-M. Constantin, M. Jabaudon, RAGE inhibition reduces acute lung injury in mice, Sci. Rep. 7 (2017) 7208.
[29] J. Audard, T. Godet, R. Blondonnet, J.-B. Joffredo, B. Paquette, C. Belville, M. Lavergne, C. Gross, J. Pasteur, D. Bouvier, L. Blanchon, V. Sapin, B. Pereira, J.-M. Constantin, M. Jabaudon, Inhibition of the receptor for advanced glycation end-products in acute respiratory distress syndrome: a randomised laboratory trial in piglets, Sci. Rep. 9 (2019) 9227.
[30] L.L. Rong, S.-F. Yan, T. Wendt, D. Hans, S. Pachydaki, L.G. Bucciarelli, A. Adebayo, W. Qu, Y. Lu, K. Kostov, E. Lalla, S.D. Yan, C. Gooch, M. Szabolcs, W. Trojaborg, A.P. Hays, A.M. Schmidt, RAGE modulates peripheral nerve regeneration via recruitment of both inflammatory and axonal outgrowth pathways, FASEB J 18 (2004) 1818–1825.
[31] O.O. Ojo, M.H. Ryu, A. Jha, H. Unruh, A.J. Halayko, High-mobility group box 1 promotes extracellular matrix synthesis and wound repair in human bronchial epithelial cells, Am. J. Physiol. Lung Cell Mol. Physiol. 309 (2015) L1354–L1366.
[32] T. Arumugam, V. Ramachandran, S.B. Gomez, A.M. Schmidt, C.D. Logsdon, S100P-derived RAGE antagonistic peptide reduces tumor growth and metastasis, Clin. Canc. Res. 18 (2012) 4356–4364.
[33] S. Bongarzone, V. Savickas, F. Luzi, A.D. Gee, Targeting the receptor for advanced glycation endproducts (RAGE): a medicinal chemistry perspective, J. Med. Chem. 60 (2017) 7213–7232.
[34] S. Uderhardt, A.J. Martins, J.S. Tsang, T. Lämmermann, R.N. Germain, Resident macrophages cloak tissue microlesions to prevent neutrophil-driven inflammatory damage, Cell 177 (2019) 541–555.e17.
[35] J. Schindelin, I. Arganda-Carreras, E. Frise, V. Kaynig, M. Longair, T. Pietzsch, S. Preibisch, C. Rueden, S. Saalfeld, B. Schmid, J.-Y. Tinevez, D.J. White, V. Hartenstein, K. Eliceiri, P. Tomancak, A. Cardona, Fiji: an open-source platform for biological-image analysis, Nat. Methods 9 (2012) 676–682.
[36] C. Gross, C. Belville, M. Lavergne, H. Choltus, M. Jabaudon, R. Blondonnet, J.-M. Constantin, F. Chiambaretta, L. Blanchon, V. Sapin, Advanced glycation end products and receptor (RAGE) promote wound healing of human corneal epithelial cells, Invest. Ophthalmol. Vis. Sci. 61 (2020) 14.
[37] S. Straino, A. Di Carlo, A. Mangoni, R. De Mori, L. Guerra, R. Maurelli, L. Panacchia, F. Di Giacomo, R. Palumbo, C. Di Campli, L. Uccioli, P. Biglioli, M.E. Bianchi, M.C. Capogrossi, A. Germani, High-mobility group box 1 protein in human and murine skin: involvement in wound healing, J. Invest. Dermatol. 128 (2008) 1545–1553.
[38] J.-F. Pittet, H. Koh, X. Fang, K. Iles, S. Christiaans, N. Anjun, B.M. Wagener, D.W. Park, J.W. Zmijewski, M.A. Matthay, J. Roux, HMGB1 accelerates alveolar epithelial repair via an IL-1β- and αvβ6 integrin-dependent activation of TGF-β1, PloS One 8 (2013) e63907.
[39] A.M. Schmidt, O. Hori, R. Cao, S.D. Yan, J. Brett, J.L. Wautier, S. Ogawa, K. Kuwabara, M. Matsumoto, D. Stern, RAGE: a novel cellular receptor for advanced glycation end products, Diabetes 45 (Suppl 3) (1996) S77–S80.
[40] A. Bierhaus, P.M. Humpert, M. Morcos, T. Wendt, T. Chavakis, B. Arnold, D.M. Stern, P.P. Nawroth, Understanding RAGE, the receptor for advanced glycation end products, J. Mol. Med. 83 (2005) 876–886.
[41] L.M. Crosby, C. Luellen, Z. Zhang, L.L. Tague, S.E. Sinclair, C.M. Waters, Balance of life and death in alveolar epithelial type II cells: proliferation, apoptosis, and the effects of cyclic stretch on wound healing, Am. J. Physiol. Lung Cell Mol. Physiol. 301 (2011) L536–L546.
[42] W. Huang, H. Zhao, H. Dong, Y. Wu, L. Yao, F. Zou, S. Cai, High-mobility group box 1 impairs airway epithelial barrier function through the activation of the RAGE/ERK pathway, Int. J. Mol. Med. 37 (2016) 1189–1198.
[43] J. Yang, L. Chen, J. Yang, J. Ding, H. Rong, W. Dong, X. Li, High mobility group box-1 induces migration of vascular smooth muscle cells via TLR4-dependent PI3K/Akt pathway activation, Mol. Biol. Rep. 39 (2012) 3361–3367.
[44] J. Zhu, J. Luo, Y. Li, M. Jia, Y. Wang, Y. Huang, S. Ke, HMGB1 induces human non-small cell lung cancer cell motility by activating integrin αvβ3/FAK through TLR4/NF-κB signaling pathway, Biochem. Biophys. Res. Commun. 480 (2016) 522–527.
[45] Y. Zhang, B. You, X. Liu, J. Chen, Y. Peng, Z. Yuan, High-mobility group box 1 (HMGB1) induces migration of endothelial progenitor cell via receptor for advanced glycation end-products (RAGE)-Dependent PI3K/Akt/eNOS signaling pathway, Med. Sci. Mon. Int. Med. J. Exp. Clin. Res. 25 (2019) 6462–6473.
[46] S. Vogel, D. Rath, O. Borst, A. Mack, P. Loughran, M.T. Lotze, M.D. Neal, T.R. Billiar, M. Gawaz, Platelet-derived high-mobility group box 1 promotes recruitment and suppresses apoptosis of monocytes, Biochem. Biophys. Res. Commun. 478 (2016) 143–148.
[47] V. Meneghini, M.T. Francese, L. Carraro, M. Grilli, A novel role for the Receptor for Advanced Glycation End-products in neural progenitor cells derived from adult SubVentricular Zone, Mol. Cell. Neurosci. 45 (2010) 139–150.
[48] A. Taguchi, D.C. Blood, G. del Toro, A. Canet, D.C. Lee, W. Qu, N. Tanji, Y. Lu, E. Lalla, C. Fu, M.A. Hofmann, T. Kislinger, M. Ingram, A. Lu, H. Tanaka, O. Hori, S. Ogawa, D.M. Stern, A.M. Schmidt, Blockade of RAGE-amphoterin signalling suppresses tumour growth and metastases, Nature 405 (2000) 354–360.
[49] H.J. Huttunen, C. Fages, J. Kuja-Panula, A.J. Ridley, H. Rauvala, Receptor for advanced glycation end products-binding COOH-terminal motif of amphoterin inhibits invasive migration and metastasis, Cancer Res 62 (2002) 4805–4811.
[50] D. Yang, Q. Chen, H. Yang, K.J. Tracey, M. Bustin, J.J. Oppenheim, High mobility group box-1 protein induces the migration and activation of human dendritic cells and acts as an alarmin, J. Leukoc. Biol. 81 (2007) 59–66.
[51] Y.S. Kim, J. Kim, K.M. Kim, D.H. Jung, S. Choi, C.-S. Kim, J.S. Kim, Myricetin inhibits advanced glycation end product (AGE)-induced migration of retinal pericytes through phosphorylation of ERK1/2, FAK-1, and paxillin in vitro and in vivo, Biochem. Pharmacol. 93 (2015) 496–505.
[52] S. Lee, C. Piao, G. Kim, J.Y. Kim, E. Choi, M. Lee, Production and application of HMGB1 derived recombinant RAGE-antagonist peptide for anti-inflammatory therapy in acute lung injury, Eur. J. Pharmaceut. Sci. 114 (2017) 275–284.
[53] H. Fehrenbach, R. Weiskirchen, M. Kasper, A.M. Gressner, Up-regulated expression of the receptor for advanced glycation end products in cultured rat hepatic stellate cells during transdifferentiation to myofibroblasts, Hepatology 34 (2001) 943–952.
[54] N. Demling, C. Ehrhardt, M. Kasper, M. Laue, L. Knels, E.P. Rieber, Promotion of cell adherence and spreading: a novel function of RAGE, the highly selective differentiation marker of human alveolar epithelial type I cells, Cell Tissue Res. 323 (2006) 475–488.
[55] A.E. Vaughan, A.N. Brumwell, Y. Xi, J.E. Gotts, D.G. Brownfield, B. Treutlein, K. Tan, V. Tan, F.C. Liu, M.R. Looney, M.A. Matthay, J.R. Rock, H.A. Chapman, Lineage-negative progenitors mobilize to regenerate lung epithelium after major injury, Nature 517 (2015) 621–625.

STUDY N°4

Effects of sevoflurane on lung epithelial permeability in experimental models of acute respiratory distress syndrome

Ruoyang Zhai, Woodys Lenga Ma Bonda, Charlotte Leclaire, Cécile Saint-Béat, Camille Theilliere, Corinne Belville, Randy Coupet, Raiko Blondonnet, Damien Bouvier, Loic Blanchon, Vincent Sapin, Matthieu Jabaudon (*Submitted for Publication*)

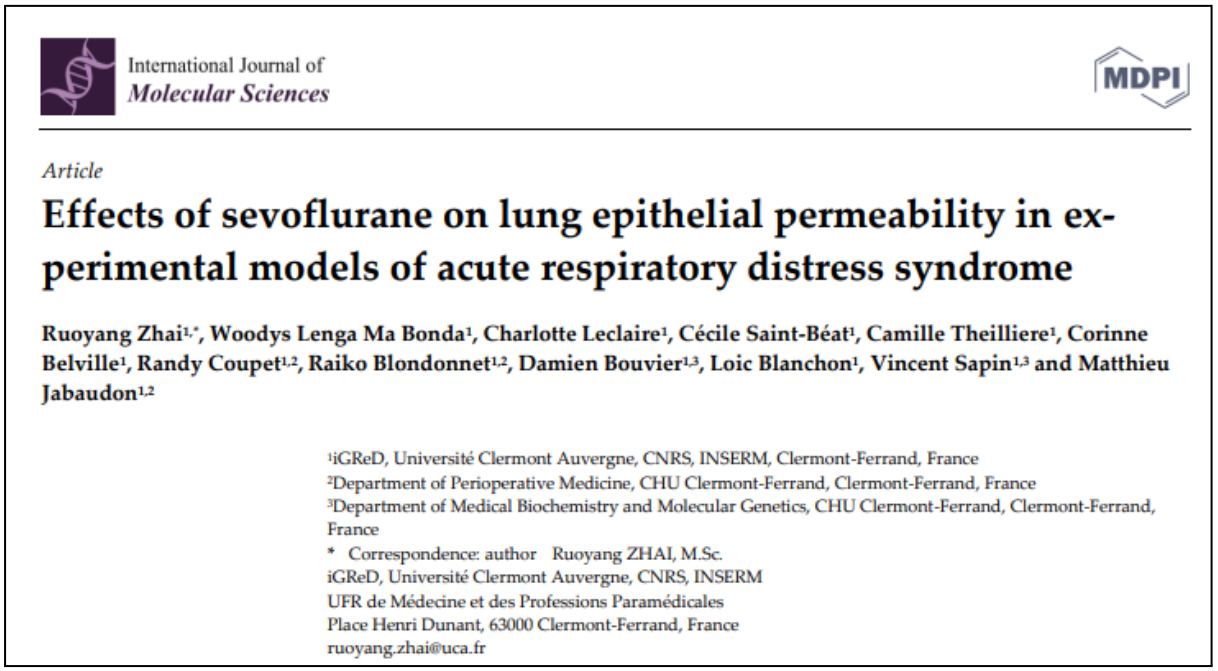

International Journal of *Molecular Sciences*

MDPI

Article

Effects of sevoflurane on lung epithelial permeability in experimental models of acute respiratory distress syndrome

Ruoyang Zhai[1,*], Woodys Lenga Ma Bonda[1], Charlotte Leclaire[1], Cécile Saint-Béat[1], Camille Theilliere[1], Corinne Belville[1], Randy Coupet[1,2], Raiko Blondonnet[1,2], Damien Bouvier[1,3], Loic Blanchon[1], Vincent Sapin[1,3] and Matthieu Jabaudon[1,2]

[1]iGReD, Université Clermont Auvergne, CNRS, INSERM, Clermont-Ferrand, France
[2]Department of Perioperative Medicine, CHU Clermont-Ferrand, Clermont-Ferrand, France
[3]Department of Medical Biochemistry and Molecular Genetics, CHU Clermont-Ferrand, Clermont-Ferrand, France
* Correspondence: author Ruoyang ZHAI, M.Sc.
iGReD, Université Clermont Auvergne, CNRS, INSERM
UFR de Médecine et des Professions Paramédicales
Place Henri Dunant, 63000 Clermont-Ferrand, France
ruoyang.zhai@uca.fr

Scientific Knowledge of the Subject

Acute respiratory distress syndrome (ARDS) is a major cause of respiratory failure with a high mortality rate (mortality of 30–50%), ARDS is characterized by diffuse alveolar damage, alveolar edema, and hypoxemic respiratory failure which cause heavy healthcare cost, and lead to reduced quality of life or long-term physical and cognitive outcomes among survivors. There is still no pharmacological approach successfully translated into clinical application, and currently available treatments for ARDS are largely supportive and based on lung-protective mechanical ventilation and conservative fluid management[3,4,35,224].

The degree of injury to the alveolar epithelium is an important determinant of ARDS severity in patients[224]. Epithelial injury includes the dissociation of intercellular junctions with increased paracellular permeability, a process involving the dysregulation of tight junction proteins (e.g., zonula occludens (ZO) proteins) or adherens junction proteins (e.g., E–cadherin) and actin cytoskeletal rearrangement[6,183,224,235].

Sevoflurane is a volatile halogenated anesthetic that is frequently used as a sedative in intensive care units[57,236,237]. In preclinical studies of ARDS, Sevoflurane was found to improve gas exchange, reduce alveolar edema, and attenuate pulmonary and systemic inflammation in multiple preclinical models of ARDS[57,62,73,238–240]. one pilot randomized controlled trial in patients with ARDS found that sevoflurane, compared to intravenous midazolam, improved arterial oxygenation and decreased alveolar and plasma levels of some inflammatory cytokines and of soluble receptor for advanced glycation end-products (sRAGE), a marker of lung epithelial injury[77]. However, the precise mechanisms accounting for the lung-protective properties of sevoflurane remain largely unknown.

Contributions of this study to the field

Our study has shown the exposure to sevoflurane improved features of experimental ARDS in our mouse model, such as impaired arterial oxygenation, alveolar inflammation, histological evidence of lung tissue injury, and the extent of lung edema. In addition, focusing on the the integrity of the epithelial barrier function, our study showed decreased indices of permeability and preserved epithelial structures in cells and mice exposed to sevoflurane after injury, with increased the protein expression of ZO-1 but no effect on E-cadherin. Our study provides novel evidence supporting the molecular mechanisms of the effects of sevoflurane on lung epithelial barrier function after injury. Notably, sevoflurane was associated with decreased lung levels of pMLC and decreased actin cytoskeletal rearrangement after injury in vivo and in vitro. Sevoflurane also decreased cytomix-induced RhoA activity in vitro, suggesting that sevoflurane could decrease lung epithelial permeability through inhibition of the RhoA/pMLC/F-actin cytoskeleton pathway, as also suggested by studies on other cell types.

In addition, we showed that RAGE-/- mice had better oxygenation levels, decreased lung permeability, and improved inflammatory response compared to littermate wild-type animals. *In vitro*, treatment with RAP decreased cytomix-induced RhoA activity in MLE-12 cells, and treatment with RAP alleviated the beneficial effects of sevoflurane on the electrical resistance of MLE-12 cell monolayers and on actin cytoskeletal rearrangement. *In vivo,* RAGE-/- mice received the same benefits from sevoflurane as littermate controls in terms of indices of lung alveolar-capillary permeability. In contrast to wild-type mice, however, the RAGE-/- animals did not exhibit the effects of improved arterial oxygenation and decreased BALF levels of IL-6 and TNF-α observed with sevoflurane, suggesting that RAGE plays a

mediating role in the effects of sevoflurane on acute lung injury. Further studies are needed to determine whether the RAGE pathway mediates some of these effects.

International Journal of
Molecular Sciences

MDPI

Article

Effects of sevoflurane on lung epithelial permeability in experimental models of acute respiratory distress syndrome

Ruoyang Zhai[1,*], Woodys Lenga Ma Bonda[1], Charlotte Leclaire[1], Cécile Saint-Béat[1], Camille Theilliere[1], Corinne Belville[1], Randy Coupet[1,2], Raiko Blondonnet[1,2], Damien Bouvier[1,3], Loic Blanchon[1], Vincent Sapin[1,3] and Matthieu Jabaudon[1,2]

[1]iGReD, Université Clermont Auvergne, CNRS, INSERM, Clermont-Ferrand, France
[2]Department of Perioperative Medicine, CHU Clermont-Ferrand, Clermont-Ferrand, France
[3]Department of Medical Biochemistry and Molecular Genetics, CHU Clermont-Ferrand, Clermont-Ferrand, France
* Correspondence: author Ruoyang ZHAI, M.Sc.
iGReD, Université Clermont Auvergne, CNRS, INSERM
UFR de Médecine et des Professions Paramédicales
Place Henri Dunant, 63000 Clermont-Ferrand, France
ruoyang.zhai@uca.fr

ABSTRACT: Acute respiratory distress syndrome (ARDS) is a major cause of respiratory failure and death that still lacks specific therapies. Inhaled sevoflurane is an anesthetic agent that can be used for the sedation of patients with ARDS. In preclinical studies, sevoflurane is associated with decreased inflammation, improved arterial oxygenation, and attenuated lung edema. However, the precise mechanisms of such potential lung-protective effects of sevoflurane are still largely unknown. Here, we used a translational model of acid-induced lung injury in mice and an in vitro model of sterile injury in mouse lung epithelial cells to investigate whether sevoflurane could decrease lung alveolar epithelial permeability through the Ras homolog family member A (RhoA)/phospho-Myosin Light Chain 2 (Ser19) (pMLC)/filamentous (F)-actin pathway. We further hypothesized that these effects could be mediated by the receptor for advanced glycation end-products (RAGE). Lung permeability was assessed by measuring alveolar levels of total protein, the alveolar-to-plasma ratio in human albumin, and lung extravasation of a fluorescent dye in C57BL/6JRj mice on the day they received intratracheal hydrochloric acid, alone or followed by exposure at 1% sevoflurane for 1 hour, and on days 1, 2, and 4 after acid injury. In vitro, the resistance of a monolayer of mouse lung epithelial cells was assessed as a surrogate for permeability using electric cell-substrate impedance sensing after treatment with cytomix, a mixture of TNFα, IL-1β, and IFNγ, alone or followed by exposure at 1% sevoflurane for up to 24 hours. In both models, junction proteins (ZO-1, E-cadherin) and pMLC were quantified, and F-actin was immunostained. RhoA activity was further evaluated in vitro. In vivo and in vitro, exposure to sevoflurane decreased lung epithelial injury and restored epithelial barrier function after injury, which was associated with increased expression of ZO-1, decreased levels of pMLC, and decreased actin cytoskeletal rearrangement. Sevoflurane also decreased cytomix-induced RhoA activity in vitro. $RAGE^{-/-}$ mice had better oxygenation levels and decreased lung permeability and inflammatory response than littermate wild-type animals. Further, treatment with a RAGE antagonist peptide (RAP) decreased cytomix-induced RhoA activity in vitro. Treatment with RAP alleviated some beneficial effects of sevoflurane in vitro, such as on the electrical resistance of an MLE-12 cell monolayer or on actin cytoskeletal rearrangement. In vivo, RAGE deletion did not influence the beneficial effects of sevoflurane on indices of lung alveolar-capillary permeability seen in wild-type animals. However, in contrast to wild-type mice, $RAGE^{-/-}$ animals did not show improved arterial oxygenation or decreased BAL levels of IL-6 and TNF-α with sevoflurane. Taken together, the current results suggest that sevoflurane could decrease lung epithelial permeability through the RhoA/pMLC/F-actin pathway. Determining whether the RAGE pathway mediates some of these effects requires further investigation.

Keywords: Acute respiratory distress syndrome; Sevoflurane; Lung epithelial barrier function; Junction proteins; Intracellular pathways; Receptor for advanced glycation end-products

INTRODUCTION

Acute respiratory distress syndrome (ARDS) is a clinical syndrome characterized by diffuse alveolar injury, lung edema, and hypoxemic respiratory failure from septic or sterile causes, which frequently occurs in critically ill patients and is associated with a high mortality rate (mortality of 30–50%), greater healthcare utilization, and reduced quality of life or long-term physical and cognitive outcomes among survivors [1–4]. The recent COVID-19 pandemic further highlighted the high morbidity and mortality of ARDS and the high case numbers challenged most healthcare organizations worldwide [5,6]. Currently, the available treatments for ARDS are largely supportive and based on lung-protective mechanical ventilation and conservative fluid management. To date, no pharmacological approach has been successfully translated into clinical practice. Among other mechanisms leading to the accumulation of protein-rich edema fluid in the alveolar spaces, such as endothelial barrier disruption, immune cell recruitment or thrombo-inflammatory disorders, the degree of injury to the alveolar epithelium is an important determinant of ARDS severity in patients [3]. Epithelial injury includes the dissociation of intercellular junctions with increased paracellular permeability, a process involving the dysregulation of tight junction proteins (e.g., zonula occludens (ZO) proteins) or adherens junction proteins (e.g., E–cadherin) and actin cytoskeletal rearrangement [3,7–9].

Inhaled halogenated anesthetics, such as isoflurane or sevoflurane, are primarily used for general anesthesia but have gained recent attention for their use in sedation in the intensive care unit [10–12]. Sevoflurane was found to improve gas exchange, reduce alveolar edema, and attenuate pulmonary and systemic inflammation in multiple preclinical models of ARDS [10,13–17], and one pilot randomized controlled trial in patients with ARDS found that sevoflurane, compared to intravenous midazolam, improved arterial oxygenation and decreased alveolar and plasma levels of some inflammatory cytokines and of soluble receptor for advanced glycation end-products (sRAGE), a marker of lung epithelial injury [18]. However, the precise mechanisms accounting for the lung-protective properties of sevoflurane remain largely unknown, although, in a "double hit" mouse model of nebulized lipopolysaccharide (LPS) and ventilator-induced lung injury, isoflurane restored epithelial tight junction integrity via increased ZO-1 protein levels [19].

Because sevoflurane prevented LPS-induced barrier dysfunction in lung microvascular endothelial cells [20], we hypothesized that sevoflurane could decrease lung epithelial permeability. Accordingly, we used both an in vivo model of acid-induced lung injury in mice and an in vitro model of sterile injury in mouse lung epithelial cells to investigate whether sevoflurane could decrease lung alveolar epithelial permeability through the Ras homolog family member A (RhoA)/phospho-Myosin Light Chain 2 (Ser19) (pMLC)/filamentous (F)-actin pathway. As preclinical studies also reported various potential effects of sevoflurane on the RAGE and RhoA/F-actin pathways in cells of the central nervous system [21,22] and as the RAGE pathway plays a pivotal role in epithelial injury and repair during ARDS [3,23–26], we further hypothesized that the effects of sevoflurane on lung epithelial permeability could be, at least partially, mediated by RAGE.

MATERIALS AND METHODS

Mouse model of acid-induced lung injury

Animals were maintained and all procedures were performed in the animal facility at University Clermont Auvergne with the approval of the ethics committee of the French *Ministère de l'Education Nationale, de l'Enseignement Supérieur et de la Recherche* (approval number CE 67–12). The experiments were performed in accordance with relevant regulations, the 3R principles (Replacement, Reduction, and Refinement), and the "Animal Research: Reporting In Vivo Experiments" (ARRIVE) guidelines 2.0 [27].

C57BL/6JRj littermate control (Janvier Labs, Saint-Berthevin, France) and RAGE$^{-/-}$ mice (kindly provided by Prof. Ann Marie Schmidt, NYU Langone Health, New York, USA), aged 10–12 weeks and weighing 25–30 g, were anesthetized via an intraperitoneal injection of ketamine (100 mg/kg) and xylazine (10 mg/kg) and given a subcutaneous fluid bolus of 10 μL/g 0.9% isotonic saline as preemptive resuscitation. As previously described [28,29], 75 μL of a 322 mOsm/L solution (iso-osmolar to mouse plasma) of 0.1 M hydrochloric acid (pH 1.0) was instilled to model ARDS in injured mice. For the next 4 h, mice were kept in a transparent recovery box under humidified supplemental oxygen (inspiratory oxygen fraction (FiO_2), reduced gradually from 1.0 to 0.21) and carefully monitored. Their body temperature was maintained using external heat sources, after which they were transferred to individually ventilated cages with air and free access to food and water.

To examine the effects of sevoflurane, lung-injured wild-type and RAGE$^{-/-}$ mice were divided into a Sham group, an HCl group, and an HCl+Sevo group. In the intervention groups, sevoflurane 1% was delivered for 1 hour and its ambient concentration was maintained using a gas monitor (AMG-06, Sedana Medical, Danderyd, Sweden).

Physiological measurements in vivo

The criteria for experimental ARDS were evaluated as recommended by the American Thoracic Society [30], at baseline (day 0) in injured and sham animals, and at specified time-points (days 1, 2, and 4) after acid-induced injury [25,29]. Animals were ventilated for 30 min using volume-controlled ventilation with a tidal volume of 6 $\mu L.g^{-1}$, a positive end-expiratory pressure of 6 cmH_2O, a respiratory rate of 160 per minute, an inspiration-to-expiration ratio of 1:2, and an FiO_2 of 1.0 (VentElite, Harvard Apparatus, Cambridge, USA). At the end of ventilation, the mice were sacrificed via anesthetic overdose with intraperitoneal pentobarbital (150 $\mu g.g^{-1}$), and arterial blood was sampled for blood gas analysis (Epoc® Blood Analysis System, Siemens Healthineers, Erlangen, Germany), bronchoalveolar lavage (BAL) was performed with 750 μL of saline, and lungs were harvested for molecular biology and histology examination. Acid-injured animals were compared with sham mice, receiving only surgical preparation and 30 min of ventilation. One hour before sacrifice, 10 $\mu g.g^{-1}$ of human serum albumin (HSA) dissolved in 100 μL of saline was retro-orbitally injected for the measurement of the lung permeability index, defined as the ratio of HSA in the BAL fluid to that in the plasma collected at the end of the experiments (human albumin ELISA Kit, R&D Systems, Minneapolis, MN) [29]. In some mice, instead of HSA, a fluorescent tracer IRDye® 800CW (LI-COR Biosciences, Lincoln, USA) was administered retro-orbitally to visualize and quantify its accumulation in isolated lung samples and BAL fluid samples (Pearl® Trilogy Small animal Imaging System, LI-COR Biosciences, Lincoln, USA).

Cell culture

Virus-transformed murine lung epithelial (MLE-12) cells were obtained from the American Type Culture Collection (CRL-2110™, ATCC, Manassas, USA). The cells were maintained in Gibco Dulbecco's Modified Eagle Medium/Nutrient Mixture F12 (DMEM F12, a 1:1 mixture of DMEM and Ham's F-12) (Thermo Fisher Scientific, Waltham, USA) supplemented with 2% fetal bovine serum (FBS) (Thermo Fisher Scientific, Waltham, USA), 1% penicillin-streptomycin-amphotericin (Eurobio Scientific, Les Ulis, France), 10 nM hydrocortisone and 10 nM β-estradiol (Sigma-Aldrich, St. Louis, USA), and 1X insu-

lin-transferrin-selenium (Thermo Fisher Scientific, Waltham, USA). The cells were incubated at 37°C in a humidified atmosphere containing 5% CO_2.

In vitro treatments

To test the response of MLE-12 cells to an injurious, nonseptic stimulus, the cells were treated with cytomix, a mix of 10 ng/mL each of tumor necrosis factor (TNF)-α, interleukin (IL)-1β, and interferon (IFN)-γ (R&D Systems, Minneapolis, MN) in serum-free medium [31]. To test the hypothesis that the RAGE pathway could influence the effects of sevoflurane, cells were treated with 12.5 $\mu g.mL^{-1}$ of a RAGE Antagonist Peptide (RAP) (Sigma-Aldrich, St. Louis, USA). Treatments were initiated after the cells reached a monolayer with 100% confluency, usually 48 hours after seeding to allow formation of intercellular junctions. The cells were exposed to cytomix, administered with medium, for up to 24 hours in some experiments. RAP was delivered 30 min before treatment with cytomix.

Exposure to sevoflurane in vitro was delivered through a dedicated vaporizer (Vapor 2000, Dräger, Lübeck, Germany) in a standard and sealed incubator (Thermo Fisher Scientific, Waltham, USA) with specific gas scavenging (Flurabsorb, Sedana-Medical, Danderyd, Sweden). Concentrations of sevoflurane were continuously monitored and maintained at 1% inside the incubator (AMG-06, Sedana Medical, Danderyd, Sweden), for up to 24 hours in some experiments.

Electric cell-substrate impedance sensing

MLE-12 cells were cultured to confluence on collagen-coated (50 $\mu g.mL^{-1}$) 96-well arrays overlying electrodes according to the manufacturer's protocol (96W10df PET, Applied Biophysics, Troy, USA). Alternating current applied to each electrode was used to calculate the resistance of the cell monolayer over 24 hours (ECIS® Z-Theta, Applied Biophysics, Troy, USA), which reflects barrier integrity as resistance decreases when the epithelial monolayer is compromised [32].

RhoA expression and activity measurements in vitro

RhoA activity was determined using a RhoA-specific G-LISA Activation Assay kit (BK124, Cytoskeleton, Denver, USA) following the per manufacturer's protocol. The results were normalized to the total RhoA level as measured using the Total RhoA ELISA Biochem Kit (BK150, Cytoskeleton, Denver, USA). Active RhoA was determined in duplicate with the same colorimetric RhoA activation assay in all experimental conditions.

Histological examination in vivo and immunofluorescence

Formalin-fixed paraffin embedded tissue sections (10 μm) from mice were rehydrated and deparaffinized through a series of xylem ethanol baths. The slices were stained with hematoxylin and eosin (Sigma-Aldrich, St. Louis, USA). Histological features of lung injury were scored by one independent expert, blinded to the treatment groups, using a standardized score as previously described [29,33].

For immunofluorescence studies, non-specific binding sites were blocked with phosphate-buffered saline (PBS)/1% horse serum buffer for 1 hour at room temperature. Sections were then incubated with primary antibodies overnight at 2–8°C in the incubation buffer (1% bovine serum albumin (BSA), 1% normal donkey serum, 0.3% Triton X-100, and 0.01% sodium azide in PBS). Anti-ZO-1 (61-7300, Invitrogen, Waltham, USA) and anti-E-cadherin (Cell Signaling Technology, Danvers, USA) antibodies were diluted at 1/25 and 1/200, respectively. Slices were washed three times on a rocking station for 15 min with PBS and further incubated with secondary anti-rabbit IgG coupled with AlexaFluor® 647 A-21244 (Invitrogen, Waltham, USA) diluted at 1/500 in the incubation buffer. Control slices without primary antibodies were used as negative controls for nonspecific binding of secondary antibodies.

MLE-12 cells were seeded in eight-well chamber slides (Nunc™ Lab-Tek™ II Chamber Slide™, Thermo Fisher Scientific, Waltham, USA) at a density of 10^5 per well in complete medium for 72 hours at 37°C and 5% CO_2. The cells were then exposed to 10 ng/mL cytomix, in the presence or absence of 12.5 μg/mL RAP, in serum-free medium for 6 hours before immunostaining. After treatments, cells were washed with PBS, fixed, and permeabilized in 3.7% paraformaldehyde/0.2 % Triton X-100 buffer for 10 min at room temperature. Slides were washed three times in PBS before non-specific sites were blocked with a PBS/BSA 3% solution for 30 min. Then, an anti- ZO-1 polyclonal antibody (61-7300, Invitrogen, Waltham, USA) diluted at 1/25 or an anti-E-cadherin rabbit monoclonal antibody (24E10, Cell Signaling Technology, Danvers, USA) diluted at 1/200 were incubated for 1 hour. After three additional washes again, the slides were incubated with an anti-rabbit IgG labeled with AlexaFluor® 647 (A-21244, Invitrogen, Waltham, USA) diluted at 1/1,000 for 1 hour.

Finally, the cells and tissue sections were washed three times with PBS before nuclei staining with 1 $\mu g.mL^{-1}$ Hoechst 33258 diluted at 1/10,000 (Sigma-Aldrich, St. Louis, USA) for 10 min before the slides were washed and covered with an anti-fading mounting medium (CitiFluor MWL4-88, Electron Microscopy Sciences, Hatfield, USA). Samples were observed under a fluorescence microscope (Zeiss Axio Imager M2/Colibri7 coupled Axiocam 506 monochrome camera, power supply 232, and ApoTome.2) at 10X magnification and analyzed with ZEN software v2.1 (Zeiss, Oberkochen, Germany). The same exposure time was chosen to compare fluorescence among all conditions (800 ms for ZO-1 and E-cadherin at 10 X magnification).

mRNA and protein quantification

mRNA was extracted from cultured cells or lung tissues with the Nucleospin Kit (Macherey-Nagel), in accordance with the manufacturer's instructions. Briefly, cells were scratched and approximately 30 mg of tissues were grinded with 2mL lysis buffer using the Precellys lysing kit (Bertin Technologies, Montigny-le-Bretonneux, France). For grinding, the Precellys Evolution device (Bertin Technologies, Montigny-le-Bretonneux, France) was used for 1.5 min, with intervals of 15 seconds between each 15 seconds of burst at 8,500 rpm. After quantification using the DeNovix DS-11 FX spectrophotometer/fluorometer (DeNovix, Wilmington, USA), retro-transcription was done using 1 μg of mRNA following the high-capacity cDNA reverse transcription kit protocol (Applied Biosystems, Waltham, USA). Real-time polymerase chain reaction (PCR) was performed using the SsoAdvanced SyBR Green Supermix kit (Thermo Fisher Scientific, Waltham, USA) and LightCycler 480 (Roche, Basel, Switzerland). Primers for ZO-1, E-cadherin, RAGE and GAPDH were obtained from the PrimePCR SYBR Green Assays systems (Bio-Rad Laboratories, Hercules, USA). LightCycler 480 was programmed for 40 cycles of two-step cycling for 30 seconds at 95°C and 30 seconds at 60°C, followed by a melting curve and cooling step. To monitor any changes in mRNA levels, we used the $2^{-\Delta\Delta CT}$ method after normalization with the housekeeper gene GAPDH.

Proteins from treated cells were obtained by scratching cell monolayers with a RIPA buffer containing a mixture of 1X protease inhibitors, 1 mM sodium orthovanadate (Sigma-Aldrich, St. Louis, USA), and 1X PhosSTOP (Roche, Basel, Switzerland). Tissues were grinded in a Precellys lysing kit (Bertin Technologies, Montigny-le-Bretonneux, France) with 2 mL-tubes containing ceramic beads in RIPA buffer. The tubes were first centrifuged at 14,000 x g for 10 min to remove cell debris and beads. Then, all the lysates were then sonicated for 3 min and centrifuged at 14,000 x g at 4°C for 14 min. Supernatant protein concentrations were measured using the BCA assay (Pierce™ BCA protein assay kit (Thermo Fisher Scientific, Waltham, USA). Next, 25 μg of total protein in β-mercapto-ethanol and Laemmli buffer 1X (Bio-Rad Laboratories, Hercules, USA) containing a reducing agent were separated on an SDS-PAGE 4%-15% protein gel (Mini-PROTEAN TGX Stain-Free gels, Bio-Rad Laboratories, Hercules, USA), before being transferred to nitrocellulose membranes using the Trans-Blot Turbo Transfer System

(Bio-Rad Laboratories, Hercules, USA). The membranes were then saturated for 1 hour at room temperature in the TBST buffer (50 mM Tris HCl pH 7.5, 150 mM NaCl, and 0.1% Tween 20, Abcam, Cambridge, United Kingdom) containing 5% of fat-free milk or BSA. Membranes were incubated overnight at 4°C with primary antibodies. The ZO-1 polyclonal antibody (61-7300, Invitrogen, Waltham, USA) and the anti-E-cadherin rabbit monoclonal antibody (24E10, Cell Signaling Technology, Danvers, USA) were diluted at 1/25 and 1/200, respectively. Antibodies against MLC and pMLC were obtained from the Myosin Light Chain 2 Antibody Sampler Kit #9776 (Cell Signaling Technology, Danvers, USA). After washing with the TBST buffer, the membranes were incubated for 1 hour with horseradish peroxidase (HRP)-conjugated secondary anti-rabbit IgG (BI 2407, Abliance, Compiègne, France) diluted at 1/2,500–1/5,000. Then, the membranes were processed for chemiluminescence detection using Clarity Max ECL Western blotting substrates (Bio-Rad Laboratories, Hercules, USA). Protein detection was performed using a Bio-Rad Imager, and densitometry analysis of protein bands from the Western blot images was performed using Bio-Rad imaging software (Bio-Rad Laboratories, Hercules, USA). The results were normalized to the band intensity in the control condition.

Cytokines (TNF-α, IL-1β, and IL-6) in the BAL fluid from mice or supernatants from cell cultures were measured using the Ella Automated Immunoassay System (ProteinSimple, Bio-Techne, Minneapolis, USA) following the manufacturer's instructions. Relative fluorescence units were converted to cytokine concentrations using calibration curves provided by the manufacturer. Final results represent the average of triplicate measurements for each analyte.

For mouse sRAGE quantification, the Quantikine® ELISA mouse RAGE immunoassay (MRG00, R&D Systems, Minneapolis, USA) was used as per the manufacturer's instructions. Samples were diluted at 1/10. Measurements of HSA were performed using ELISA (R&D Systems, Minneapolis, MN).

Statistical analysis

The data analysis was performed using Prism 9 software (GraphPaD software, La Jolla, USA) and Stata version 17 (StataCorp, College Station, USA). Tests were two-sided, with a bilateral type I error set at 5%. Continuous data were expressed as mean ± standard deviation or median with interquartile range depending on their statistical distribution after evaluating normality using the Shapiro–Wilk test and homoscedasticity using the Fisher–Snedecor test. Continuous parameters were compared between the experimental groups using an analysis of variance or the Kruskal–Wallis test (when t-test assumptions were not met). Random-effects models were used to analyze the longitudinal evolution of the variables, (i) by considering the between- and within-experiment variability (random effects of the subject: intercept and random slope) and (ii) by assessing fixed effects: group, time, and time–group interaction. The normality of the residuals was checked for all models. A limited number of animals was used for baseline comparisons (n = 3-4), and 4–6 animals were used in each group on days 1, 2, and 4 [29,34]. For the cell experiments, three independent series (n = 3-4 per series) were performed in duplicate.

RESULTS

In vivo effects of sevoflurane on lung injury and alveolar-capillary permeability

Arterial oxygenation impairment, the degree of alveolar inflammation, and histological evidence of lung tissue injury were higher on days 1–2 after injury in acid-injured mice, as compared with sham animals. However, these phenomena were not observed in animals treated with sevoflurane (Figure S1–3, online supplement).

Alveolar-capillary barrier permeability, as assessed by the permeability index and BAL levels of total proteins, peaked on days 1–2 after injury in acid-injured mice (Figure 1). This was less marked in animals treated with sevoflurane, although the differences did not reach statistical significance (Time x Group interaction for the permeability index: p = 0.88, for BAL total proteins: p = 0.95). The

extent of edema was further determined through imaging of isolated lung samples and BAL fluid, and fluorescent signals were more intense after acid injury in the control animals than in those treated with sevoflurane (Figure 1).

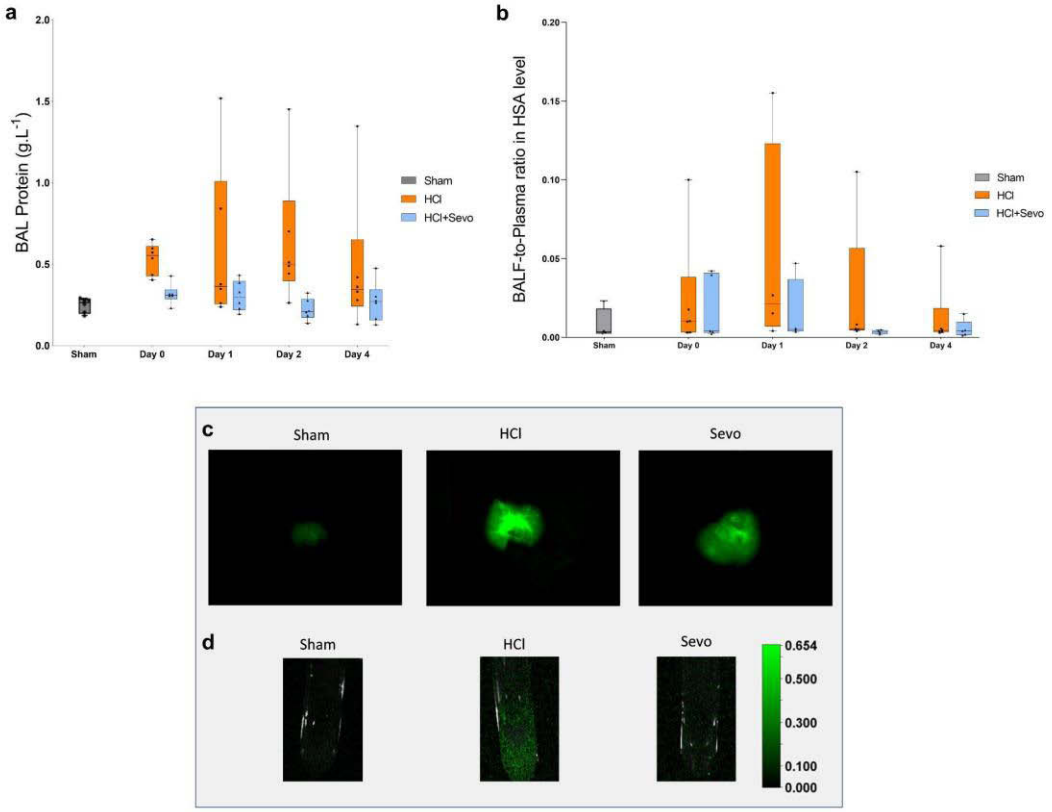

Figure 1. Measures of alveolar-capillary permeability in mice after acid-induced lung injury. a) Total protein content (in $g.L^{-1}$) of the bronchoalveolar lavage (BAL) fluid and **b**) Permeability index, as calculated as the BAL fluid-to-plasma ratio of the human serum albumin (HSA) concentration, in uninjured (Sham), acid-injured (HCl), and acid-injured mice treated with sevoflurane (HCl+Sevo) from day 0 to day 4 after injury. Values are presented as box and whisker plots with medians and interquartile ranges. Two-way ANOVA tests were performed, and post-hoc comparisons were performed if ANOVA results showed significance. **c**) Representative images of accumulation on day 2 after injury of an intravenously injected, near-infrared fluorescent dye, as reported as relative fluorescence units (RFU), in isolated lungs and **d**) in the BAL fluid of uninjured (Sham), acid-injured (HCl), and acid-injured mice treated with sevoflurane (HCl+Sevo).

In vivo effects of sevoflurane on mechanisms of lung epithelial integrity

Immunostaining studies revealed that ZO-1 and E-cadherin expressions were both markedly decreased in mouse lungs on day 1 after acid injury; in injured animals treated with sevoflurane, however, ZO-1 expression was restored (Figure 2). This effect of restored ZO-1 expression with sevoflurane following acid injury was confirmed after quantification by Western blot, although there were no differences in ZO-1 mRNA expressions (Figures S4–S5, online supplement). There were no between-group differences in E-cadherin expressions assessed by Western blot or RT-qPCR.

Increased pMLC was observed in lungs from mice on day 0 and day 1 after injury, as compared with sham animals. In mice treated with sevoflurane, such an increase was not seen (Figure 2).

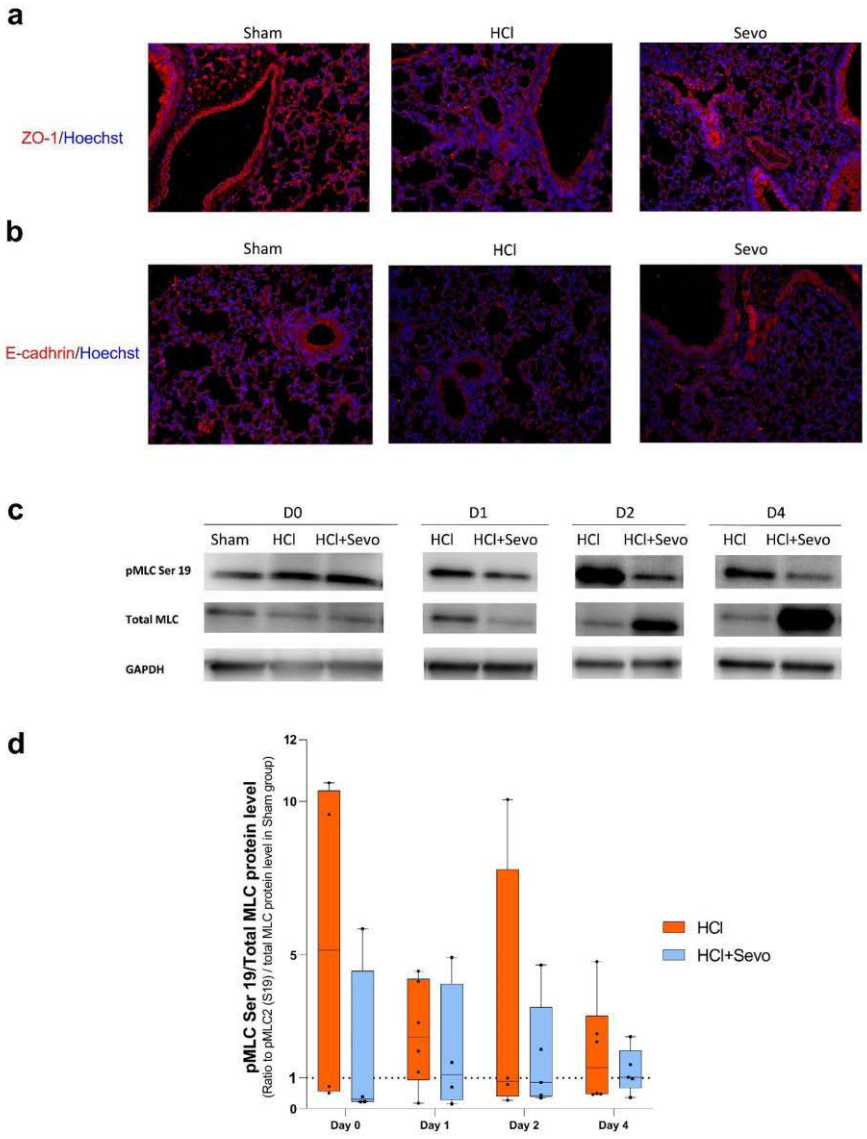

Figure 2. Lung junction proteins zonula occludens (ZO)-1 and E-cadherin and lung myosin light chain 2 (Ser19) phosphorylation (pMLC) in vivo. Immunostaining of lung a) ZO-1 and b) E-cadherin in lung tissues from uninjured (Sham), acid-injured (HCl), and acid-injured mice treated with sevoflurane (HCl+Sevo) on day 1 after injury. Tissues were fixed, permeabilized, and stained with ZO-1 and E-cadherin antibodies, followed by A488 secondary antibodies and Hoechst staining. All images were acquired by a fluorescent microscope with a 20x objective. a) ZO-1 protein is red-stained, and the cell nucleus is blue-stained. b) E-cadherin protein is red-stained, and the cell nucleus is blue-stained. Scale bar: 50 μm. c) Western blots of total myosin light chain (MLC) and phosphorylated myosin light chain 2 (Ser19) (pMLC) in lung of uninjured (Sham), acid-injured (HCl), and acid-injured mice treated with sevoflurane (HCl+Sevo) from day 0 to day 4 after injury. d) Protein expression levels were quantified and standardized by GAPDH protein level, and pMLC (Ser 19) levels were additionally standardized by total MLC level, expressed as ratios to those in Sham animals, and reported as box and whisker plots with medians and interquartile ranges. Two-way ANOVA test was performed, with post-hoc comparisons if ANOVA results showed significance.

In vitro effects of sevoflurane on lung epithelial barrier function

The electrical resistance of the MLE-12 monolayer, assessed using ECIS, was markedly decreased after treatment with cytomix, which was not found in cells exposed to sevoflurane (Time x Group interaction: $p < 10^{-4}$) (Figure 3). Post-hoc comparisons revealed significant differences in resistance at 12 and 24 hours between cytomix-treated cells exposed or not exposed to sevoflurane (Time x Group interaction: $p < 10^{-3}$ and $p < 10^{-4}$, respectively).

Treatment with cytomix was associated with increased cytokine release at 6 hours, but such a release was significantly prevented by exposure to sevoflurane (Figure 3).

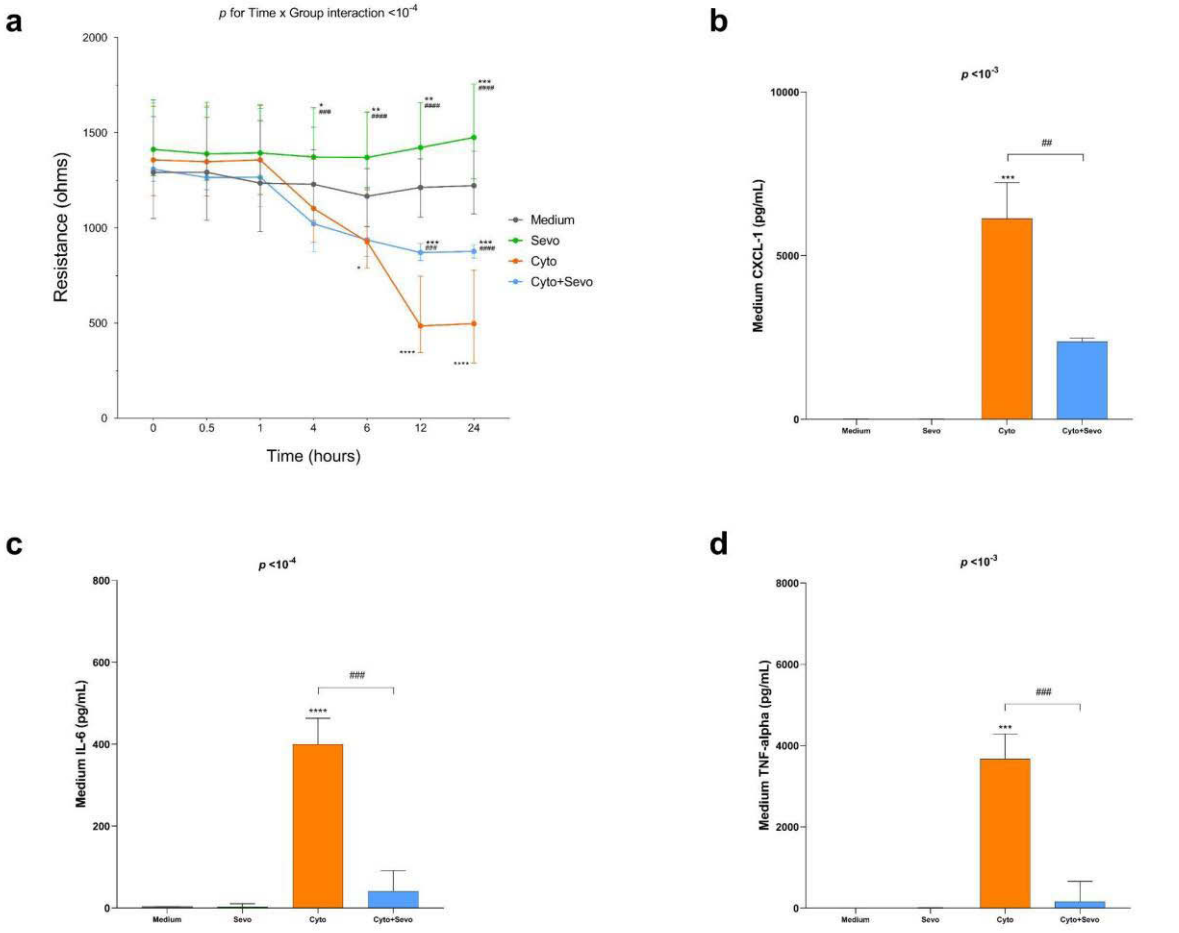

Figure 3. Effects of sevoflurane on electrical resistance and proinflammatory cytokines levels in conditioned medium of mouse lung epithelial (MLE-12) cell monolayer. a) Electrical resistance of a monolayer of MLE-12 cells was measured at a frequency at 4000 Hz by electric cell-substrate impedance sensing (ECIS) in untreated cells (Medium) or in cells treated for 24 hours with cytomix alone (Cyto), sevoflurane alone (Sevo) or with cytomix and sevoflurane (Cyto+Sevo). Results are shown as medians with interquartile ranges (n=35-40 per group and per timepoint). b) Medium levels of Chemokine C-X-C motif ligand-1(CXCL-1), c) Interleukin 6(IL-6) and d) Tumor necrosis factor-alpha (TNF-α) at 6h in identical conditions. Results are shown as medians with interquartile ranges. Two-way ANOVA test was performed, with post-hoc comparisons if ANOVA results showed significance (compared to the Medium group: *, $p < 0.05$; **, $p < 0.01$; ***, $p < 10^{-3}$; ****, $p < 10^{-4}$; compared to the Cyto group: ##, $p < 0.01$; ###, $p < 10^{-3}$; ####, $p < 10^{-4}$).

In vitro effects of sevoflurane on mechanisms of lung epithelial integrity

Protein expressions of ZO-1 and E-cadherin decreased at 6 hours after treatment with cytomix, but exposure to sevoflurane was associated with a higher expression of ZO-1 protein (Figure 4 and Figure S6, online supplement).

After 6 hours of exposure, sevoflurane reduced the cytomix-induced increase in pMLC and actin cytoskeletal rearrangement and contraction, with decreased F-actin staining intensity, in MLE-12 cells (Figure 4).

After 30 min of treatment, RhoA activity was increased in MLE-12 cells treated with cytomix, as compared with those treated with medium only. Exposure of cells to sevoflurane treated with cytomix significantly prevented such an increase (Figure 4).

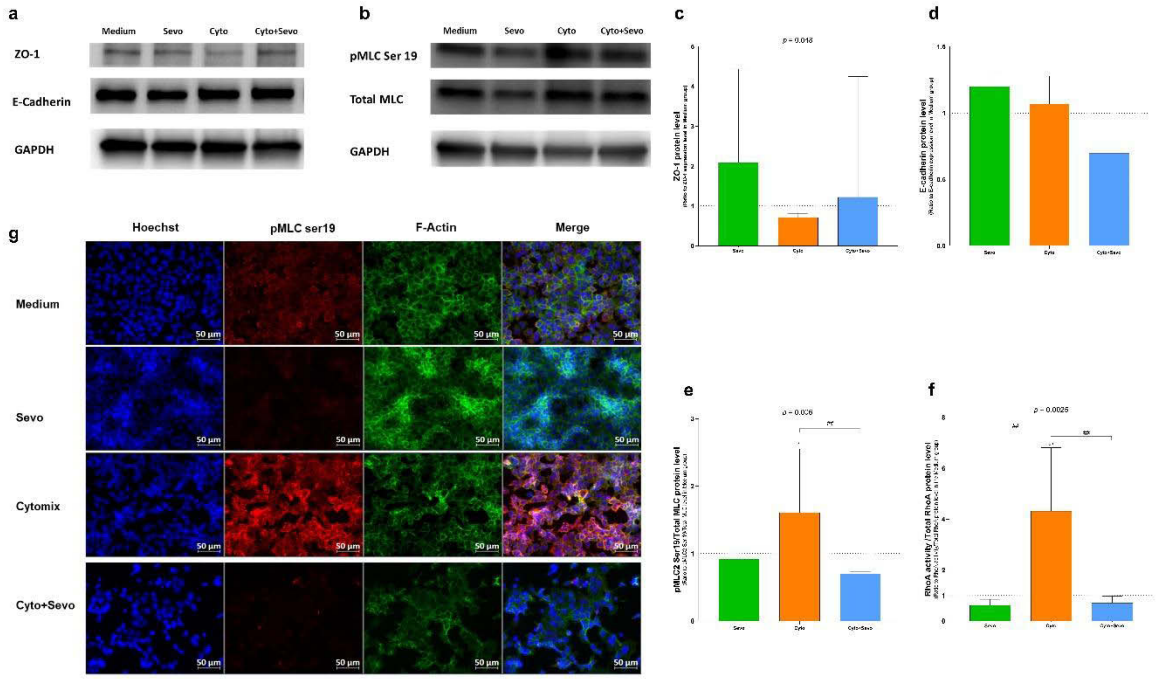

Figure 4. Effects of sevoflurane on junction proteins and RhoA/pMLC/F-actin pathway of mouse lung epithelial (MLE-12) cells. Western blots of **a**) ZO-1 and E-cadherin, **b**) total myosin light chain (MLC) and phosphorylated myosin light chain 2 (Ser19) (pMLC2) levels at 6h in untreated MLE-12 cells (Medium) and cells exposed to sevoflurane alone (Sevo), cytomix alone (Cyto) or cytomix and sevoflurane (Cyto+Sevo). **c**-**e**) Protein expression levels were quantified and standardized by GAPDH protein level, and pMLC levels were standardized by total MLC levels, expressed as ratios to those in the Medium group. **f**) RhoA activity was standardized by total RhoA protein level at 30 min in identical conditions. All results are reported as medians with interquartile ranges. One-way ANOVA was performed, with post-hoc comparisons if ANOVA results showed significance (compared to the Medium group: *, p <0.05; **, p <0.01; compared to the Cyto group: ##, p <0.01).**g**) Immunostaining after 6 hours of treatment of pMLC and F-actin was performed in identical conditions. Cells were fixed, permeabilized, and stained with antibodies, followed by A488 secondary antibodies and Hoechst. All images were acquired by fluorescent microscope with a 40x objective. Scale bar: 50 µm.

RAGE-dependent effects of sevoflurane on lung epithelial barrier function in vitro

Treatment with RAP of cells exposed to cytomix did not restore the electrical resistance of MLE-12 cell monolayers in ECIS. Further, when the cells were co-treated with sevoflurane and RAP, the beneficial effect previously found with sevoflurane alone was no longer observed (Figure 5). Treatment with RAP alone did not significantly alter the cytomix-induced release of cytokines by MLE-12 cells at 6 hours, and RAP alone did not influence the effects of sevoflurane on cytomix-induced cytokine release. However, co-treatment with RAP and sevoflurane was associated with higher medium levels of

TNF-α after cytomix, as compared with those after treatment with sevoflurane alone (Figure 5). Although the experiments with RAP showed no between-group differences in E-cadherin protein levels after 6 hours of treatment, RAP was associated with restored protein levels of ZO-1 in cells exposed to cytomix, whether or not they were co-exposed to sevoflurane (Figure 5).

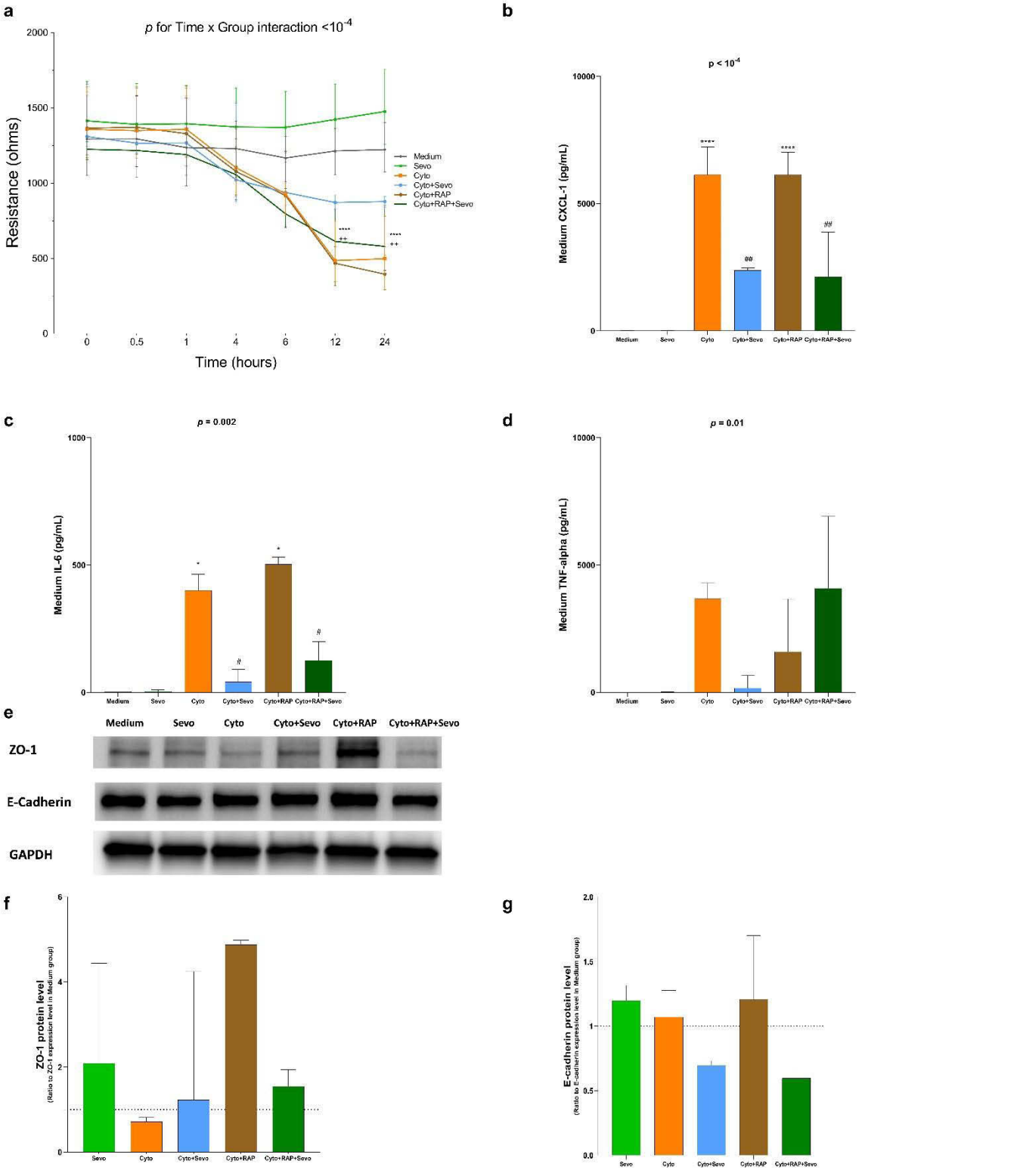

Figure 5. Effects of sevoflurane on lung epithelial barrier function of mouse lung epithelial (MLE-12) cell monolayer, treated or not with RAGE antagonist peptide (RAP). a) Electrical resistance over 24 hours of a monolayer of MLE-12 cells was measured at a frequency at 4000 Hz by electric cell-substrate impedance sensing (ECIS) in untreated cells (Medium) or in cells treated for 24 hours with cytomix alone (Cyto), sevoflurane alone (Sevo), cytomix and sevoflurane (Cyto+Sevo), cytomix and RAP (Cyto+RAP) or with cytomix, RAP, and sevoflurane (Cyto+RAP+Sevo). Results are shown as medians with interquartile ranges (n=35-40 per group and per timepoint). Two-way ANOVA test was performed, with post-hoc comparisons if ANOVA results showed significance (compared to the Medium group: ****, $p < 10^{-4}$; compared to the Cyto+Sevo group: ++, $p < 0.01$). b) Medium level of Chemokine C-X-C motif ligand-1(CXCL-1), c) Interleukin 6(IL-6) and d) Tumor necrosis factor alpha (TNF-α) at 6h in identical conditions. e) western blots of ZO-1 and E-cadherin at 6h in identical conditions. f) Protein expression levels were quantified and standardized by GAPDH protein level and expressed as ratios to those in the Medium group. Results of b-f are shown as medians with interquartile ranges. One-way ANOVA was performed, with post-hoc comparisons if ANOVA results showed significance (compared to the Medium group: *, $p < 0.05$; ****, $p < 10^{-4}$; compared to the Cyto group: #, $p < 0.05$;##, $p < 0.01$).

The immunostaining signal and protein quantification based on the Western blot of pMLC were decreased when MLE-12 cells exposed to cytomix were treated with RAP, compared to those who were not treated with RAP (Figure 6). Although treatment with RAP did not influence the effects of sevoflurane on pMLC levels after exposure to cytomix, F-actin cytoskeletal rearrangement and contraction were increased by RAP in MLE-12 cells exposed to cytomix and sevoflurane (Figure 6). Treatment with RAP decreased the cytomix-induced increase in the RhoA activity of MLE-12 cells, as assessed at 30 min. However, RAP did not influence the effects of sevoflurane on RhoA activity after exposure to cytomix (Figure 6).

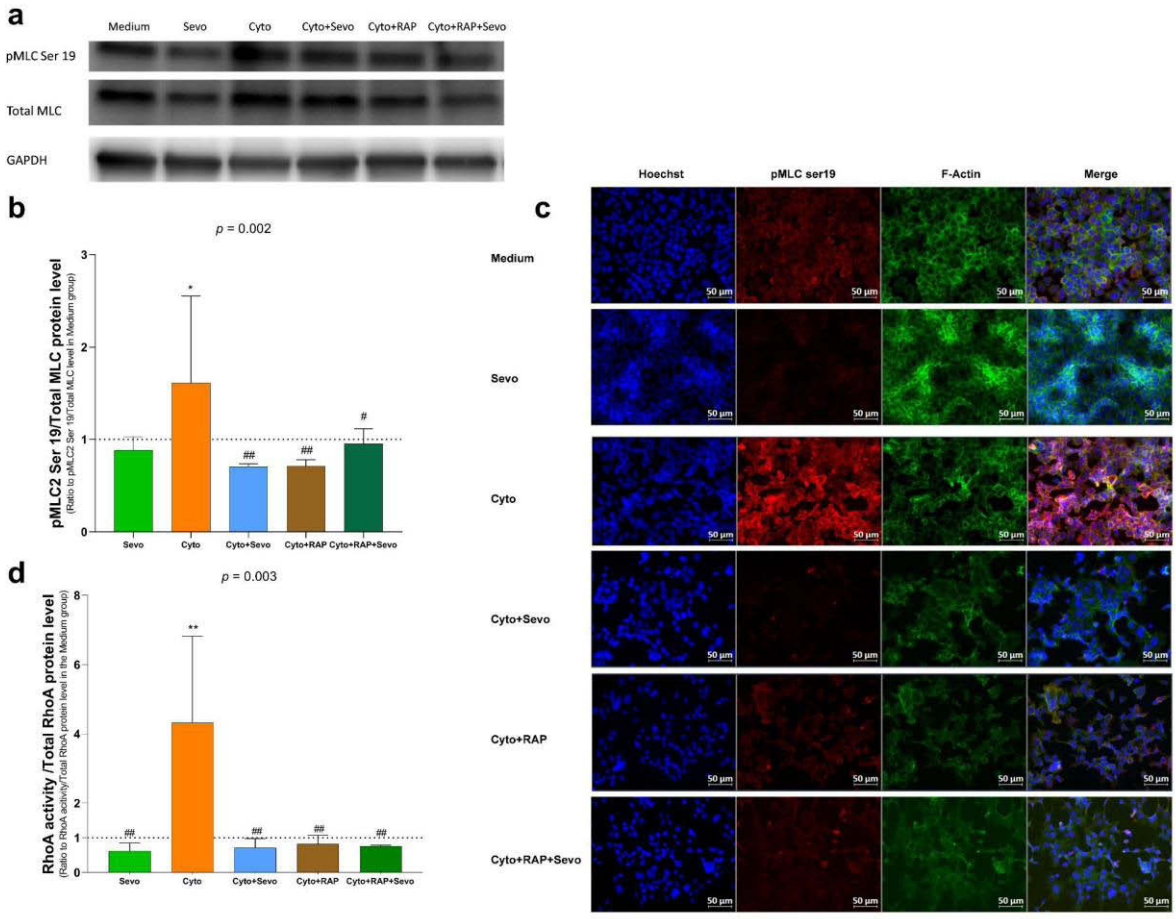

Figure 6. Effects of sevoflurane on RhoA/pMLC/F-actin pathway in mouse lung epithelial (MLE-12) cells, treated or not with RAGE antagonist peptide (RAP). a) total myosin light chain (MLC) and phosphorylated myosin light chain 2 (Ser19) (pMLC2) levels at 6h in untreated MLE-12 cells (Medium) and cells exposed to sevoflurane alone (Sevo), cytomix alone (Cyto), cytomix and sevoflurane (Cyto+Sevo), cytomix and RAP (Cyto+RAP) or with cytomix, RAP, and sevoflurane (Cyto+RAP+Sevo). b) Protein expression levels were quantified and standardized by GAPDH protein level, and pMLC levels were standardized by total MLC levels, expressed as ratios to those in the Medium group, and reported as medians with interquartile ranges. c) Immunostaining after 6 hours of treatment of pMLC and F-actin was performed in identical conditions. Cells were fixed, permeabilized, and stained with antibodies, followed by A488 secondary antibodies and Hoechst. All images were acquired by fluorescent microscope with a 40x objective. Scale bar: 50 μm. d) RhoA activity was standardized by total RhoA protein level at 30 min in identical conditions. All quantitative results are reported as medians with interquartile ranges. One-way ANOVA was performed, with post-hoc comparisons if ANOVA results showed significance (compared to the Medium group: *, p <0.05; **, p <0.01; compared to the Cyto group: #, p <0.05; ##, p <0.01).

RAGE-dependent effects of sevoflurane on lung injury and mechanisms of lung epithelial barrier function in vivo

The permeability index and BAL levels of total proteins were lower from day 0 to day 2 after acid injury in RAGE$^{-/-}$ mice than in littermate controls. However, RAGE deletion did not influence the effects of sevoflurane related to permeability indices after injury (Figure S7, online supplement). Similarly, lung accumulation of an intravenous fluorescent tracer on day 2 after injury was decreased in RAGE$^{-/-}$ mice, compared to littermate controls, without additional influence of RAGE deletion on the effects of sevoflurane (Figure S8, online supplement). There were no obvious differences in lung immunostaining of ZO-1 and E-cadherin in RAGE$^{-/-}$ versus wild-type mice on day 1 after injury (Figure S9, online supplement). In RAGE$^{-/-}$ mice, sevoflurane restored both ZO-1 and E-cadherin fluorescent signals after injury in comparison to injured mice not receiving sevoflurane. Overall, ZO-1 and E-cadherin protein levels were overall lower in RAGE$^{-/-}$ animals than in littermate controls (Figure S10, online supplement). In RAGE$^{-/-}$ mice, sevoflurane was not associated with a significant effect on ZO-1 and E-cadherin protein expressions in the lungs over the four-day experiment. Lung pMLC levels peaked on day 1 after acid injury in RAGE$^{-/-}$ mice, a phenomenon abolished by treatment with sevoflurane (Figure S11, online supplement).

RAGE deletion in treated mice was associated with improvements in physiological, inflammatory, and histological features of acid-induced lung injury over time, as compared with wild-type controls (Figures S12–14, online Supplement). However, the beneficial effect of sevoflurane previously observed in wild-type mice on day 1 after injury in terms of higher PaO_2/FiO_2 and decreased BAL levels of IL-6 and TNF-α was not found in RAGE$^{-/-}$ mice.

DISCUSSION

In this study, we used an in vivo model of acid-induced lung injury in mice and an in vitro model of sterile injury in mouse lung epithelial cells to investigate whether sevoflurane could decrease lung alveolar epithelial permeability through the RhoA/pMLC/F-actin pathway.

Exposure to sevoflurane improved features of experimental ARDS in our mouse model, such as impaired arterial oxygenation, alveolar inflammation, histological evidence of lung tissue injury, and the extent of lung edema, in line with previous reports of models of lipopolysaccharide-induced lung injury in rats and a pig model of surfactant saline lavage [13,15,16,35]. Our study focused on the integrity of the epithelial barrier function, finding decreased indices of permeability and preserved epithelial structures in cells and mice exposed to sevoflurane after injury. Alterations of inter-epithelial tight and adherens junction proteins are major contributors to lung epithelial barrier dysfunction

in ARDS [3,36]. Sevoflurane increased the protein expression of ZO-1 in our in vivo and in vitro models, further supporting previous findings of alleviated lung permeability due to the upregulation of occludin and ZO-1 with sevoflurane preconditioning before ischemia-reperfusion in rats [37]. In another double-hit mouse model, isoflurane restored epithelial tight junction integrity and increased ZO-1 levels [19]. However, no effect of sevoflurane on E-cadherin was observed in our study, contrasting with previous findings on human lung microvascular endothelial cells injured by LPS and on colon carcinoma cell lines [38,39]. In particular, our study provides novel evidence supporting the molecular mechanisms of the effects of sevoflurane on lung epithelial barrier function after injury. Notably, sevoflurane was associated with decreased lung levels of pMLC and decreased actin cytoskeletal rearrangement after injury in vivo and in vitro. Sevoflurane also decreased cytomix-induced RhoA activity in vitro, suggesting that sevoflurane could decrease lung epithelial permeability through inhibition of the RhoA/pMLC/F-actin cytoskeleton pathway, as also suggested by studies on other cell types [38,40–44].

In addition, we showed that RAGE$^{-/-}$ mice had better oxygenation levels, decreased lung permeability, and improved inflammatory response compared to littermate wild-type animals, as previously reported for RAGE inhibition strategies using recombinant sRAGE as a decoy receptor or an anti-RAGE monoclonal antibody as an antagonist [29]. In vitro, treatment with RAP decreased cytomix-induced RhoA activity in MLE-12 cells, and treatment with RAP alleviated the beneficial effects of sevoflurane on the electrical resistance of MLE-12 cell monolayers and on actin cytoskeletal rearrangement. In vivo, RAGE$^{-/-}$ mice received the same benefits from sevoflurane as littermate controls in terms of indices of lung alveolar-capillary permeability. In contrast to wild-type mice, however, the RAGE$^{-/-}$ animals did not exhibit the effects of improved arterial oxygenation and decreased BAL levels of IL-6 and TNF-α observed with sevoflurane, suggesting that RAGE plays a mediating role in the effects of sevoflurane on acute lung injury.

Our study has limitations. First, we used in vitro and vivo models of injury from sterile causes, and thus our findings may not be generalizable to other settings. Second, we used MLE-12 cells (i.e., type-2-like, tumor-derived epithelial cells), and future validation studies on primary mouse or human alveolar epithelial cells are warranted. Third, our mechanistic analyses focused on a short time frame since we hypothesized this would be more relevant for studying the RhoA/pMLC/F-actin signaling pathway, which was only feasible *in vitro*. Fourth, although we

investigated lung epithelial permeability using modern and relevant approaches focusing on the barrier function and intercellular junctions, the extent of lung epithelial injury also depends on other important mechanisms, such as cell death [39], wound healing or fluid and ion clearance. Further investigation is needed to determine whether sevoflurane affects such mechanisms.

Our study also has several strengths. We used a mouse model of direct lung epithelial injury over multiple days [25,28,29] and an in vitro model of alveolar epithelial injury [31,45], which are validated and have translational value. In addition, the sevoflurane concentrations used in our study are similar to those used in clinical practice for deep sedation, which is often required in the early management of clinical ARDS [12,46]. Further, a better description of the mechanisms of lung epithelial injury, among other features of ARDS pathogeny, is important to identify endotypes within ARDS (i.e., subgroups with distinct biological or functional features) and to inform the future development of more targeted, endotype-based therapies for ARDS [47–49].

In conclusion, sevoflurane was shown to have protective effects on lung epithelial permeability and epithelial junction proteins in experimental models of sterile ARDS. These protective effects could be explained, at least in part, by the inhibition of increased RhoA activity and pMLC as well as actin cytoskeleton rearrangement following lung epithelial injury. Further studies are needed to determine whether the RAGE pathway mediates some of these effects.

Funding

This work was supported by grants from the French Agence Nationale de la Recherche (RESPIRE Project, ANR-20-CE17-0015) and the Fonds Européen de Développement Régional (FEDER), Région Auvergne, and Université Clermont Auvergne (ASTRA Project). The funders had no influence in the study design, conduct, and analysis or in the preparation of this article.

Acknowledgments

The authors wish to thank the technicians and staff from the department of Medical Biochemistry and Molecular Genetics and the technicians and staff from Université Clermont Auvergne. The authors also thank Prof. Ann Marie Schmidt (NYU Langone Health, New York, USA) for kindly providing RAGE$^{-/-}$ mice.

Author Contributions

Conceptualization, M.J., V.S.; Methodology, M.J., R.Z., R.B., W.L.M.B., L.B., V.S.; Formal Analysis, R.Z., W.L.M.B.,C.B., and M.J.; Investigations, R.Z., W.L.M.B., R.B., C.B., C.L., C.S.B., C.T., C.B., R.C., D.B., L.B., M.J.; Writing – Original Draft Preparation, R.Z., W.L.M.B. and M.J.; Writing – Review & Editing, all authors; Supervision, M.J. and V.S.; Project Administration, M.J. and V.S.; Funding Acquisition, M.J, V.S.

Ethics Statement

Mouse experiments were approved by the Animal Ethics Committee of the French *Ministère de l'Education Nationale, de l'Enseignement Supérieur et de la Recherche* (approval number CE 67–12; December 4, 2012). All experiments were performed following relevant guidelines and regulations for animal and cell experimentations.

REFERENCES

1. Bellani, G.; Laffey, J.G.; Pham, T.; Fan, E.; Brochard, L.; Esteban, A.; Gattinoni, L.; van Haren, F.; Larsson, A.; McAuley, D.F.; et al. Epidemiology, Patterns of Care, and Mortality for Patients With Acute Respiratory Distress Syndrome in Intensive Care Units in 50 Countries. *JAMA* **2016**, *315*, 788–800.
2. Thompson, B.T.; Chambers, R.C.; Liu, K.D. Acute Respiratory Distress Syndrome. *N. Engl. J. Med.* 2017, *377*, 1904–1905.
3. Matthay, M.A.; Zemans, R.L.; Zimmerman, G.A.; Arabi, Y.M.; Beitler, J.R.; Mercat, A.; Herridge, M.; Randolph, A.G.; Calfee, C.S. Acute Respiratory Distress Syndrome. *Nat Rev Dis Primers* **2019**, *5*, 18.
4. Bos, L.D.J.; Ware, L.B. Acute Respiratory Distress Syndrome: Causes, Pathophysiology, and Phenotypes. *Lancet* **2022**, *400*, 1145–1156.
5. Grasselli, G.; Pesenti, A.; Cecconi, M. Critical Care Utilization for the COVID-19 Outbreak in Lombardy, Italy: Early Experience and Forecast During an Emergency Response. *JAMA* **2020**, *323*, 1545–1546.
6. Verdonk, F.; Feyaerts, D.; Badenes, R.; Bastarache, J.A.; Bouglé, A.; Ely, W.; Gaudilliere, B.; Howard, C.; Kotfis, K.; Lautrette, A.; et al. Upcoming and Urgent Challenges in Critical Care Research Based on COVID-19 Pandemic Experience. *Anaesth Crit Care Pain Med* **2022**, 101121.
7. Lucas, R.; Verin, A.D.; Black, S.M.; Catravas, J.D. Regulators of Endothelial and Epithelial Barrier Integrity and Function in Acute Lung Injury. *Biochem. Pharmacol.* **2009**, *77*, 1763–1772.
8. van Roy, F.; Berx, G. The Cell-Cell Adhesion Molecule E-Cadherin. *Cell. Mol. Life Sci.* **2008**, *65*, 3756–3788.
9. Schlingmann, B.; Overgaard, C.E.; Molina, S.A.; Lynn, K.S.; Mitchell, L.A.; Dorsainvil White, S.; Mattheyses, A.L.; Guidot, D.M.; Capaldo, C.T.; Koval, M. Regulation of Claudin/zonula Occludens-1 Complexes by Hetero-Claudin Interactions. *Nat. Commun.* **2016**, *7*, 12276.
10. Jerath, A.; Parotto, M.; Wasowicz, M.; Ferguson, N.D. Volatile Anesthetics. Is a New Player Emerging in Critical Care Sedation? *Am. J. Respir. Crit. Care Med.* **2016**, *193*, 1202–1212.
11. Beitler, J.R.; Talmor, D. Volatile Anesthetics for ICU Sedation: The Future of Critical Care or Niche Therapy? *Intensive Care Med.* **2022**, *48*, 1413–1417.
12. Jabaudon, M.; Zhai, R.; Blondonnet, R.; Bonda, W.L.M. Inhaled Sedation in the Intensive Care Unit. *Anaesth Crit Care Pain Med* **2022**, 101133.
13. Ferrando, C.; Aguilar, G.; Piqueras, L.; Soro, M.; Moreno, J.; Belda, F.J. Sevoflurane, but Not Propofol, Reduces the Lung Inflammatory Response and Improves Oxygenation in an Acute Respiratory Distress Syndrome Model: A Randomised Laboratory Study. *European Journal of Anaesthesiology| EJA* **2013**, *30*, 455–463.
14. Watanabe, K.; Iwahara, C.; Nakayama, H.; Iwabuchi, K.; Matsukawa, T.; Yokoyama, K.; Ya-

maguchi, K.; Kamiyama, Y.; Inada, E. Sevoflurane Suppresses Tumour Necrosis Factor-α-Induced Inflammatory Responses in Small Airway Epithelial Cells after Anoxia/reoxygenation. *Br. J. Anaesth.* **2013**, *110*, 637–645.

15. Fortis, S.; Spieth, P.M.; Lu, W.-Y.; Parotto, M.; Haitsma, J.J.; Slutsky, A.S.; Zhong, N.; Mazer, C.D.; Zhang, H. Effects of Anesthetic Regimes on Inflammatory Responses in a Rat Model of Acute Lung Injury. *Intensive Care Med.* **2012**, *38*, 1548–1555.
16. Schläpfer, M.; Leutert, A.C.; Voigtsberger, S.; Lachmann, R.A.; Booy, C.; Beck-Schimmer, B. Sevoflurane Reduces Severity of Acute Lung Injury Possibly by Impairing Formation of Alveolar Oedema. *Clin. Exp. Immunol.* **2012**, *168*, 125–134.
17. O'Gara, B.; Talmor, D. Lung Protective Properties of the Volatile Anesthetics. *Intensive Care Med.* **2016**, *42*, 1487–1489.
18. Jabaudon, M.; Boucher, P.; Imhoff, E.; Chabanne, R.; Faure, J.-S.; Roszyk, L.; Thibault, S.; Blondonnet, R.; Clairefond, G.; Guérin, R.; et al. Sevoflurane for Sedation in Acute Respiratory Distress Syndrome. A Randomized Controlled Pilot Study. *Am. J. Respir. Crit. Care Med.* **2017**, *195*, 792–800.
19. Englert, J.A.; Macias, A.A.; Amador-Munoz, D.; Pinilla Vera, M.; Isabelle, C.; Guan, J.; Magaoay, B.; Suarez Velandia, M.; Coronata, A.; Lee, A.; et al. Isoflurane Ameliorates Acute Lung Injury by Preserving Epithelial Tight Junction Integrity. *Anesthesiology* **2015**, *123*, 377–388.
20. Huang, Y.; Tan, Q.; Chen, R.; Cao, B.; Li, W. Sevoflurane Prevents Lipopolysaccharide-Induced Barrier Dysfunction in Human Lung Microvascular Endothelial Cells: Rho-Mediated Alterations of VE-Cadherin. *Biochem. Biophys. Res. Commun.* **2015**, *468*, 119–124.
21. Liu, Y.; Gao, M.; Ma, L.; Zhang, L.; Pan, N. Sevoflurane Alters the Expression of Receptors and Enzymes Involved in Aβ Clearance in Rats. *Acta Anaesthesiol. Scand.* **2013**, *57*, 903–910.
22. Zimering, J.H.; Dong, Y.; Fang, F.; Huang, L.; Zhang, Y.; Xie, Z. Anesthetic Sevoflurane Causes Rho-Dependent Filopodial Shortening in Mouse Neurons. *PLoS One* **2016**, *11*, e0159637.
23. Guo, W.A.; Knight, P.R.; Raghavendran, K. The Receptor for Advanced Glycation End Products and Acute Lung Injury/acute Respiratory Distress Syndrome. *Intensive Care Med.* **2012**, *38*, 1588–1598.
24. Calfee, C.S.; Ware, L.B.; Eisner, M.D.; Parsons, P.E.; Thompson, B.T.; Wickersham, N.; Matthay, M.A.; NHLBI ARDS Network Plasma Receptor for Advanced Glycation End Products and Clinical Outcomes in Acute Lung Injury. *Thorax* **2008**, *63*, 1083–1089.
25. Jabaudon, M.; Blondonnet, R.; Roszyk, L.; Bouvier, D.; Audard, J.; Clairefond, G.; Fournier, M.; Marceau, G.; Déchelotte, P.; Pereira, B.; et al. Soluble Receptor for Advanced Glycation End-Products Predicts Impaired Alveolar Fluid Clearance in Acute Respiratory Distress Syndrome. *Am. J. Respir. Crit. Care Med.* **2015**, *192*, 191–199.
26. Jabaudon, M.; Blondonnet, R.; Pereira, B.; Cartin-Ceba, R.; Lichtenstern, C.; Mauri, T.; Deter-

mann, R.M.; Drabek, T.; Hubmayr, R.D.; Gajic, O.; et al. Plasma sRAGE Is Independently Associated with Increased Mortality in ARDS: A Meta-Analysis of Individual Patient Data. *Intensive Care Med.* **2018**, *44*, 1388–1399.

27. Percie du Sert, N.; Ahluwalia, A.; Alam, S.; Avey, M.T.; Baker, M.; Browne, W.J.; Clark, A.; Cuthill, I.C.; Dirnagl, U.; Emerson, M.; et al. Reporting Animal Research: Explanation and Elaboration for the ARRIVE Guidelines 2.0. *PLoS Biol.* **2020**, *18*, e3000411.
28. Patel, B.V.; Wilson, M.R.; Takata, M. Resolution of Acute Lung Injury and Inflammation: A Translational Mouse Model. *Eur. Respir. J.* **2012**, *39*, 1162–1170.
29. Blondonnet, R.; Audard, J.; Belville, C.; Clairefond, G.; Lutz, J.; Bouvier, D.; Roszyk, L.; Gross, C.; Lavergne, M.; Fournet, M.; et al. RAGE Inhibition Reduces Acute Lung Injury in Mice. *Sci. Rep.* **2017**, *7*, 7208.
30. Kulkarni, H.S.; Lee, J.S.; Bastarache, J.A.; Kuebler, W.M.; Downey, G.P.; Albaiceta, G.M.; Altemeier, W.A.; Artigas, A.; Bates, J.H.T.; Calfee, C.S.; et al. Update on the Features and Measurements of Experimental Acute Lung Injury in Animals: An Official American Thoracic Society Workshop Report. *Am. J. Respir. Cell Mol. Biol.* **2022**, *66*, e1–e14.
31. Goolaerts, A.; Pellan-Randrianarison, N.; Larghero, J.; Vanneaux, V.; Uzunhan, Y.; Gille, T.; Dard, N.; Planès, C.; Matthay, M.A.; Clerici, C. Conditioned Media from Mesenchymal Stromal Cells Restore Sodium Transport and Preserve Epithelial Permeability in an in Vitro Model of Acute Alveolar Injury. *Am. J. Physiol. Lung Cell. Mol. Physiol.* **2014**, *306*, L975–L985.
32. Kuck, J.L.; Bastarache, J.A.; Shaver, C.M.; Fessel, J.P.; Dikalov, S.I.; May, J.M.; Ware, L.B. Ascorbic Acid Attenuates Endothelial Permeability Triggered by Cell-Free Hemoglobin. *Biochem. Biophys. Res. Commun.* **2018**, *495*, 433–437.
33. Matute-Bello, G.; Downey, G.; Moore, B.B.; Groshong, S.D.; Matthay, M.A.; Slutsky, A.S.; Kuebler, W.M.; Acute Lung Injury in Animals Study Group An Official American Thoracic Society Workshop Report: Features and Measurements of Experimental Acute Lung Injury in Animals. *Am. J. Respir. Cell Mol. Biol.* **2011**, *44*, 725–738.
34. Lenga Ma Bonda, W.; Fournet, M.; Zhai, R.; Lutz, J.; Blondonnet, R.; Bourgne, C.; Leclaire, C.; Saint-Béat, C.; Theilliere, C.; Belville, C.; et al. Receptor for Advanced Glycation End-Products Promotes Activation of Alveolar Macrophages through the NLRP3 Inflammasome/TXNIP Axis in Acute Lung Injury. *Int. J. Mol. Sci.* **2022**, *23*, 11659.
35. Voigtsberger, S.; Lachmann, R.A.; Leutert, A.C.; Schläpfer, M.; Booy, C.; Reyes, L.; Urner, M.; Schild, J.; Schimmer, R.C.; Beck-Schimmer, B. Sevoflurane Ameliorates Gas Exchange and Attenuates Lung Damage in Experimental Lipopolysaccharide-Induced Lung Injury. *Anesthesiology* **2009**, *111*, 1238–1248.
36. Brune, K.; Frank, J.; Schwingshackl, A.; Finigan, J.; Sidhaye, V.K. Pulmonary Epithelial Barrier Function: Some New Players and Mechanisms. *Am. J. Physiol. Lung Cell. Mol. Physiol.* **2015**, *308*, L731–L745.

37. Chai, J.; Long, B.; Liu, X.; Li, Y.; Han, N.; Zhao, P.; Chen, W. Effects of Sevoflurane on Tight Junction Protein Expression and PKC-α Translocation after Pulmonary Ischemia-Reperfusion Injury. *Exp. Mol. Med.* **2015**, *47*, e167.
38. Huang, Y.; Tan, Q.; Chen, R.; Cao, B.; Li, W. Sevoflurane Prevents Lipopolysaccharide-Induced Barrier Dysfunction in Human Lung Microvascular Endothelial Cells: Rho-Mediated Alterations of VE-Cadherin. *Biochem. Biophys. Res. Commun.* **2015**, *468*, 119–124.
39. Yang, X.; Zheng, Y.-T.; Rong, W. Sevoflurane Induces Apoptosis and Inhibits the Growth and Motility of Colon Cancer in Vitro and in Vivo via Inactivating Ras/Raf/MEK/ERK Signaling. *Life Sci.* **2019**, *239*, 116916.
40. Samarin, S.N.; Ivanov, A.I.; Flatau, G.; Parkos, C.A.; Nusrat, A. Rho/Rho-Associated Kinase-II Signaling Mediates Disassembly of Epithelial Apical Junctions. *Mol. Biol. Cell* **2007**, *18*, 3429–3439.
41. Ivanov, A.I.; Parkos, C.A.; Nusrat, A. Cytoskeletal Regulation of Epithelial Barrier Function during Inflammation. *Am. J. Pathol.* **2010**, *177*, 512–524.
42. Li, J.; Yuan, T.; Zhao, X.; Lv, G.-Y.; Liu, H.-Q. Protective Effects of Sevoflurane in Hepatic Ischemia-Reperfusion Injury. *Int. J. Immunopathol. Pharmacol.* **2016**, *29*, 300–307.
43. Restin, T.; Kajdi, M.-E.; Schläpfer, M.; Roth Z'graggen, B.; Booy, C.; Dumrese, C.; Beck-Schimmer, B. Sevoflurane Protects Rat Brain Endothelial Barrier Structure and Function after Hypoxia-Reoxygenation Injury. *PLoS One* **2017**, *12*, e0184973.
44. Pronk, M.C.A.; van Bezu, J.S.M.; van Nieuw Amerongen, G.P.; van Hinsbergh, V.W.M.; Hordijk, P.L. RhoA, RhoB and RhoC Differentially Regulate Endothelial Barrier Function. *Small GTPases* **2019**, *10*, 466–484.
45. Zhai, R.; Bonda, W.L.M.; Matute-Bello, G.; Jabaudon, M. From Preclinical to Clinical Models of Acute Respiratory Distress Syndrome. *Signa Vitae* **2022**, doi:10.22514/sv.2021.228.
46. Chanques, G.; Constantin, J.-M.; Devlin, J.W.; Ely, E.W.; Fraser, G.L.; Gélinas, C.; Girard, T.D.; Guérin, C.; Jabaudon, M.; Jaber, S.; et al. Analgesia and Sedation in Patients with ARDS. *Intensive Care Med.* **2020**, *46*, 2342–2356.
47. Jabaudon, M.; Blondonnet, R.; Audard, J.; Fournet, M.; Godet, T.; Sapin, V.; Constantin, J.-M. Recent Directions in Personalised Acute Respiratory Distress Syndrome Medicine. *Anaesth Crit Care Pain Med* **2018**, *37*, 251–258.
48. Bos, L.D.J.; Laffey, J.G.; Ware, L.B.; Heijnen, N.F.L.; Sinha, P.; Patel, B.; Jabaudon, M.; Bastarache, J.A.; McAuley, D.F.; Summers, C.; et al. Towards a Biological Definition of ARDS: Are Treatable Traits the Solution? *Intensive Care Med Exp* **2022**, *10*, 8.
49. Wick, K.D.; Aggarwal, N.R.; Curley, M.A.Q.; Fowler, A.A., 3rd; Jaber, S.; Kostrubiec, M.; Lassau, N.; Laterre, P.F.; Lebreton, G.; Levitt, J.E.; et al. Opportunities for Improved Clinical Trial Designs in Acute Respiratory Distress Syndrome. *Lancet Respir Med* **2022**, *10*, 916–924.

ONLINE DATA SUPPLEMENT

Effects of sevoflurane on lung epithelial permeability in experimental models of acute respiratory distress syndrome

Ruoyang Zhai, Woodys Lenga Ma Bonda, Charlotte Leclaire, Cécile Saint-Béat, Camille Theilliere, Corinne Belville, Randy Coupet, Raiko Blondonnet, Damien Bouvier, Loic Blanchon, Vincent Sapin, Matthieu Jabaudon

Supplementary figure legends

Figure S1. Arterial oxygen tension (PaO_2)/inspiratory oxygen fraction (FiO_2) in mice after acid-induced lung injury. Arterial oxygen tension (PaO2)/inspiratory oxygen fraction (FiO2) of uninjured (Sham), acid-injured (HCl), and acid-injured mice treated with sevoflurane (HCl+Sevo) from day 0 to day 4 after injury. Values are presented as box and whisker plots with medians and interquartile ranges. Two-way ANOVA tests were performed, and post-hoc comparisons were performed if ANOVA results showed significance (compared to the Sham group: *, $p < 0.05$; ****, $p < 10^{-4}$; compared to the HCl group: ###, $p < 0.001$).

Figure S2. Bronchoalveolar lavage fluid (BALF) proinflammatory cytokines levels in mice after acid-induced lung injury. BALF level of **a**) Chemokine C-X-C motif ligand-1(CXCL-1), **b**) Interleukin 6(IL-6) and **c**) Tumor necrosis factor alpha (TNF-α) of uninjured (Sham), acid-injured (HCl), and acid-injured mice treated with sevoflurane (HCl+Sevo) from day 0 to day 4 after injury. Values are presented as box and whisker plots with medians and interquartile ranges. Two-way ANOVA tests were performed, and post-hoc comparisons were performed if ANOVA results showed significance (compared to the WT_Sham group: ****,$p < 10^{-4}$; compared to the WT_HCl group: ##, $p < 0.01$).

Figure S3. **Histological features of lung injury in mice after acid-induced lung injury. a**) Lung histological stainings and **b**) Lung injury scores of uninjured (Sham), acid-injured (HCl), and acid-injured mice treated with sevoflurane (HCl+Sevo) from day 0 to day 4 after injury. Values are presented as box and whisker plots with medians and interquartile ranges. Two-way ANOVA tests were performed, and post-hoc comparisons were performed if ANOVA results showed significance. Two-way ANOVA tests were performed, and post-hoc comparisons were performed if ANOVA results showed significance (compared to the Sham group: ****, $p < 10^{-4}$; compared to the HCl group: ###, $p < 10^{-3}$; ####, $p < 10^{-4}$).

Figure S4. Western blots of lung junction proteins zonula occludens (ZO)-1 and E-cadherin in vivo. a) Western blots of ZO-1 and E-cadherin in lung tissues from uninjured (Sham), acid-injured (HCl), and acid-injured mice treated with sevoflurane (HCl+Sevo) from day 0 to day 4 after injury. **b**) ZO-1 and **c**) E-cadherin expression levels were quantified and standardized by GAPDH protein level, expressed as ratios to those in sham animals, and represented as box and whisker plots with medians and interquartile ranges. Two-way ANOVA tests were performed, with post-hoc comparisons if ANOVA results showed significance (compared to the Sham group: ****, $p < 10^{-4}$; compared to the HCl group: ###, $p < 10^{-3}$).

Figure S5. Lung mRNA levels of lung junction protein zonula occludens (ZO)-1 and E-cadherin in vivo. a) ZO-1 and **b)** E-cadherin mRNA levels measured by RT-qPCR in lung tissues from uninjured (Sham), acid-injured (HCl), and acid-injured mice treated with sevoflurane (HCl+Sevo) from day 0 to day 4 after injury. mRNA levels were calculated by the delta-delta Ct method standardized with the housekeeping gene GAPDH. mRNA levels are expressed as ratios to those in sham animals, represented as box and whisker plots with medians and interquartile ranges. Two-way ANOVA test was performed, with post-hoc comparisons if ANOVA results showed significance.

Figure S6. **mRNA levels of lung junction protein zonula occludens (ZO)-1 and E-cadherin in mouse lung epithelial (MLE-12) cells. a)** ZO-1 and **b)** E-cadherin mRNA levels measured by RT-qPCRin untreated MLE-12 cells (Medium) and cells exposed to sevoflurane alone (Sevo), cytomix alone (Cyto) or cytomix and sevoflurane (Cyto+Sevo). mRNA levels were calculated by the delta-delta Ct method standardized with the housekeeping gene GAPDH. mRNA levels are expressed as ratios to those in the Medium group, represented as medians and interquartile ranges. Two-way ANOVA test was performed, with post-hoc comparisons if ANOVA results showed significance.

Figure S7. **Measures of alveolar-capillary permeability in RAGE-/- and littermate wild-type mice after acid-induced lung injury. a**) Total protein content (in g.L-1) of the bronchoalveolar lavage (BAL) fluid and **b**) Permeability index, as calculated as the BAL fluid-to-plasma ratio of the human serum albumin (HSA) concentration, in wild-type (WT) or RAGE-/- uninjured (Sham), acid-injured (HCl), and acid-injured mice treated with sevoflurane (HCl+Sevo) from day 0 to day 4 after injury. Values are presented as box and whisker plots with medians and interquartile ranges. Two-way ANOVA tests were performed, and post-hoc comparisons were performed if ANOVA results showed significance.

Figure S8. Effects of sevoflurane on lung accumulation of an intravenous fluorescent tracer in RAGE$^{-/-}$ and wild-type mice on day 2 after acid-induced injury. Representative images of accumulation on day 2 after injury of an intravenously-injected, near-infrared

fluorescent dye, as reported as relative fluorescence units (RFU), a) in isolated lungs and **b**) in the bronchoalveolar lavage fluid from RAGE$^{-/-}$ (KO) and littermate wild-type (WT) mice: uninjured (Sham), acid-injured (HCl), and acid-injured treated with sevoflurane (HCl+Sevo).

Figure S9. **Immunostaining of lung junction proteins Zonula Occludens (ZO)-1 and E-cadherin in RAGE$^{-/-}$ and wild-type mice on day 1 after acid-induced injury.** Immunostaining of lung **a**) ZO-1 and **b**) E-cadherin in lung tissues from RAGE$^{-/-}$ (KO) and littermate wild-type (WT) mice, either uninjured (Sham), acid-injured (HCl) or acid-injured treated with sevoflurane (HCl+Sevo), on day 1 after injury. Tissues were fixed, permeabilized, and stained with ZO-1 and E-cadherin antibodies, followed by A488 secondary antibodies and Hoechst staining. All images were acquired by a fluorescent microscope with a 20x objective. **a**) ZO-1 protein is red-stained, and the cell nucleus is blue-stained. **b**) E-cadherin protein is red-stained, and the cell nucleus is blue-stained. Scale bar: 50 μm.

Figure S10. **Western blots of lung junction proteins zonula occludens (ZO)-1 and E-cadherin in lung tissues from RAGE$^{-/-}$ and wild-type mice after acid-induced injury. a**) Western blots of ZO-1 and E-cadherin in lung tissues from RAGE$^{-/-}$ (KO) and littermate wild-type (WT) mice, either uninjured (Sham), acid-injured (HCl) or acid-injured treated with sevoflurane (HCl+Sevo), from day 0 to day 4 after injury. **b**) ZO-1 and **c**) E-cadherin expression levels were quantified and standardized by GAPDH protein level, expressed as ratios to those in sham WT animals, and represented as box and whisker plots with medians and interquartile ranges. Two-way ANOVA tests were performed, with post-hoc comparisons if ANOVA results showed significance.

Figure S11. Myosin Light Chain phosphorylation (Ser 19) in lung tissues from RAGE$^{-/-}$ and wild-type mice after acid-induced injury. a) Western blots of total myosin light chain (MLC) and phosphorylated myosin light chain 2 (Ser19) (pMLC) in lung tissues from RAGE$^{-/-}$ (KO) and littermate wild-type (WT) mice, either uninjured (Sham), acid-injured (HCl) or acid-injured treated with sevoflurane (HCl+Sevo), from day 0 to day 4 after injury. **b**) Protein expression levels were quantified and standardized by GAPDH protein level, and pMLC levels were standardized by total MLC levels and expressed as ratios to those in the Medium group. Two-way ANOVA test was performed, with post-hoc comparisons if ANOVA results showed significance.

Figure S12. Arterial oxygen tension (PaO_2)/inspiratory oxygen fraction (FiO_2) in mice after acid-induced lung injury. Arterial oxygen tension (PaO_2)/inspiratory oxygen fraction (FiO_2) of littermate control (WT) and RAGE$^{-/-}$ mice, uninjured (Sham), after acid-induced injury (HCl) or after acid-induced injury with treatment by sevoflurane (HCl+Sevo) from day

0 to day 4 after injury. Values are presented as box and whisker plots with medians and interquartile ranges. Two-way ANOVA tests were performed, and post-hoc comparisons were performed if ANOVA results showed significance (compared to the WT_Sham group: *, $p < 0.05$; ***, $p < 0.001$; ****, $p < 0.0001$; compared to the WT_HCl group: ###, $p < 0.001$; compared to the WT_HCl+Sevo group: +, $p < 0.05$).

Figure **S13. Bronchoalveolar lavage fluid (BALF) proinflammatory cytokines levels in mice after acid-induced lung injury.** BALF level of **a**) Chemokine C-X-C motif ligand-1(CXCL-1), **b**) Interleukin 6(IL-6) and **c**) Tumor necrosis factor alpha (TNF-α) of littermate control (WT) and RAGE-/- mice, uninjured (Sham), after acid-induced injury (HCl) or after acid-induced injury with treatment by sevoflurane (HCl+Sevo) from day 0 to day 4 after injury. Values are presented as box and whisker plots with medians and interquartile ranges. Two-way ANOVA tests were performed, and post-hoc comparisons were performed if ANOVA results showed significance (compared to the WT_Sham group: ****, $p < 0.0001$; compared to the WT_HCl group: ##, $p < 0.01$; compared to the WT_HCl+Sevo group: +, $p < 0.05$).

Figure **S14**. **Histological features of lung injury in mice after acid-induced lung injury. a**) Section images and **b**) Lung injury scores of littermate control (WT) and RAGE-/- mice, uninjured (Sham), after acid-induced injury (HCl) or after acid-induced injury with treatment by sevoflurane (HCl+Sevo) from day 0 to day 4 after injury. Values are presented as box and whisker plots with medians and interquartile ranges. Two-way ANOVA tests were performed, and post-hoc comparisons were performed if ANOVA results showed significance (compared to the WT_Sham group: *, $p < 0.05$; ****, $p < 0.0001$; compared to the WT_HCl group: ###, $p < 0.001$; ####, $p < 0.0001$; compared to the KO_HCl group: ++++, $p < 0.0001$).

Figure S1

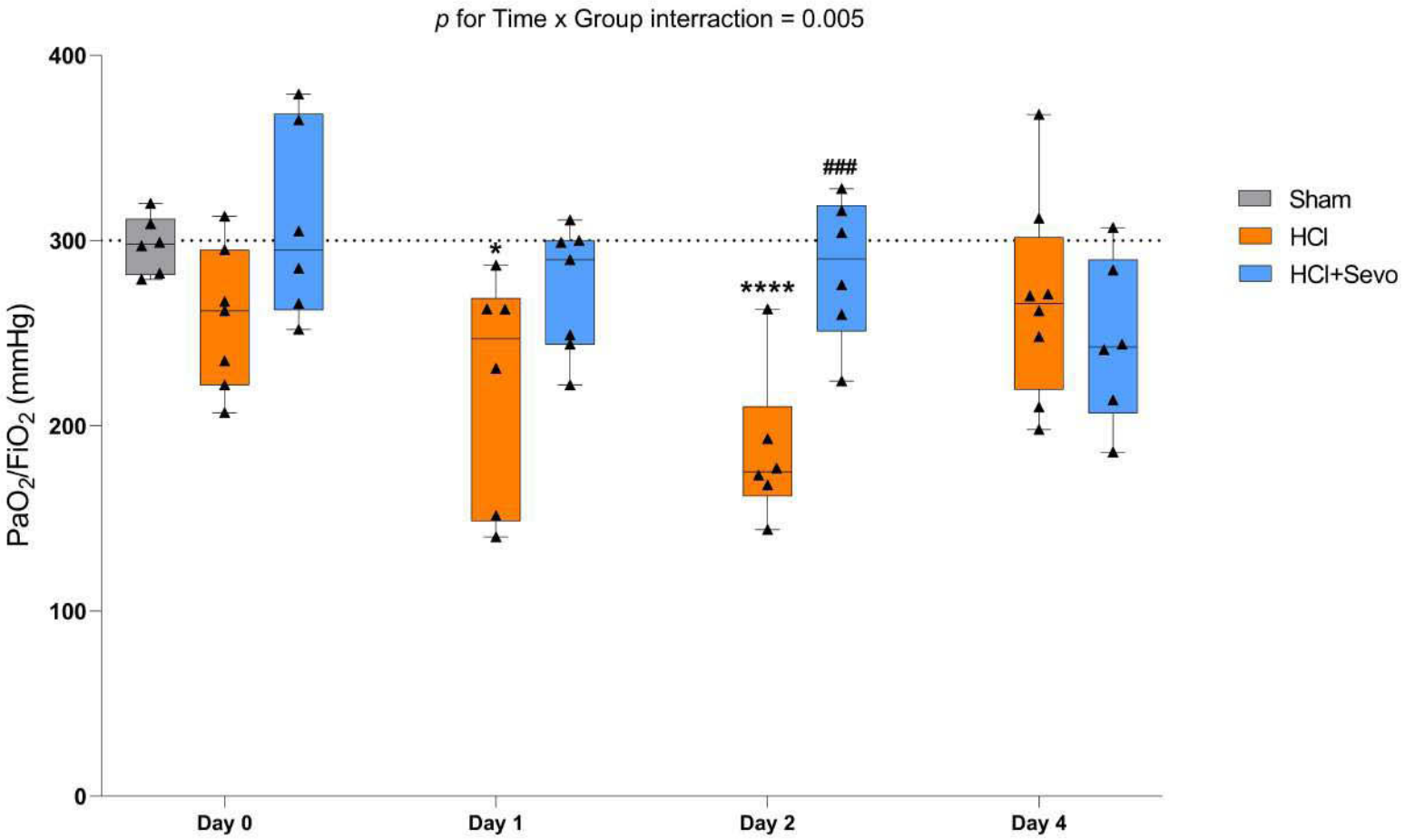
p for Time x Group interraction = 0.005
400
300
200
100
0
PaO2/FiO2 (mmHg)
Day 0
Day 1
Day 2
Day 4
*
****
###
Sham
HCl
HCl+Sevo

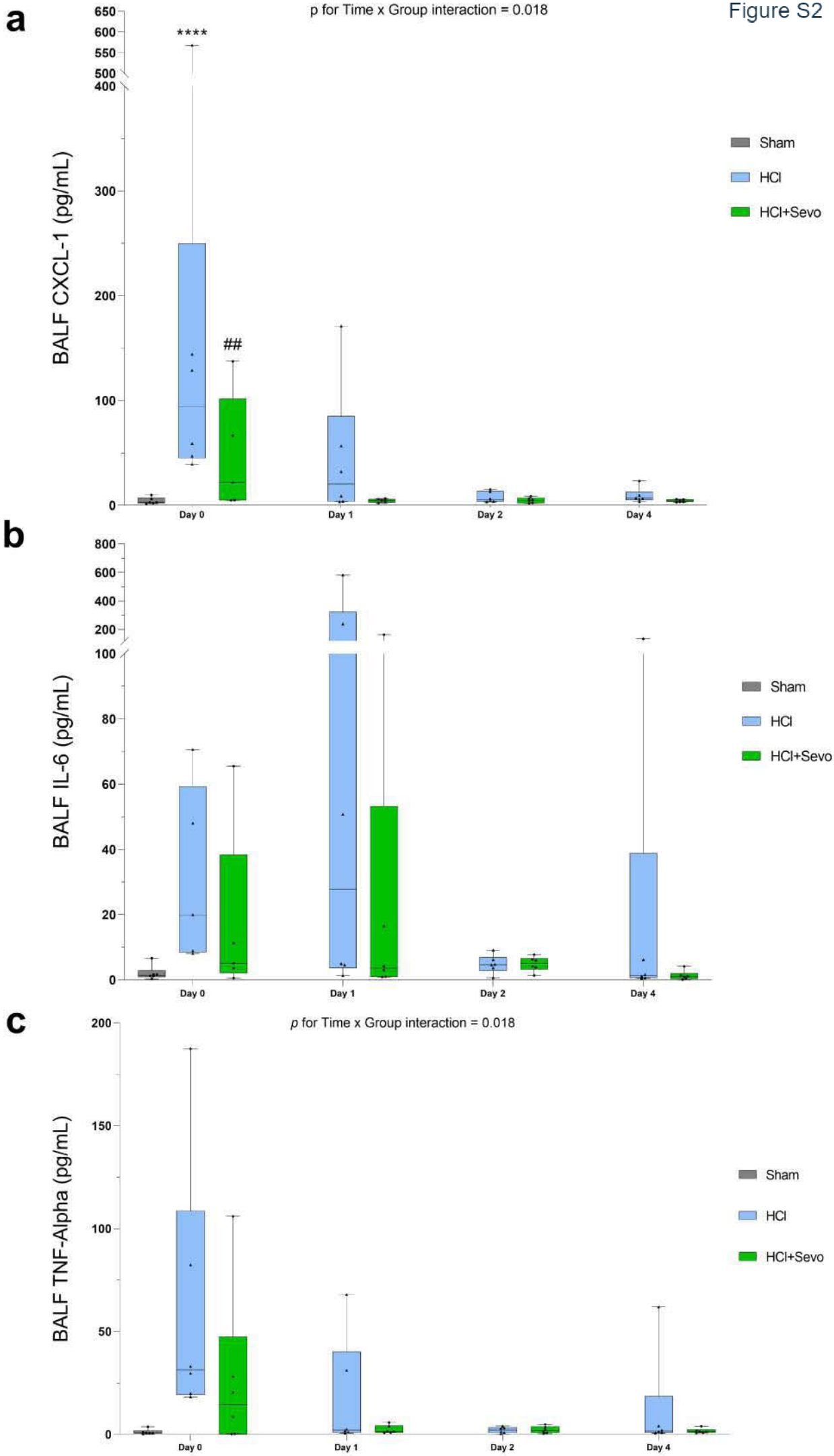
a
p for Time x Group interaction = 0.018
BALF CXCL-1 (pg/mL)
****
##
Day 0
Day 1
Day 2
Day 4
Sham
HCl
HCl+Sevo
b
BALF IL-6 (pg/mL)
Day 0
Day 1
Day 2
Day 4
Sham
HCl
HCl+Sevo
c
p for Time x Group interaction = 0.018
BALF TNF-Alpha (pg/mL)
Day 0
Day 1
Day 2
Day 4
Sham
HCl
HCl+Sevo

Figure S3

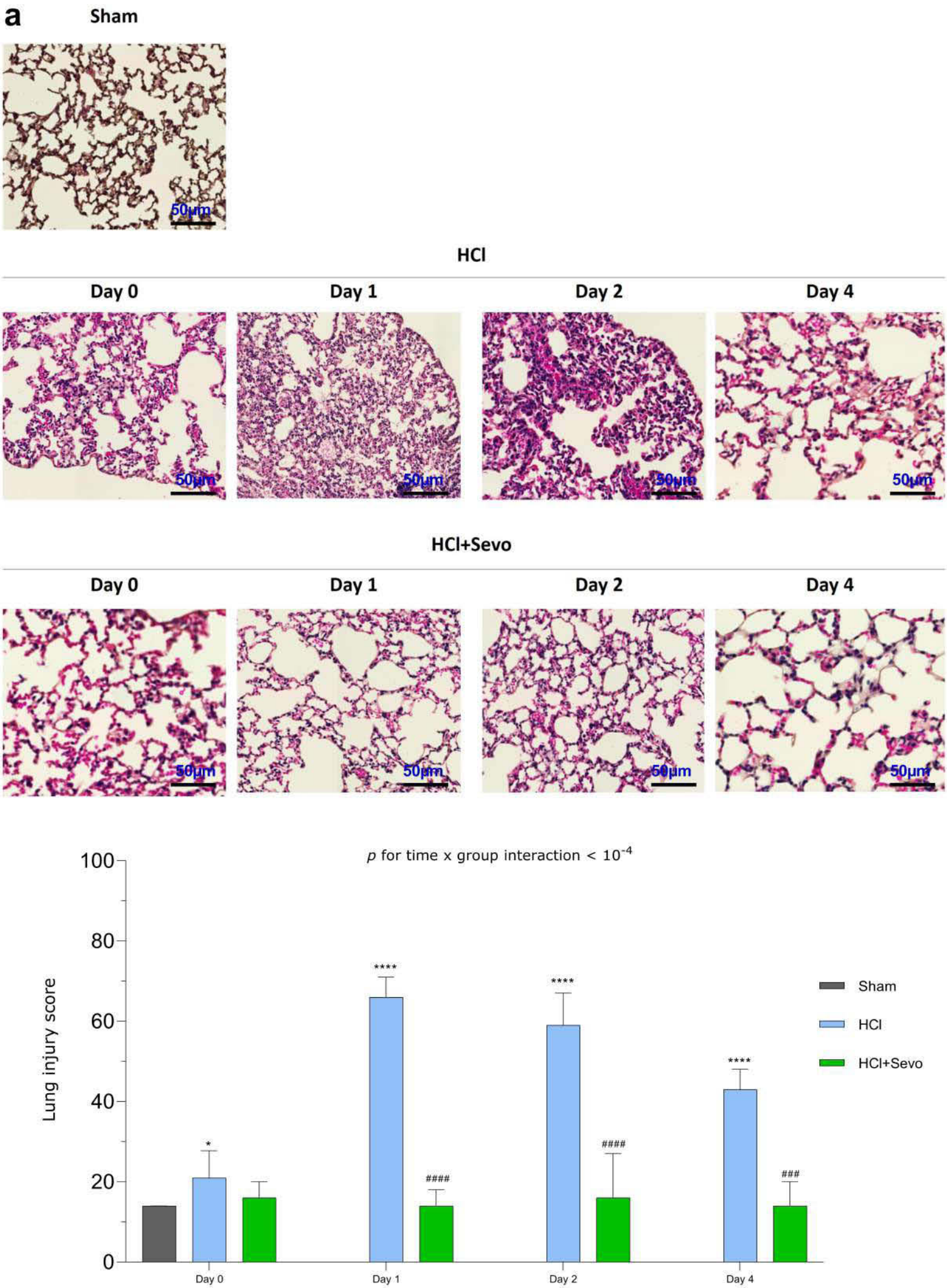
a
Sham
50μm
HCl
Day 0
Day 1
Day 2
Day 4
50μm
HCl+Sevo
Day 0
Day 1
Day 2
Day 4
50μm
p for time x group interaction < 10-4
Lung injury score
100
80
60
40
20
0
*
****
####
****
####
****
###
Day 0
Day 1
Day 2
Day 4
Sham
HCl
HCl+Sevo

Figure S4

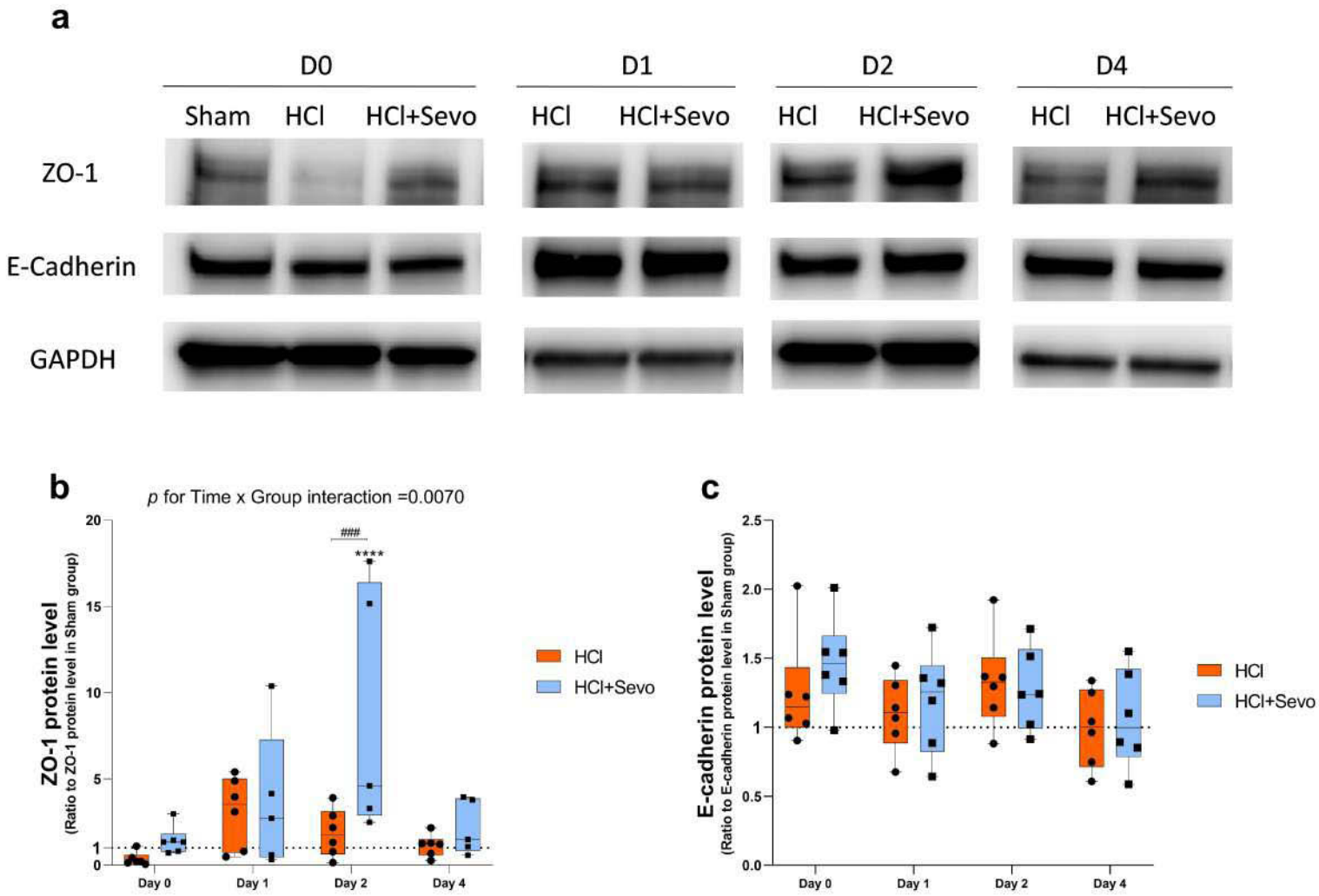
a
D0
D1
D2
D4
Sham
HCl
HCl+Sevo
HCl
HCl+Sevo
HCl
HCl+Sevo
HCl
HCl+Sevo
ZO-1
E-Cadherin
GAPDH
b
p for Time x Group interaction =0.0070
###
****
ZO-1 protein level
(Ratio to ZO-1 protein level in Sham group)
20
15
10
5
1
0
Day 0
Day 1
Day 2
Day 4
HCl
HCl+Sevo
c
E-cadherin protein level
(Ratio to E-cadherin protein level in Sham group)
2.5
2.0
1.5
1
0.5
0.0
Day 0
Day 1
Day 2
Day 4
HCl
HCl+Sevo

Figure S5

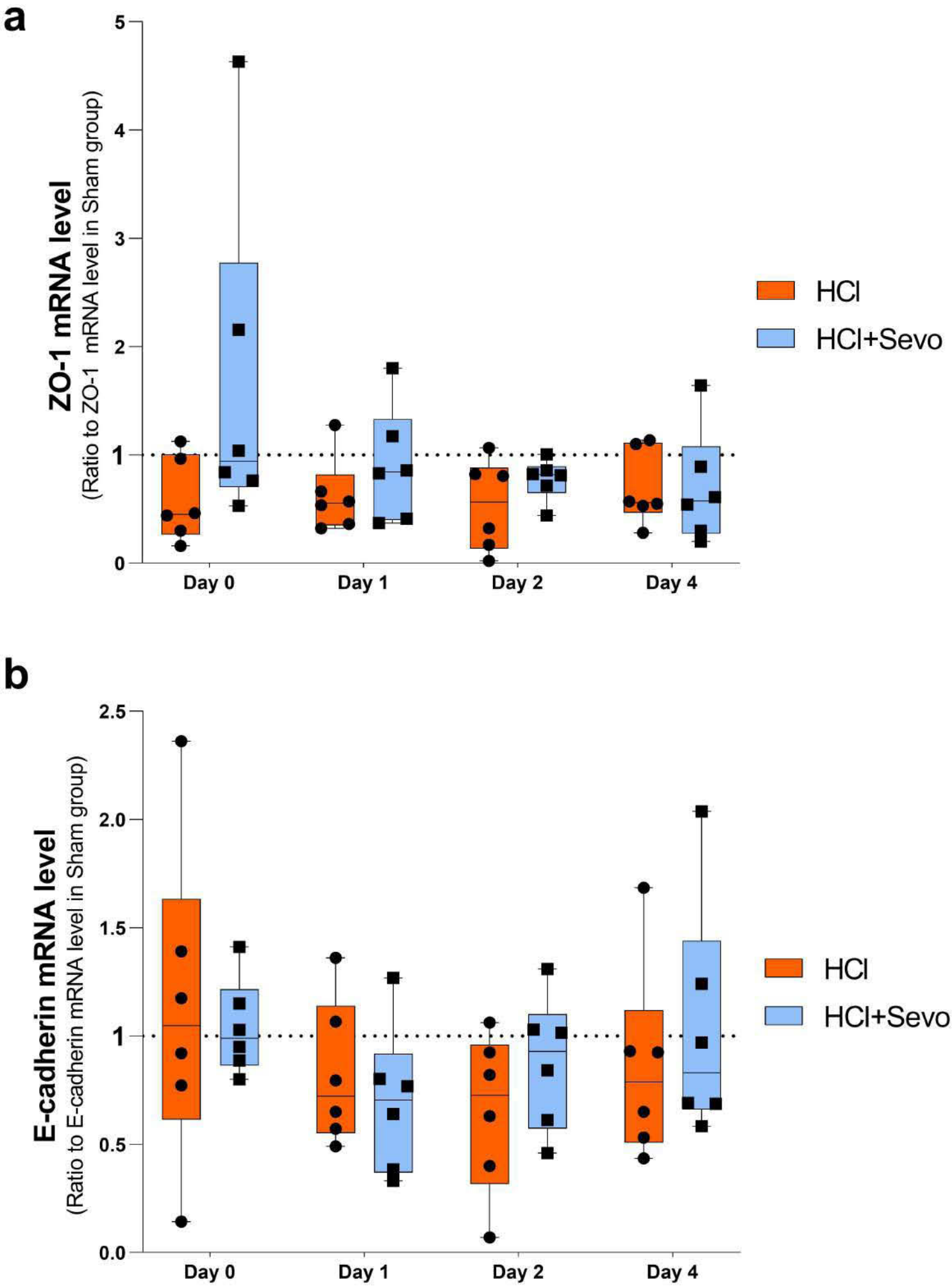
a
ZO-1 mRNA level
(Ratio to ZO-1 mRNA level in Sham group)
5
4
3
2
1
0
Day 0
Day 1
Day 2
Day 4
HCl
HCl+Sevo
b
E-cadherin mRNA level
(Ratio to E-cadherin mRNA level in Sham group)
2.5
2.0
1.5
1
0.5
0.0
Day 0
Day 1
Day 2
Day 4
HCl
HCl+Sevo

Figure S6

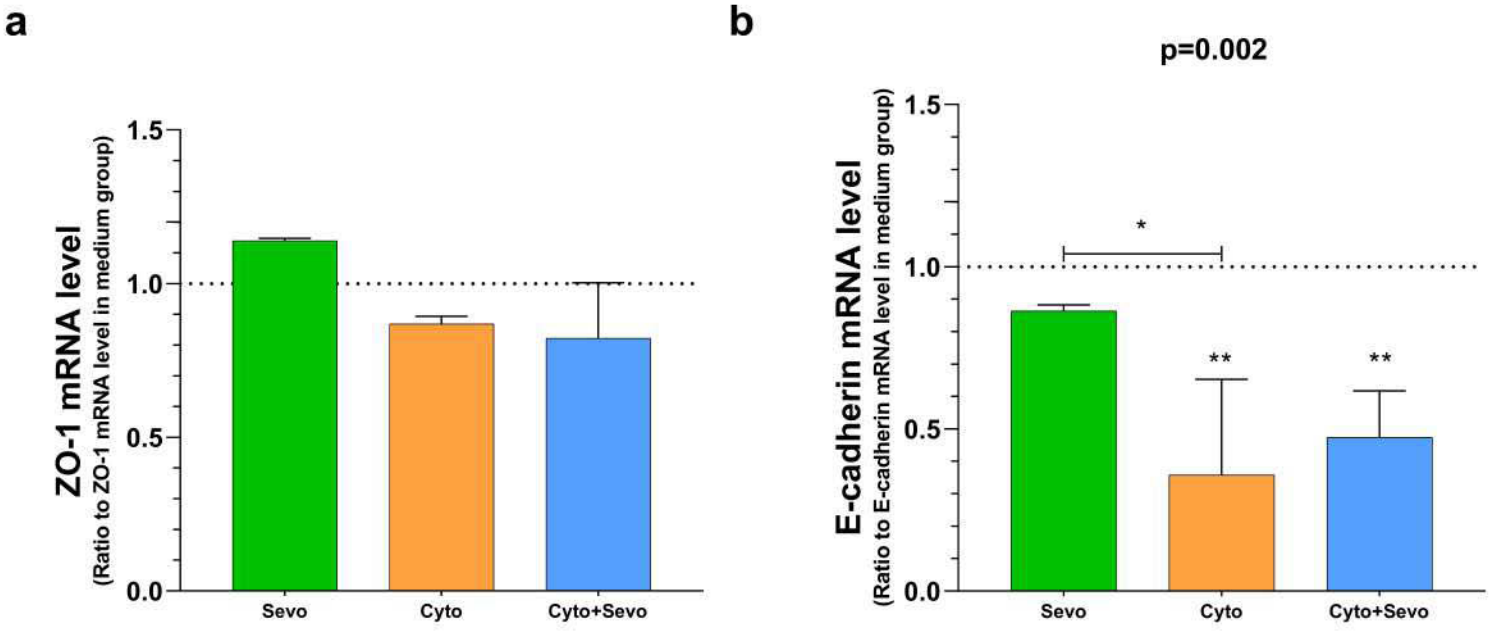
a
ZO-1 mRNA level
(Ratio to ZO-1 mRNA level in medium group)
1.5
1.0
0.5
0.0
Sevo
Cyto
Cyto+Sevo
b
p=0.002
E-cadherin mRNA level
(Ratio to E-cadherin mRNA level in medium group)
1.5
1.0
0.5
0.0
*
**
**
Sevo
Cyto
Cyto+Sevo

Figure S7

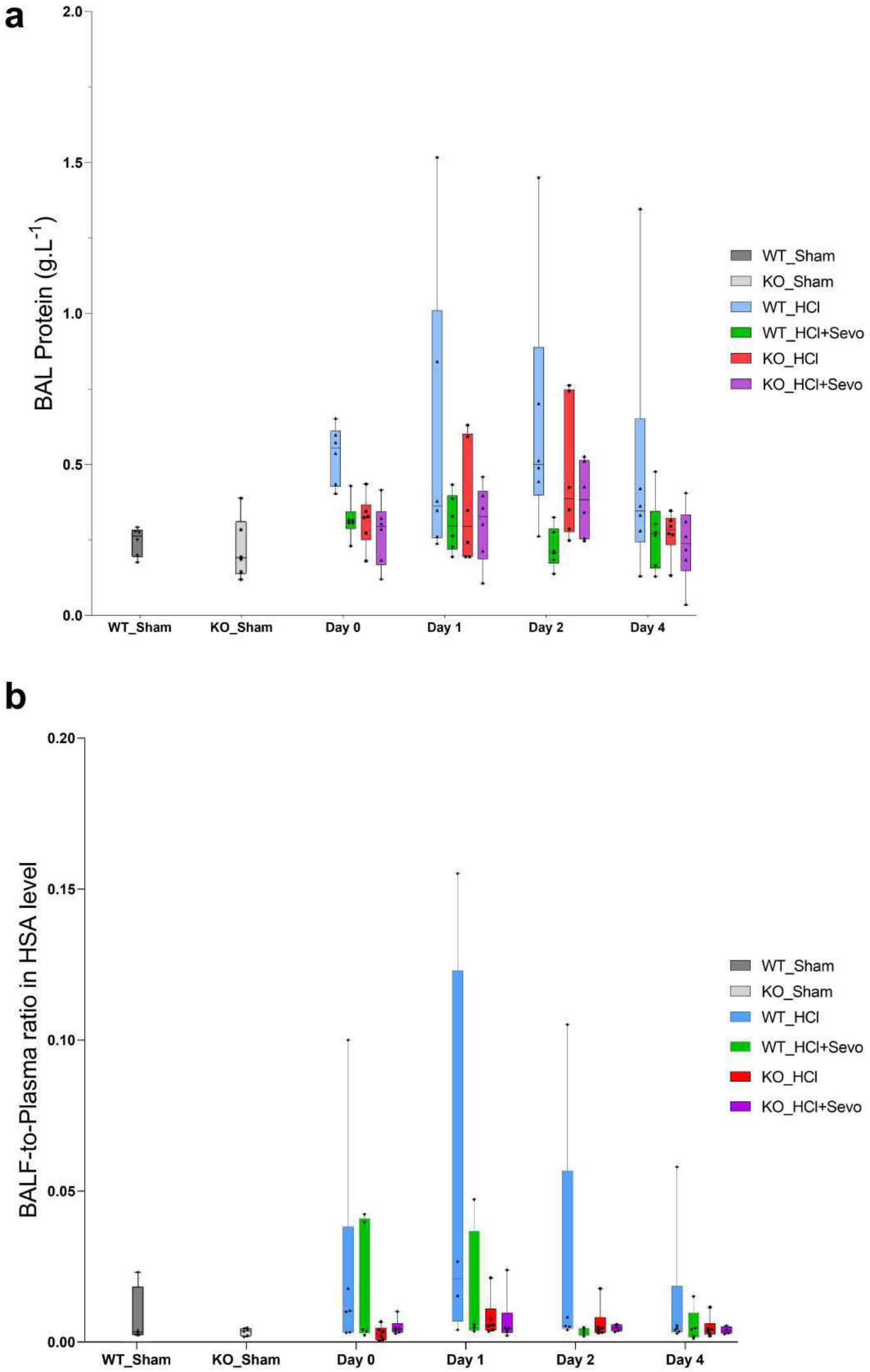
a
BAL Protein (g.L-1)
2.0
1.5
1.0
0.5
0.0
WT_Sham
KO_Sham
Day 0
Day 1
Day 2
Day 4
WT_Sham
KO_Sham
WT_HCl
WT_HCl+Sevo
KO_HCl
KO_HCl+Sevo
b
BALF-to-Plasma ratio in HSA level
0.20
0.15
0.10
0.05
0.00
WT_Sham
KO_Sham
Day 0
Day 1
Day 2
Day 4
WT_Sham
KO_Sham
WT_HCl
WT_HCl+Sevo
KO_HCl
KO_HCl+Sevo

Figure S8

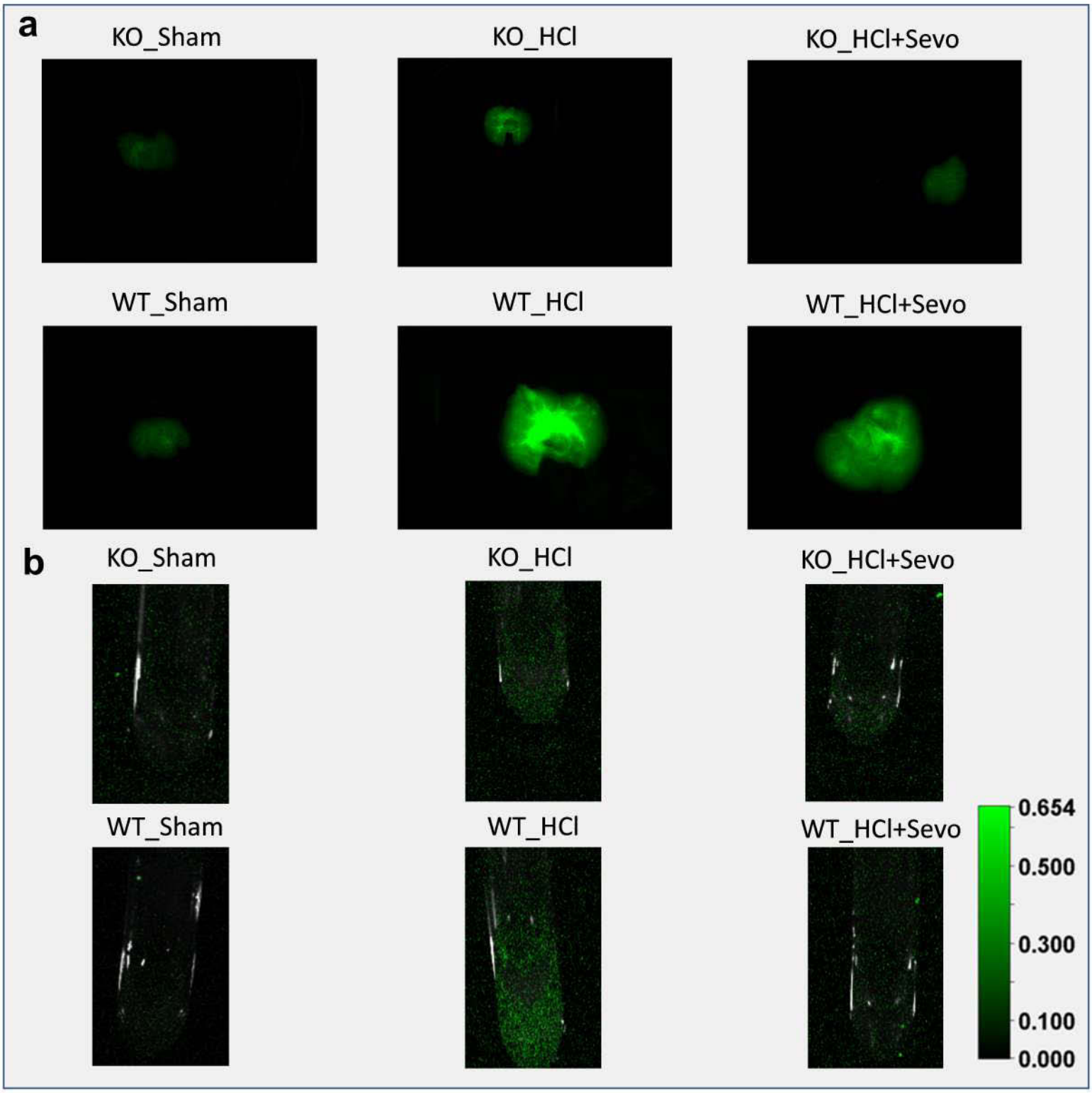
a
KO_Sham
KO_HCl
KO_HCl+Sevo
WT_Sham
WT_HCl
WT_HCl+Sevo
b
KO_Sham
KO_HCl
KO_HCl+Sevo
WT_Sham
WT_HCl
WT_HCl+Sevo
0.654
0.500
0.300
0.100
0.000

Figure S9

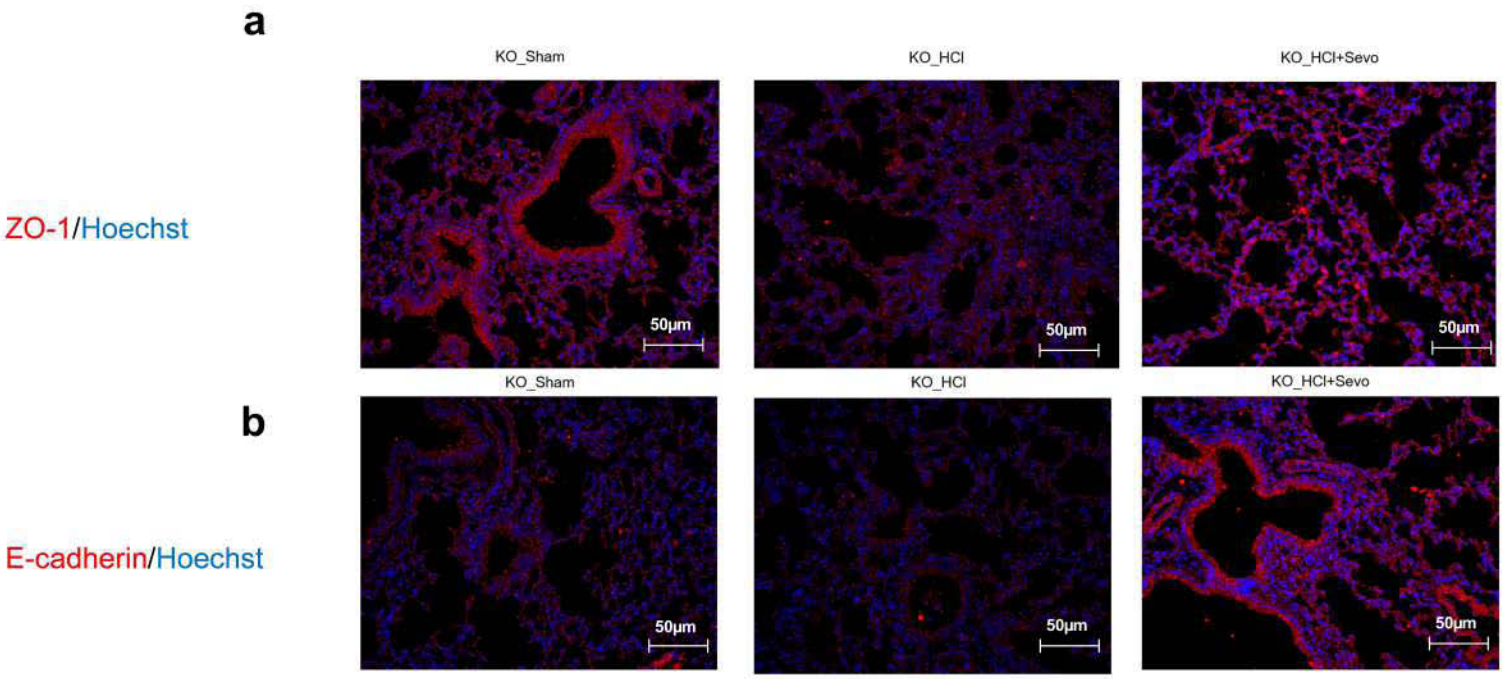
a
KO_Sham
KO_HCl
KO_HCl+Sevo
ZO-1/Hoechst
50μm
50μm
50μm
b
KO_Sham
KO_HCl
KO_HCl+Sevo
E-cadherin/Hoechst
50μm
50μm
50μm

Figure S10

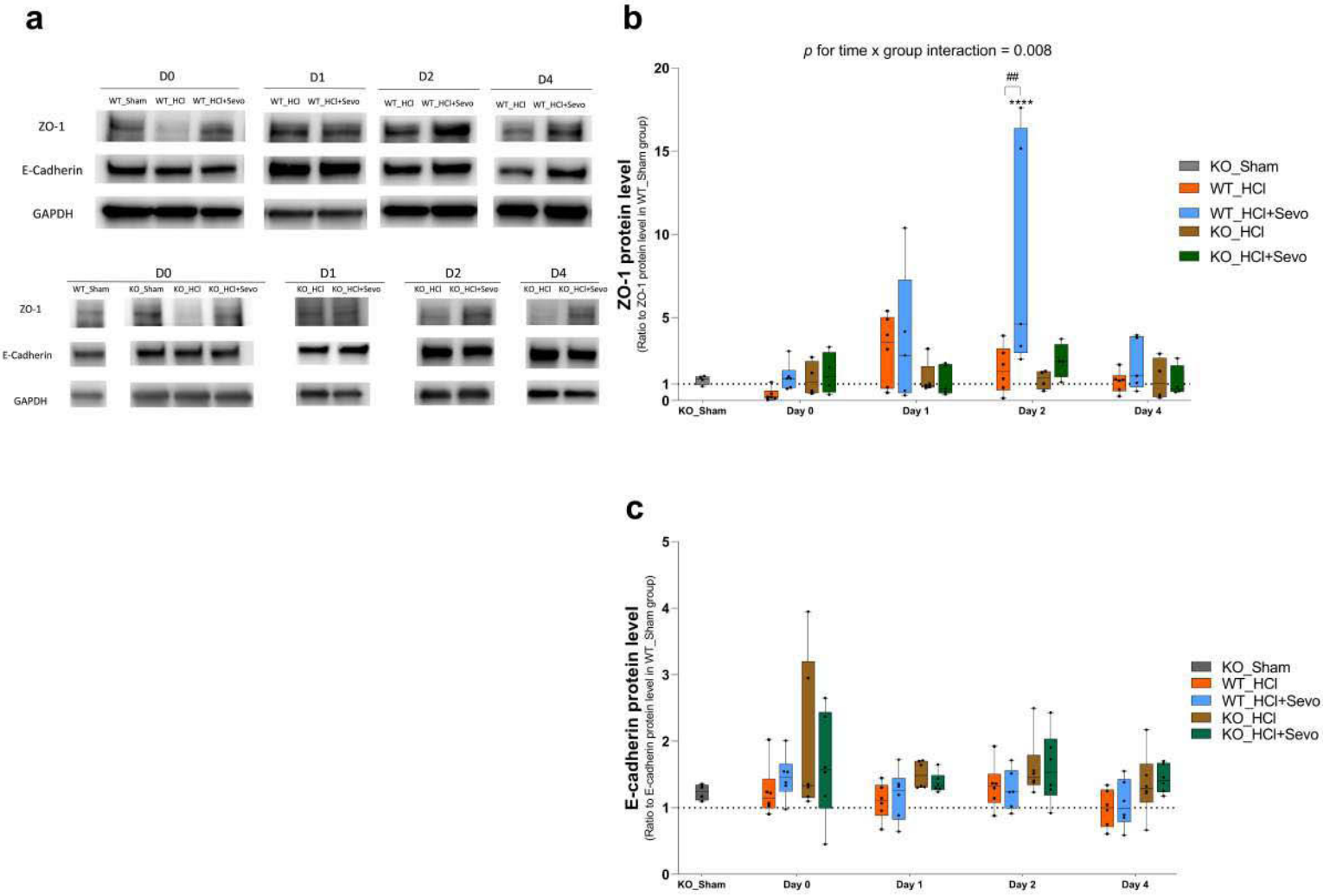
a
D0
D1
D2
D4
WT_Sham
WT_HCl
WT_HCl+Sevo
ZO-1
E-Cadherin
GAPDH
KO_Sham
KO_HCl
KO_HCl+Sevo
b
p for time x group interaction = 0.008
##
****
ZO-1 protein level
(Ratio to ZO-1 protein level in WT_Sham group)
KO_Sham
Day 0
Day 1
Day 2
Day 4
c
E-cadherin protein level
(Ratio to E-cadherin protein level in WT_Sham group)

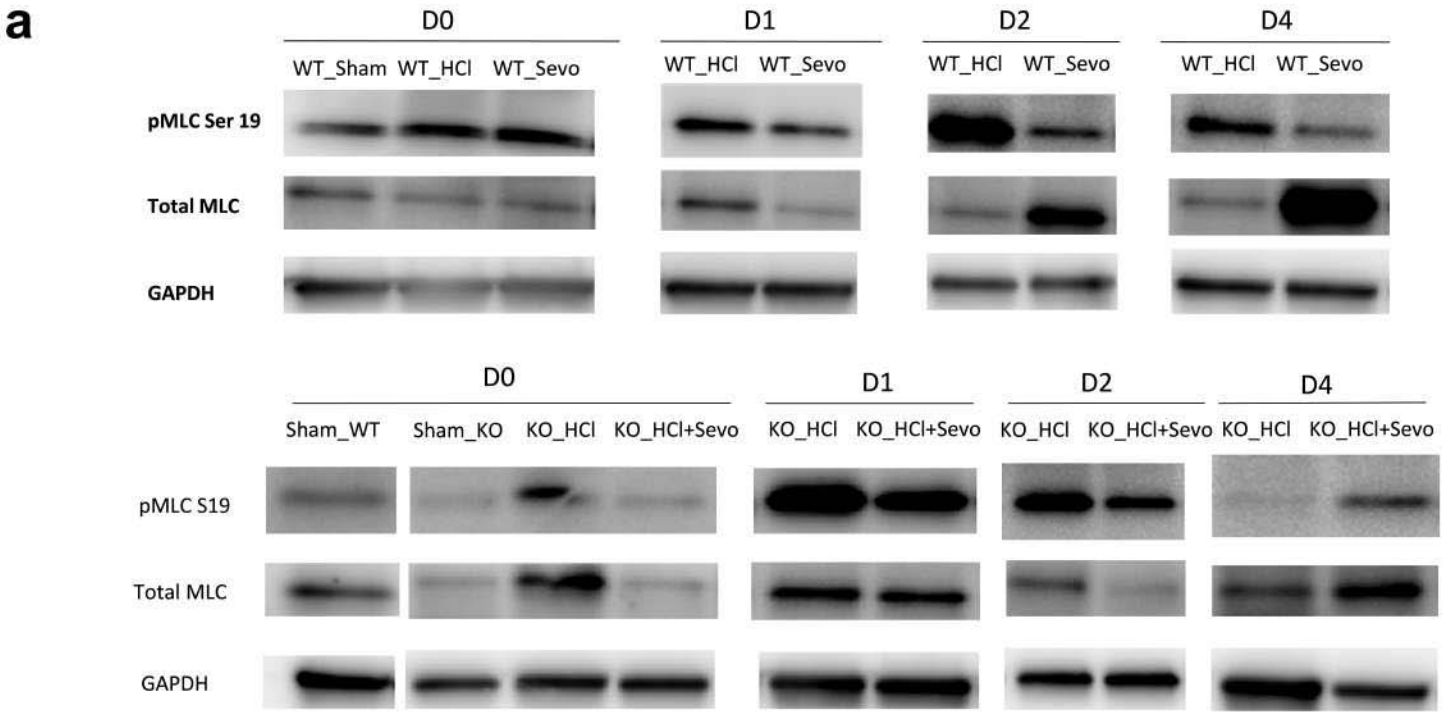
a
D0
D1
D2
D4
WT_Sham WT_HCl WT_Sevo
WT_HCl WT_Sevo
WT_HCl WT_Sevo
WT_HCl WT_Sevo
pMLC Ser 19
Total MLC
GAPDH
D0
D1
D2
D4
Sham_WT Sham_KO KO_HCl KO_HCl+Sevo
KO_HCl KO_HCl+Sevo
KO_HCl KO_HCl+Sevo
KO_HCl KO_HCl+Sevo
pMLC S19
Total MLC
GAPDH

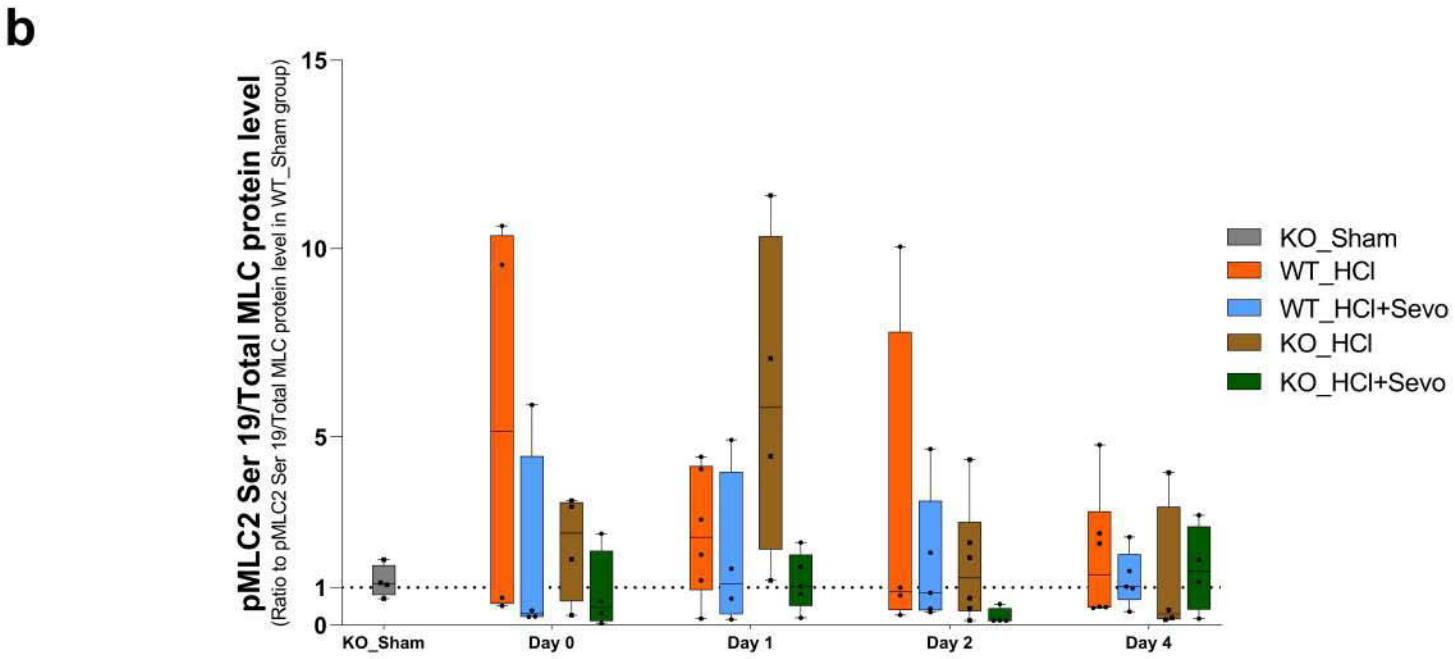
b
pMLC2 Ser 19/Total MLC protein level
(Ratio to pMLC2 Ser 19/Total MLC protein level in WT_Sham group)
15
10
5
1
0
KO_Sham
Day 0
Day 1
Day 2
Day 4
KO_Sham
WT_HCl
WT_HCl+Sevo
KO_HCl
KO_HCl+Sevo

Figure S12

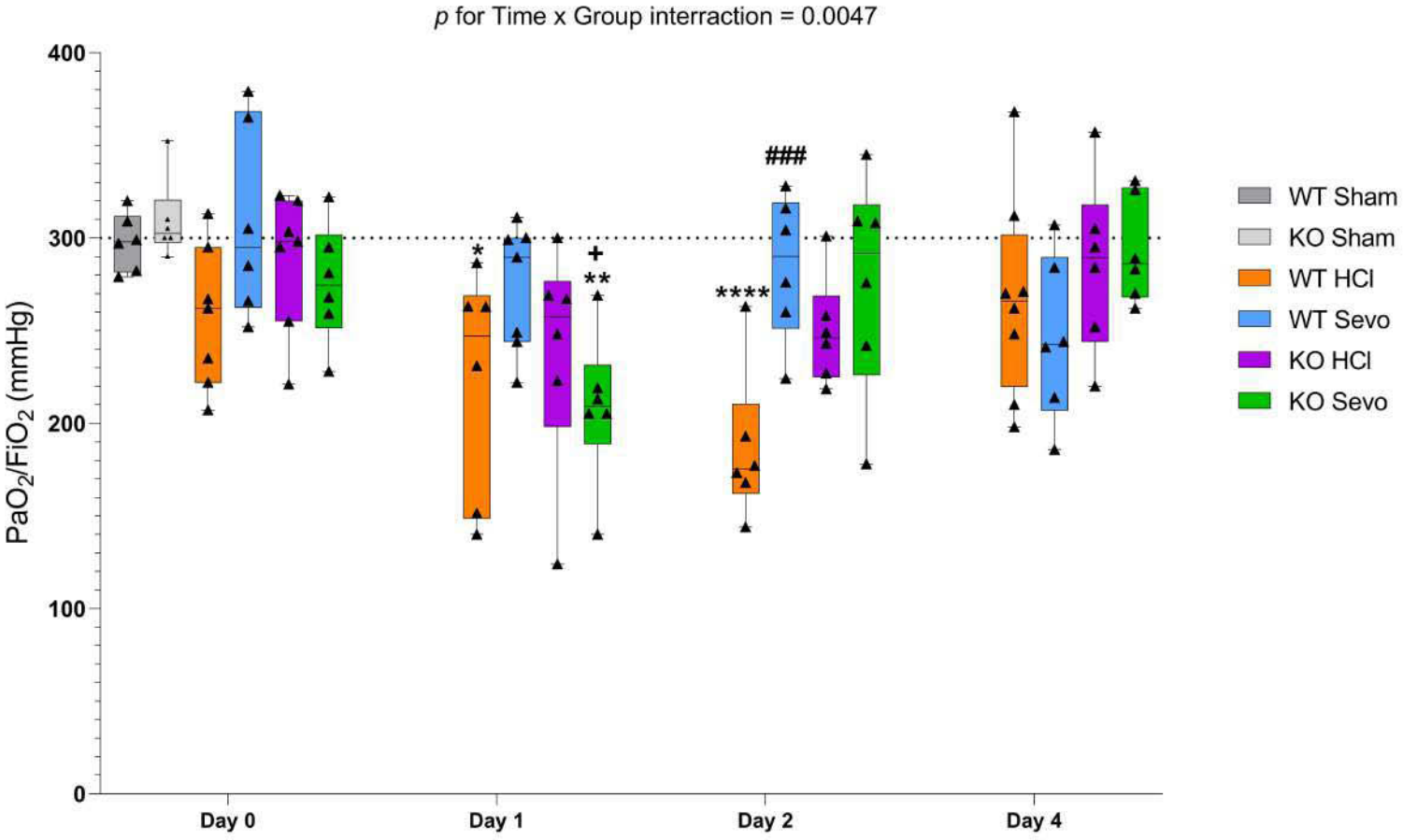
p for Time x Group interraction = 0.0047
400
300
200
100
0
PaO2/FiO2 (mmHg)
Day 0
Day 1
Day 2
Day 4
*
**
+
****
###
WT Sham
KO Sham
WT HCl
WT Sevo
KO HCl
KO Sevo

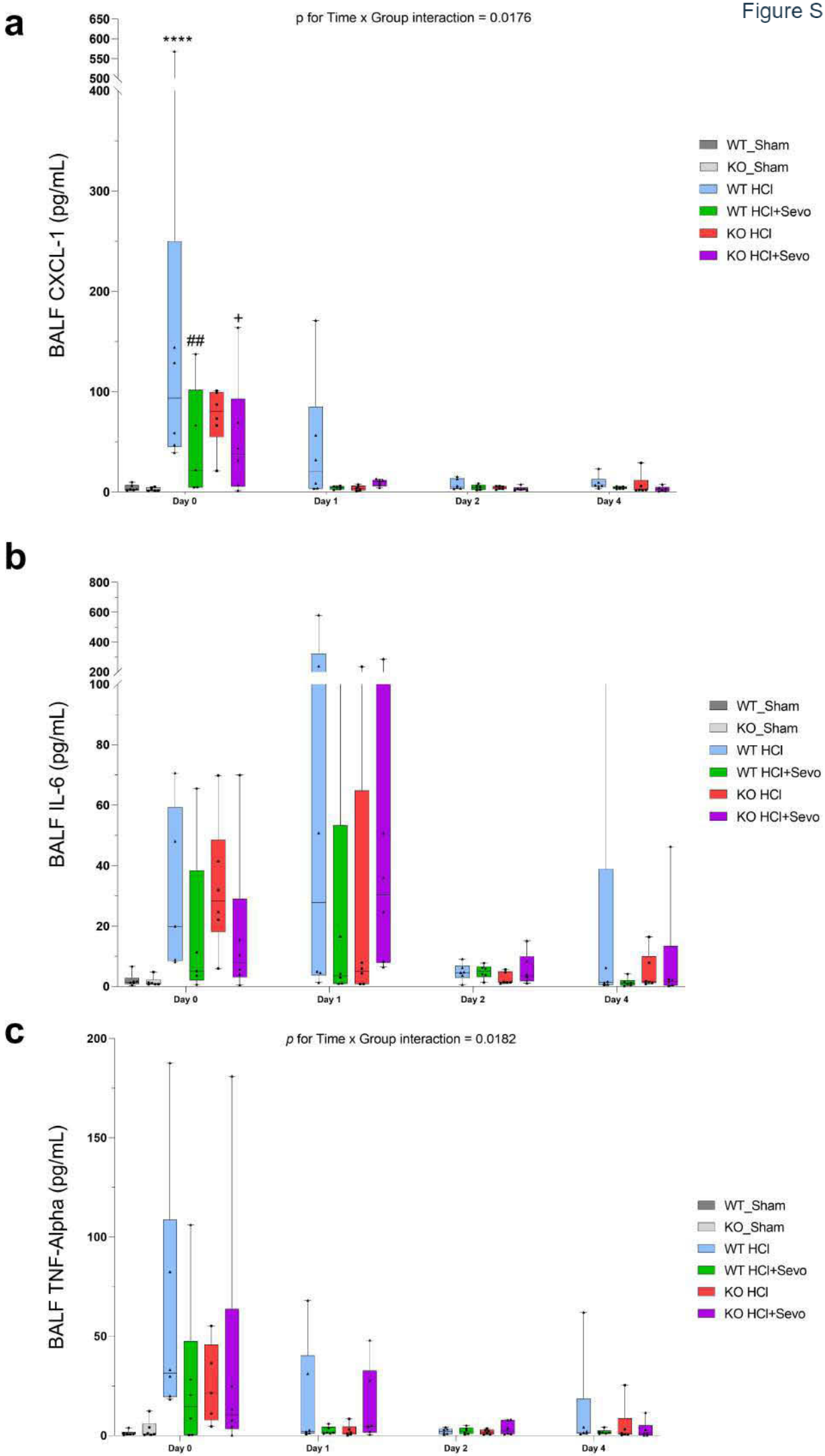
a
p for Time x Group interaction = 0.0176
BALF CXCL-1 (pg/mL)
****
##
+
Day 0
Day 1
Day 2
Day 4
WT_Sham
KO_Sham
WT HCl
WT HCl+Sevo
KO HCl
KO HCl+Sevo
b
BALF IL-6 (pg/mL)
c
p for Time x Group interaction = 0.0182
BALF TNF-Alpha (pg/mL)

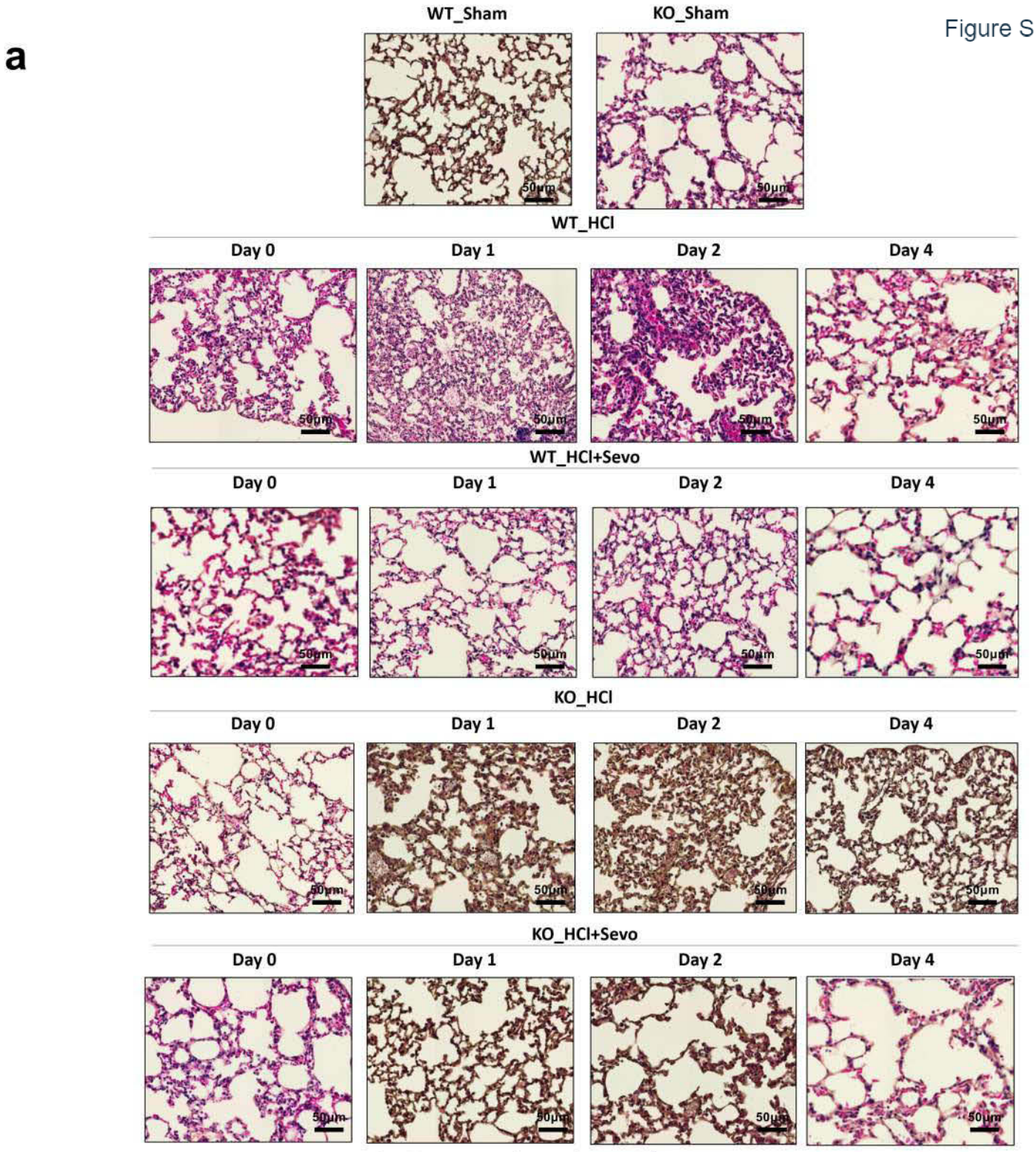
a
WT_Sham
KO_Sham
WT_HCl
Day 0
Day 1
Day 2
Day 4
WT_HCl+Sevo
KO_HCl
KO_HCl+Sevo
50μm

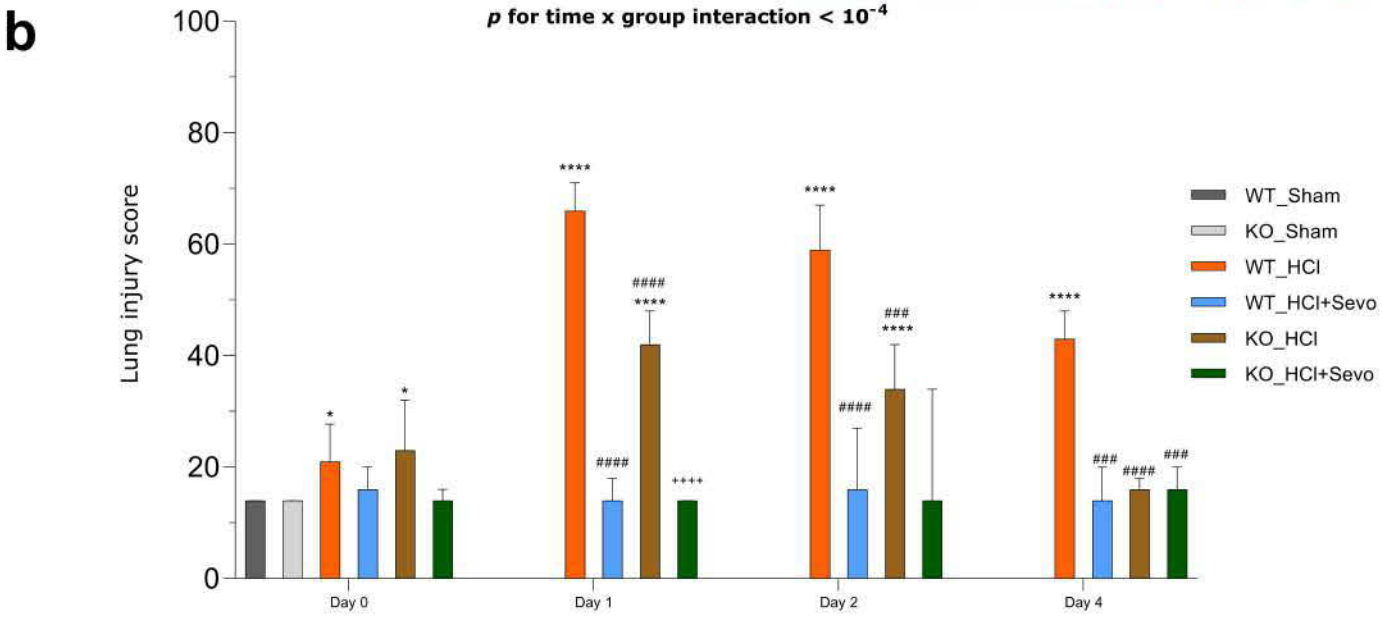
b
p for time x group interaction < 10-4
Lung injury score
100
80
60
40
20
0
Day 0
Day 1
Day 2
Day 4
WT_Sham
KO_Sham
WT_HCl
WT_HCl+Sevo
KO_HCl
KO_HCl+Sevo

STUDY N°5

Halogenated Agents Sevoflurane And Isoflurane Effects In Alveolar Epithelial Pulmonar Function : A Randomized Laboratory Trial in Piglets

Zhai R, Blondonnet R, Paquette B, Belville C, Pereira B, Lenga W, Damon-Soubeyran C, Blanchon L, Sapin V, Jabaudon M. ***(Manuscript in preparation)***

Halogenated Agents Sevoflurane And Isoflurane Effects In Alveolar Epithelial Pulmonar Function : A Randomized Laboratory Trial in Piglets

Ruoyang Zhai[1], Raiko Blondonnet[1], Bertille Paquette[1,2], Corinne Belville[1], Bruno Pereira[4], Woodys Lenga[1], Christelle Damon-Soubeyran[1], Loic Blanchon[1], Vincent Sapin[1,3], Matthieu Jabaudon[1,2]

1_Université Clermont Auvergne, CNRS, INSERM, iGReD, Clermont-Ferrand, France.
2_Department of Perioperative Medicine, CHU Clermont-Ferrand, Clermont-Ferrand, France.
3_Department of Medical Biochemistry and Molecular Genetics, CHU Clermont-Ferrand, Clermont-Ferrand, France.
4._Biostatistics Unit, Department of Clinical Research and Innovation (DRCI), CHU Clermont-Ferrand, Clermont-Ferrand, France

Scientific Knowledge of the Subject

In ARDS, impaired alveolar fluid clearance function (AFC) is a key pathophysiological process that is partly associated with the impaired epithelial function, influencing patients' prognosis [197,198,224].

Increasing evidence showed the potential beneficial effects of inhaled sedation including improved gas exchange, decreased alveolar edema and decreased inflammation in experimental models of lung injury[240–242]. Furthermore, sevoflurane appears to specifically decrease type 2 pneumocyte damage [243] and isoflurane maintains the integrity of the alveolar-capillary barrier by modulating tight junctions [241].

The objective of this study is to investigate the effects of halogenated agents (sevoflurane and isoflurane) on pulmonary epithelial function with its potential improvement in oxygenation and AFC in a piglet ARDS model.

Contributions of this study to the field

Compared to intravenous sedation, the use of inhaled sedation with sevoflurane or isoflurane in our porcine model of ARDS was shown to be associated with improved oxygenation, restored alveolar permeability, and improved AFC.

Furthermore, lung expression levels of the three main epithelial channels AQP-5, Na, K, ATPase and ENaC are impaired during hydrochloric acid-induced lung injury. The use of inhaled sedation compared to intravenous sedation seems to restore the protein expression of these channels.

Halogenated Agents Sevoflurane And Isoflurane Effects In Alveolar Epithelial Pulmonar Function : A Randomized Laboratory Trial in Piglets

Ruoyang Zhai[1], Raiko Blondonnet[1], Bertille Paquette[1,2], Corinne Belville[1], Bruno Pereira[4], Woodys Lenga[1], Christelle Damon-Soubeyran[1], Loic Blanchon[1], Vincent Sapin[1,3], Matthieu Jabaudon[1,2]

1_Université Clermont Auvergne, CNRS, INSERM, iGReD, Clermont-Ferrand, France.
2_Department of Perioperative Medicine, CHU Clermont-Ferrand, Clermont-Ferrand, France.
3_Department of Medical Biochemistry and Molecular Genetics, CHU Clermont-Ferrand, Clermont-Ferrand, France.
4_Biostatistics Unit, Department of Clinical Research and Innovation (DRCI), CHU Clermont-Ferrand, Clermont-Ferrand, France

CORRESPONDING AUTHOR:
Raiko Blondonnet, MD, Ph.D.
Université Clermont Auvergne, iGReD, CNRS, INSERM
Clermont-Ferrand Cedex 1, France
(Mail) rblondonnet@chu-clermontferrand.fr

INTRODUCTION

Acute respiratory distress syndrome (ARDS) is a syndrome of diffuse inflammatory lung injury with increased pulmonary oedema and the rapid onset of hypoxemic respiratory failure characterized by both diffuse alveolar epithelial and endothelial lung injuries. ARDS is still undertreated, with high mortality and currently lacks effective therapies. Impairment of alveolar fluid clearance (AFC) is a major feature of AFC that is associated with the mortality [1]. One of the main mechanisms responsible for the resolution of alveolar oedema is ion transport across the alveolar epithelium, primarily through epithelial sodium (ENaC), Na,K-ATPase and aquaporin (AQP)-5 channels, thus creating a local osmotic gradient to reabsorb the water fraction of the edema fluid from the airspaces of the lungs [2–4].

Halogenated anesthetics, such as isoflurane or sevoflurane, have been widely used for general anesthesia in the operating room. Sevoflurane is associated with decreased inflammation in the lungs of patients undergoing thoracic surgery and with a decrease in postoperative pulmonary complications, such as ARDS[5]. Similar results have been found in a meta-analysis of patients after cardiac surgery[6]. Halogenated volatiles also have a bronchodilatory effect[7,8] and perhaps some properties that protect several organs, such as the heart[9,10] and the kidneys[11–13]. Recently, there has been growing interest in the clinical use of inhaled anesthetics as sedatives in the intensive care unit (ICU). Both animal and human studies support the protective effects of pretreatment with halogenated agents before prolonged ischemia of the liver[14], the brain[15], or the heart[9]. Halogenated agents also have potential pharmacokinetic and pharmacodynamic advantages over other intravenous agents for the sedation of critically ill patients, including a rapid onset of action and fast offset due to little accumulation in tissues. Inhaled halogenated agents decrease intubation times in comparison with intravenous sedation in patients undergoing cardiac surgery[16]. Several studies support the safety and efficacy of halogenated agents in the sedation of ICU patients[17–19]. In experimental models of ARDS, inhaled sevoflurane improves gas exchange[20,21], reduces alveolar edema[20,21], and attenuates both pulmonary and systemic inflammation[22]. Isoflurane also ameliorates lung repair after injury by maintaining the integrity of the alveolar–capillary barrier, possibly by modulating the expression of a key tight junction protein[23–25]. In addition, mouse macrophages that were cultured and treated with isoflurane had better phagocytic effects on neutrophils than macrophages that were not treated with isoflurane[26].

Our objectives were to investigate the *in vivo* effects of inhaled sevoflurane and isoflurane on of lung injury and repair (namely lung epithelial injury and alveolar fluid clearance) and to test the hypothesis that sevoflurane and/or isoflurane may exert beneficial effects on lung injury, oxygenation and alveolar fluid clearance.

MATERIAL AND METHODS

Animal model. We used the porcine model previously described by our team [27] and derived from the work from Ambrosio et al [28] Animal experiments were performed in the *Centre International de Chirurgie Endoscopique, Faculté de Médecine, Université d'Auvergne* (Clermont-Ferrand, France), as approved by our national animal ethics committee (approval number 01505.03).

Landrace white two-year old piglets, weighing 10-15 kg, were used. The animals were restricted from food overnight but had free access to water. Pigs were premedicated using intramuscular azaperone (2 $mg.kg^{-1}$) behind the ear. Anesthesia was induced with intravenous propofol (3 $mg.kg^{-1}$) and sufentanil (0.3 $\mu g.kg^{-1}$) and animals were intubated orally with a 6-mm internal diameter cuffed endotracheal tube. Central venous access using a surgical exposure of the right internal jugular vein and the Seldinger method to insert a 3-lumen catheter (7 French, 16 cm) was inserted. The femoral artery was catheterized to insert both an arterial line and a thermodilution catheter (3–5 French, 20) allowing blood samples and continuous hemodynamic monitoring (e.g., cardiac output, extravascular lung water) with PiCCO+ device (Pulsion SA).

A total of 24 piglets were randomly allocated to four groups. The randomization was performed by means of computer software (Microsoft Office Excel 2003, Microsoft Corporation). A Sham-IV group (N=6) was made with control animals, without lung injury, and receiving intravenous sedation with propofol and remifentanil. A HCl-IV group (N=6) defined animals with acid-induced lung injury and receiving intravenous sedation (N=6). The HCl-Sevo group (N=6) and HCl-Iso group (N=6) formed groups of animals with

acid-induced lung injury and receiving an inhaled sedation post-conditioning with either sevoflurane or isoflurane, respectively.

Mechanical ventilation was delivered using volume-controlled ventilation, tidal volume of 6–8 $ml.kg^{-1}$, PEEP of 5 cmH_2O and oxygen inspired fraction (FiO_2) of 40% (Engström, GE Healthcare). Respiratory rate was adjusted to maintain end-tidal carbon dioxide between 35 and 45 mmHg. The temperature of the pigs was kept at approximately 38°C by using warm blankets (Medi-therm II, Gaymar Industries). The electrocardiogram and arterial pressure were monitored continuously (IntelliVue MP40, Phillips and PiCCO, Pulsion SA). Pigs were placed in the supine position. Continuous anesthesia consisting of intravenous infusion of propofol (5 $mg.kg^{-1}.h^{-1}$) and continuous intravenous infusion of remifentanil (10–20 $\mu g.kg^{-1}.h^{-1}$=0.15–0.33$\mu g.kg^{-1}.min^{-1}$) before acid-induced lung injury was standardized. Continuous intravenous infusion of cisatracurium (0.2 $mg.kg^{-1}.h^{-1}$) was used for a neuromuscular blockade.

Sedation using halogenated anesthetics (sevoflurane or isoflurane) was started once the acid-induced lung injury was achieved. The intravenous sedation was then interrupted for both the HCl-sevo and HCl-iso groups. Inhaled sedation was delivered through the anesthetic conserving device (Cedaconda, Sedana Medical) connected between the Y-piece of the respiratory circuit and the endotracheal tube. After priming the agent line with a bolus of 1.5 mL of the halogenated anesthetics, the syringe pump rate was adapted to reach a certain concentration depends on the minute volume and the targeted concentration, with rates of 2–7 mL.h-1 and 4–10 ml.h-1 being, in general, associated with expired fractions of 0.2–0.7% and 0.5–1.4% for isoflurane[29] and sevoflurane[30,31], respectively. For this study, continue administration of the halogenated anesthetics with FEsevo and FEiso targets were of 0.8–1.1 and 0.5–0.8, respectively.

Acid aspiration–Induced acute lung injury was induced by intratracheal instillation of 100ml hydrochloric acid 0.05 N, pH 1.4 (4 $ml.kg^{-1}$ body weight), at the level of the carina over 3 min using a Ch14 suction catheter through the endotracheal tube. Based on previous studies, lung injury was established when PaO_2/FiO_2 ratio decreased to 25% from the baseline (blood

samples collected at 5 cmH_2O of PEEP, FiO_2 of 40 %), approximately one hour after airway hydrochloric acid instillation[28,32].

At the end of ventilation, and after lung bronchoalveolar lavage (BAL) and arterial blood sampling, piglets were sacrificed with intravenous pentobarbital (150 $mg.kg^{-1}$). Whole lungs were harvested after sacrifice for histological analysis.

Physiological measurements. Criteria for experimental ARDS were evaluated as recommended by the *American Thoracic Society [33]* at baseline in injured and Sham animals, and after four hours of mechanical ventilation. We evaluated PaO_2/FiO_2 ratio (also measured hourly during the experimental procedure), as assessed by arterial blood gases using a bedside solution (EPOC, Siemens), alveolar-capillary permeability, as assessed by total protein level in BAL, and by measurements of extravascular lung water (EVLW, as indexed to body weight [34]) after transpulmonary thermodilution (PiCCO+, Pulsion SA). Hemodynamic variables, measured at baseline, and every hour until the end of the ventilation period (four hours): cardiac index, mean arterial pressure and plasma lactate level. Lung compliance was measured at baseline, and every hour until the end of the ventilation period (four hours), as a surrogate marker of lung injury severity.

Alveolar fluid clearance. Undiluted pulmonary edema fluid samples were also collected from animals at baseline and four hours later, as previously described[35,36]. Briefly, a soft 14-Fr-gauge suction catheter (PharmaPlast, Maersk Medical, Denmark) was advanced into a wedged position in a distal bronchus via an endotracheal tube. Pulmonary edema fluid was collected in a suction trap by gentle suction. All samples were centrifuged at 3,000 rpm at 4°C for 10 min in a refrigerated centrifuge. Supernatants was collected, and the total protein concentration in edema fluid was measured by the biuret method[35,36]. On the basis of the observation that the rate of clearance of edema fluid from the alveolar space is much faster than the rate of protein removal[37], the net AFC rate was calculated: Percent AFC = 100 x [1 - (initial edema protein/final edema total protein)]. This method has been validated in prior clinical and experimental studies [1,36,38–40]. All samples had a coefficient of variation less than 10%.

Lung mRNA and protein expression. The animals were sacrificed after the ventilation period and AFC measurements, and subjected to lung sampling for the assessment of protein expression levels. A Mem-PER Plus Membrane Protein Extraction Kit (Thermo Scientific, Weltham, MA) was used to extract membrane proteins of the right lung tissues of pig in each treatment group, following the manufacturer's instructions. Briefly, 50 mg left lung tissue were washed with cell wash solution, cut to pieces and homogenized in permeabilization buffer to an even suspension. The cells were scraped off, resuspended in Hites medium and centrifuged at 300 × g for 5 minutes. The cell pellet was washed with 3 mL of cell wash solution and centrifuged at 300 × g for 5 min. After the complete removal of the supernatant containing the cytosolic extract, the cells were resuspended in wash solution and centrifuged at 300 × g for 5 min. Again, the supernatant was discarded and permeabilization buffer was added to cell pellet. Then the homogeneous tissue and cell suspension in permeabilization buffer was obtained and incubated at 4°C with mixing for 20 min. Again, the pellet was centrifuged at 16,000 × g for 15 minutes and the supernatant was discarded. The pellet was resuspended in solution buffer and incubated at 4°C with mixing for 40 min. The suspension was centrifuged at 16,000 × g for 15 minutes at 4°C. Finally, the membrane protein contained in supernatant was obtained and further quantified in duplicate using pig α1-ENaC (MBS7218398, MyBiosource, San Diego, CA) α1-Na,K-ATPase (MBS9333154, MyBiosource, San Diego, CA) and AQP-5 (MBS9334691, MyBiosource, San Diego, CA) ELISA kits.

In parallel, total RNA was isolated from the left lung with an RNA extraction kit (RNeasy® Mini Kit, Qiagen, Valencia, CA). The gene expression levels of RAGE (mRNA Refseq NM_007425), α1-ENaC (NM_011324), α1-Na,K-ATPase (NM_144900), and AQP-5 (NM_009701) were assessed using semi-quantitative real-time polymerase chain reaction (PCR)(RT² Profiler™ PCR Array, Qiagen, Valencia, CA). Threshold levels of mRNA expression (ΔΔCt) were normalized to housekeeping gene, and the values represent the mean of triplicate samples ± standard deviation (SD). Data are representative of three independent observations. Housekeeping gene included the following: glyceraldehyde-3-phosphate dehydrogenase (GADPH).

Statistical Analysis. A computer-based randomization was applied to allocate animals to different study groups, thus minimizing inclusion bias. All measures (e.g. blood gas analyses, measurements of epithelial channels) were done by investigators blind to randomization groups, thus limiting analysis bias. Categorical data were expressed as numbers and percentages, and quantitative data as mean and standard deviation (SD) or median and interquartile range (IQR) according to statistical distribution. Statistical analyses of physiological parameters were carried out by two-way repeated measures analyses of variance (ANOVA) when appropriate. Kruskal-Wallis test with Bonferroni tests were used for pairwise comparisons. All analyses were performed using Prism 6 (Graphpad Software, La Jolla, CA). A $P < 0.05$ (two-sided) was considered statistically significant.

According to the principles of the 3Rs (Replacement, Reduction and Refinement), a limited number of animals was used (six animals under a given ventilator setting in each group) (Table 2) in order to detect a difference of 1 $mg.mL^{-1}$ (SD=0.5) in BAL protein concentration and of 5% per hour (SD=2.5) in net AFC rate 4 hours after mechanical ventilation, when considering alpha and beta risks of 5% (bilateral) and 10%, respectively. Statistical power of 90% was considered sufficient to allow multiple comparisons between groups.

RESULTS

Measurements of Alveolar Fluid Clearance. A significant between-group diference was detected in net AFC rates measured afer four hours of mechanical ventilation (P=0.03) (**Fig. 1**). The net AFC rate was decreased in HCl-injured piglets with intravenous sedation (8.4 ± 9.2 %/h) when compared with Sham animals (26 ± 4.3 %/h). By contrast, inhaled sedation with sevoflurane (23 ± 9.1 %/h) or isoflurane (19 ± 11 %/h) restored AFC in the HCl-injured animals.

Measurements of Physiological Dysfunction. In HCl-injured piglet with intravenous sedation, arterial oxygenation had deteriorated one hour after injury, as compared with sham animals, with gradual improvement by hour 4 in HCl-injured piglet with inhaled sedation (**Fig. 2**). Mean arterial oxygenation (PaO2/FiO2 ratios) therefore met clinical ARDS criteria on hour 1-2 in injured piglets, but not in injured piglets treated with sevoflurane or isoflurane, in which PaO2/FiO2 were similar to those seen in sham animals.

Alteration of the Alveolar Capillary Barrier. Alveolar-capillary barrier permeability, as assessed by the permeability index, showed a substantial increase in HCl-injured animals with intravenous sedation, as compared with sham animals. Inhaled sedation with either sevoflurane or isoflurane was efficient in normalising the permeability index after acid injury **(Fig. 3)**.

Two-way repeated-measurement ANOVA indicated a group time x group effect (P=0.04) with an incremental effect of HCl-induced injury on the course of extravascular lung water (EVLW), when compared with the absence of injury or with the use of inhaled sedation by sevoflurane or isoflurane (**Fig. 4**)

Lung expression of alveolar epithelial channels. The protein expression of AQP-5, Na,K,ATP-ase and ENaC in the lung was decreased in the HCl-injured piglets with intravenous sedation. In contrast, inhaled sedation by sevoflurane and isoflurane restored the the lung protein expression of Na,K,ATP-ase and ENaC compared to intravenous sedation (**Fig. 5**). No obvious changes were observed in lung AQP-5, Na,K,ATP-ase and ENaC mRNA levels in HCl-injured piglets with intravenous sedation and with sevoflurane or isoflurane (**Fig. 6)**

Effects of halogenated agents on respiratory and hemodynamic variables. The effets of both sevoflurane and isoflurane on respiratory and hemodynamic variables were summarized in the supplemental content.

DISCUSSION

This study reports that the use of inhaled sedation with both sevoflurane and isoflurane compared to intravenous sedation improves arterial oxygenation and alveolar fluid clearance in an experimental model of alveolar injury. This improvement is associated with a restoration of protein level of epithelial channels.

Growing preclinical evidence suggests that inhaled sedation by sevoflurane or isoflurane may possess important lung-protective effects mediated via mechanisms that could be very

relevant to the pathogenesis and resolution of ARDS, although some uncertainty persists [41]. *In vitro*, sevoflurane reduced the secretion of inflammatory mediators and the chemotactic activity and adherence of neutrophils in cultured alveolar epithelial cells after lipopolysaccharide (LPS) challenge [42,43], and alveolar macrophages treated with sevoflurane after LPS had increased phosphorylation of the extracellular-regulated kinase, an anti-inflammatory and anti-apoptotic kinase [44,45]. *In vivo*, studies in various mouse, rat and pig models of ARDS found that isoflurane and sevoflurane reduced alveolar and systemic levels of proinflammatory cytokines [26,46–49]. Inhaled sedation was also associated with improved arterial oxygenation and decreased lung alveolar edema in experimental ARDS [49,50]. In particular, isoflurane was able to restore epithelial tight junction integrity in a double-hit mouse model of nebulised LPS plus ventilator-induced lung injury [23], and sevoflurane may have protective effects on some mechanisms of transepithelial fluid transport *in vitro* and *in vivo* [20,46].

Currently, at least two large trials are enrolling patients with ARDS to assess the effects of inhaled sedation on major clinical outcomes. The Canadian Sedating with Volatile Anesthetics Critically Ill COVID-19 Patients in ICU: Effects On Ventilatory Parameters And Survival (SAVE-ICU) trial is a multicentre, open-label, pragmatic, randomised controlled trial that aims at randomising 752 mechanically ventilated patients with hypoxemic acute respiratory failure and proven or suspected COVID-19 to either intravenous sedation (with any sedation supplied by the participating hospital) or inhaled sedation with isoflurane or sevoflurane, depending on the availability of both drugs (ClinicalTrials.gov: NCT04415060). Primary outcome measures will be hospital mortality, ventilator-free days and ICU-free days at day 30, and quality of life at 3 and 12 months after discharge. In parallel, the French Sevoflurane for Sedation in ARDS (SESAR) trial aims at recruiting a total of 700 patients within 24 h of moderate-severe ARDS onset (PaO_2/FiO_2 <150 mmHg under a positive end-expiratory pressure of at least 8 cmH_2O) to evaluate whether sedation with inhaled sevoflurane (administered through the Sedaconda-ACD-S device) will increase the number of ventilator-free days through day 28, as defined as the number of days alive and off the ventilator at 28 days (thereby considering death as a competing event) (primary outcome) and decrease all-cause 90-day mortality (key secondary outcome), compared to a sedation strategy of intravenous propofol (ClinicalTrials.gov: NCT04235608). Findings from the

SAVE-ICU and SESAR trials will also be invaluable to inform the impact of inhaled sedation on neurocognitive function and long-term outcomes, in addition to contributing to better understanding of the potential clinical benefits of halogenated agents for ICU sedation. Meanwhile, although this sedation strategy is already being applied routinely in some centres, a recent panel of experts suggested that inhaled sedation with isoflurane or sevoflurane could be considered as a second or third-line strategy (propofol being the first line) within an "ABCDEF-R" bundle (R for Respiratory-drive-control) for patients with ARDS [51].

Nevertheless, large-scale studies are urgently awaited to further confirm the efficacy and safety of inhaled ICU sedation. The phase III multicentre randomised controlled SEDACONDA trial found that isoflurane is efficacious as a sole sedative and non-inferior to propofol in maintaining targeted sedation levels [15]. This trial is the largest trial of inhaled sedation that has been completed to date, with 301 adult patients under mechanical ventilation enrolled across 21 centres in Germany and three centres in Slovenia. It will also allow pre-planned analyses in patients with acute respiratory failure/ARDS and evaluation of long-term neuropsychological effects (up to one year after randomisation).

Using halogenated agents for ICU sedation is gaining popularity, and a 2019 survey of French ICUs highlighted that 80% of respondents were "satisfied or very satisfied" with the technique [52]. In this declarative survey, the main indications of inhaled sedation were severe asthma or bronchospasm, ARDS, and failure of intravenous sedation. However, most of them had only used inhaled sedation for <5 years and in <20 patients per year, and the main reasons for not using inhaled sedation included the unavailability of the device (40% of responses) and lack of familiarity with the technique (35% of responses). Overall, almost 75% of respondents answered that inhaled sedation was probably a seducing and viable alternative to intravenous sedation, thus prompting further diffusion and evaluation of this strategy, the pursuit of continuous efforts to specifically train ICU staff in charge of sedation, and efforts to further simplify the set-up and use of systems dedicated to inhaled sedation, such as the Sedaconda-ACD and the Mirus

Our study has some potential limitations. First, one of the factors limiting the clinical translation of preclinical findings is the limitations of *in vivo* disease models, but animal

experiments remain essential to understanding the fundamental mechanisms underlying the onset of diseases and to discovering improved methods to preventing, diagnosing and treating them. Second, we limited our evaluation at hour 4 after injury that only allowed to collect parameters during the early phase of ARDS and not assess later time-points. Nevertheless our experimental model of ARDS in piglets has significant advantages compared to existing ones including a rapid onset (within 1 h in general), good reproducibility and stability over time and a low mortality rate. Third, we did not set up exactly the same lines on the ventilatory between the group. Indeed piglets received inhaled sedation had the Sedaconda-ACD whearas other piglet had an simple HFE filter. This point could change rheological properties of fluid and impact the findings. Nevertheless same differences on line exist for mecanical ventilation in ARDS humans.

CONCLUSION

In conclusion, the use of inhaled sedation with both sevoflurane and isoflurane alleviated lung injury, improved arterial oxygenation, improved AFC, and restored lung epithelial channels expression in a translational piglet model of ARDS. Our findings should prompt further mechanistic studies of the pathways from inhaled sedation use to AFC and regulation of alveolar epithelial channels.

FIGURES

Figure 1. Inhaled sedation with sevoflurane or isoflurane improves alveolar fluid clearance. Values are reported as means±standard error of the mean.

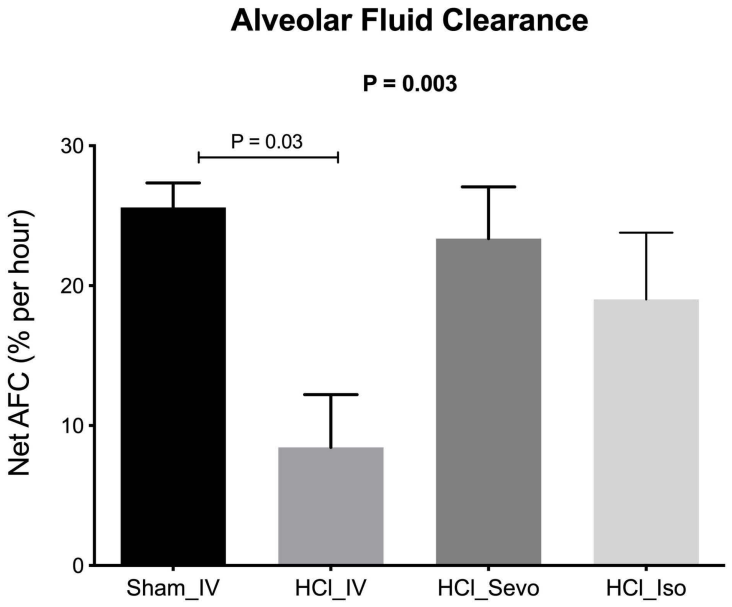

Figure 2. Inhaled sedation with sevoflurane or isoflurane improves arterial oxygenation. Values are reported as means±standard error of the mean.

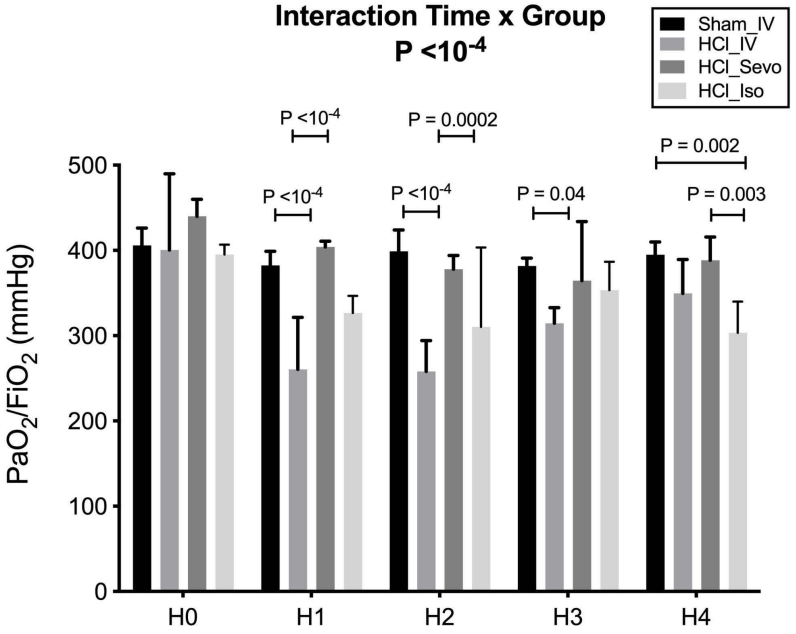

Figure 3. Inhaled sedation with sevoflurane or isoflurane decreases both alveolar permeability. Values are reported as means±standard error of the mean.

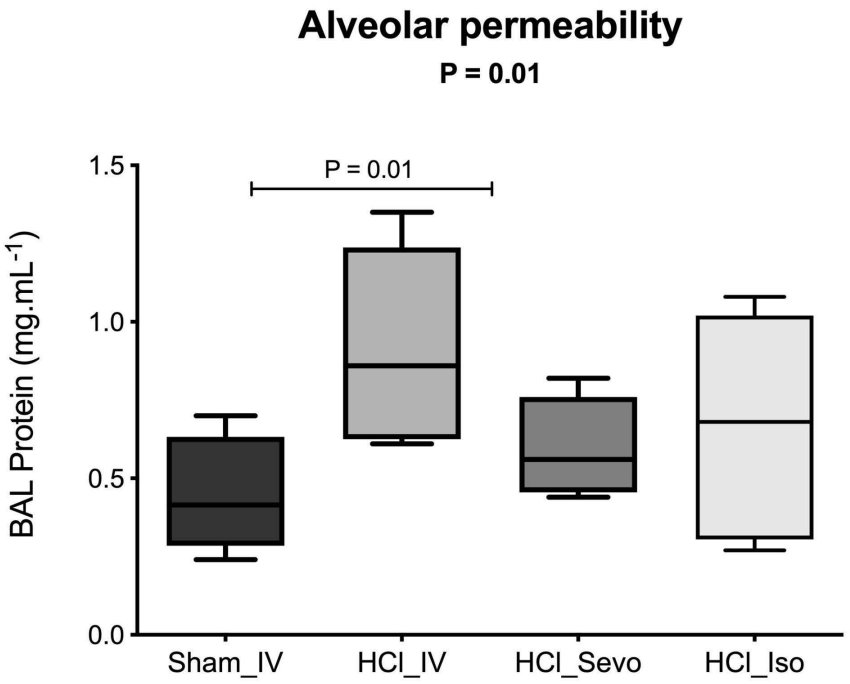

Figure 4. Inhaled sedation with sevoflurane or isoflurane decreases extravascular lung water. Values are reported as means±standard error of the mean.

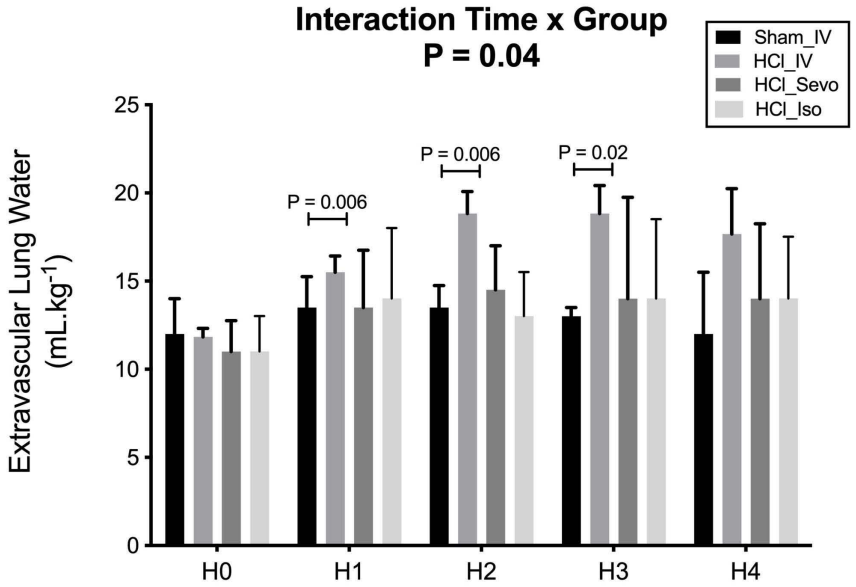

Figure 5. Inhaled sedation with sevoflurane or isoflurane restaures protein expression of epithelial channels AQP-5 (A), Na,K,ATP-ase (B) and ENaC (C). Values are reported as means±standard error of the mean.

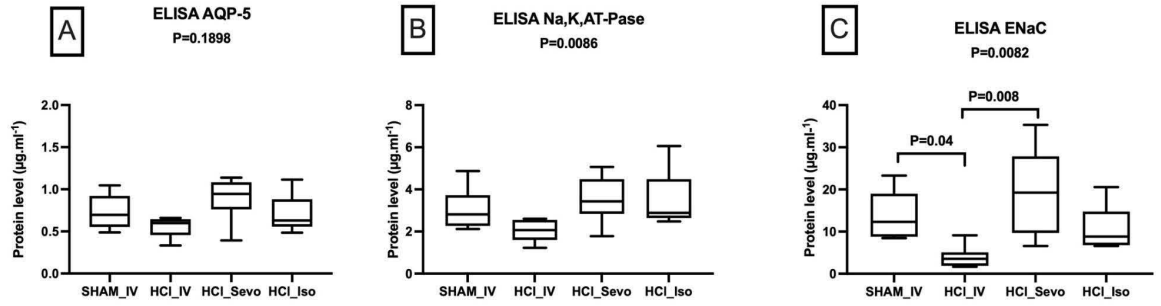

Figure 6. Inhaled sedation with sevoflurane or isoflurane has not effect on mRNA levels of AQP-5 (A), Na,K,ATP-ase (B) and ENaC (C). Values are reported as means±standard error of the mean.

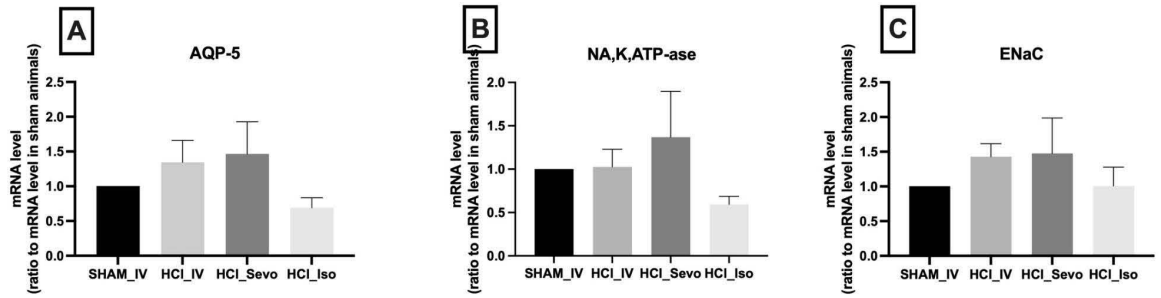

REFERENCES

1. Ware LB, Matthay MA. Alveolar fluid clearance is impaired in the majority of patients with acute lung injury and the acute respiratory distress syndrome. Am J Respir Crit Care Med. 2001;163: 1376–1383.

2. Matthay MA. Resolution of pulmonary edema. Thirty years of progress. Am J Respir Crit Care Med. 2014;189: 1301–1308.

3. Matthay MA, Folkesson HG, Clerici C. Lung epithelial fluid transport and the resolution of pulmonary edema. Physiol Rev. 2002;82: 569–600.

4. Dobbs LG, Gonzalez R, Matthay MA, Carter EP, Allen L, Verkman AS. Highly water-permeable type I alveolar epithelial cells confer high water permeability between the airspace and vasculature in rat lung. Proc Natl Acad Sci U S A. 1998;95: 2991–2996.

5. De Conno E, Steurer MP, Wittlinger M, Zalunardo MP, Weder W, Schneiter D, et al. Anesthetic-induced improvement of the inflammatory response to one-lung ventilation. Anesthesiology. 2009;110: 1316–1326.

6. Uhlig C, Bluth T, Schwarz K, Deckert S, Heinrich L, De Hert S, et al. Effects of Volatile Anesthetics on Mortality and Postoperative Pulmonary and Other Complications in Patients Undergoing SurgeryA Systematic Review and Meta-analysis. Anesthesiology: The Journal of the American Society of Anesthesiologists. 2016;124: 1230–1245.

7. Campagna JA, Miller KW, Forman SA. Mechanisms of actions of inhaled anesthetics. N Engl J Med. 2003;348: 2110–2124.

8. Dikmen Y, Eminoglu E, Salihoglu Z, Demiroluk S. Pulmonary mechanics during isoflurane, sevoflurane and desflurane anaesthesia. Anaesthesia. 2003;58: 745–748.

9. Hert SGD, De Hert SG, Van der Linden PJ, Cromheecke S, Meeus R, ten Broecke PW, et al. Choice of Primary Anesthetic Regimen Can Influence Intensive Care Unit Length of Stay after Coronary Surgery with Cardiopulmonary Bypass. Anesthesiology. 2004. pp. 9–20. doi:10.1097/00000542-200407000-00005

10. Uhlig C, Bluth T, Schwarz K, Deckert S, Heinrich L, De Hert S, et al. Effects of Volatile Anesthetics on Mortality and Postoperative Pulmonary and Other Complications in Patients Undergoing Surgery. Anesthesiology. 2016. pp. 1230–1245. doi:10.1097/aln.0000000000001120

11. Hashiguchi H, Morooka H, Miyoshi H, Matsumoto M, Koji T, Sumikawa K. Isoflurane Protects Renal Function Against Ischemia and Reperfusion Through Inhibition of Protein Kinases, JNK and ERK. Anesthesia & Analgesia. 2005. pp. 1584–1589. doi:10.1213/01.ane.0000184044.51749.b8

12. Fukazawa K, Lee HT. Volatile anesthetics and AKI: risks, mechanisms, and a potential therapeutic window. J Am Soc Nephrol. 2014;25: 884–892.

13. Obal D, Rascher K, Favoccia C, Dettwiler S, Schlack W. Post-conditioning by a short

administration of desflurane reduced renal reperfusion injury after differing of ischaemia times in rats. Br J Anaesth. 2006;97: 783–791.

14. Lv X, Yang L, Tao K, Liu Y, Yang T, Chen G, et al. Isoflurane preconditioning at clinically relevant doses induce protective effects of heme oxygenase-1 on hepatic ischemia reperfusion in rats. BMC Gastroenterol. 2011;11: 31.

15. Sakai H, Sheng H, Yates RB, Ishida K, Pearlstein RD, Warner DS. Isoflurane Provides Long-term Protection against Focal Cerebral Ischemia in the Rat. Anesthesiology. 2007. pp. 92–99. doi:10.1097/00000542-200701000-00017

16. Jerath A, Beattie SW, Chandy T, Karski J, Djaiani G, Rao V, et al. Volatile-based short-term sedation in cardiac surgical patients: a prospective randomized controlled trial. Crit Care Med. 2015;43: 1062–1069.

17. Jerath A, Parotto M, Wasowicz M, Ferguson ND. Volatile Anesthetics. Is a New Player Emerging in Critical Care Sedation? Am J Respir Crit Care Med. 2016;193: 1202–1212.

18. Perbet S, Bourdeaux D, Sautou V, Pereira B, Chabanne R, Constantin JM, et al. A pharmacokinetic study of 48-hour sevoflurane inhalation using a disposable delivery system (AnaConDa®) in ICU patients. Minerva Anestesiol. 2014;80: 655–665.

19. Mesnil M, Capdevila X, Bringuier S, Trine P-O, Falquet Y, Charbit J, et al. Long-term sedation in intensive care unit: a randomized comparison between inhaled sevoflurane and intravenous propofol or midazolam. Intensive Care Med. 2011;37: 933–941.

20. Schläpfer M, Leutert AC, Voigtsberger S, Lachmann RA, Booy C, Beck-Schimmer B. Sevoflurane reduces severity of acute lung injury possibly by impairing formation of alveolar oedema. Clin Exp Immunol. 2012;168: 125–134.

21. Voigtsberger S, Lachmann RA, Leutert AC, Schläpfer M, Booy C, Reyes L, et al. Sevoflurane Ameliorates Gas Exchange and Attenuates Lung Damage in Experimental Lipopolysaccharide-induced Lung Injury. Anesthesiology. 2009. pp. 1238–1248. doi:10.1097/aln.0b013e3181bdf857

22. Steurer M, Schläpfer M, Steurer M, Roth Z'graggen B, Booy C, Reyes L, et al. The volatile anaesthetic sevoflurane attenuates lipopolysaccharide-induced injury in alveolar macrophages. Clinical & Experimental Immunology. 2009. pp. 224–230. doi:10.1111/j.1365-2249.2008.03807.x

23. Englert JA, Macias AA, Amador-Munoz D, Pinilla Vera M, Isabelle C, Guan J, et al. Isoflurane Ameliorates Acute Lung Injury by Preserving Epithelial Tight Junction Integrity. Anesthesiology. 2015;123: 377–388.

24. Li QF, Zhu YS, Jiang H, Xu H, Sun Y. Isoflurane preconditioning ameliorates endotoxin-induced acute lung injury and mortality in rats. Anesth Analg. 2009;109: 1591–1597.

25. Reutershan J, Chang D, Hayes JK, Ley K. Role of a Reduction of Cytokine Levels in Isoflurane-mediated Protection from Endotoxin-induced Lung Injury. Anesthesiology. 2006. pp. 1280–1281. doi:10.1097/00000542-200612000-00037

26. Du X, Jiang C, Lv Y, Dull RO, Zhao Y-Y, Schwartz DE, et al. Isoflurane promotes phagocytosis of apoptotic neutrophils through AMPK-mediated ADAM17/Mer signaling. PLoS One. 2017;12: e0180213.

27. Blondonnet R, Paquette B, Audard J, Guler R, Roman F-X, Zhai R, et al. Halogenated Agent Delivery in Porcine Model of Acute Respiratory Distress Syndrome via an Intensive Care Unit Type Device. J Vis Exp. 2020. doi:10.3791/61644

28. Ambrosio AM, Luo R, Fantoni DT, Gutierres C, Lu Q, Gu W-J, et al. Effects of positive end-expiratory pressure titration and recruitment maneuver on lung inflammation and hyperinflation in experimental acid aspiration-induced lung injury. Anesthesiology. 2012;117: 1322–1334.

29. Sackey PV, Martling C-R, Granath F, Radell PJ. Prolonged isoflurane sedation of intensive care unit patients with the Anesthetic Conserving Device. Crit Care Med. 2004;32: 2241–2246.

30. Jabaudon M, Boucher P, Imhoff E, Chabanne R, Faure J-S, Roszyk L, et al. Sevoflurane for Sedation in Acute Respiratory Distress Syndrome. A Randomized Controlled Pilot Study. Am J Respir Crit Care Med. 2017;195: 792–800.

31. Blanchard F, Perbet S, James A, Verdonck F, Godet T, Bazin J-E, et al. Minimal alveolar concentration for deep sedation (MAC-DS) in intensive care unit patients sedated with sevoflurane: A physiological study. Anaesth Crit Care Pain Med. 2020. doi:10.1016/j.accpm.2020.04.002

32. Marumo CK, Otsuki DA, Fantoni DT, Margarido CB, Ambrósio AM, Pelosi P, et al. Hemodynamic effects of PEEP in a porcine model of HCl-induced mild acute lung injury. Acta Anaesthesiol Scand. 2009;53: 190–202.

33. Matute-Bello G, Downey G, Moore BB, Groshong SD, Matthay MA, Slutsky AS, et al. An official American Thoracic Society workshop report: features and measurements of experimental acute lung injury in animals. Am J Respir Cell Mol Biol. 2011;44: 725–738.

34. Jozwiak M, Teboul J-L, Monnet X. Extravascular lung water in critical care: recent advances and clinical applications. Ann Intensive Care. 2015;5: 38.

35. Constantin J-M, Cayot-Constantin S, Roszyk L, Futier E, Sapin V, Dastugue B, et al. Response to recruitment maneuver influences net alveolar fluid clearance in acute respiratory distress syndrome. Anesthesiology. 2007;106: 944–951.

36. Matthay MA, Wiener-Kronish JP. Intact epithelial barrier function is critical for the resolution of alveolar edema in humans. Am Rev Respir Dis. 1990;142: 1250–1257.

37. Berthiaume Y, Staub NC, Matthay MA. Beta-adrenergic agonists increase lung liquid clearance in anesthetized sheep. J Clin Invest. 1987;79: 335–343.

38. Verghese GM, Ware LB, Matthay BA, Matthay MA. Alveolar epithelial fluid transport and the resolution of clinically severe hydrostatic pulmonary edema. J Appl Physiol. 1999;87: 1301–1312.

39. Sakuma T, Okaniwa G, Nakada T, Nishimura T, Fujimura S, Matthay MA. Alveolar fluid clearance in the resected human lung. Am J Respir Crit Care Med. 1994;150: 305–310.

40. Ware LB, Golden JA, Finkbeiner WE, Matthay MA. Alveolar epithelial fluid transport capacity in reperfusion lung injury after lung transplantation. Am J Respir Crit Care Med. 1999;159: 980–988.

41. O'Gara B, Talmor D. Lung protective properties of the volatile anesthetics. Intensive Care Med. 2016 [cited 19 Jul 2016]. doi:10.1007/s00134-016-4429-x

42. Suter D, Spahn DR, Blumenthal S, Reyes L, Booy C, Z'graggen BR, et al. The immunomodulatory effect of sevoflurane in endotoxin-injured alveolar epithelial cells. Anesth Analg. 2007;104: 638–645.

43. Yue T, Roth Z'graggen B, Blumenthal S, Neff SB, Reyes L, Booy C, et al. Postconditioning with a volatile anaesthetic in alveolar epithelial cells in vitro. Eur Respir J. 2008;31: 118–125.

44. Steurer M, Schläpfer M, Steurer M, Z'graggen BR, Booy C, Reyes L, et al. The volatile anaesthetic sevoflurane attenuates lipopolysaccharide-induced injury in alveolar macrophages. Clin Exp Immunol. 2009;155: 224–230.

45. Kim S-H, Li M, Pyeon T-H, So K-Y, Kwak S-H. The volatile anesthetic sevoflurane attenuates ventilator-induced lung injury through inhibition of ERK1/2 and Akt signal transduction. Korean J Anesthesiol. 2015;68: 62–69.

46. Fortis S, Spieth PM, Lu W-Y, Parotto M, Haitsma JJ, Slutsky AS, et al. Effects of anesthetic regimes on inflammatory responses in a rat model of acute lung injury. Intensive Care Med. 2012;38: 1548–1555.

47. Ohsumi A, Marseu K, Slinger P, McRae K, Kim H, Guan Z, et al. Sevoflurane Attenuates Ischemia-Reperfusion Injury in a Rat Lung Transplantation Model. Ann Thorac Surg. 2017;103: 1578–1586.

48. Voigtsberger S, Lachmann RA, Leutert AC, Schläpfer M, Booy C, Reyes L, et al. Sevoflurane ameliorates gas exchange and attenuates lung damage in experimental lipopolysaccharide-induced lung injury. Anesthesiology. 2009;111: 1238–1248.

49. Ferrando C, Aguilar G, Piqueras L, Soro M, Moreno J, Belda FJ. Sevoflurane, but not propofol, reduces the lung inflammatory response and improves oxygenation in an acute respiratory distress syndrome model: A randomised laboratory study. Eur J Anaesthesiol. 2013;30: 455–463.

50. Kellner P, Müller M, Piegeler T, Eugster P, Booy C, Schläpfer M, et al. Sevoflurane Abolishes Oxygenation Impairment in a Long-Term Rat Model of Acute Lung Injury. Anesth Analg. 2017;124: 194–203.

51. Chanques G, Constantin J-M, Devlin JW, Ely EW, Fraser GL, Gélinas C, et al. Analgesia and sedation in patients with ARDS. Intensive Care Med. 2020;46: 2342–2356.

52. Blondonnet R, Quinson A, Lambert C, Audard J, Godet T, Zhai R, et al. Use of volatile agents for sedation in the intensive care unit: A national survey in France. PLoS One. 2021;16: e0249889.

05. Perspectives and conclusion

After years of research and numerous negative trials, there are, to date, only a few therapies that have shown a reduction in mortality in ARDS patients[14,15,244], and new trials have failed to confirm the interest of some of these therapies[245–248]. Taken together with all of the results from the literature already published on the subject, there is an increasing interest in the use of inhaled sedation in intensive care. Current evidence supports a safe profile for the use of inhaled sedation in intensive care patients. Nevertheless, the description of the precise physio-pathological mechanisms that can explain the beneficial effects, require the pursuit of translational research with the implementation of new clinical studies and experimental studies with *in vivo* and *in vitro* models.

The main objective of this thesis project, as mentioned in its title, is to explore sevoflurane effects by translational *in vivo* and *in vitro* models and its potential mechanistic. Nevertheless, literature reviews during this thesis project were very meaningful and permitted the established basis before the beginning of the experimental project. Our review of inhaled sedation (**Study #1**) summarized the pharmacological basis and practical aspects of the use of volatile anesthetics for ICU sedation, and also reviewed and discussed available evidence which highlighted the huge potential and increasing acceptance in intensive care as sedative agents. This review has also permitted us to conceptualize experimental projects which reflect the reality of intensive care settings in a translational research perspective.

Following this first review, our second review on preclinical ARDS models (**Study #2**) in which we had the chance to work with the Pr. Matute-Bello (the first author of an important review highlighted and has given systematic guidelines for experimental animal models of ARDS[249], summarized the strengths and limitations of the available models until today. This review may help future experimental designers to choose the adequate model for

their research objective, hopefully along with the acquisition of granular clinical, physiological, and biological data within clinical studies, lead to perspectives of identifying new drug targets, developing targeted therapies, or moreover the development of personalized medicine and predictive medicine strategies which may deeply improve patient outcomes in ARDS.

Our investigation of alveolar re-epithelization and the RAGE role in the alveolar epithelial wound repair in A549 cell models (**Study #3**), this study underlying the activation of RAGE by HMGB1 and AGEs promote in vitro wound healing of human alveolar epithelial cells in a RAGE-dependent manner with evidence which supports that this effect was at least in a part by increased cell migration and proliferation following RAGE activation. Those discoveries, though need to be precisely investigated via mechanistic investigation, encourage us to continue to clarify the involvement of RAGE during lung injury, especially on mechanistic pathways.

As one of the principal studies to achieve the research objectives of this thesis project, our study on the effects of sevoflurane on lung epithelial permeability in both *in vitro* and *in vivo* mice models (**Study #4**) has shown, besides numerous results which are in line with previous results reported in other studies such as impaired arterial oxygenation, alveolar inflammation, histological evidence of lung tissue injury, and the extent of lung edema[238–240,243], protective effects of sevoflurane on lung epithelial permeability and epithelial junction proteins in experimental models of sterile ARDS and mechanistically explain this effects, at least in part by the inhibition of increased RhoA activity and pMLC as well as actin cytoskeleton rearrangement following lung epithelial injury. Also, in this study, we observed that $RAGE^{-/-}$ mice had better oxygenation levels, decreased lung permeability, and improved inflammatory response compared to littermate wild-type animals, this discovery is in line

with our previous research, in which RAGE inhibition may protect mice from an acute lung injury[152,153]. $RAGE^{-/-}$ mice received the same benefits from sevoflurane as littermate wild-type animals, however, despite RAP treatment in our *in vitro* cell model showing decreasing effects on cytomix-induced RhoA activation, the use of RAP alleviated the beneficial effects of sevoflurane on decreased permeability and cytoskeleton rearrangement.

Finally, our study on the effects of sevoflurane but also isoflurane on alveolar fluid clearance in an *in vivo* piglet model of ARDS (**Study #5**) confirmed the effects of sevoflurane and isoflurane on improved arterial oxygenation and alveolar-capillary permeability restoration after acid-induced acute lung injury. This study has also shown both sevoflurane and isoflurane effects on the improvement of AFC and this improvement was shown to be associated with restored lung protein levels of Na, K, ATPase, and ENaC. These discoveries on the improvement of AFC and restored lung epithelial channels take steps of advancement on the mechanistic research of halogenated agents' protective effects on the resolution of lung edema during ARDS[239–241]. Which encourages further research focusing on the sevoflurane effects on the AFC and the regulation of epithelial channels with a more precise mechanism.

Taken together of all of our results with the literature already published in this field, our studies, with results found in both *in vitro* and two different *in vivo* models, explain more precisely the protective effects of halogenated agents and new revelation of its potential mechanism, and hence support the high interest in the use of inhaled sedation in intensive care for ARDS patients. However, despite all efforts in our studies to figure out the precise mechanism of halogenated agents' protective effects on improved arterial oxygenation, improved inflammation, alveolar epithelial permeability, epithelial junction, restoration of AFC, and epithelial channel regulation, However, there is still a strong need in the future to

clarify more precisely different mechanisms which may be involved in halogenated agents' beneficial effects.

First of all, despite our advancements in this research project, the mediating role of RhoA/pMLC pathway in acute lung injury and sevoflurane effects on it, the mechanism is not wholly understood, in other studies, the upregulation of Rho kinase (ROCKI and ROCKII) was also reported in acute lung injury[194,195] indicates the role and involvement of ROCKI and ROCKII, and its possible link with sevoflurane need to be better discussed in acute lung injury. The Rho activation was observed with induced increased endothelial permeability but also inflammation[192,250,251], in addition to its involvement in the ROS formation, suggest the mechanistic link between the RhoA/ROCK activation and the induction of inflammation should also be clarified. Furthermore, the mechanistic discussion in this thesis work was limited to the investigation of Myosin Light Chain Kinase(MLCK) which is straightly involved in the RhoA/ROCK/pMLC pathway, recent studies reported its involvement in acute lung injury and the disassembly of epithelial junctions[191,192]. Moreover, some studies reported, from a genetic view, its link to the risk of development of ARDS[252,253]. RhoA/ROCK pathway was also reported to be involved in the regulation of epithelial channels of water transport, including its involvement in the downregulation of Na, K-ATPase[254,255], and ENAC[256], indicating a possible link between effects of sevoflurane on the restored epithelial channels and RhoA/ROCK regulation. Taken together, further investigations of RhoA/ROCK pathways in ARDS along with the encouraging effects observed in our study may have high potential therapeutic interest[207].

Besides sevoflurane effects via the RhoA/pMLC/F-actin pathway that our project focused on, other possible mechanistic pathways are involved in the mechanism of halogenated agents. Numerous studies suggest the mediation of halogenated agents' effects

by the PI3K/Akt signaling pathway[196,257–260]. Moreover, recent studies suggest the regulator role of sevoflurane on autophagy[261,262] and apoptosis[258,263], two downstream cell signaling activity of activation of this pathway. other studies suggest also the regulator role of sevoflurane/isoflurane but on wnt/beta-catenin pathway[264,265]. However, although these cell death mechanisms are also described in the altered epithelial barrier function in ARDS, no studies have investigated the potential effects of sevoflurane on these cell survival and cell death pathways, such as autophagy and apoptosis, in a suitable model of pulmonary alveolar epithelial injury. Further studies of halogenated agents' effects may explain whether they protect alveolar epithelial integrity through improved cell survival from epithelial injury.

Another important mechanistic factor for further studies is RAGE, which is also directly involved with the Rho pathway[266,267], PI3K/Akt pathway[268,269]. Although the mediation of sevoflurane protective effects by RAGE was just partially revealed in our *in vitro* and *in vivo* models(**Study #4**), our study revealed the protective effect on acute lung injury of RAGE deletion. Associated with our discoveries about RAGE modulation effects on epithelial wound repair including cell proliferation and migration, our project indicates the critical role of RAGE on epithelial integrity and its repair. Furthermore, our in vivo $RAGE^{-/-}$ animal model showed a solid and robust performance of its high translational potential for further studies which, along with *in vitro* studies, may better explore this pathway.

Our study(**Study #2**) discussed different models with their strengths and limits and pointed out the limits of monolayer cell culture. Additionally, in our studies using A549 cell lines and MLE-12 cell lines, results remain in a limited reproduction of the alveolar environment. Furthermore, some results showed on MLE-12 cell lines were not in line with those obtained *in vivo*, some studies observed the different effects of sevoflurane on cell

proliferation[270,271], future validation studies on the primary mouse or human alveolar epithelial cells, or even more like organoids. lung-on-a-chip, *ex vivo* human lungs are warranted[272].

The ultimate objective of all those preclinical translational studies is no doubt to be able to contribute to clinical advancements from a translational view. In spite of the abundance of data on the benefits of using inhaled sedation in the operating bloc, there exists few solid clinical data about the benefit of inhaled sedation in intensive care units with ARDS patients. Our first pilot study has shown that an inhaled sevoflurane sedation strategy compared to intravenous sedation in patients with moderate to severe ARDS resulted in improved oxygenation and decreased plasma and alveolar concentrations of pro-inflammatory cytokines[77]. Recently, a large multicenter prospective randomized trial SESAR (Sevoflurane for Sedation in Acute Respiratory Distress Syndrome, ClinicalTrials.gov Identifier: NCT04235608) coordinated by our clinic team has been started in 2019. The principal objective of this trial is to assess the efficacy of sedation with inhaled sevoflurane in improving a composite outcome of mortality and ventilator-free time at 28 days in 700 patients with moderate-severe ARDS in comparison to a control group receiving intravenous sedation with propofol. Another multicenter randomized trial SAVE-ICU (SedAting With Volatile Anesthetics Critically Ill COVID-19 Patients in ICU: Effects On Ventilatory Parameters And Survival, ClinicalTrials.gov Identifier: NCT04415060), aims to assess the outcome of hospital mortality and ventilator-free time of patients with COVID-19 disease or suffering from hypoxic lung failure receiving sevoflurane or isoflurane.

The difficulties in finding new therapies are probably partly explained by the heterogeneity of this syndrome with the existence of distinct clinical and biological-molecular profiles, and having different responses to different therapies[273,274]. It is now recognized that patient response to candidate therapies largely varies because of the

underlying biology, even in patients with a shared etiology, such as COVID-19[45]. It may now be possible to identify ARDS subtypes (or phenotypes) that could confer different responses to therapy, in addition to identifying patients with distinct prognosis[275]. However, currently, no consensus on the most appropriate approach to understanding ARDS heterogeneity exists, and significant gaps remain to develop more personalized therapeutic approaches for ARDS[276]. In order to respond to the need for the identification of ARDS phenotype and endotype toward personalized medicine strategies. The first clinical study evaluating a point-of-care assay to prospectively identify hyper- and hypo-inflammatory phenotypes[34] in patients with ARDS and hypoxemic acute respiratory failure is started since 2019 (ClinicalTrials.gov Identifier: NCT04009330), and the preliminary results in patients with COVID-19 have been published[277]. Furthermore, In the SESAR trial, to find out if there are different profiles between patients regarding the response to sevoflurane. The two patient phenotypes described by Calfee et al.[34] will be tested in a SESAR ancillary study to find out if there are different profiles between patients regarding the response to sevoflurane.

ARDS phenotypes are not necessarily only biological but can also be morphological. During ARDS, patients have different prognosis and responses to therapies, which depends on whether the pulmonary involvement is focal or non-focal. Different profiles responding to mechanical ventilation and to different recruitment maneuvers have already been shown[278], with an impact on the future of patients, depending on the morphology of the lung involvement during ARDS. In order to better characterize the diffusion of halogenated agents according to the morphology of the pulmonary involvement, a study of the pharmacokinetics/pharmacodynamics of sevoflurane according to the morphology of the pulmonary involvement in patients with ARDS is currently undergoing. The results will make it possible to better characterize the administration of halogenated agents during ARDS. Finally, in order to try to describe the sub-phenotypes of ARDS and their potential

response to halogenated agents in experimental models, a systematic review of the literature and a meta-analysis of preclinical studies will be carried out.

Furthermore, in order to respond to the necessity of biomarkers development for the identification of ARDS phenotype and endotype, as suggested by Bos and Ware recently[35]. In the SESAR trial, patients' plasma concentrations of sRAGE will be assessed from biological samples taken from patients in the SESAR study (n=350 per group), at the time of inclusion (D0) and on D1, D2 , D4, D6 and D14 (or upon leaving intensive care if this occurs before) for the validation of sRAGE as a biomarker of epithelial injury and ARDS severity. Furthermore, plasmatic Angiopoietin-2 will be assessed as an endothelial injury biomarker and, plasmatic interleukin IL-6, IL-8, and tumor necrosis factor-receptor will be assessed as biomarkers of hyperinflammatory phenotype.

Additionally, measured sRAGE with the patient’s profile will be analyzed by inferential statistical methods to assess plasma sRAGE as a predictive and prognostic enrichment method in patients meeting the criteria for ARDS.

Since longitudinal sampling could provide additional insights into biological dynamics and treatment responses over time, a biological collection of plasma, alveolar, and urine samples of enrolled patients will be constructed, for future mechanistic and endotyping studies of the biological effects of sevoflurane. The whole blood will be collected for both genetic studies (e.g., evaluation of single nucleotide polymorphisms (SNPs), RNA sequencing (RNA-Seq)) and phenotypic characterization of macrophages using FACS.

All of those actual promising studies and future enviable studies, including preclinical and clinical studies, should finally make it possible to better understand the effects and mechanisms of halogenated agents, to better describe their place in therapeutic use, and to better develop future clinical studies on the effect of halogenated agents during ARDS, and to

establish future clinical trial enrichment which will be hopefully beneficial for patients who suffer from this syndrome.

6. References

1. Ashbaugh, D. G., Bigelow, D. B., Petty, T. L. & Levine, B. E. Acute respiratory distress in adults. *Lancet* **2**, 319–323 (1967).
2. Murray, J. F., Matthay, M. A., Luce, J. M. & Flick, M. R. An expanded definition of the adult respiratory distress syndrome. *Am. Rev. Respir. Dis.* **138**, 720–723 (1988).
3. Bellani, G. *et al.* Epidemiology, Patterns of Care, and Mortality for Patients With Acute Respiratory Distress Syndrome in Intensive Care Units in 50 Countries. *JAMA* **315**, 788–800 (2016).
4. Thompson, B. T., Chambers, R. C. & Liu, K. D. Acute Respiratory Distress Syndrome. *The New England journal of medicine* vol. 377 1904–1905 (2017).
5. Confalonieri, M., Salton, F. & Fabiano, F. Acute respiratory distress syndrome. *Eur. Respir. Rev.* **26**, (2017).
6. Lucas, R., Verin, A. D., Black, S. M. & Catravas, J. D. Regulators of endothelial and epithelial barrier integrity and function in acute lung injury. *Biochem. Pharmacol.* **77**, 1763–1772 (2009).
7. Lusuardi, M. *et al.* Role of surfactant in chronic obstructive pulmonary disease: therapeutic implications. *Respiration* **59 Suppl 1**, 28–32 (1992).
8. Huppert, L. A. & Matthay, M. A. Alveolar Fluid Clearance in Pathologically Relevant Conditions: In Vitro and In Vivo Models of Acute Respiratory Distress Syndrome. *Front. Immunol.* **8**, 371 (2017).
9. Vaughan, A. E. *et al.* Lineage-negative progenitors mobilize to regenerate lung epithelium after major injury. *Nature* **517**, 621–625 (2015).
10. Jansing, N. L. *et al.* Unbiased Quantitation of Alveolar Type II to Alveolar Type I Cell Transdifferentiation during Repair after Lung Injury in Mice. *Am. J. Respir. Cell Mol.*

Biol. **57**, 519–526 (2017).

11. Fan, E., Brodie, D. & Slutsky, A. S. Acute Respiratory Distress Syndrome: Advances in Diagnosis and Treatment. *JAMA* **319**, 698–710 (2018).
12. Acute Respiratory Distress Syndrome Network *et al.* Ventilation with lower tidal volumes as compared with traditional tidal volumes for acute lung injury and the acute respiratory distress syndrome. *N. Engl. J. Med.* **342**, 1301–1308 (2000).
13. Calfee, C. S. & Matthay, M. A. Nonventilatory treatments for acute lung injury and ARDS. *Chest* **131**, 913–920 (2007).
14. Papazian, L. *et al.* Neuromuscular blockers in early acute respiratory distress syndrome. *N. Engl. J. Med.* **363**, 1107–1116 (2010).
15. Guérin, C. *et al.* Prone positioning in severe acute respiratory distress syndrome. *N. Engl. J. Med.* **368**, 2159–2168 (2013).
16. Agarwal, R., Aggarwal, A. N. & Gupta, D. Role of noninvasive ventilation in acute lung injury/acute respiratory distress syndrome: a proportion meta-analysis. *Respir. Care* **55**, 1653–1660 (2010).
17. Caironi, P. *et al.* Lung opening and closing during ventilation of acute respiratory distress syndrome. *Am. J. Respir. Crit. Care Med.* **181**, 578–586 (2010).
18. Amato, M. B. P. *et al.* Driving pressure and survival in the acute respiratory distress syndrome. *N. Engl. J. Med.* **372**, 747–755 (2015).
19. Gattinoni, L. Ultra-protective ventilation and hypoxemia. *Crit. Care* **20**, 130 (2016).
20. Pelosi, P. *et al.* Recruitment and derecruitment during acute respiratory failure: an experimental study. *Am. J. Respir. Crit. Care Med.* **164**, 122–130 (2001).
21. Ricard, J. D., Dreyfuss, D. & Saumon, G. Ventilator-induced lung injury. *Eur. Respir. J. Suppl.* **42**, 2s–9s (2003).
22. Beitler, J. R., Malhotra, A. & Thompson, B. T. Ventilator-induced Lung Injury. *Clin.*

Chest Med. **37**, 633–646 (2016).

23. Dreyfuss, D. & Saumon, G. Ventilator-induced lung injury: lessons from experimental studies. *Am. J. Respir. Crit. Care Med.* **157**, 294–323 (1998).
24. Dreyfuss, D., Soler, P., Basset, G. & Saumon, G. High inflation pressure pulmonary edema. Respective effects of high airway pressure, high tidal volume, and positive end-expiratory pressure. *Am. Rev. Respir. Dis.* **137**, 1159–1164 (1988).
25. Bowton, D. L. & Kong, D. L. High tidal volume ventilation produces increased lung water in oleic acid-injured rabbit lungs. *Crit. Care Med.* **17**, 908–911 (1989).
26. Corbridge, T. C. *et al.* Adverse effects of large tidal volume and low PEEP in canine acid aspiration. *Am. Rev. Respir. Dis.* **142**, 311–315 (1990).
27. Attar, M. A. & Donn, S. M. Mechanisms of ventilator-induced lung injury in premature infants. *Semin. Neonatol.* **7**, 353–360 (2002).
28. Pinhu, L., Whitehead, T., Evans, T. & Griffiths, M. Ventilator-associated lung injury. *Lancet* **361**, 332–340 (2003).
29. Brower, R. G. *et al.* Higher versus lower positive end-expiratory pressures in patients with the acute respiratory distress syndrome. *N. Engl. J. Med.* **351**, 327–336 (2004).
30. Meade, M. O. *et al.* Ventilation strategy using low tidal volumes, recruitment maneuvers, and high positive end-expiratory pressure for acute lung injury and acute respiratory distress syndrome: a randomized controlled trial. *JAMA* **299**, 637–645 (2008).
31. Marra, A., Ely, E. W., Pandharipande, P. P. & Patel, M. B. The ABCDEF Bundle in Critical Care. *Crit. Care Clin.* **33**, 225–243 (2017).
32. Chanques, G. *et al.* Analgesia and sedation in patients with ARDS. *Intensive Care Med.* **46**, 2342–2356 (2020).
33. Thille, A. W. *et al.* Comparison of the Berlin definition for acute respiratory distress

syndrome with autopsy. *Am. J. Respir. Crit. Care Med.* **187**, 761–767 (2013).

34. Calfee, C. S. *et al.* Subphenotypes in acute respiratory distress syndrome: latent class analysis of data from two randomised controlled trials. *Lancet Respir Med* **2**, 611–620 (2014).
35. Bos, L. D. J. & Ware, L. B. Acute respiratory distress syndrome: causes, pathophysiology, and phenotypes. *Lancet* **400**, 1145–1156 (2022).
36. Bos, L. D., Martin-Loeches, I. & Schultz, M. J. ARDS: challenges in patient care and frontiers in research. *Eur. Respir. Rev.* **27**, (2018).
37. Prescott, H. C., Calfee, C. S., Thompson, B. T., Angus, D. C. & Liu, V. X. Toward Smarter Lumping and Smarter Splitting: Rethinking Strategies for Sepsis and Acute Respiratory Distress Syndrome Clinical Trial Design. *Am. J. Respir. Crit. Care Med.* **194**, 147–155 (2016).
38. Calfee, C. S. *et al.* Subphenotypes in acute respiratory distress syndrome: latent class analysis of data from two randomised controlled trials. *Lancet Respir Med* **2**, 611–620 (2014).
39. Famous, K. R. *et al.* Acute Respiratory Distress Syndrome Subphenotypes Respond Differently to Randomized Fluid Management Strategy. *Am. J. Respir. Crit. Care Med.* **195**, 331–338 (2017).
40. Sinha, P. *et al.* Development and validation of parsimonious algorithms to classify acute respiratory distress syndrome phenotypes: a secondary analysis of randomised controlled trials. *The Lancet Respiratory Medicine* vol. 8 247–257 Preprint at https://doi.org/10.1016/s2213-2600(19)30369-8 (2020).
41. Delucchi, K. *et al.* Stability of ARDS subphenotypes over time in two randomised controlled trials. *Thorax* (2018) doi:10.1136/thoraxjnl-2017-211090.
42. Sinha, P. *et al.* Latent class analysis-derived subphenotypes are generalisable to

observational cohorts of acute respiratory distress syndrome: a prospective study. *Thorax* **77**, 13–21 (2022).

43. Maddali, M. V. *et al.* Validation and utility of ARDS subphenotypes identified by machine-learning models using clinical data: an observational, multicohort, retrospective analysis. *Lancet Respir Med* (2022) doi:10.1016/S2213-2600(21)00461-6.
44. Sinha, P. *et al.* Latent class analysis of ARDS subphenotypes: a secondary analysis of the statins for acutely injured lungs from sepsis (SAILS) study. *Intensive Care Med.* (2018) doi:10.1007/s00134-018-5378-3.
45. Sinha, P. *et al.* Latent Class Analysis Reveals COVID-19-related Acute Respiratory Distress Syndrome Subgroups with Differential Responses to Corticosteroids. *Am. J. Respir. Crit. Care Med.* **204**, 1274–1285 (2021).
46. Calfee, C. S. *et al.* Acute respiratory distress syndrome subphenotypes and differential response to simvastatin: secondary analysis of a randomised controlled trial. *Lancet Respir Med* **6**, 691–698 (2018).
47. Shah, F. A. *et al.* A Research Agenda for Precision Medicine in Sepsis and Acute Respiratory Distress Syndrome: An Official American Thoracic Society Research Statement. *Am. J. Respir. Crit. Care Med.* **204**, 891–901 (2021).
48. Bos, L. D. J. *et al.* Towards a biological definition of ARDS: are treatable traits the solution? *Intensive Care Med Exp* **10**, 8 (2022).
49. Bos, L. D. J. *et al.* Precision medicine in acute respiratory distress syndrome: workshop report and recommendations for future research. *Eur. Respir. Rev.* **30**, (2021).
50. Harhay, M. O. *et al.* Contemporary strategies to improve clinical trial design for critical care research: insights from the First Critical Care Clinical Trialists Workshop. *Intensive Care Med.* **46**, 930–942 (2020).
51. Casey, J. D. *et al.* Use of pragmatic and explanatory trial designs in acute care research:

lessons from COVID-19. *Lancet Respir. Med.* (2022) doi:10.1016/S2213-2600(22)00044-3.

52. Weinert, C. R. & Calvin, A. D. Epidemiology of sedation and sedation adequacy for mechanically ventilated patients in a medical and surgical intensive care unit. *Crit. Care Med.* **35**, 393–401 (2007).
53. Baldwin, D. S. *et al.* Benzodiazepines: risks and benefits. A reconsideration. *J. Psychopharmacol.* **27**, 967–971 (2013).
54. Saraghi, M., Badner, V. M., Golden, L. R. & Hersh, E. V. Propofol: an overview of its risks and benefits. *Compend. Contin. Educ. Dent.* **34**, 252–258 (2013).
55. Jerath, A., Ferguson, N. D. & Cuthbertson, B. Inhalational volatile-based sedation for COVID-19 pneumonia and ARDS. *Intensive Care Med.* (2020) doi:10.1007/s00134-020-06154-8.
56. Campagna, J. A., Miller, K. W. & Forman, S. A. Mechanisms of actions of inhaled anesthetics. *N. Engl. J. Med.* **348**, 2110–2124 (2003).
57. Jerath, A., Parotto, M., Wasowicz, M. & Ferguson, N. D. Volatile Anesthetics. Is a New Player Emerging in Critical Care Sedation? *Am. J. Respir. Crit. Care Med.* **193**, 1202–1212 (2016).
58. Georgevici, A.-I. *et al.* Negative drift of sedation depth in critically ill patients receiving constant minimum alveolar concentration of isoflurane, sevoflurane, or desflurane: a randomized controlled trial. *Crit. Care* **25**, 141 (2021).
59. Sackey, P. V., Radell, P. J., Granath, F. & Martling, C. R. Bispectral index as a predictor of sedation depth during isoflurane or midazolam sedation in ICU patients. *Anaesth. Intensive Care* **35**, 348–356 (2007).
60. Blanchard, F. *et al.* Minimal alveolar concentration for deep sedation (MAC-DS) in intensive care unit patients sedated with sevoflurane: A physiological study. *Anaesth*

Crit Care Pain Med **39**, 429–434 (2020).

61. Weiser, T. G. *et al.* An estimation of the global volume of surgery: a modelling strategy based on available data. *Lancet* **372**, 139–144 (2008).
62. O'Gara, B. & Talmor, D. Lung protective properties of the volatile anesthetics. *Intensive Care Med.* **42**, 1487–1489 (2016).
63. Bellgardt, M. *et al.* Survival after long-term isoflurane sedation as opposed to intravenous sedation in critically ill surgical patients: Retrospective analysis. *Eur. J. Anaesthesiol.* **33**, 6–13 (2016).
64. Bisbal, M. *et al.* [Efficacy, safety and cost of sedation with sevoflurane in intensive care unit]. *Ann. Fr. Anesth. Reanim.* **30**, 335–341 (2011).
65. Perbet, S. *et al.* A pharmacokinetic study of 48-hour sevoflurane inhalation using a disposable delivery system (AnaConDa®) in ICU patients. *Minerva Anestesiol.* **80**, 655–665 (2014).
66. Soukup, J. *et al.* Efficiency and safety of inhalative sedation with sevoflurane in comparison to an intravenous sedation concept with propofol in intensive care patients: study protocol for a randomized controlled trial. *Trials* **13**, 135 (2012).
67. Mesnil, M. *et al.* Long-term sedation in intensive care unit: a randomized comparison between inhaled sevoflurane and intravenous propofol or midazolam. *Intensive Care Med.* **37**, 933–941 (2011).
68. Ferrando, C. *et al.* Sevoflurane, but not propofol, reduces the lung inflammatory response and improves oxygenation in an acute respiratory distress syndrome model: A randomised laboratory study. *Eur. J. Anaesthesiol.* **30**, 455–463 (2013).
69. Voigtsberger, S. *et al.* Sevoflurane ameliorates gas exchange and attenuates lung damage in experimental lipopolysaccharide-induced lung injury. *Anesthesiology* **111**, 1238–1248 (2009).

70. Schläpfer, M. *et al.* Sevoflurane reduces severity of acute lung injury possibly by impairing formation of alveolar oedema. *Clin. Exp. Immunol.* **168**, 125–134 (2012).

71. Suter, D. *et al.* The immunomodulatory effect of sevoflurane in endotoxin-injured alveolar epithelial cells. *Anesth. Analg.* **104**, 638–645 (2007).

72. Steurer, M. *et al.* The volatile anaesthetic sevoflurane attenuates lipopolysaccharide-induced injury in alveolar macrophages. *Clin. Exp. Immunol.* **155**, 224–230 (2009).

73. Watanabe, K. *et al.* Sevoflurane suppresses tumour necrosis factor-α-induced inflammatory responses in small airway epithelial cells after anoxia/reoxygenation. *Br. J. Anaesth.* **110**, 637–645 (2013).

74. Englert, J. A. *et al.* Isoflurane Ameliorates Acute Lung Injury by Preserving Epithelial Tight Junction Integrity. *Anesthesiology* **123**, 377–388 (2015).

75. Li, Q. F., Zhu, Y. S., Jiang, H., Xu, H. & Sun, Y. Isoflurane preconditioning ameliorates endotoxin-induced acute lung injury and mortality in rats. *Anesth. Analg.* **109**, 1591–1597 (2009).

76. Reutershan, J., Chang, D., Hayes, J. K. & Ley, K. Role of a Reduction of Cytokine Levels in Isoflurane-mediated Protection from Endotoxin-induced Lung Injury. *Anesthesiology* vol. 105 1280–1281 Preprint at https://doi.org/10.1097/00000542-200612000-00037 (2006).

77. Jabaudon, M. *et al.* Sevoflurane for Sedation in Acute Respiratory Distress Syndrome. A Randomized Controlled Pilot Study. *Am. J. Respir. Crit. Care Med.* **195**, 792–800 (2017).

78. Fritz, G. RAGE: a single receptor fits multiple ligands. *Trends Biochem. Sci.* **36**, 625–632 (2011).

79. Jangde, N., Ray, R. & Rai, V. RAGE and its ligands: from pathogenesis to therapeutics.

Crit. Rev. Biochem. Mol. Biol. **55**, 555–575 (2020).

80. Hanford, L. E. *et al.* Purification and characterization of mouse soluble receptor for advanced glycation end products (sRAGE). *J. Biol. Chem.* **279**, 50019–50024 (2004).
81. Mukherjee, T. K., Mukhopadhyay, S. & Hoidal, J. R. Implication of receptor for advanced glycation end product (RAGE) in pulmonary health and pathophysiology. *Respir. Physiol. Neurobiol.* **162**, 210–215 (2008).
82. Cheng, C. *et al.* Expression profiling of endogenous secretory receptor for advanced glycation end products in human organs. *Mod. Pathol.* **18**, 1385–1396 (2005).
83. Parkin, E. & Harris, B. A disintegrin and metalloproteinase (ADAM)-mediated ectodomain shedding of ADAM10. *J. Neurochem.* **108**, 1464–1479 (2009).
84. Raucci, A. *et al.* A soluble form of the receptor for advanced glycation endproducts (RAGE) is produced by proteolytic cleavage of the membrane-bound form by the sheddase a disintegrin and metalloprotease 10 (ADAM10). *FASEB J.* **22**, 3716–3727 (2008).
85. Zhang, L. *et al.* Receptor for advanced glycation end products is subjected to protein ectodomain shedding by metalloproteinases. *J. Biol. Chem.* **283**, 35507–35516 (2008).
86. Thorpe, S. R. & Baynes, J. W. Maillard reaction products in tissue proteins: new products and new perspectives. *Amino Acids* **25**, 275–281 (2003).
87. Yan, S. F. *et al.* The biology of RAGE and its ligands: Uncovering mechanisms at the heart of diabetes and its complications. *Curr. Diab. Rep.* **7**, 146–153 (2007).
88. Hofmann, M. A. *et al.* RAGE mediates a novel proinflammatory axis: a central cell surface receptor for S100/calgranulin polypeptides. *Cell* **97**, 889–901 (1999).
89. Schmidt, A. M., Yan, S. D., Yan, S. F. & Stern, D. M. The multiligand receptor RAGE as a progression factor amplifying immune and inflammatory responses. *J. Clin. Invest.* **108**, 949–955 (2001).

90. Bucciarelli, L. G. *et al.* RAGE is a multiligand receptor of the immunoglobulin superfamily: implications for homeostasis and chronic disease. *Cell. Mol. Life Sci.* **59**, 1117–1128 (2002).

91. Schmidt, A. M., Yan, S. D., Yan, S. F. & Stern, D. M. The multiligand receptor RAGE as a progression factor amplifying immune and inflammatory responses. *J. Clin. Invest.* **108**, 949–955 (2001).

92. Du Yan, S. *et al.* Amyloid-beta peptide-receptor for advanced glycation endproduct interaction elicits neuronal expression of macrophage-colony stimulating factor: a proinflammatory pathway in Alzheimer disease. *Proc. Natl. Acad. Sci. U. S. A.* **94**, 5296–5301 (1997).

93. Yan, S. D. *et al.* RAGE and amyloid-beta peptide neurotoxicity in Alzheimer's disease. *Nature* **382**, 685–691 (1996).

94. Yan, S. D. *et al.* Receptor-dependent cell stress and amyloid accumulation in systemic amyloidosis. *Nat. Med.* **6**, 643–651 (2000).

95. Hofmann, M. A. *et al.* RAGE mediates a novel proinflammatory axis: a central cell surface receptor for S100/calgranulin polypeptides. *Cell* **97**, 889–901 (1999).

96. Marenholz, I., Heizmann, C. W. & Fritz, G. S100 proteins in mouse and man: from evolution to function and pathology (including an update of the nomenclature). *Biochem. Biophys. Res. Commun.* **322**, 1111–1122 (2004).

97. Hori, O. *et al.* The receptor for advanced glycation end products (RAGE) is a cellular binding site for amphoterin. Mediation of neurite outgrowth and co-expression of rage and amphoterin in the developing nervous system. *J. Biol. Chem.* **270**, 25752–25761 (1995).

98. Wang, H. *et al.* HMG-1 as a late mediator of endotoxin lethality in mice. *Science* **285**, 248–251 (1999).

99. Andersson, U. & Tracey, K. J. HMGB1 in sepsis. *Scand. J. Infect. Dis.* **35**, 577–584 (2003).

100. Treutiger, C. J. *et al.* High mobility group 1 B-box mediates activation of human endothelium. *J. Intern. Med.* **254**, 375–385 (2003).

101. Chapman, M. R. *et al.* Role of Escherichia coli curli operons in directing amyloid fiber formation. *Science* **295**, 851–855 (2002).

102. Sasaki, N. *et al.* Advanced glycation end products (AGE) and their receptor (RAGE) in the brain of patients with Creutzfeldt-Jakob disease with prion plaques. *Neurosci. Lett.* **326**, 117–120 (2002).

103. Chavakis, T. *et al.* The pattern recognition receptor (RAGE) is a counterreceptor for leukocyte integrins: a novel pathway for inflammatory cell recruitment. *J. Exp. Med.* **198**, 1507–1515 (2003).

104. Liliensiek, B. *et al.* Receptor for advanced glycation end products (RAGE) regulates sepsis but not the adaptive immune response. *J. Clin. Invest.* **113**, 1641–1650 (2004).

105. Gordon, S. Pattern recognition receptors: doubling up for the innate immune response. *Cell* **111**, 927–930 (2002).

106. Akira, S., Takeda, K. & Kaisho, T. Toll-like receptors: critical proteins linking innate and acquired immunity. *Nat. Immunol.* **2**, 675–680 (2001).

107. Tamura, Y. *et al.* FEEL-1 and FEEL-2 are endocytic receptors for advanced glycation end products. *J. Biol. Chem.* **278**, 12613–12617 (2003).

108. Ohgami, N. *et al.* Cd36, a member of the class b scavenger receptor family, as a receptor for advanced glycation end products. *J. Biol. Chem.* **276**, 3195–3202 (2001).

109. Xie, J., Méndez, J. D., Méndez-Valenzuela, V. & Aguilar-Hernández, M. M. Cellular signalling of the receptor for advanced glycation end products (RAGE). *Cell. Signal.* **25**, 2185–2197 (2013).

110. Bierhaus, A. *et al.* Diabetes-associated sustained activation of the transcription factor nuclear factor-kappaB. *Diabetes* **50**, 2792–2808 (2001).

111. Barnes, P. J. & Karin, M. Nuclear factor-kappaB: a pivotal transcription factor in chronic inflammatory diseases. *N. Engl. J. Med.* **336**, 1066–1071 (1997).

112. Li, J. & Schmidt, A. M. Characterization and functional analysis of the promoter of RAGE, the receptor for advanced glycation end products. *J. Biol. Chem.* **272**, 16498–16506 (1997).

113. Bierhaus, A., Chen, J., Liliensiek, B. & Nawroth, P. P. LPS and cytokine-activated endothelium. *Semin. Thromb. Hemost.* **26**, 571–587 (2000).

114. Thompson, J. E., Phillips, R. J., Erdjument-Bromage, H., Tempst, P. & Ghosh, S. IκB-β regulates the persistent response in a biphasic activation of NF-κB. *Cell* **80**, 573–582 (1995).

115. Johnson, D. R., Douglas, I., Jahnke, A., Ghosh, S. & Pober, J. S. A sustained reduction in IkappaB-beta may contribute to persistent NF-kappaB activation in human endothelial cells. *J. Biol. Chem.* **271**, 16317–16322 (1996).

116. Manfredi, A. A. *et al.* Maturing dendritic cells depend on RAGE for in vivo homing to lymph nodes. *J. Immunol.* **180**, 2270–2275 (2008).

117. Kang, R. *et al.* HMGB1 in health and disease. *Mol. Aspects Med.* **40**, 1–116 (2014).

118. Chen, R.-C. *et al.* The role of HMGB1-RAGE axis in migration and invasion of hepatocellular carcinoma cell lines. *Mol. Cell. Biochem.* **390**, 271–280 (2014).

119. Taguchi, A. *et al.* Blockade of RAGE–amphoterin signalling suppresses tumour growth and metastases. *Nature* **405**, 354–360 (2000).

120. Chou, D. K. H., Zhang, J., Smith, F. I., McCaffery, P. & Jungalwala, F. B. Developmental expression of receptor for advanced glycation end products (RAGE), amphoterin and sulfoglucuronyl (HNK-1) carbohydrate in mouse cerebellum and their

role in neurite outgrowth and cell migration. *J. Neurochem.* **90**, 1389–1401 (2004).

121. Gross, C. *et al.* Advanced Glycation End Products and Receptor (RAGE) Promote Wound Healing of Human Corneal Epithelial Cells. *Invest. Ophthalmol. Vis. Sci.* **61**, 14 (2020).

122. Dahlmann, M. *et al.* RAGE mediates S100A4-induced cell motility via MAPK/ERK and hypoxia signaling and is a prognostic biomarker for human colorectal cancer metastasis. *Oncotarget* **5**, 3220–3233 (2014).

123. Ko, S.-Y. *et al.* Cell migration is regulated by AGE-RAGE interaction in human oral cancer cells in vitro. *PLoS One* **9**, e110542 (2014).

124. Riuzzi, F., Sorci, G. & Donato, R. The amphoterin (HMGB1)/receptor for advanced glycation end products (RAGE) pair modulates myoblast proliferation, apoptosis, adhesiveness, migration, and invasiveness. *J. Biol. Chem.* **281**, 8242–8253 (2006).

125. Riuzzi, F., Sorci, G. & Donato, R. RAGE expression in rhabdomyosarcoma cells results in myogenic differentiation and reduced proliferation, migration, invasiveness, and tumor growth. *Am. J. Pathol.* **171**, 947–961 (2007).

126. Huttunen, H. J. *et al.* Coregulation of neurite outgrowth and cell survival by amphoterin and S100 proteins through receptor for advanced glycation end products (RAGE) activation. *J. Biol. Chem.* **275**, 40096–40105 (2000).

127. Sorci, G. *et al.* S100B protein in tissue development, repair and regeneration. *World J. Biol. Chem.* **4**, 1–12 (2013).

128. Tang, D. *et al.* Endogenous HMGB1 regulates autophagy. *J. Cell Biol.* **190**, 881–892 (2010).

129. Tang, D. *et al.* HMGB1 release and redox regulates autophagy and apoptosis in cancer cells. *Oncogene* **29**, 5299–5310 (2010).

130. Notsu, M. *et al.* Advanced Glycation End Product 3 (AGE3) Increases Apoptosis and

the Expression of Sclerostin by Stimulating TGF-β Expression and Secretion in Osteocyte-Like MLO-Y4-A2 Cells. *Calcif. Tissue Int.* **100**, 402–411 (2017).

131. Wautier, M. P. *et al.* Activation of NADPH oxidase by AGE links oxidant stress to altered gene expression via RAGE. *Am. J. Physiol. Endocrinol. Metab.* **280**, E685–94 (2001).
132. Lander, H. M. *et al.* Activation of the receptor for advanced glycation end products triggers a p21(ras)-dependent mitogen-activated protein kinase pathway regulated by oxidant stress. *J. Biol. Chem.* **272**, 17810–17814 (1997).
133. Ramasamy, R., Yan, S. F. & Schmidt, A. M. RAGE: therapeutic target and biomarker of the inflammatory response--the evidence mounts. *J. Leukoc. Biol.* **86**, 505–512 (2009).
134. Yao, D. & Brownlee, M. Hyperglycemia-induced reactive oxygen species increase expression of the receptor for advanced glycation end products (RAGE) and RAGE ligands. *Diabetes* **59**, 249–255 (2010).
135. Xiang, M. & Fan, J. Pattern recognition receptor-dependent mechanisms of acute lung injury. *Mol. Med.* **16**, 69–82 (2010).
136. Brett, J. *et al.* Survey of the distribution of a newly characterized receptor for advanced glycation end products in tissues. *Am. J. Pathol.* **143**, 1699–1712 (1993).
137. Hanford, L. E. *et al.* Regulation of receptor for advanced glycation end products during bleomycin-induced lung injury. *Am. J. Respir. Cell Mol. Biol.* **29**, S77–81 (2003).
138. Hanford, L. E. *et al.* Purification and characterization of mouse soluble receptor for advanced glycation end products (sRAGE). *J. Biol. Chem.* **279**, 50019–50024 (2004).
139. Englert, J. M. *et al.* A role for the receptor for advanced glycation end products in idiopathic pulmonary fibrosis. *Am. J. Pathol.* **172**, 583–591 (2008).
140. Queisser, M. A. *et al.* Loss of RAGE in pulmonary fibrosis: molecular relations to functional changes in pulmonary cell types. *Am. J. Respir. Cell Mol. Biol.* **39**, 337–345

(2008).

141. Schmidt, A. M., Yan, S. D., Yan, S. F. & Stern, D. M. The biology of the receptor for advanced glycation end products and its ligands. *Biochim. Biophys. Acta* **1498**, 99–111 (2000).

142. Chavakis, T., Bierhaus, A. & Nawroth, P. P. RAGE (receptor for advanced glycation end products): a central player in the inflammatory response. *Microbes Infect.* **6**, 1219–1225 (2004).

143. Bierhaus, A. *et al.* Understanding RAGE, the receptor for advanced glycation end products. *J. Mol. Med.* **83**, 876–886 (2005).

144. Bianchi, R., Adami, C., Giambanco, I. & Donato, R. S100B binding to RAGE in microglia stimulates COX-2 expression. *J. Leukoc. Biol.* **81**, 108–118 (2007).

145. Kuipers, M. T., van der Poll, T., Schultz, M. J. & Wieland, C. W. Bench-to-bedside review: Damage-associated molecular patterns in the onset of ventilator-induced lung injury. *Crit. Care* **15**, 235 (2011).

146. Vazzana, N., Santilli, F., Cuccurullo, C. & Davì, G. Soluble forms of RAGE in internal medicine. *Intern. Emerg. Med.* **4**, 389–401 (2009).

147. Santilli, F., Vazzana, N., Bucciarelli, L. & Davi, G. Soluble Forms of RAGE in Human Diseases: Clinical and Therapeutical Implications. *Current Medicinal Chemistry* vol. 16 940–952 Preprint at https://doi.org/10.2174/092986709787581888 (2009).

148. Shirasawa, M. *et al.* Receptor for advanced glycation end-products is a marker of type I lung alveolar cells. *Genes Cells* **9**, 165–174 (2004).

149. Uchida, T. *et al.* Receptor for advanced glycation end-products is a marker of type I cell injury in acute lung injury. *Am. J. Respir. Crit. Care Med.* **173**, 1008–1015 (2006).

150. Zhang, H. *et al.* Role of soluble receptor for advanced glycation end products on endotoxin-induced lung injury. *Am. J. Respir. Crit. Care Med.* **178**, 356–362 (2008).

151. Su, X., Looney, M. R., Gupta, N. & Matthay, M. A. Receptor for advanced glycation end-products (RAGE) is an indicator of direct lung injury in models of experimental lung injury. *Am. J. Physiol. Lung Cell. Mol. Physiol.* **297**, L1–5 (2009).

152. Blondonnet, R. *et al.* RAGE inhibition reduces acute lung injury in mice. *Sci. Rep.* **7**, 7208 (2017).

153. Audard, J. *et al.* Inhibition of the Receptor for Advanced Glycation End-Products in Acute Respiratory Distress Syndrome: A Randomised Laboratory Trial in Piglets. *Sci. Rep.* **9**, 9227 (2019).

154. Jabaudon, M., Blondonnet, R. & Ware, L. B. Biomarkers in acute respiratory distress syndrome. *Curr. Opin. Crit. Care* (2020) doi:10.1097/MCC.0000000000000786.

155. Jabaudon, M. *et al.* Soluble form of the receptor for advanced glycation end products is a marker of acute lung injury but not of severe sepsis in critically ill patients. *Crit. Care Med.* **39**, 480–488 (2011).

156. Jabaudon, M. *et al.* Soluble Forms and Ligands of the Receptor for Advanced Glycation End-Products in Patients with Acute Respiratory Distress Syndrome: An Observational Prospective Study. *PLoS One* **10**, e0135857 (2015).

157. Mrozek, S. *et al.* Elevated Plasma Levels of sRAGE Are Associated With Nonfocal CT-Based Lung Imaging in Patients With ARDS: A Prospective Multicenter Study. *Chest* **150**, 998–1007 (2016).

158. Jabaudon, M. *et al.* Plasma sRAGE is independently associated with increased mortality in ARDS: a meta-analysis of individual patient data. *Intensive Care Med.* (2018) doi:10.1007/s00134-018-5327-1.

159. Jabaudon, M. *et al.* Effects of a recruitment maneuver on plasma levels of soluble RAGE in patients with diffuse acute respiratory distress syndrome: a prospective randomized crossover study. *Intensive Care Med.* **41**, 846–855 (2015).

160. Jabaudon, M. *et al.* Association between intraoperative ventilator settings and plasma levels of soluble receptor for advanced glycation end-products in patients without pre-existing lung injury. *Respirology* (2015) doi:10.1111/resp.12583.

161. Lee, S. *et al.* Production and application of HMGB1 derived recombinant RAGE-antagonist peptide for anti-inflammatory therapy in acute lung injury. *Eur. J. Pharm. Sci.* **114**, 275–284 (2018).

162. Mason, R. J. Biology of alveolar type II cells. *Respirology* **11 Suppl**, S12–5 (2006).

163. Guillot, L. *et al.* Alveolar epithelial cells: master regulators of lung homeostasis. *Int. J. Biochem. Cell Biol.* **45**, 2568–2573 (2013).

164. Agassandian, M. & Mallampalli, R. K. Surfactant phospholipid metabolism. *Biochim. Biophys. Acta* **1831**, 612–625 (2013).

165. Mittal, R. A. *et al.* SFTA2—A Novel Secretory Peptide Highly Expressed in the Lung—Is Modulated by Lipopolysaccharide but Not Hyperoxia. *PLoS One* **7**, e40011 (2012).

166. Weibel, E. R. On the tricks alveolar epithelial cells play to make a good lung. *Am. J. Respir. Crit. Care Med.* **191**, 504–513 (2015).

167. Danto, S. I., Shannon, J. M., Borok, Z., Zabski, S. M. & Crandall, E. D. Reversible transdifferentiation of alveolar epithelial cells. *Am. J. Respir. Cell Mol. Biol.* **12**, 497–502 (1995).

168. Fujino, N. *et al.* Isolation of alveolar epithelial type II progenitor cells from adult human lungs. *Lab. Invest.* **91**, 363–378 (2011).

169. Zhao, L., Yee, M. & O'Reilly, M. A. Transdifferentiation of alveolar epithelial type II to type I cells is controlled by opposing TGF-β and BMP signaling. *Am. J. Physiol. Lung Cell. Mol. Physiol.* **305**, L409–18 (2013).

170. Desai, T. J., Brownfield, D. G. & Krasnow, M. A. Alveolar progenitor and stem cells in

lung development, renewal and cancer. *Nature* **507**, 190–194 (2014).

171. Wang, F. *et al.* Heterogeneity of claudin expression by alveolar epithelial cells. *Am. J. Respir. Cell Mol. Biol.* **29**, 62–70 (2003).

172. Jin, W. *et al.* Increased claudin-3, -4 and -18 levels in bronchoalveolar lavage fluid reflect severity of acute lung injury. *Respirology* **18**, 643–651 (2013).

173. Coyne, C. B., Gambling, T. M., Boucher, R. C., Carson, J. L. & Johnson, L. G. Role of claudin interactions in airway tight junctional permeability. *Am. J. Physiol. Lung Cell. Mol. Physiol.* **285**, L1166–78 (2003).

174. Mitchell, L. A., Overgaard, C. E., Ward, C., Margulies, S. S. & Koval, M. Differential effects of claudin-3 and claudin-4 on alveolar epithelial barrier function. *Am. J. Physiol. Lung Cell. Mol. Physiol.* **301**, L40–9 (2011).

175. Wray, C. *et al.* Claudin-4 augments alveolar epithelial barrier function and is induced in acute lung injury. *Am. J. Physiol. Lung Cell. Mol. Physiol.* **297**, L219–27 (2009).

176. Rokkam, D., Lafemina, M. J., Lee, J. W., Matthay, M. A. & Frank, J. A. Claudin-4 levels are associated with intact alveolar fluid clearance in human lungs. *Am. J. Pathol.* **179**, 1081–1087 (2011).

177. Kage, H. *et al.* Claudin 4 knockout mice: normal physiological phenotype with increased susceptibility to lung injury. *Am. J. Physiol. Lung Cell. Mol. Physiol.* **307**, L524–36 (2014).

178. Itoh, M., Nagafuchi, A., Moroi, S. & Tsukita, S. Involvement of ZO-1 in cadherin-based cell adhesion through its direct binding to alpha catenin and actin filaments. *J. Cell Biol.* **138**, 181–192 (1997).

179. Itoh, M. *et al.* Direct binding of three tight junction-associated MAGUKs, ZO-1, ZO-2, and ZO-3, with the COOH termini of claudins. *J. Cell Biol.* **147**, 1351–1363 (1999).

180. Denker, B. M. & Nigam, S. K. Molecular structure and assembly of the tight junction.

Am. J. Physiol. **274**, F1–9 (1998).

181. Brune, K., Frank, J., Schwingshackl, A., Finigan, J. & Sidhaye, V. K. Pulmonary epithelial barrier function: some new players and mechanisms. *Am. J. Physiol. Lung Cell. Mol. Physiol.* **308**, L731–45 (2015).

182. Weibel, E. R. On the tricks alveolar epithelial cells play to make a good lung. *Am. J. Respir. Crit. Care Med.* **191**, 504–513 (2015).

183. van Roy, F. & Berx, G. The cell-cell adhesion molecule E-cadherin. *Cell. Mol. Life Sci.* **65**, 3756–3788 (2008).

184. Rao, R. Oxidative stress-induced disruption of epithelial and endothelial tight junctions. *Front. Biosci.* **13**, 7210–7226 (2008).

185. Turner, J. R. Intestinal mucosal barrier function in health and disease. *Nat. Rev. Immunol.* **9**, 799–809 (2009).

186. Ivanov, A. I., Parkos, C. A. & Nusrat, A. Cytoskeletal regulation of epithelial barrier function during inflammation. *Am. J. Pathol.* **177**, 512–524 (2010).

187. Capaldo, C. T. & Nusrat, A. Cytokine regulation of tight junctions. *Biochim. Biophys. Acta* **1788**, 864–871 (2009).

188. Gonzalez-Mariscal, L., Garay, E. & Lechuga, S. Virus interaction with the apical junctional complex. *Front. Biosci.* **14**, 731–768 (2009).

189. Song, C. *et al.* Evidence for the critical role of the PI3K signaling pathway in particulate matter-induced dysregulation of the inflammatory mediators COX-2/PGE2 and the associated epithelial barrier protein Filaggrin in the bronchial epithelium. *Cell Biol. Toxicol.* **36**, 301–313 (2020).

190. Bhat, A. A. *et al.* Tight Junction Proteins and Signaling Pathways in Cancer and Inflammation: A Functional Crosstalk. *Front. Physiol.* **9**, 1942 (2018).

191. Samarin, S. N., Ivanov, A. I., Flatau, G., Parkos, C. A. & Nusrat, A. Rho/Rho-associated

kinase-II signaling mediates disassembly of epithelial apical junctions. *Mol. Biol. Cell* **18**, 3429–3439 (2007).

192. McKenzie, J. A. G. & Ridley, A. J. Roles of Rho/ROCK and MLCK in TNF-alpha-induced changes in endothelial morphology and permeability. *J. Cell. Physiol.* **213**, 221–228 (2007).

193. Elamin, E., Masclee, A., Dekker, J. & Jonkers, D. Ethanol disrupts intestinal epithelial tight junction integrity through intracellular calcium-mediated Rho/ROCK activation. *Am. J. Physiol. Gastrointest. Liver Physiol.* **306**, G677–85 (2014).

194. Tasaka, S. *et al.* Attenuation of endotoxin-induced acute lung injury by the Rho-associated kinase inhibitor, Y-27632. *Am. J. Respir. Cell Mol. Biol.* **32**, 504–510 (2005).

195. Köksel, O. *et al.* Rho-kinase (ROCK-1 and ROCK-2) upregulation in oleic acid-induced lung injury and its restoration by Y-27632. *Eur. J. Pharmacol.* **510**, 135–142 (2005).

196. Zhang, Y. *et al.* Pharmacological postconditioning with sevoflurane activates PI3K/AKT signaling and attenuates cardiopulmonary bypass-induced lung injury in dog. *Life Sci.* **173**, 68–72 (2017).

197. Ware, L. B. & Matthay, M. A. Alveolar fluid clearance is impaired in the majority of patients with acute lung injury and the acute respiratory distress syndrome. *Am. J. Respir. Crit. Care Med.* **163**, 1376–1383 (2001).

198. Berthiaume, Y. & Matthay, M. A. Alveolar edema fluid clearance and acute lung injury. *Respir. Physiol. Neurobiol.* **159**, 350–359 (2007).

199. Ramasamy, R., Yan, S. F. & Schmidt, A. M. RAGE: therapeutic target and biomarker of the inflammatory response--the evidence mounts. *J. Leukoc. Biol.* **86**, 505–512 (2009).

200. Watanabe, N., Kato, T., Fujita, A., Ishizaki, T. & Narumiya, S. Cooperation between mDia1 and ROCK in Rho-induced actin reorganization. *Nat. Cell Biol.* **1**, 136–143

(1999).

201. Etienne-Manneville, S. & Hall, A. Rho GTPases in cell biology. *Nature* **420**, 629–635 (2002).

202. Birukova, A. A. *et al.* Microtubule disassembly induces cytoskeletal remodeling and lung vascular barrier dysfunction: role of Rho-dependent mechanisms. *J. Cell. Physiol.* **201**, 55–70 (2004).

203. Loirand, G., Guérin, P. & Pacaud, P. Rho kinases in cardiovascular physiology and pathophysiology. *Circ. Res.* **98**, 322–334 (2006).

204. Shimizu, Y., Dobashi, K., Sano, T. & Yamada, M. ROCK activation in lung of idiopathic pulmonary fibrosis with oxidative stress. *Int. J. Immunopathol. Pharmacol.* **27**, 37–44 (2014).

205. Maekawa, M. *et al.* Signaling from Rho to the actin cytoskeleton through protein kinases ROCK and LIM-kinase. *Science* **285**, 895–898 (1999).

206. Ware, L. B. Pathophysiology of acute lung injury and the acute respiratory distress syndrome. *Semin. Respir. Crit. Care Med.* **27**, 337–349 (2006).

207. Abedi, F., Hayes, A. W., Reiter, R. & Karimi, G. Acute lung injury: The therapeutic role of Rho kinase inhibitors. *Pharmacol. Res.* **155**, 104736 (2020).

208. González-Mariscal, L., Betanzos, A., Nava, P. & Jaramillo, B. E. Tight junction proteins. *Prog. Biophys. Mol. Biol.* **81**, 1–44 (2003).

209. Schneeberger, E. E. & Lynch, R. D. The tight junction: a multifunctional complex. *Am. J. Physiol. Cell Physiol.* **286**, C1213–28 (2004).

210. Ely, E. W. The ABCDEF Bundle: Science and Philosophy of How ICU Liberation Serves Patients and Families. *Crit. Care Med.* **45**, 321–330 (2017).

211. Devlin, J. W. *et al.* Clinical Practice Guidelines for the Prevention and Management of Pain, Agitation/Sedation, Delirium, Immobility, and Sleep Disruption in Adult Patients

in the ICU. *Crit. Care Med.* **46**, e825–e873 (2018).

212. Devlin, J. W. *et al.* Clinical Practice Guidelines for the Prevention and Management of Pain, Agitation/Sedation, Delirium, Immobility, and Sleep Disruption in Adult Patients in the ICU. *Crit. Care Med.* **46**, e825–e873 (2018).
213. Shehabi, Y. *et al.* Early Sedation with Dexmedetomidine in Critically Ill Patients. *N. Engl. J. Med.* **380**, 2506–2517 (2019).
214. Payen, J.-F. *et al.* Current practices in sedation and analgesia for mechanically ventilated critically ill patients: a prospective multicenter patient-based study. *Anesthesiology* **106**, 687–95; quiz 891–2 (2007).
215. Soukup, J. *et al.* State of the art: sedation concepts with volatile anesthetics in critically Ill patients. *J. Crit. Care* **24**, 535–544 (2009).
216. DAS-Taskforce 2015 *et al.* Evidence and consensus based guideline for the management of delirium, analgesia, and sedation in intensive care medicine. Revision 2015 (DAS-Guideline 2015) - short version. *Ger. Med. Sci.* **13**, Doc19 (2015).
217. Blondonnet, R. *et al.* Use of volatile agents for sedation in the intensive care unit: A national survey in France. *PLoS One* **16**, e0249889 (2021).
218. Ferrière, N., Bodenes, L., Bailly, P. & L'Her, E. Shortage of anesthetics: Think of inhaled sedation! *J. Crit. Care* (2020) doi:10.1016/j.jcrc.2020.09.009.
219. Matthay, M. A. *et al.* Future research directions in acute lung injury: summary of a National Heart, Lung, and Blood Institute working group. *Am. J. Respir. Crit. Care Med.* **167**, 1027–1035 (2003).
220. Matthay, M. A., McAuley, D. F. & Ware, L. B. Clinical trials in acute respiratory distress syndrome: challenges and opportunities. *The Lancet Respiratory Medicine* **5**, 524–534 (2017/6).
221. Calfee, C. S. *et al.* Trauma-associated lung injury differs clinically and biologically from

acute lung injury due to other clinical disorders. *Crit. Care Med.* **35**, 2243–2250 (2007).

222. Tejera, P. *et al.* Distinct and replicable genetic risk factors for acute respiratory distress syndrome of pulmonary or extrapulmonary origin. *J. Med. Genet.* **49**, 671–680 (2012).

223. Delucchi, K. *et al.* Stability of ARDS subphenotypes over time in two randomised controlled trials. *Thorax* thoraxjnl–2017–211090 (2018) doi:10.1136/thoraxjnl-2017-211090.

224. Matthay, M. A. *et al.* Acute respiratory distress syndrome. *Nat Rev Dis Primers* **5**, 18 (2019).

225. Wilson, J. G. & Calfee, C. S. ARDS Subphenotypes: Understanding a Heterogeneous Syndrome. *Crit. Care* **24**, 102 (2020).

226. Juffermans, N. P., Radermacher, P., Laffey, J. G. & Translational Biology Group. The importance of discovery science in the development of therapies for the critically ill. *Intensive Care Med Exp* **8**, 17 (2020).

227. Villar, J. *et al.* Dexamethasone treatment for the acute respiratory distress syndrome: a multicentre, randomised controlled trial. *Lancet Respir Med* **8**, 267–276 (2020).

228. Matthay, M. A. & Wiener-Kronish, J. P. Intact epithelial barrier function is critical for the resolution of alveolar edema in humans. *Am. Rev. Respir. Dis.* **142**, 1250–1257 (1990).

229. Villar, J., Zhang, H. & Slutsky, A. S. Lung Repair and Regeneration in ARDS: Role of PECAM1 and Wnt Signaling. *Chest* **155**, 587–594 (2019).

230. Adamson, I. Y. & Bowden, D. H. The type 2 cell as progenitor of alveolar epithelial regeneration. A cytodynamic study in mice after exposure to oxygen. *Lab. Invest.* **30**, 35–42 (1974).

231. McQualter, J. L., Yuen, K., Williams, B. & Bertoncello, I. Evidence of an epithelial stem/progenitor cell hierarchy in the adult mouse lung. *Proc. Natl. Acad. Sci. U. S. A.*

107, 1414–1419 (2010).

232. Huttunen, H. J., Fages, C. & Rauvala, H. Receptor for advanced glycation end products (RAGE)-mediated neurite outgrowth and activation of NF-kappaB require the cytoplasmic domain of the receptor but different downstream signaling pathways. *J. Biol. Chem.* **274**, 19919–19924 (1999).
233. Rong, L. L. *et al.* RAGE modulates peripheral nerve regeneration via recruitment of both inflammatory and axonal outgrowth pathways. *FASEB J.* **18**, 1818–1825 (2004).
234. Ojo, O. O., Ryu, M. H., Jha, A., Unruh, H. & Halayko, A. J. High-mobility group box 1 promotes extracellular matrix synthesis and wound repair in human bronchial epithelial cells. *Am. J. Physiol. Lung Cell. Mol. Physiol.* **309**, L1354–66 (2015).
235. Schlingmann, B. *et al.* Regulation of claudin/zonula occludens-1 complexes by hetero-claudin interactions. *Nat. Commun.* **7**, 12276 (2016).
236. Beitler, J. R. & Talmor, D. Volatile anesthetics for ICU sedation: the future of critical care or niche therapy? *Intensive Care Med.* **48**, 1413–1417 (2022).
237. Jabaudon, M., Zhai, R., Blondonnet, R. & Bonda, W. L. M. Inhaled sedation in the intensive care unit. *Anaesth Crit Care Pain Med* 101133 (2022) doi:10.1016/j.accpm.2022.101133.
238. Ferrando, C. *et al.* Sevoflurane, but not propofol, reduces the lung inflammatory response and improves oxygenation in an acute respiratory distress syndrome model: a randomised laboratory study. *European Journal of Anaesthesiology| EJA* **30**, 455–463 (2013).
239. Fortis, S. *et al.* Effects of anesthetic regimes on inflammatory responses in a rat model of acute lung injury. *Intensive Care Med.* **38**, 1548–1555 (2012).
240. Schläpfer, M. *et al.* Sevoflurane reduces severity of acute lung injury possibly by impairing formation of alveolar oedema. *Clin. Exp. Immunol.* **168**, 125–134 (2012).

241. Englert, J. A. *et al.* Isoflurane Ameliorates Acute Lung Injury by Preserving Epithelial Tight Junction Integrity. *Anesthesiology* **123**, 377–388 (2015).

242. Reutershan, J., Chang, D., Hayes, J. K. & Ley, K. Protective effects of isoflurane pretreatment in endotoxin-induced lung injury. *Anesthesiology* **104**, 511–517 (2006).

243. Voigtsberger, S. *et al.* Sevoflurane ameliorates gas exchange and attenuates lung damage in experimental lipopolysaccharide-induced lung injury. *Anesthesiology* **111**, 1238–1248 (2009).

244. Rubenfeld, G. D. & Shankar-Hari, M. Lessons From ARDS for Non-ARDS Research: Remembrance of Trials Past. *JAMA: the journal of the American Medical Association* vol. 320 1863–1865 (2018).

245. National Heart, Lung, and Blood Institute PETAL Clinical Trials Network *et al.* Early Neuromuscular Blockade in the Acute Respiratory Distress Syndrome. *N. Engl. J. Med.* **380**, 1997–2008 (2019).

246. Beitler, J. R. *et al.* Effect of titrating positive end-expiratory pressure (PEEP) with an esophageal pressure--guided strategy vs an empirical high PEEP-Fio2 strategy on death and days free from mechanical ventilation among patients with acute respiratory distress syndrome: a randomized clinical trial. *JAMA* **321**, 846–857 (2019).

247. Hodgson, C. L. *et al.* Maximal Recruitment Open Lung Ventilation in Acute Respiratory Distress Syndrome (PHARLAP). A Phase II, Multicenter Randomized Controlled Clinical Trial. *Am. J. Respir. Crit. Care Med.* **200**, 1363–1372 (2019).

248. Ranieri, V. M. *et al.* Effect of Intravenous Interferon β-1a on Death and Days Free From Mechanical Ventilation Among Patients With Moderate to Severe Acute Respiratory Distress Syndrome: A Randomized Clinical Trial. *JAMA* **323**, 725–733 (2020).

249. Matute-Bello, G. *et al.* An official American Thoracic Society workshop report: features and measurements of experimental acute lung injury in animals. *Am. J. Respir. Cell Mol.*

Biol. **44**, 725–738 (2011).

250. Karki, P. & Birukov, K. G. Rho and Reactive Oxygen Species at Crossroads of Endothelial Permeability and Inflammation. *Antioxid. Redox Signal.* **31**, 1009–1022 (2019).

251. Sun, H., Breslin, J. W., Zhu, J., Yuan, S. Y. & Wu, M. H. Rho and ROCK signaling in VEGF-induced microvascular endothelial hyperpermeability. *Microcirculation* **13**, 237–247 (2006).

252. Gong, M. N. Myosin light chain kinase gene and acute lung injury in trauma and sepsis: opposite effects but confirmatory. *Critical care medicine* vol. 36 2943–2945 (2008).

253. Szilágyi, K. L. *et al.* Epigenetic contribution of the myosin light chain kinase gene to the risk for acute respiratory distress syndrome. *Transl. Res.* **180**, 12–21 (2017).

254. Lecuona, E., Ridge, K., Pesce, L., Batlle, D. & Sznajder, J. I. The GTP-binding protein RhoA mediates Na,K-ATPase exocytosis in alveolar epithelial cells. *Mol. Biol. Cell* **14**, 3888–3897 (2003).

255. Stanimirovic, J. *et al.* Regulation of hepatic Na+/K+-ATPase in obese female and male rats: involvement of ERK1/2, AMPK, and Rho/ROCK. *Mol. Cell. Biochem.* **440**, 77–88 (2018).

256. Pavlov, T. S., Levchenko, V. & Staruschenko, A. Role of Rho GDP dissociation inhibitor α in control of epithelial sodium channel (ENaC)-mediated sodium reabsorption. *J. Biol. Chem.* **289**, 28651–28659 (2014).

257. Yang, S., Wu, Q., Huang, S., Wang, Z. & Qi, F. Sevoflurane and isoflurane inhibit KCl-induced Class II phosphoinositide 3-kinase α subunit mediated vasoconstriction in rat aorta. *BMC Anesthesiol.* **16**, 63 (2016).

258. Qin, J., Ma, Q. & Ma, D. Low-dose Sevoflurane Attenuates Cardiopulmonary Bypass (CPB)- induced Postoperative Cognitive Dysfunction (POCD) by Regulating

Hippocampus Apoptosis via PI3K/AKT Pathway. *Curr. Neurovasc. Res.* **17**, 232–240 (2020).

259. Yu, Q., Dai, H., Jiang, Y., Zha, Y. & Zhang, J. Sevoflurane alleviates oxygen-glucose deprivation/reoxygenation-induced injury in HT22 cells through regulation of the PI3K/AKT/GSK3β signaling pathway. *Exp. Ther. Med.* **21**, 376 (2021).
260. Wang, F. *et al.* Sevoflurane ameliorates adriamycin-induced myocardial injury in rats through the PI3K/Akt/GSK-3β pathway. *Eur. Rev. Med. Pharmacol. Sci.* **25**, 968–975 (2021).
261. Shiomi, M. *et al.* Sevoflurane induces cardioprotection through reactive oxygen species-mediated upregulation of autophagy in isolated guinea pig hearts. *J. Anesth.* **28**, 593–600 (2014).
262. Lv, G. *et al.* Inhibiting specificity protein 1 attenuated sevoflurane-induced mitochondrial stress and promoted autophagy in hippocampal neurons through PI3K/Akt/mTOR and α7-nAChR signaling. *Neurosci. Lett.* **794**, 136995 (2022).
263. He, H. *et al.* Sevoflurane post-conditioning attenuates traumatic brain injury-induced neuronal apoptosis by promoting autophagy via the PI3K/AKT signaling pathway. *Drug Des. Devel. Ther.* **12**, 629–638 (2018).
264. Ma, J.-F., Li, C.-G., Sun, M.-Y., Shao, G.-F. & Li, K.-Z. Isoflurane and sevoflurane affects Wnt/β-catenin signaling pathways in hippocampal formation of neonatal rats. *Eur. Rev. Med. Pharmacol. Sci.* **21**, 1980–1989 (2017).
265. Liu, S. *et al.* Sevoflurane affects neurogenesis through cell cycle arrest via inhibiting wnt/β-catenin signaling pathway in mouse neural stem cells. *Life Sci.* **209**, 34–42 (2018).
266. Oliveira, A. L. *et al.* Enhanced RAGE Expression and Excess Reactive-Oxygen Species Production Mediates Rho Kinase-Dependent Detrusor Overactivity After Methylglyoxal

Exposure. *Front. Physiol.* **13**, 860342 (2022).

267. Zhao, M.-J. *et al.* Roles of RAGE/ROCK1 Pathway in HMGB1-Induced Early Changes in Barrier Permeability of Human Pulmonary Microvascular Endothelial Cell. *Front. Immunol.* **12**, 697071 (2021).

268. Qin, Q. *et al.* Heparanase induced by advanced glycation end products (AGEs) promotes macrophage migration involving RAGE and PI3K/AKT pathway. *Cardiovasc. Diabetol.* **12**, 37 (2013).

269. Li, G., Xu, J. & Li, Z. Receptor for advanced glycation end products inhibits proliferation in osteoblast through suppression of Wnt, PI3K and ERK signaling. *Biochem. Biophys. Res. Commun.* **423**, 684–689 (2012).

270. Kvolik, S., Dobrosevic, B., Marczi, S., Prlic, L. & Glavas-Obrovac, L. Different apoptosis ratios and gene expressions in two human cell lines after sevoflurane anaesthesia. *Acta Anaesthesiol. Scand.* **53**, 1192–1199 (2009).

271. Hirai, T. *et al.* Differential effects of sevoflurane on the growth and apoptosis of human cancer cell lines. *J. Anesth.* **34**, 47–57 (2020).

272. Zhai, R., Bonda, W. L. M., Matute-Bello, G. & Jabaudon, M. From preclinical to clinical models of acute respiratory distress syndrome. *Signa Vitae* (2021) doi:10.22514/sv.2021.228.

273. Matthay, M. A. *et al.* Phenotypes and personalized medicine in the acute respiratory distress syndrome. *Intensive Care Med.* **46**, 2136–2152 (2020).

274. Sinha, P. & Calfee, C. S. Phenotypes in acute respiratory distress syndrome: moving towards precision medicine. *Curr. Opin. Crit. Care* **25**, 12–20 (2019).

275. Jabaudon, M. *et al.* Recent directions in personalised acute respiratory distress syndrome medicine. *Anaesth Crit Care Pain Med* **37**, 251–258 (2018).

276. Martin, T. R. *et al.* New Insights into Clinical and Mechanistic Heterogeneity of the

Acute Respiratory Distress Syndrome: Summary of the Aspen Lung Conference 2021. *Am. J. Respir. Cell Mol. Biol.* (2022) doi:10.1165/rcmb.2022-0089WS.

277. Sinha, P. *et al.* Prevalence of phenotypes of acute respiratory distress syndrome in critically ill patients with COVID-19: a prospective observational study. *Lancet Respir Med* **8**, 1209–1218 (2020).

278. Pelosi, P. *et al.* Personalized mechanical ventilation in acute respiratory distress syndrome. *Crit. Care* **25**, 250 (2021).